Data accompanying

Episodic burial and exhumation in NE Brazil after opening of the South Atlantic

by Japsen et al.

Item 1a: Extract of Geotrack report GC990 by Paul F. Green (Onshore Northeast Brazil. Thermal history reconstruction based on AFTA and VR). Details about data and interpretations for wells A and B (wells FPO-1 and 6-MGP-34), and outcrop samples in NE Brazil.

Item 1b: AFTA data for 2 basement samples near the outcrop of the Fonseca Formation; results from sample RD93-5 is discussed in the paper.

Item 2: Extract of GEUS report 2009/8 by Peter Japsen (Burial anomalies and magnitude of exhumation estimated from sonic data for 19 wells, onshore and offshore NE Brazil; Almada, Camamu, Recôncavo, Sanfranciscana and Tucano Basins with details about data and interpretations for wells A and B, and outcrop samples in NE Brazil). Details about data and interpretation of onshore wells A and B wells FPO-1 and 6-MGP-34, and offshore reference wells BAS-21, -88, 113.

Item 3: GEUS report 2009/9 by Johan M. Bonow (Relative denudation chronology in NE Brazil based on mapping of large-scale landforms)

Contents of Extract of Geotrack report GC990

2. Interpretation strategy: p. 9.

6. Thermal history interpretation of AFTA and VR data in the 1-FPO-1-BA: p. 76.

6. Thermal history interpretation of AFTA and VR data in the 6-MGP-34-BA well: p. 166.

11. AFTA and VR data in outcrop samples from NE Brazil and associated thermal history interpretations: p. 194.

13. Regional synthesis: definition of major regional paleo-thermal episodes, mechanisms of heating and cooling, and regional variation: p. 324.

References: p. 405.

Contents of Extract of GEUS Report 2009/8

2. Introduction: p. 8.

3. Data: p. 9.

4. Velocity anomalies and burial anomalies: p. 11.

5. Normal velocity-depth trends for different lithologies: p. 16.

8. References: p. 34.

Appendix B. Interpretation and plots of sonic data: p. 53.

- **BAS-21**
- **BAS-88**
- **BAS-113**
- **FPO-1 (well A)**
- **MGP-34 (well B)**
-

1. Summary....3

2. Background....5

2.1 Geomorphology....6
2.2 The approach of landscape analysis....6
2.3 The study area 6

3. Method of landscape analysis....9

3.1 Method of surface mapping....9

4. Geomorphological results....13

4.1 Topographical overview....13
4.2 The denudation surfaces....20
4.2.1 The higher surface....21
4.2.2 The lower surface....22
4.2.3 The coastal plain....22
4.2.4 Illustrations of the surface mapping....22
4.3 The surfaces in relationship to geology....24

5. Geomorphological implications and discussion....27

5.1 Surface chronology and timing of events....28

6. Conclusions....29

7. References....30

ONSHORE NORTHEAST BRAZIL

THERMAL HISTORY RECONSTRUCTION BASED ON AFTA AND VR DATA IN THE 1-AO-1-BA, 1-BRN-1-BA, 1-FLU-1-BA, 1-FPO-1-BA, 1-FVM-1-BA, 1-RSO-1-BA, 3-MB-3-BA AND 6-MGP-34-BA WELLS, TUCANO AND RECÔNCAVO BASINS, TOGETHER WITH AFTA AND ASSOCIATED THERMAL HISTORY INTERPRETATIONS IN 89 OUTCROP SAMPLES FROM BAHIA, NE BRAZIL, AND 20 SAMPLES FROM THE SERRA DO MAR

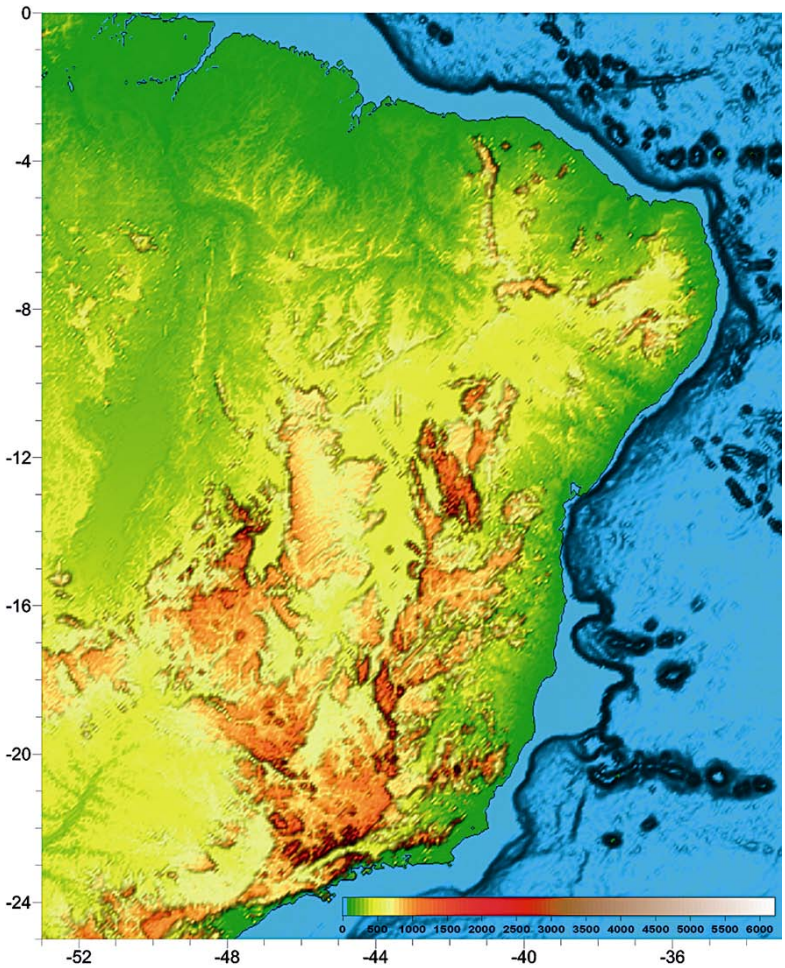

GEOTRACK REPORT #990

A report prepared for Statoil do Brasil, Rio de Janeiro, as part of a research project coordinated by the Geological Survey of Denmark and Greenland (GEUS), Copenhagen

Report prepared by: P.F. Green

February 2009

Geotrack International Pty Ltd ABN 16006 899 209

37 Melville Road, Brunswick West, Victoria 3055 Australia tel: +613 9380 1077 fax: +613 9380 1477

email: mail@geotrack.com.au website: www.geotrack.com.au

Geotrack International Pty Ltd and its officers and employees assume no responsibility and make no representation as to the productivity or profitability of any mineralisation, oil, gas or other material in connection with which this report may be used.

AFTA® and Geotrack® are registered trademarks owned and maintained by Geotrack International Pty Ltd.

2. Interpretation strategy

2.1 Thermal history interpretation of AFTA data

Basic principles

Interpretation of AFTA data in this report begins by assessing whether the fission track age and track length data in each sample could have been produced if the sample has never been hotter than its present temperature at any time since deposition. To this end, we consider a "Default Thermal History" for each sample, which forms the basis of interpretation. Default Thermal Histories throughout a well are derived from the stratigraphy of the preserved sedimentary section, combined with constant values for paleogeothermal gradient and paleo-surface temperature which are adopted from present-day values. For outcrop samples, the Default Thermal Histories simply represent long-term residence at the prevailing surface temperature.

Using this history, AFTA parameters are predicted for each sample. If the measured data show a greater degree of fission track annealing (in terms of either fission track age reduction or track length reduction) than expected on the basis of this history, the sample must have been hotter at some time in the past. In this case, the AFTA data are analysed to provide estimates of the magnitude of the maximum paleotemperature in that sample, and the timing of cooling from the thermal maximum.

Because of the possible presence of tracks inherited from sediment source terrains, it is possible that track length data might show definite evidence that the sample has been hotter in the past (since deposition) while fission track ages are still greater than predicted from the Default Thermal History (which only refers to tracks formed after deposition). Similarly in samples in which all or most fission tracks were totally annealed in a paleo-thermal episode, and which have subsequently been cooled and then reburied, fission track age data might show clear evidence of exposure to higher temperatures in the past while track length data may be dominated by the present-day thermal regime and will not directly reveal the paleo-thermal effects. In circumstances such as these, evidence from either track length or fission track age data alone is sufficient to establish that a sample has been hotter in the past.

As AFTA data provide no information on the *approach* to a thermal maximum, they cannot independently constrain the heating rate and a value must therefore be assumed in order to interpret the data. The resulting paleotemperature estimates are

therefore conditional on this assumed value. AFTA data do provide some control on the history after cooling from maximum paleotemperatures, through the lengths of tracks formed during this period.

Wherever possible, data from each sample are normally interpreted in terms of two episodes of heating and cooling, using assumed heating and cooling rates during each episode. The maximum paleotemperature is assumed to be reached during the earlier episode. The timing of the onset of cooling and the peak paleotemperatures during the two episodes are varied systematically, and by comparing predicted and measured parameters the range of conditions which are co7220/6-1tible with the data can be defined. One additional episode during the cooling history is the limit of resolution from typical AFTA data. Alternatively, if the data can be explained by a single episode of heating and cooling, then a heating rate is assumed and the range of values of maximum paleotemperature and the time of cooling is defined as before.

If AFTA data show a lower degree of fission track annealing (age and/or length reduction) than expected on the basis of the Default Thermal History, this either suggests present temperatures may be overestimated or temperatures have increased very recently. In such cases, the data may allow a more realistic estimate of the present temperature, or an estimate of the time over which temperatures have increased.

AFTA data are predicted using a multi-compositional kinetic model for fission track annealing in apatite developed by Geotrack, described in more detail in Appendix C.

Specific to this report

For all samples analysed for this report, chlorine content has been determined in every apatite grain analysed (i.e., for both fission track age and track length measurement), as explained in more detail in Appendix A. For rigorous thermal history interpretation the age and length data have been grouped into 0.1 wt% Cl divisions (see Table B.3, Appendix B).

In this report, AFTA data in all samples have been interpreted using heating rates of 1°C/Myr and cooling rates of 10°C/Myr. These values are assumed arbitrarily, and all paleotemperature estimates are conditional on the assumed rates. For the kinetics characterising both AFTA and VR, increasing or decreasing heating rates by an order of magnitude is equivalent to raising or lowering the required maximum paleotemperature by about 10°C.

2.2 Thermal history interpretation of VR data

Basic principles

Interpretation of VR data follows similar principles to those used in interpreting the AFTA data (Section 2.1). If a measured VR value is higher than the value predicted from the Default Thermal History (making due allowance for analytical uncertainty), the sample must have been hotter at some time in the past. In this case, VR data provide an independent estimate of maximum paleotemperature, which can be calculated using an assumed heating rate and timing information provided from AFTA data, if available (assumed, otherwise). Cooling rates do not significantly affect VR data, which are dominated by the maximum paleotemperature provided that cooling occurs immediately after reaching the thermal maximum. If both AFTA and VR data are available from the same sample or well, then an identical heating rate must be used to obtain consistent paleotemperature estimates.

If a measured VR value is lower than expected on the basis of the Default Thermal History, either present temperatures may have been overestimated or temperatures have increased very recently. In such cases, the measured VR value may allow an estimate of the true present-day temperature. Alternatively the measured VR value may underestimate the true maturity for some other reason, e.g., suppression of reflectance in certain organic macerals, misidentification of true "in-situ" vitrinite, presence of caved material etc. Comparison of AFTA and VR data usually allows such factors to be identified, and where applicable they are discussed in the relevant section of text.

Vitrinite reflectance data (specifically $R_o$max values) are predicted using the distributed activation energy model describing the evolution of VR, with temperature and time developed by Burnham and Sweeney (1989) (see also Sweeney and Burnham, 1990).

Values of VR less than ~0.3% and greater than 4% cannot be assigned to a specific maximum paleotemperature with confidence, and such values are given maximum and minimum limits, respectively, appropriate to the particular heating rate used (see Appendix D). Further discussion of the methodology employed in interpreting VR data are given in Appendix D, which also briefly discusses the benefits of integrating AFTA and VR data.

Specific to this report

For this report, VR data in all samples have been interpreted using heating and cooling rates of 1 and 10°C/Myr (respectively), for consistency with interpretation of the AFTA data, as specified in Section 2.1.

Maximum paleotemperatures determined for the VR samples are attributed to one of the paleo-thermal episodes identified by AFTA on the basis of comparison of the VR-derived maximum paleotemperature with observed paleo-heating of a similar style in adjacent AFTA samples.

2.3 Comparison of paleotemperature estimates from AFTA and VR

Maximum paleotemperatures derived from AFTA and VR ($R_o$max) using the strategies outlined above are usually highly consistent. Estimates of maximum paleotemperature from AFTA (Table i) are often quoted in terms of a range of paleotemperatures, as the data can often be explained by a variety of scenarios. Paleotemperature estimates from VR (Table i) are usually quoted to the nearest degree Celsius, as the value which predicts the exact measured reflectance. This is not meant to imply VR data can be used to estimate paleotemperatures to this degree of precision. VR data from individual samples typically show a scatter equivalent to a range of between ±5 and ±10°C. Estimates from a series of samples are normally used to define a paleotemperature profile in samples from a well, or a regional trend in paleotemperatures from outcrop samples.

2.4 Estimates of paleogeothermal gradients and mechanisms of heating and cooling

Basic principles

A series of paleotemperature estimates from AFTA and/or VR over a range of depths can be used to reconstruct a paleotemperature profile through the preserved section. The slope of this profile defines the paleogeothermal gradient. As explained by Bray et al. (1992), and as illustrated in Figure 2.1, the shape of the paleotemperature profile and the magnitude of the paleogeothermal gradient provides unique insights into the origin and nature of the heating and cooling episodes expressed in the observed paleotemperatures.

Linear paleotemperature profiles with paleogeothermal gradients close to the present-day geothermal gradient provide strong evidence that heating was caused by greater depth of burial with no significant increase in basal heat flow, implying in turn that cooling was due to uplift and erosion. Paleogeothermal gradients significantly higher than the present-day geothermal gradient suggest that heating was due, at least in part, to increased basal heat flow, while a component of deeper burial may also be important as discussed in the next section. Paleogeothermal gradients significantly lower than the present-day geothermal gradient suggest that a simple conductive model is inappropriate, and more complex mechanisms must be sought for the observed heating. One common cause of low paleogeothermal gradients is transport of hot fluids shallow in the section. However the presence of large thicknesses of sediment with uniform lithology dominated by high thermal conductivities can produce similar paleotemperature profiles and each case has to be considered individually.

A paleotemperature profile can only be characterised by a single value of paleogeothermal gradient when the profile is linear. Departures from linearity may occur where strong contrasts in thermal conductivities occur within the section, or where hot fluid movement or intrusive bodies have produced localised heating effects. In such cases a single value of paleogeothermal gradient cannot be calculated, and different values (possibly negative) may apply through different parts of the section. However it is important to recognise that the validity of the paleotemperatures determined from AFTA and/or VR are independent of these considerations, and can still be used to control possible thermal history models.

Estimation of paleogeothermal gradients in this report

Paleogeothermal gradients for this report have been estimated from paleotemperature estimates over a range of depths using methods outlined in Appendix C. These methods provide a best estimate of the gradient ("maximum likelihood value") and upper and lower 95% confidence limits on this estimate (analogous to $\pm 2\sigma$ limits). The "goodness of fit" is displayed in the form of a log-likelihood profile, which is expected to show good quadratic behaviour for a dataset which agrees with a linear profile. This analysis depends on the assumption that the paleogeothermal gradient through the preserved section is linear. Visual inspection is usually sufficient to confirm or reject this assumption.

2.5 Determination of removed section

Basic principles

Subject to a number of important assumptions, extrapolation of a linear paleotemperature profile to a paleo-surface temperature allows estimation of the amount of eroded section represented by an unconformity, as explained in more detail in Section C.9 (Appendix C).

Specifically, this analysis assumes:

- The paleotemperature profile through the preserved section is linear
- The paleogeothermal gradient through the preserved section can be extrapolated linearly through the missing section.
- The paleo-surface temperature is known.
- The heating rate used to estimate the paleotemperatures defining the paleogeothermal gradient is correct

It is important to realise that any method of determining the amount of eroded section based on thermal methods is subject to these and/or additional assumptions. For example methods based on heat-flow modelling must assume values of thermal conductivities in the eroded section, which can never be known with confidence. Such models also require some initial assumption of the amount of eroded section to allow for the effect of compaction on thermal conductivity. Methods based on geothermal gradients, as used in this study, are unaffected by this consideration, and can therefore provide independent estimates of the amount of eroded section. But these estimates are always subject to the assumptions set out above, and should be considered with this in mind.

The analysis used to estimate paleogeothermal gradients is easily extended to provide maximum likelihood values of eroded section for an assumed paleo-surface temperature, together with ±95% confidence limits. These parameters are quoted for each well in which the paleotemperature profile suggests that heating may have been due, at least in part, to deeper burial.

Estimates of paleogeothermal gradient and eroded section derived from fitting linear profiles to paleotemperature data as a function of depth are highly correlated, since the profile is constrained to pass through the main body of the data. Thus, higher paleo-gradients within the allowed range correspond to lower amounts of section

removed, while lower paleo-gradients correspond to higher amounts of removed section. In plots of paleogeothermal gradient against removed section, paired values of each parameter which are consistent with the paleotemperature data can be defined, thus allowing the range of allowed values at various levels of statistical significance to be contoured. In general, the greater the depth interval over which paleotemperature constraints are available, the tighter the resulting constraints on both the paleogeothermal gradient and the amount of removed section.

However, it is emphasised that reconstructed burial histories produced in this way do not produce unique solutions, and alternative interpretations are always possible. For instance, where the eroded section was dominated by units with high thermal conductivities the paleogeothermal gradient through the missing section may have been much higher than in the preserved section, and extrapolation of a linear gradient will lead to overestimation of the eroded section.

Specific to this report

For the well analysed in this report, estimates of eroded section are conditional on:

- Heating rates of 1°C/Myr and cooling rates of 10°C/Myr in each episode, and
- Paleo-surface temperatures as specified in Section 3

as well as the other assumptions outlined above.

The effects of higher paleo-surface temperatures can be simply allowed for by subtracting the depth increment corresponding to the increase in temperature, for the appropriate value of paleogeothermal gradient. For instance, if the paleogeothermal gradient was 33°C/km and the paleo-surface temperature was *10°C higher* than the value assumed in this report, the estimated eroded section should be *reduced by 300 metres*. Different heating rates can be allowed for in similar fashion, with an order of magnitude change in heating rate equivalent to a 10°C change in paleotemperature (paleotemperatures increase for higher heating rates, and decrease for lower heating rates). For typical values, the assumed value of heating rate will not affect the shape or slope of the paleotemperature profile significantly.

Multiple exhumation episodes

In the previous discussion, it is important to emphasise that estimates of removed section derived in this way represent the total amount of sediment removed since the onset of cooling (i.e. exhumation) from the maximum (or peak) paleotemperatures from which the estimates were derived. In this sense, these estimates can be thought

of as representing "paleo-burial", i.e. the amount by which the preserved section (in which the paleotemperatures were recorded) was more deeply buried, prior to the onset of the exhumation episode.

In the case of a single cooling episode, in which the additional section was fully removed prior to the onset of deposition of sediment which has been preserved to the present day, such estimates of paleo-burial are identical to the amount of removed section in that episode. In such cases, it is clear that the unconformity surface, on which the additional section was deposited, returned to the surface before the re-commencement of deposition. However, where multiple exhumation episodes occur within a relatively long interval for which no sediments are preserved, this is not necessarily true. In this case, there is no evidence to demonstrate whether the unconformity surface at the top of the now preserved section returned entirely to the surface following an initial exhumational episode (i.e. if the entire amount of additional sediment was eroded), or if only part of the additional section was eroded prior to the re-commencement of deposition (after which a later exhumation episode resulted in removal of all the additional section). This situation is summarised in Figure 2.2, in the context of an outcrop sample, although similar principles apply to well samples.

In the notional example shown in Figure 2.2, two cooling episodes are identified by AFTA (grey zones) within a time interval represented by a single unconformity. The sampled unit cooled from its maximum paleotemperature in the Early Tertiary, and subsequently cooled from a lower paleotemperature peak in the Late Tertiary. Since AFTA only records the maximum or peak paleotemperatures in each event, which provide the estimates of paleo-burial for those episodes, no information on the approach to those paleotemperatures is preserved. For this reason, although the amount of section removed in the Late Tertiary episode, E_2, is well constrained, the amount of additional section deposited in that episode, D_2, is not. Conversely, while the total amount of section removed since the onset of Early Tertiary cooling (i.e. the Early Tertiary paleo-burial), D_1, is well constrained, the amount of section removed by erosion in the earlier exhumation episode (E_1) is not well constrained. Only for the case where the unit returned to the surface (red path) before burial re-commenced, are D_1 and E_1 equal, and E_1 is well constrained. But if sediments laid down in the mid-Tertiary are not preserved to the present-day, then no record of this return to the surface is available, and therefore the absolute magnitude of E_1 is not clear. Similar considerations apply to well samples, except that the present-day depth should be substituted for the surface.

2.6 Present-day temperatures

Construction of Default Thermal Histories as described in Section 2.1 requires estimation of present-day thermal gradients in each well. As described in Appendix A (Section A.3), values of present-day thermal gradient are normally derived from corrected BHT values or DST values, which are used uncorrected. But in several wells analysed for this Report, no BHT or DST values were available. In these wells we have used present-day thermal gradients derived from the compilation by Meister (1973) as illustrated in Figure 2.3. This Figure shows the 1-BRN-1-BA, 1-FPO-1-BA and 1-FVN-1-BA wells within a tongue of low values <17°C/km. In the 1-FPO-1-BA and 1-FVN-1-BA wells, corrected BHT values define thermal gradients of 20.7 and 18.7°C/km, respectively (Appendix A), but as discussed in Sections 5.2 and 6.2 of this Report, AFTA data from these wells suggest lower values around 15°C/km. This revised value is more consistent with the values suggested by Meister (1973), and therefore we have used a value of 15°C/km as a basis for extracting thermal history information from AFTA and VR data in all three Tucano Basin wells analysed in this Report.

Similarly, corrected BHT values in the 6-MGP-34-BA well define a present-day thermal gradient of 32.7°C/km (Appendix A) but as discussed in Section 10.2 of this Report, AFTA data from this well suggest a lower value around 20°C/km. As shown in Figure 2.3, present-day thermal gradients defined by Meister (1973) in the vicinity of the 6-MGP-34-BA well show considerable scatter, but a value around 20°C/km applies to a significant region around this well.

We consider it likely that this scatter in Figure 2.3 reflects some factor that produces transient variation in the present-day thermal regime, such as ground water movements. On the basis of the AFTA data in the wells discussed above, and the information they provide on present-day temperatures, we have adopted a regional thermal gradient of 20°C/km for the four wells analysed from the Recôncavo Basin. Note that in the 1-AO-1-BA, 1-RSO-1-BA and 3-BMB-3-BA wells, samples are sufficiently shallow that present-day temperatures do not affect the interpretation of data from these wells.

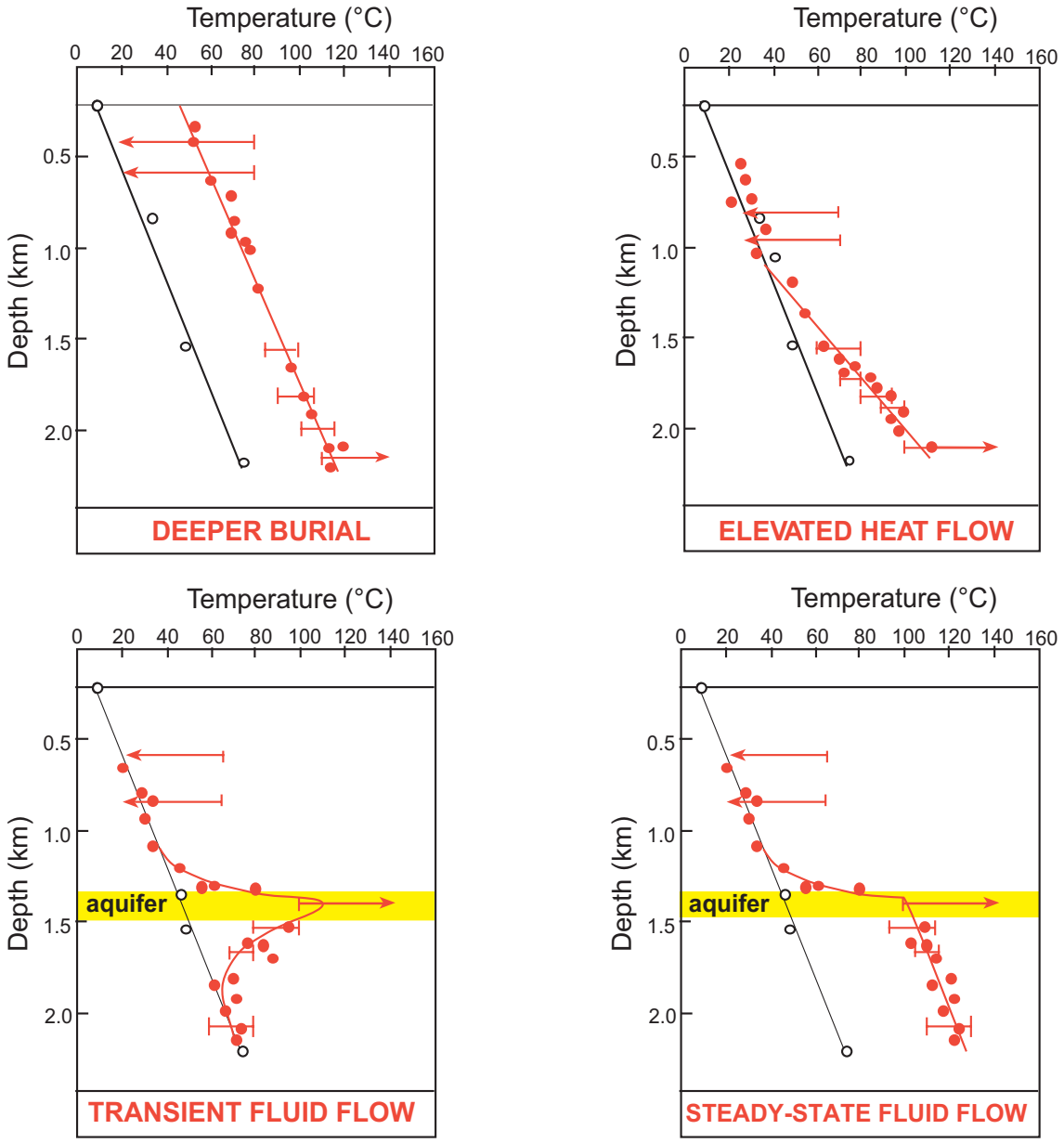

Figure 2.1: The way in which paleotemperatures characterising a particular paleo-thermal episode vary with depth, or the "paleotemperature profile", provides key information on the mechanisms of heating and cooling. Deeper burial followed by exhumation, with little or no change in basal heat flow, typically results in paleotemperatures defining a linear profile sub-parallel to the present-day thermal profile but offset to higher temperatures. Elevated heat flow results in a linear paleotemperature profile with a higher slope compared to the present-day profile. In contrast, transient hot fluid flow through a localised aquifer results in a markedly non linear profile with a maximum centred on the aquifer, while prolonged fluid flow can result in a linear profile below the aquifer as the deeper section reaches a "steady-state" situation. Combinations of these four simple cases are possible.

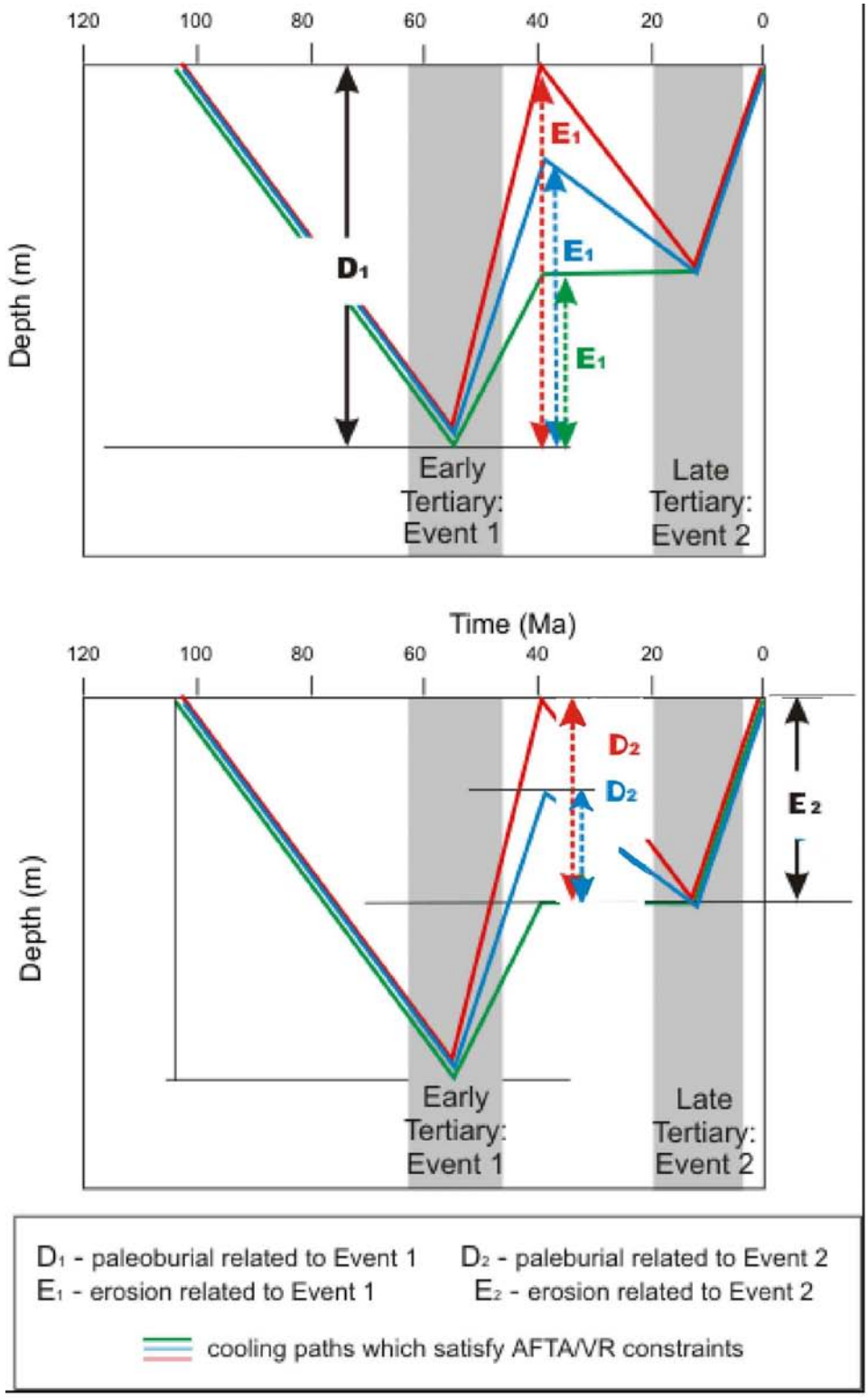

Figure 2.2: Where multiple exhumation episodes occur within an interval represented by a single unconformity, it is not possible to determine the total amount of section removed during the earlier exhumation episode, only the total amount removed between the onset of cooling in that episode and the present day. In this example, E_2 is uniquely defined by the total section removed during the later episode, while D_1 is uniquely defined by the total amount of additional burial required to explain the paleotemperatures in the earlier episode. But E_1 and D_2 are not uniquely defined.

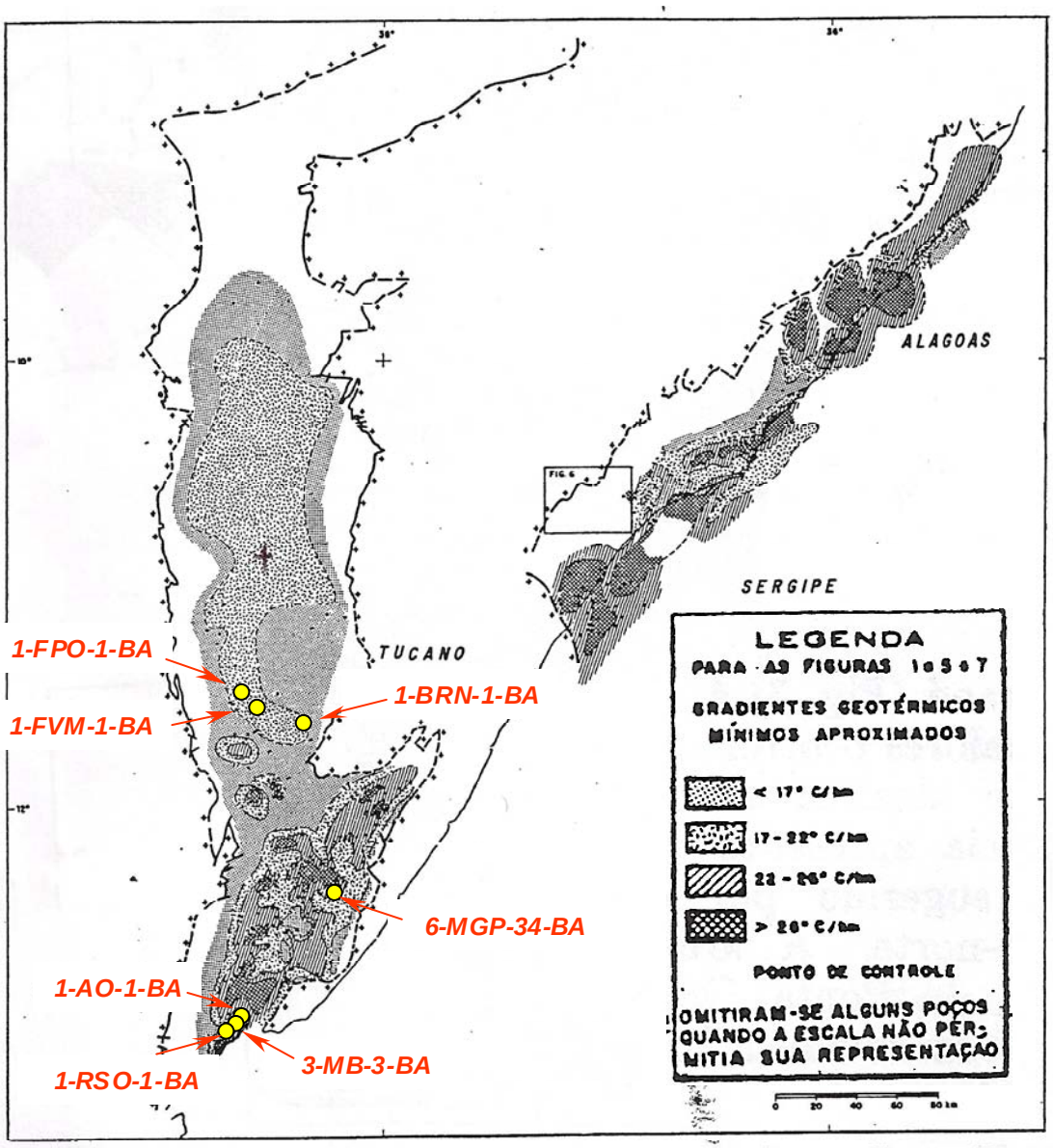

Fig. 5 — Gradientes geotérmicos nas bacias Sergipe/Alagoas, Recôncavo e Tucano. Mesma legenda da Fig. 1.

Figure 2.3: Present-day thermal gradient map from Meister (1973), showing locations of wells from which samples have been analysed for this study.

6. Thermal history interpretation of AFTA and VR data in the 1-FPO-1-BA well

6.1 Geological background

The 1-FPO-1-BA well intersected around 270 m of the post-rift Marizal Formation of Aptian age, separated by an unconformity from the underlying São Sebastião, Ilhas and Candelas Formations (Barremian-Berriasian), separated by a further unconformity from the Late Jurassic Sergi Formation, reaching TD at a depth of 4203 m (rkb) in this latter unit. The detailed stratigraphic succession is summarised in Table A.2. Major unconformities occur at the ground surface, representing the interval ~110 to 0 Ma, at a depth of 282 m, representing the interval 123 to 115 Ma, and at 4163 m, representing the interval 146 to 144 Ma.

A present-day thermal gradient of 20.7°C/km was initially calculated for this well, based on three corrected BHT values as described in Appendix A. This gradient, together with an assumed surface temperature of 20°C, has been used to calculate present-day temperatures for samples from this well, and in initial construction of Default Thermal Histories. But as explained in Section 6.2, AFTA data in deeper samples from the well suggest that present-day temperatures calculated in this way are too high, and suggest a revised present-day thermal gradient of ~15°C/km or less. Such a value is consistent with the map shown in Figure 2.3 from Meister (1973), in which this well lies within the region ascribed to gradients less than 17°C/km. Results from the nearby 1-FVM-1-BA well described in Section 7 support a value of ~15°C/km, and this value has been employed as a basis for final thermal history interpretation of the AFTA and VR data in this well, as described below.

6.2 Thermal history interpretation of AFTA data

Introduction

For this study, samples of cuttings from eight depth intervals together with two core samples were analysed by AFTA, making ten samples in all. Excellent yields of apatite were obtained from nine of the ten samples with a Fair yield in the tenth, and reliable thermal history constraints were obtained for all samples, as described below.

Fission track ages and mean track lengths in samples analysed from this well are summarised in Table 6.1 and plotted as a function of depth and present temperature

in Figure 6.1, where the fission track age data are contrasted with the variation of stratigraphic age through the section. The variation of fission track age and length vs depth predicted from the Default Thermal History (see Section 2.1) for this well using a thermal gradient of 20.7°C/km as derived from corrected BHT values are also shown in Figure 6.1a, for selected apatite chlorine contents. Mean values predicted from the corresponding Default Thermal History for each sample are also summarised in Table 6.1. These values take explicit account of the distribution of wt% Cl within each sample.

Initial visual inspection of the AFTA parameters shows that the fission track ages in the three deepest samples in Figure 6.1a, at depths around 3.5 to 4 km, are much older than the values predicted on the basis of the Default Thermal History. This is particularly pronounced in the two deepest samples, from depths of ~4 km, in which the Default Thermal History calculated using a thermal gradient of 20.7°C/km predicts near total annealing in these samples from present-day temperatures of over 100°C in this scenario, in contrast to the measured fission track ages. Thus, these deepest samples display a lower degree of annealing in the present-day thermal regime than expected using a thermal gradient of 20.7°C/km, suggesting that revision of the present-day thermal gradient is required before rigorous thermal history interpretation can begin. More detailed assessment of the AFTA data in individual samples confirms this suggestion, as discussed in the following Section.

Revision of present-day temperatures on the basis of AFTA

Certain aspects of AFTA data are sensitive to the present-day thermal regime; in particular the longest tracks in each sample and the temperatures at which the fission track ages are progressively reduced towards zero. As discussed in Table 6.2, quantitative assessment of the AFTA data in several samples from this well are incompatible with the degree of annealing predicted by the Default Thermal History calculated using a present-day thermal gradient of 20.7°C/km derived from corrected BHT values as described in Appendix A, and require downward revision of the present-day thermal gradient.

As explained in Table 6.2, samples GC990-183, -186 and -190 all contain a significant proportion of tracks which are much longer than those predicted from the respective Default Thermal Histories for these samples calculated using a present-day thermal gradient of 20.7°C/km. Modelling the length distributions in these samples for a range of scenarios and comparing with the measured data suggests that the present-day temperature of sample GC990-183 cannot be greater than 60°C, while for samples GC990-186 and -190 the corresponding upper limit is ~70°C.

Similarly, the Default Thermal Histories calculated for samples GC990-193 and -194 using a present-day thermal gradient of 20.7°C/km predict near total annealing (i.e. near-zero fission track ages) in contrast to much older measured ages. Modelling the AFTA parameters in these samples as above suggests that the present-day temperatures of both these samples cannot be greater than ~95°C.

Thus, data from the five deepest samples analysed from this well provide consistent evidence that the present-day thermal gradient of 20.7°C/km derived from corrected BHT values as described in Appendix A is too high. Note that the five shallower samples are from depths at which present-day temperatures are too low to exert a detectable influence on the measured data. The limits on present-day temperatures derived from the AFTA data in individual samples as above suggest a thermal gradient around 15°C/km or less is more appropriate. Such a value is consistent with the mapped values of thermal gradient shown in Figure 2.3 from Meister (1973), and we have therefore calculated a revised Default Thermal History scenario using a thermal gradient of 15°C/km, which has been used as a basis for extracting thermal history data from the AFTA and VR data in this study.

The pattern of AFTA parameters predicted from this scenario are compared with the measured data in Figure 6.1b, and corresponding values of fission track age and mean length are summarised for each sample in Table 6.1. Measured fission track ages in the five deepest samples are now much less than predicted from the revised Default Thermal History, showing that the sampled units have been hotter in the past. In shallower samples, fission track ages are older than the respective depositional ages, showing that the AFTA data in these samples are dominated by tracks formed prior to deposition of the host sediments. Overall, the fission track age data display the characteristic variation with depth of a rock sequence that has been hotter in the past, with a rapid decrease at shallow depths to values less than predicted from the Default Thermal History, then showing a “break-in-slope” (denoting the transition from partial to total annealing of tracks formed prior to the onset of cooling) below which the decrease with age is much slower, finally decreasing towards zero at greater depths due to annealing in the present-day thermal regime.

More detailed assessment of the AFTA data in individual samples is presented in the following Sections.

Evidence for elevated paleotemperatures from AFTA

Interpretation of the AFTA data in terms of evidence that the samples may have been hotter in the past is summarised in Table 6.2.

After downward revision of present-day temperatures as above, data in all ten samples show clear evidence that the samples must have been hotter than the revised present-day temperatures at some time since deposition. As explained in Table 6.2, for the five shallowest samples this evidence comes only from the track length data, which contains a dominant population of tracks which are shorter than expected from the (revised) Default Thermal History and cannot be explained by inheritance from sediment provenance terrains when considered in tandem with the fission track age data. The lack of significant reduction in fission track age in these samples suggests that the magnitude of paleo-thermal effects is not particularly severe. For samples GC990-183 and -186, evidence for higher temperatures in the past comes from both the track length and fission track age data, with both parameters indicating a greater degree of post-depositional annealing than can be explained by the respective Default Thermal Histories. In the three deepest samples, GC190-190, -193 and -196, only the fission track age data provide evidence that the samples have been hotter in the past, while track length data in these samples are dominated by the present-day thermal regime (although the revision of the present-day thermal gradient on the basis of track length data in these samples causes some uncertainty, since true present-day temperatures could be lower than those used in constructing revised Default Thermal Histories).

Magnitude of paleotemperatures and timing of cooling from AFTA

Following the strategy outlined in Section 2.1, estimates of the magnitude and timing of maximum paleotemperatures are summarised in Table 6.3.

AFTA data in the seven deepest samples from this well clearly require two major episodes of cooling from elevated paleotemperatures to explain all facets of the data. In samples GC990-180 and -183), the earlier episode is required to explain the length reduction of the shorter tracks within each sample while the later episode is defined by the shortening of the main mode of the track length distribution. In deeper samples (e.g. GC990-186, -190) the earlier episode is required to explain the fission track age reduction, while the later episode is defined by the shortening of the main mode of the track length distribution. And in the deepest samples (GC990-193 and -194), both episodes are defined from the fission track age data and their variation with wt% Cl (although evidence for the earlier episode in GC990-193 is only tentative, Table 6.3). In contrast, AFTA data in the three shallowest samples, GC990-169, -171 and -174, each define only a single episode, most likely because the lower magnitude of paleotemperatures at these depths do not allow reliable resolution of multiple events.

Timing constraints derived from the AFTA data in each sample are compared in Figure 6.2. If we assume that results from all samples represent the effects of synchronous cooling episodes throughout the section intersected in the well, then combining results from all ten samples shows that three dominant paleo-thermal episodes are required, involving cooling beginning in the intervals:

100 to 60 Ma	**mid-Cretaceous to Paleocene**
55 to 40 Ma	**Eocene**
20 to 3 Ma	**Miocene to Pliocene**

(Stratigraphic assignments are based on the timescale of Gradstein et al., 2004). Thermal history solutions derived from the AFTA data in each sample are summarised in Table iv.

Equivalent maturity values from AFTA

Estimates of maximum allowed paleotemperature from AFTA data in each sample have been converted to equivalent vitrinite reflectance values (using the Burnham and Sweeney, 1989, algorithm) which are summarised in Table 6.3. The quoted ranges increase from between 0.45 and 0.52% in the shallowest sample (GC990-169) to >0.73% in the deepest sample (GC990-194). Integration of AFTA data with measured VR values from the well is discussed in Section 6.4.

6.3 Thermal history interpretation of VR data

Introduction

New VR analyses were undertaken for this study on cuttings material from twenty depth intervals and one sample of core (Table D.2). These analyses were performed by Keiraville Konsultants (analyst: Alan Cook), and results are summarised in Table D.2 (Appendix D), while detailed maceral descriptions and histograms of reflectance measurements in each sample, together with a discussion of the results from this well, are also presented in Appendix D.

VR determinations were possible in most of the samples analysed, with variable quality (as expressed by the number of measurements) from sample to sample. In two samples (GC990-185.1 and -194.1), no vitrinite was present but reflectance could be measured in the inertinite maceral. Mean inertinite reflectance (IR) values

obtained in these samples by Keiraville Konsultants are also summarised in Table D.2 (Appendix D). These have been converted to equivalent VR values (VR_{eq}) using the relationship between mean VR and IR shown in Figure 6.3, with the results summarised in Table 6.4. The relationship in Figure 6.3 is based on a compilation of results from a large number of previous studies (using data only from Keiraville Konsultants).

Both VR and VR_{eq} values are plotted against depth in Figure 6.4. Also shown in Figure 6.4 is the maturity profile predicted from two versions of Default Thermal History - i.e., the thermal history predicted for samples from this well if they are currently at their maximum post-depositional temperatures, as defined in Section 2.1 of this report. Predicted profiles based on present-day thermal gradients of 20.7°C/km as derived from corrected BHT values in this well (Appendix A) and 15°C/km as suggested by the AFTA data (Section 6.2) are shown in Figure 6.4. The burial history used in calculating these Default Thermal Histories, derived from the preserved stratigraphy in the well, is shown in Figure 6.5.

Mean VR_{eq} values are systematically lower than mean VR values from similar depths in Figure 6.4. This reflects the scatter in the relationship between VR and IR in Figure 6.3, with many of the IR values from this well plotting far below the correlation used to convert IR to VR_{eq}. This is thought to be due to provinciality in the relationship between the two parameters, as illustrated by the spread in individual datapoints in this plot, with the majority of data from this study appearing to define a distinct trend in Figure 6.3, separate from our usual correlation trend. Note that use of the trend of the GC990 data to convert the IR values would result in VR_{eq} values that are more consistent with the measured VR values. But because of the existence of two distinct trends within the data, with some values plotting close to the normal correlation line, we have not attempted this procedure. Instead, we have focussed only on the measured VR values, and since the VR_{eq} values quoted in Table 6.4 are not considered to provide reliable indications of maturity levels, they have not been used in quantitative analysis.

Evidence that samples have been hotter in the past

Ignoring the VR_{eq} values derived from IR (for reasons described above), all of the measured Keiraville Konsultants VR values in Figure 6.4 plot well above both profiles predicted from the two versions of the Default Thermal History, confirming the indications from AFTA that the sampled units have been hotter in the past. Note that the trend defined by the data is sub-parallel to the profile predicted using a present-day thermal gradient of 15°C/km, supporting the suggestion from AFTA that

this value provides a more accurate description of the thermal regime in this well (Section 6.2).

Magnitude of paleotemperatures from VR

Maximum paleotemperatures derived from the Keiraville Konsultants VR values in this well, calculated using the strategy outlined in Section 2.2, are summarised in Table 6.4. Values increase with depth from around 80°C in the shallowest sample to between 130 and 150°C in the deepest samples that provided VR data. Comparison of these paleotemperatures with those derived from AFTA, and the significance of these paleotemperatures in terms of the underlying heating mechanisms, are discussed in Section 6.4.

6.4 Integration of AFTA and VR data

Paleotemperature constraints from AFTA and VR are plotted against depth (TVD rkb) in Figure 6.6. Maximum paleotemperatures derived from AFTA data representing the **mid-Cretaceous to Paleocene** episode in samples at depths between ~0.5 and ~2.5 km are highly consistent with those derived from VR data at similar depths. At greater depths, paleotemperatures in the earlier of two events revealed by AFTA correspond to the Eocene paleo-thermal event, and are generally lower than the maximum paleotemperatures defined by the VR data. But on the basis of shallower data, VR data through the deeper part of the well can also be interpreted as representing the mid-Cretaceous to Paleocene episode. The paleotemperatures characterising this episode from the two techniques thus define a consistent linear profile throughout the well. The consistency between AFTA and VR data in this well confirms that the sampled units began to cool from their maximum post-depositional paleotemperatures at some time in the interval **100 to 60 Ma (mid-Cretaceous to Paleocene)**.

As also noted in relation to the 1-BRN-1-BA well in Section 4, the timing of cooling from the paleo-thermal maximum defined by the AFTA and VR data in this well clearly post-dates deposition of the post-rift (Aptian) Marizal Formation. Thus, no paleo-thermal effects attributed to the unconformity between this unit and the underlying syn-rift section are evident in this well.

6.5 Paleotemperature profiles and mechanisms of heating and cooling

As illustrated in Figure 6.7, **mid-Cretaceous to Paleocene** paleotemperature constraints defined from AFTA and VR data define a linear depth profile, sub-parallel to the present-day temperature profile and offset to higher temperatures by around 50°C. The nature of this profile suggests that the observed paleotemperatures can be explained solely in terms of heating due to additional depth of burial, with little or no change in basal heat flow. In this case, subsequent cooling would be due solely to uplift and erosion.

Eocene paleotemperatures are only defined from AFTA in the five deeper samples, so the form of the paleotemperature profile characterising this episode cannot be defined with confidence. But the **Miocene to Pliocene** paleotemperatures are again highly consistent with a linear profile, sub-parallel to the present-day temperature profile and offset to higher temperatures by ~20°C. Thus an explanation of this episode in terms of deeper burial and subsequent exhumation appears reasonable. Given the nature of both the **mid-Cretaceous to Paleocene** and **Miocene to Pliocene** paleotemperature profiles, extension of a similar conclusion to the intervening **Eocene** episode appears reasonable.

The preferred timing for the onset of cooling in each episode derived from the AFTA data, at **100 to 60 Ma**, **55 to 40 Ma** and **20 to 3 Ma**, all coincide with the post-Aptian unconformity forming the ground surface at the location of this well, representing the approximate interval 110 to 0 Ma. Thus an interpretation involving deeper burial on this unconformity provides a viable explanation of the observed **mid-Cretaceous to Paleocene , Eocene** and **Miocene to Pliocene** paleotemperatures in this well.

Section 13 presents detailed evaluation of the range of values of paleogeothermal gradient and corresponding values of additional section required to explain the paleotemperatures in each event. Results from this well are discussed within the regional context. In Section 14 we develop thermal and burial/uplift history reconstructions for this well on the basis of the conclusions outlined above. The resulting maturation histories for units in this well are also discussed in Section 14.

Table 6.1: Summary of apatite fission track data in samples from the 1-FPO-1-BA well, Recôncavo Basin, Onshore Brazil (Geotrack Report #990)

Sample number	Average depth (m)	Present temp-erature[*1] (°C)	Stratigraphic age (Ma)	Mean track length (µm)	Predicted mean track length[*2] (µm)	Fission track age (Ma)	Predicted fission track age[*2] (Ma)
Default Thermal history calculated using a thermal gradient of 20.7°C/km from corrected BHT values							
GC990-169	551	31	130-123	11.96±0.16	14.1	332.0±23.0	118
GC990-171	900	38	130-123	12.35±0.19	13.9	348.6±23.3	117
GC990-174	1328	47	130-123	11.73±0.19	13.4	293.1±27.9	114
GC990-177	1714	55	130-123	10.64±0.20	12.7	155.2±21.2	109
GC990-180	2025	62	130-123	10.40±0.23	12.3	151.5±21.2	106
GC990-183	2510	72	130-123	11.76±0.19	11.4	88.5±13.8	99
GC990-186	2925	80	141-130	11.02±0.19	10.3	41.3±4.0	77
GC990-190	3439	91	141-130	10.81±0.27	9.7	31.0±2.7	22
GC990-193	3913	101	144-141	-	9.4	16.6±6.2	7
GC990-194	4179	106	147-141	8.49±0.80	9.2	8.3±2.1	3
Default Thermal history calculated using a thermal gradient of 15°C/km from AFTA in deepest samples							
GC990-169	551	28	130-123	11.96±0.16	14.2	332.0±23.0	119
GC990-171	900	33	130-123	12.35±0.19	14.1	348.6±23.3	119
GC990-174	1328	40	130-123	11.73±0.19	13.8	293.1±27.9	117
GC990-177	1714	46	130-123	10.64±0.20	13.4	155.2±21.2	115
GC990-180	2025	50	130-123	10.40±0.23	13.1	151.5±21.2	113
GC990-183	2510	58	130-123	11.76±0.19	12.6	88.5±13.8	110
GC990-186	2925	64	141-130	11.02±0.19	12.1	41.3±4.0	107
GC990-190	3439	71	141-130	10.81±0.27	11.3	31.0±2.7	106
GC990-193	3913	79	144-141	-	10.5	16.6±6.2	92
GC990-194	4179	83	147-141	8.49±0.80	10.6	8.3±2.1	78

[*1] See Appendix A for discussion of present temperature data.

[*2] Values predicted from the Default Thermal History (Section 2.1); i.e. assuming that each sample is now at its maximum temperature since deposition. The values refer only to tracks formed after deposition. Samples may contain tracks inherited from sediment provenance areas. Calculations refer to apatites within the measured compositional range for each sample, as discussed in Appendix A. For this reason, predicted ages may not vary smoothly with depth.

Note: all depths quoted are TVD with respect to kb elevation.

Table 6.2: Evidence for higher temperatures in the past from AFTA data in samples from the 1-FPO-1-BA well (Geotrack Report #990)

Sample details **Sample No.** Depth Present temp Strat. age	Do AFTA data require any revision of present temperature?	Evidence of higher temperatures in the past from length data?	Evidence of higher temperatures in the past from fission track age data?	Conclusion
GC990-169 501-600 m 31°C (Revised to 28°C on the basis of AFTA data.) 130-123 Ma	No	Yes [Mean track length is ~2.2 µm less than that predicted from the (revised) Default Thermal History. Modelling AFTA parameters through likely thermal history scenarios shows that the shorter tracks within this sample cannot be explained by inheritance from sediment source terrains, and must be due to higher paleotemperatures at some time after deposition.]	No [Central fission track age as well as all of the single grain ages are significantly older than the value predicted from the (revised) Default History .]	Track length data show that this sample has been hotter in the past, but heating was sufficiently moderate that no detectable age reduction has occurred.
GC990-171 849-951 m 38°C (Revised to 33°C on the basis of AFTA data.) 130-123 Ma	No	Yes [Mean track length is ~1.7 µm less than that predicted from the (revised) Default Thermal History. Modelling AFTA parameters through likely thermal history scenarios shows that the shorter tracks within this sample cannot be explained by inheritance from sediment source terrains, and must be due to higher paleotemperatures at some time after deposition.]	No [Central fission track age as well as all of the single grain ages are significantly older than the value predicted from the (revised) Default History .]	Track length data show that this sample has been hotter in the past, but heating was sufficiently moderate that no detectable age reduction has occurred.

Note: Interpretation of AFTA data is based on comparison of measured AFTA parameters with values predicted from "Default Thermal History" (Section 2.1); i.e., assuming that each sample is now at its maximum temperature since deposition. The predicted values for each sample are summarised in Table 6.1, and refer only to tracks formed after deposition. Samples may also contain tracks inherited from sediment provenance areas, which must be allowed for in interpreting the data. Calculations refer to apatites with the compositional range appropriate to each sample, as explained in Appendix A.

Table 6.2: Continued (Geotrack Report #990)

Sample details **Sample No.** Depth Present temp Strat. age	Do AFTA data require any revision of present temperature?	Evidence of higher temperatures in the past from length data?	Evidence of higher temperatures in the past from fission track age data?	Conclusion
GC990-174 1275-1380 m 47°C (Revised to 40°C on the basis of AFTA data.) 130-123 Ma	No	Yes [Mean track length is ~2 µm less than that predicted from the (revised) Default Thermal History. Modelling AFTA parameters through likely thermal history scenarios shows that the shorter tracks within this sample cannot be explained by inheritance from sediment source terrains, and must be due to higher paleotemperatures at some time after deposition.]	No [Central fission track age as well as almost all of the single grain ages are significantly older than the value predicted from the (revised) Default History .]	Track length data show that this sample has been hotter in the past, but heating was sufficiently moderate that no detectable age reduction has occurred.
GC990-177 1668-1760 m 55°C (Revised to 46°C on the basis of AFTA data.) 130-123 Ma	No	Yes [Mean track length is ~2.7 µm less than that predicted from the (revised) Default Thermal History. Modelling AFTA parameters through likely thermal history scenarios shows that the shorter tracks within this sample cannot be explained by inheritance from sediment source terrains, and must be due to higher paleotemperatures at some time after deposition.]	No [Central fission track age is close to the value predicted from the (revised) Default History, while single grain ages are close to or older than the values predicted on this basis.]	Track length data show that this sample has been hotter in the past, but heating was sufficiently moderate that no detectable age reduction has occurred.

Note: Interpretation of AFTA data is based on comparison of measured AFTA parameters with values predicted from "Default Thermal History" (Section 2.1); i.e., assuming that each sample is now at its maximum temperature since deposition. The predicted values for each sample are summarised in Table 6.1, and refer only to tracks formed after deposition. Samples may also contain tracks inherited from sediment provenance areas, which must be allowed for in interpreting the data. Calculations refer to apatites with the compositional range appropriate to each sample, as explained in Appendix A.

Table 6.2: Continued (Geotrack Report #990)

Sample details **Sample No.** Depth Present temp Strat. age	Do AFTA data require any revision of present temperature?	Evidence of higher temperatures in the past from length data?	Evidence of higher temperatures in the past from fission track age data?	Conclusion
GC990-180 1989-2061 m 62°C (Revised to 50°C on the basis of AFTA data) 130-123 Ma	No	Yes [Mean track length is ~2.6 µm less than that predicted from the (revised) Default Thermal History. Modelling AFTA parameters through likely thermal history scenarios shows that the shorter tracks within this sample cannot be explained by inheritance from sediment source terrains, and must be due to higher paleotemperatures at some time after deposition.]	No [Central fission track age is close to the value predicted from the (revised) Default History, while single grain ages are close to or older than the values predicted on this basis.]	Track length data show that this sample has been hotter in the past, but heating was sufficiently moderate that no detectable age reduction has occurred.
GC990-183 2469-2550 m 72°C (Revised to 58°C on the basis of AFTA data) 130-123 Ma	Yes [Mean track length is ~0.8 µm longer than predicted from the Default Thermal History calculated using a thermal gradient of 20.7°C/km as derived from corrected BHT values, and the measured track length distribution contains a distinct population of long tracks that cannot be explained on the basis of this history. Modelling the track length data through various thermal history scenarios suggests that the present-day temperature of this sample must be around 60°C or less.]	Yes [Mean track length is ~0.8 µm less than that predicted from the (revised) Default Thermal History. Modelling AFTA parameters through likely thermal history scenarios shows that the shorter tracks within this sample cannot be explained by inheritance from sediment source terrains, and must be due to higher paleotemperatures at some time after deposition.]	Yes [Central fission track age is close to the value predicted from the (revised) Default History, but single grain ages in the most apatite grains (<0.1 wt% Cl) define a distinct population with a central age significantly less than predicted from the (revised) Default Thermal History.]	Track length data show that this sample has been hotter in the past, and heating was sufficiently severe that detectable age reduction has occurred in the most sensitive apatite grains.

Note: Interpretation of AFTA data is based on comparison of measured AFTA parameters with values predicted from "Default Thermal History" (Section 2.1); i.e., assuming that each sample is now at its maximum temperature since deposition. The predicted values for each sample are summarised in Table 6.1, and refer only to tracks formed after deposition. Samples may also contain tracks inherited from sediment provenance areas, which must be allowed for in interpreting the data. Calculations refer to apatites with the compositional range appropriate to each sample, as explained in Appendix A.

Table 6.2: Continued (Geotrack Report #990)

Sample details **Sample No.** Depth Present temp Strat. age	Do AFTA data require any revision of present temperature?	Evidence of higher temperatures in the past from length data?	Evidence of higher temperatures in the past from fission track age data?	Conclusion
GC990-186 2898-2952 m 80°C (Revised to 64°C on the basis of AFTA data) 141-130 Ma	Yes [Mean track length is ~0.8 µm longer than predicted from the Default Thermal History calculated using a thermal gradient of 20.7°C/km as derived from corrected BHT values, and the measured track length distribution contains a distinct population of long tracks that cannot be explained on the basis of this history. Modelling the track length data through various thermal history scenarios suggests that the present-day temperature of this sample must be around 70°C or less.]	Yes [Mean track length is ~1.0 µm less than that predicted from the (revised) Default Thermal History. Modelling AFTA parameters through likely thermal history scenarios shows that the shorter tracks within this sample cannot be explained by inheritance from sediment source terrains, and must be due to higher paleotemperatures at some time after deposition.]	Yes [Central fission track age and almost all the single grain ages are significantly less than the value predicted from the (revised) Default History.]	AFTA data show that this sample has been hotter in the past.
GC990-190 3439 m 91°C (Revised to 71°C on the basis of AFTA data) 141-130 Ma	Yes [Mean track length is ~1.2 µm longer than predicted from the Default Thermal History calculated using a thermal gradient of 20.7°C/km as derived from corrected BHT values, and the measured track length distribution contains a distinct population of long tracks that cannot be explained on the basis of this history. Modelling the track length data through various thermal history scenarios suggests that the present-day temperature of this sample must be around 70°C or less.]	No [Mean track length is consistent with the value predicted from the (revised) Default Thermal History.]	Yes [Pooled fission track age is significantly less than the value predicted from the (revised) Default History.]	Fission track age data show that this sample has been hotter in the past. Track length data may be dominated by the present-day thermal regime, although this is uncertain due to the revision of present-day temperatures.

Note: Interpretation of AFTA data is based on comparison of measured AFTA parameters with values predicted from "Default Thermal History" (Section 2.1); i.e., assuming that each sample is now at its maximum temperature since deposition. The predicted values for each sample are summarised in Table 6.1, and refer only to tracks formed after deposition. Samples may also contain tracks inherited from sediment provenance areas, which must be allowed for in interpreting the data. Calculations refer to apatites with the compositional range appropriate to each sample, as explained in Appendix A.

Table 6.2: Continued (Geotrack Report #990)

Sample details **Sample No.** Depth Present temp Strat. age	Do AFTA data require any revision of present temperature?	Evidence of higher temperatures in the past from length data?	Evidence of higher temperatures in the past from fission track age data?	Conclusion
GC990-193 3913 m 101°C (Revised to 79°C on the basis of AFTA data) 144-141 Ma	Yes [The default Thermal History calculated using a thermal gradient of 20.7°C/km as derived from corrected BHT values, predicts fission track ages close to zero in the most sensitive (i.e. low Cl) apatite grains. In contrast, these apatites give finite ages, and show a less severe degree of annealing, suggesting a lower present-day temperature around 95°C or less.]	No track lengths	Yes [Central fission track age and almost all single grain ages are significantly less than the value predicted from the (revised) Default History.]	Fission track age data show that this sample has been hotter in the past.
GC990-194 4158-4200 m 106°C (Revised to 83°C on the basis of AFTA data) 147-141 Ma	Yes [The Default Thermal History calculated using a thermal gradient of 20.7°C/km as derived from corrected BHT values, predicts fission track ages close to zero in the most sensitive (i.e. low Cl) apatite grains. In contrast, these apatites give finite ages, and show a less severe degree of annealing, suggesting a lower present-day temperature around 95°C or less.]	No [Track length are consistent with the predictions of the (revised) Default Thermal History.]	Yes [Central fission track age and all single grain ages significantly less than predicted from the (revised) Default History.]	Fission track age data show that this sample has been hotter in the past. Track length data may be dominated by the present-day thermal regime, although this is uncertain due to the revision of present-day temperatures.

Note: Interpretation of AFTA data is based on comparison of measured AFTA parameters with values predicted from "Default Thermal History" (Section 2.1); i.e., assuming that each sample is now at its maximum temperature since deposition. The predicted values for each sample are summarised in Table 6.1, and refer only to tracks formed after deposition. Samples may also contain tracks inherited from sediment provenance areas, which must be allowed for in interpreting the data. Calculations refer to apatites with the compositional range appropriate to each sample, as explained in Appendix A.

Table 6.3: Estimates of timing and magnitude of elevated paleotemperatures from AFTA data in samples from the 1-FPO-1-BA well (Geotrack Report #990)

Sample Details	**Paleo-thermal constraints**			**Comments**
Sample No. Depth Present temp Strat. age	Event	Maximum paleo-temperature (°C)	Onset Of Cooling (Ma)	
GC990-169 501-600 m 31°C (Revised to 28°C on the basis of AFTA data.) 130-123 Ma	1:	75-85	105-15	AFTA data clearly can be explained in terms of a single paleo-thermal episode, as shown (left). Cooling from between 75 and 85°C beginning at some time between 105 and 15 Ma is required to explain the reduction of the main mode of the length distribution. No later episode can be resolved. Very high quality data (20 ages, 113 lengths) provide very good definition of this single dominant episode. The thermal history solution is therefore regarded as reliable within the stated uncertainty limits. **Equivalent $R_o$max: 0.45-0.52%.** Measured VR values of 0.51 and 0.48% from bracketing depths (Table D.2), equivalent to maximum paleotemperatures of 84 and 80°C (Table 6.4), respectively, are highly consistent with the interpretation of the AFTA data in this sample.
GC990-171 849-951 m 38°C (Revised to 33°C on the basis of AFTA data.) 130-123 Ma	1:	75-90	115-20	AFTA data clearly can be explained in terms of a single paleo-thermal episode, as shown (left). Cooling from between 75 and 90°C beginning at some time between 115 and 20 Ma is required to explain the reduction of the main mode of the length distribution. No later episode can be resolved. Very high quality data (20 ages, 105 lengths) provide very good definition of this single dominant episode. The thermal history solution is therefore regarded as reliable within the stated uncertainty limits. **Equivalent $R_o$max: 0.45-0.54%.** A measured VR value of 0.48% from a slightly shallower depth (Table D.2), equivalent to a maximum paleotemperature of 80°C (Table 6.4), respectively, is highly consistent with the interpretation of the AFTA data in this sample.

All thermal history constraints are based on assumed heating rates of 1°C/Myr and cooling rates of 10°C/Myr.

Events shown in italics are not required by the AFTA data, though they are allowed within the limits shown.

Table 6.3: Continued (Geotrack Report #990)

Sample Details	**Paleo-thermal constraints**			**Comments**
Sample No. Depth Present temp Strat. age	Event	Maximum paleo-temperature (°C)	Onset Of Cooling (Ma)	
GC990-174 1275-1380 m 47°C (Revised to 40°C on the basis of AFTA data.) 130-123 Ma	1:	85-95	115-35	AFTA data clearly can be explained in terms of a single paleo-thermal episode, as shown (left). Cooling from between 85 and 95°C beginning at some time between 115 and 35 Ma is required to explain the reduction of the main mode of the length distribution. No later episode can be resolved. Very high quality data (20 ages, 109 lengths) provide very good definition of this single dominant episode. The thermal history solution is therefore regarded as reliable within the stated uncertainty limits. **Equivalent $R_o$max: 0.52-0.58%.** Measured VR values of 0.49% and 0.58% from bracketing depths (Table D.2), equivalent to maximum paleotemperatures of 81 and 96°C (Table 6.4) are broadly consistent with the interpretation of the AFTA data in this sample.
GC990-177 1668-1760 m 55°C (Revised to 46°C on the basis of AFTA data.) 130-123 Ma	1: 2:	95-105 65-85	105-40 40-2	AFTA data in this sample require two paleo-thermal episodes to explain all facets of the data. Cooling from a paleotemperature between 95 and 105°C, beginning some time between 105 and 40 Ma, is required to explain the shorter tracks within the track length distribution, while subsequent cooling from between 65 and 85°C beginning between 40 and 2 Ma is required to explain the shortening of the longer tracks. This result is based on very high quality AFTA data (20 single grain ages and 142 track lengths), and the thermal history solution given here is regarded as reliable within stated limits. **Equivalent $R_o$max: 0.57-0.63%.** Measured VR values of 0.58% and 0.63% from bracketing depths (Table D.2), equivalent to maximum paleotemperatures of 96 and 104°C (Table 6.4), respectively, are highly consistent with the interpretation of the AFTA data in this sample.

All thermal history constraints are based on assumed heating rates of 1°C/Myr and cooling rates of 10°C/Myr.

Events shown in italics are not required by the AFTA data, though they are allowed within the limits shown.

Table 6.3: Continued (Geotrack Report #990)

Sample Details	**Paleo-thermal constraints**			**Comments**
Sample No. Depth Present temp Strat. age	Event	Maximum paleo-temperature (°C)	Onset Of Cooling (Ma)	
GC990-180 1989-2061 m 62°C (Revised to 50°C on the basis of AFTA data) 130-123 Ma	1: 2:	*95-110* 50-90	*>18* 40-0	AFTA data in this sample are best explained in terms of two paleo-thermal episodes, but the earlier episode could represent the effects of shorter tracks inherited from sediment source terrains. Cooling from a paleotemperature between 95 and 110°C, beginning some time prior to 18 Ma, is required to explain the shorter tracks within the track length distribution (although note the comment above), while subsequent cooling from between 50 and 90°C some time in the last 40 Myr is required to explain the shortening of the longer tracks. This result is based on high quality AFTA data (20 single grain ages and 103 track lengths), and the thermal history solution given here is regarded as reliable within stated limits. **Equivalent $R_o$max: 0.58-0.67% (if the earlier episode was post-depositional).** Measured VR values of 0.63% and 0.64% from bracketing depths (Table D.2), equivalent to maximum paleotemperatures of 104 and 106°C (Table 6.4), respectively, are highly consistent with the interpretation of the AFTA data in this sample, confirming that the earlier episode identified from AFTA was post-depositional.
GC990-183 2469-2550 m 72°C (Revised to 58°C on the basis of AFTA data) 130-123 Ma	1: 2:	100-110 80-95	100-60 55-20	AFTA data in this sample require two paleo-thermal episodes to explain all facets of the data. Cooling from a paleotemperature between 100 and 110°C, beginning some time between 100 and 60 Ma, is required to explain the slight degree of age reduction in the most sensitive apatites, as well as the very shortest tracks within the track length distribution, while subsequent cooling from between 80 and 95°C beginning between 55 and 20 Ma is required to explain the shortening of the main mode in the length distribution. This result is based on high quality AFTA data (21 single grain ages and 101 track lengths), and the thermal history solution given here is regarded as reliable within stated limits. **Equivalent $R_o$max: 0.61-0.67%.** Measured VR values of 0.65% and 0.69% from bracketing depths (Table D.2), equivalent to maximum paleotemperatures of 108 and 115°C (Table 6.4), respectively, are broadly consistent with the interpretation of the AFTA data in this sample.

All thermal history constraints are based on assumed heating rates of 1°C/Myr and cooling rates of 10°C/Myr.

Events shown in italics are not required by the AFTA data, though they are allowed within the limits shown.

Table 6.3: Continued (Geotrack Report #990)

Sample Details	**Paleo-thermal constraints**			**Comments**
Sample No. Depth Present temp Strat. age	Event	Maximum paleo-temperature (°C)	Onset Of Cooling (Ma)	
GC990-186 2898-2952 m 80°C (Revised to 64°C on the basis of AFTA data) 141-130 Ma	1: 2:	100-105 80-90	60-25 20-0	AFTA data in this sample require at least two paleo-thermal episodes to explain all facets of the data. Cooling from a paleotemperature between 100 and 105°C, beginning some time between 60 and 25 Ma, is required to explain the fission track age reduction in the most sensitive apatites, as well as the very shortest tracks within the track length distribution, while subsequent cooling from between 80 and 90°C beginning between 20 and 0 Ma is required to explain the shortening of the main mode in the length distribution. This result is based on high quality AFTA data (21 single grain ages and 115 track lengths), and the thermal history solution given here is regarded as reliable within stated limits. Integration with VR data (below) suggests a third, earlier episode also affected this sample, the effects of which cannot be resolved due to the dominance of the two episodes described above. **Equivalent R_0max: 0.61-0.63%.** Two measured VR values of 0.69% from bracketing depths (Table D.2), equivalent to maximum paleotemperatures of 115°C (Table 6.4) are higher than expected on the basis of the interpretation of the AFTA data in this sample. We interpret this as revealing an earlier event that is not resolved in the AFTA data. Synthesis of events revealed by AFTA throughout the well confirms this conclusion, as discussed in the text.
GC990-190 3439 m 91°C (Revised to 71°C on the basis of AFTA data) 141-130 Ma	1: 2:	>105 90-100	75-40 20-3	AFTA data in this sample require at least two paleo-thermal episodes to explain all facets of the data. Cooling from a paleotemperature greater than 105°C, beginning some time between 75 and 40 Ma, is required to explain the fission track age reduction, while subsequent cooling from between 90 and 100°C beginning between 20 and 3 Ma is required to explain the shortening of the main mode in the length distribution. This result is based on high quality AFTA data (20 single grain ages and 57 track lengths), and the thermal history solution given here is regarded as reliable within stated limits. **Equivalent R_0max: >0.63%.** Measured VR values of 0.71% and 0.73% from bracketing depths (Table D.2), equivalent to maximum paleotemperatures of 117 and 120°C (Table 6.4), respectively, are highly consistent with the interpretation of the AFTA data in this sample.

All thermal history constraints are based on assumed heating rates of 1°C/Myr and cooling rates of 10°C/Myr.

Events shown in italics are not required by the AFTA data, though they are allowed within the limits shown.

Table 6.3: Continued (Geotrack Report #990)

Sample Details	**Paleo-thermal constraints**			**Comments**
Sample No. Depth Present temp Strat. age	Event	Maximum paleo-temperature (°C)	Onset Of Cooling (Ma)	
GC990-193 3913 m 101°C (Revised to 79°C on the basis of AFTA data) 144-141 Ma	1: 2:	*>105* 95-105	*>25* 25-0	AFTA data in this sample require at least one and probably two paleo-thermal episodes. Cooling from a paleotemperature between 95 and 105°C, beginning some time between 25 and 0 Ma, is required to explain the fission track age reduction, while earlier cooling from a higher paleotemperature is tentatively indicated but cannot be rigorously defined. This result is based on moderate quality AFTA data (14 single grain ages and no track lengths), and the thermal history solution given here is regarded as reliable within stated limits. **Equivalent $R_o$max: >0.63% (for an earlier event).** A measured VR value of 1.10% from the same core sample (Table D.2), equivalent to a maximum paleotemperature of 148°C (Table 6.4), confirms the earlier episode tentatively identified from AFTA data in this sample.
GC990-194 4158-4200 m 106°C (Revised to 83°C on the basis of AFTA data) 147-141 Ma	1: 2:	>120 100-110	75-20 20-0	AFTA data in this sample require at least two paleo-thermal episodes to explain all facets of the data. Cooling from a paleotemperature greater than 120°C, beginning some time between 75 and 20 Ma, is required to explain the fission track age reduction in apatites containing >0.2 wt% Cl, while subsequent cooling from between 100 and 110°C beginning between 20 and 0 Ma is required to explain the fission track ages in the most sensitive apatites containing <0.2 wt% Cl. This result is based on high quality fission track age data (20 single grain ages showing a consistent increase with wt% Cl) and although only 10 track lengths were measured, the thermal history solution given here is regarded as reliable within stated limits. **Equivalent $R_o$max: >0.73%.** A measured VR value of 0.83% from a slightly shallower depth (Table D.2), equivalent to a maximum paleotemperature of 130°C (Table 6.4), is highly consistent with the interpretation of the AFTA data in this sample.

All thermal history constraints are based on assumed heating rates of 1°C/Myr and cooling rates of 10°C/Myr.

Events shown in italics are not required by the AFTA data, though they are allowed within the limits shown.

Table 6.4: Maximum paleotemperatures from VR data in the 1-FPO-1-BA well (Geotrack Report #990)

Sample number GC990-	Average depth (m)	Present temp-erature[*1] (°C)	Strati-graphic Age (Ma)	Keiraville VR[*3]2 (%)	Equivalent VR from IR[*3] (%)	Maximum paleotemp-erature[*4] (°C)
167.1	312	26	130-123	-	-	-
168.1	492	30	130-123	0.51 (1)		84
170.1	801	36	130-123	0.48 19)		80
172.1	966	40	130-123	0.62 (1)		102
173.1	1182	44	130-123	0.49 (5)		81
175.1	1395	49	130-123	0.58 (8)		96
176.1	1605	53	130-123	0.58 (4)		96
178.1	1800	57	130-123	0.63 (3)		104
179.1	1983	61	130-123	0.63 (5)		104
181.1	2199	65	130-123	0.64 (6)		106
182.1	2406	70	130-123	0.65 (3)		108
184.1	2613	74	130-123	0.69 (14)		115
185.1	2823	78	130-123	-	0.49 (8)	81[*3]
187.1	3042	83	141-130	0.69 (4)		115
188.1	3210	86	141-130	0.80 (4)		127
189.1	3429	91	144-141	0.71 (3)		117
191.1	3612	95	144-141	1.25, 0.73 (1, 1)		157, 120
192.1	3813	99	144-141	0.88 (5)		134
193	3913	101	144-141	1.10 (25)		148
193.1	3996	103	144-141	0.83 (6)		130
194.1	4185	106	147-146	-	0.63 (2)	104[*3]

[*1] Present temperatures calculated as explained in Appendix A. Values in brackets are revised on the basis of AFTA data (see Table 6.2 and Section 6.2).

[*2] From Table D.2. Numbers in brackets show the numbers of fields measured for each sample.

[*3] Equivalent VR (VR_{eq}) derived from mean inertinite reflectance using Figure 6.2, as described in the text. Numbers in brackets refer to the numbers of inertinite fields measured for each sample. Paleotemperatures derived from these values are not considered reliable – see text.

[*4] Estimates of maximum paleotemperature derived from mean VR or VR_{eq} using assumed heating and cooling rates of 1°C/Myr and 10°C/Myr, respectively.

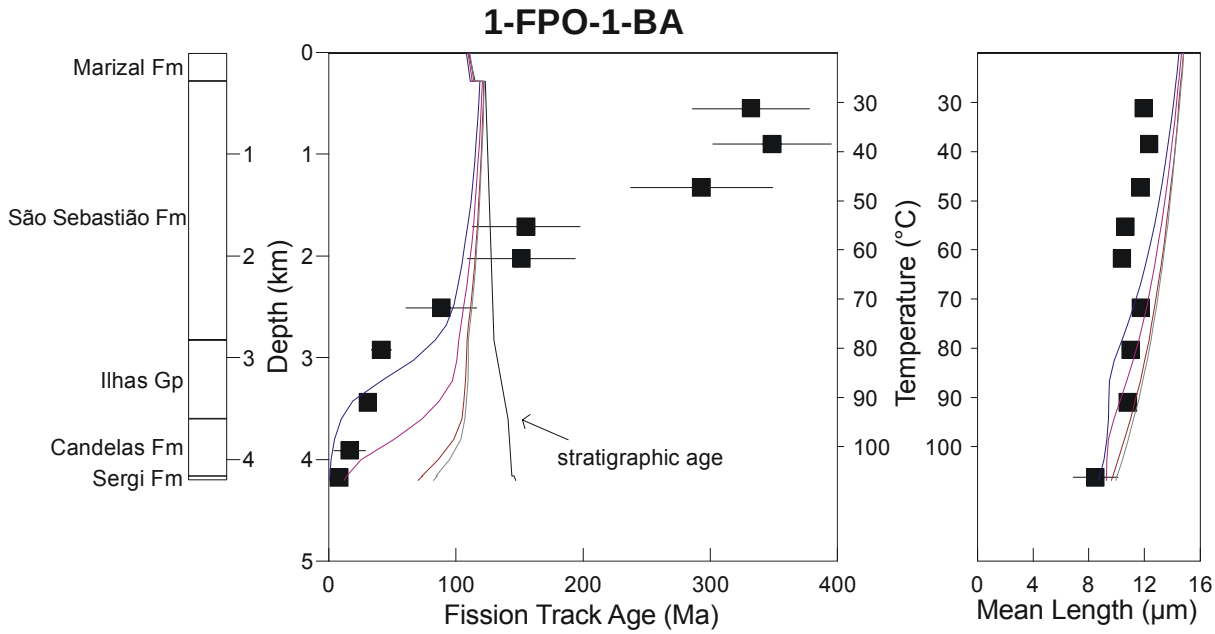

Figure 6.1a: AFTA parameters plotted against sample depth and present temperature for samples from the **1-FPO-1-BA well, Recôncavo Basin, Onshore Brazil**. The variation of stratigraphic age with depth is also shown, as the solid black line in the central panel. Present-day temperatures shown here are based on a surface temperature of 20°C and present-day thermal gradient of 20.7°C/km derived from corrected BHT values as described in Appendix A. Coloured lines show the pattern of fission track age and mean track length predicted from the Default Thermal History (see Section 2.1) for apatites containing 0.0-0.1, 0.4-0.5, 0.9-1.0 and 1.5-1.6 wt% Cl. The Default Thermal History is based on the thermal structure reported above, combined with the burial history shown in Figure 6.2.

Initial visual assessment of these data shows that measured apatite fission track ages in the three deepest samples are significantly older than predicted for the most sensitive apatite compositions, suggesting that present-day temperatures may have been overestimated. Shallower in the well, fission track ages are much older than depositional ages, showing that the samples contain a major proportion of tracks inherited from sediment source terrains. More detailed assessment of data in individual samples is therefore required before any firm conclusions can be reached.

Detailed interpretation of data in individual samples, including extraction of formal thermal history solutions for each sample, is summarised in Tables 6.2 and 6.3.

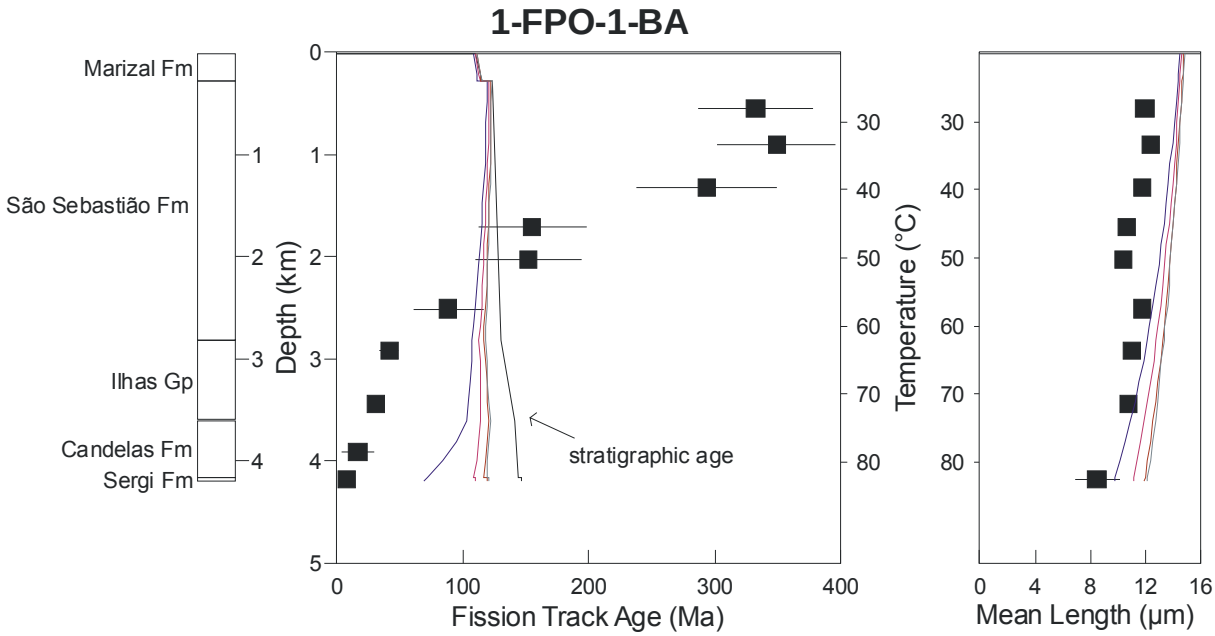

Figure 6.1b: AFTA parameters plotted against sample depth and present temperature for samples from the **1-FPO-1-BA well, Recôncavo Basin, Onshore Brazil**, as in Figure 6.1a. The variation of stratigraphic age with depth is again also shown, as the solid black line in the central panel. Present-day temperatures shown here are based on a surface temperature of 20°C and a revised present-day thermal gradient of 15°C/km based on AFTA data in deeper samples and also on Meister (l973) as discussed in Section 2.6. Coloured lines show the pattern of fission track age and mean track length predicted from the Default Thermal History (see Section 2.1) for apatites containing 0.0-0.1, 0.4-0.5, 0.9-1.0 and 1.5-1.6 wt% Cl. The Default Thermal History is based on the thermal structure reported above, combined with the burial history shown in Figure 6.2.

Visual assessment of these data now shows that measured apatite fission track ages in deeper samples are significantly less than predicted from, the revised Default Thermal History. The fission track age data define a classic pattern characteristic of a sedimentary section that has been hotter in the past, with a rapid decrease in age with increasing depth and a "break in slope" at a depth of ~3 km defining the transition from partial to total annealing of tracks formed prior to the onset of cooling. Track length data show a sympathetic pattern of variation with an increase in mean track length at a slightly shallower depth denoting the diminishing influence of shorter tracks as total annealing is approached.

Detailed interpretation of data in individual samples, including extraction of formal thermal history solutions for each sample, is summarised in Tables 6.2 and 6.3.

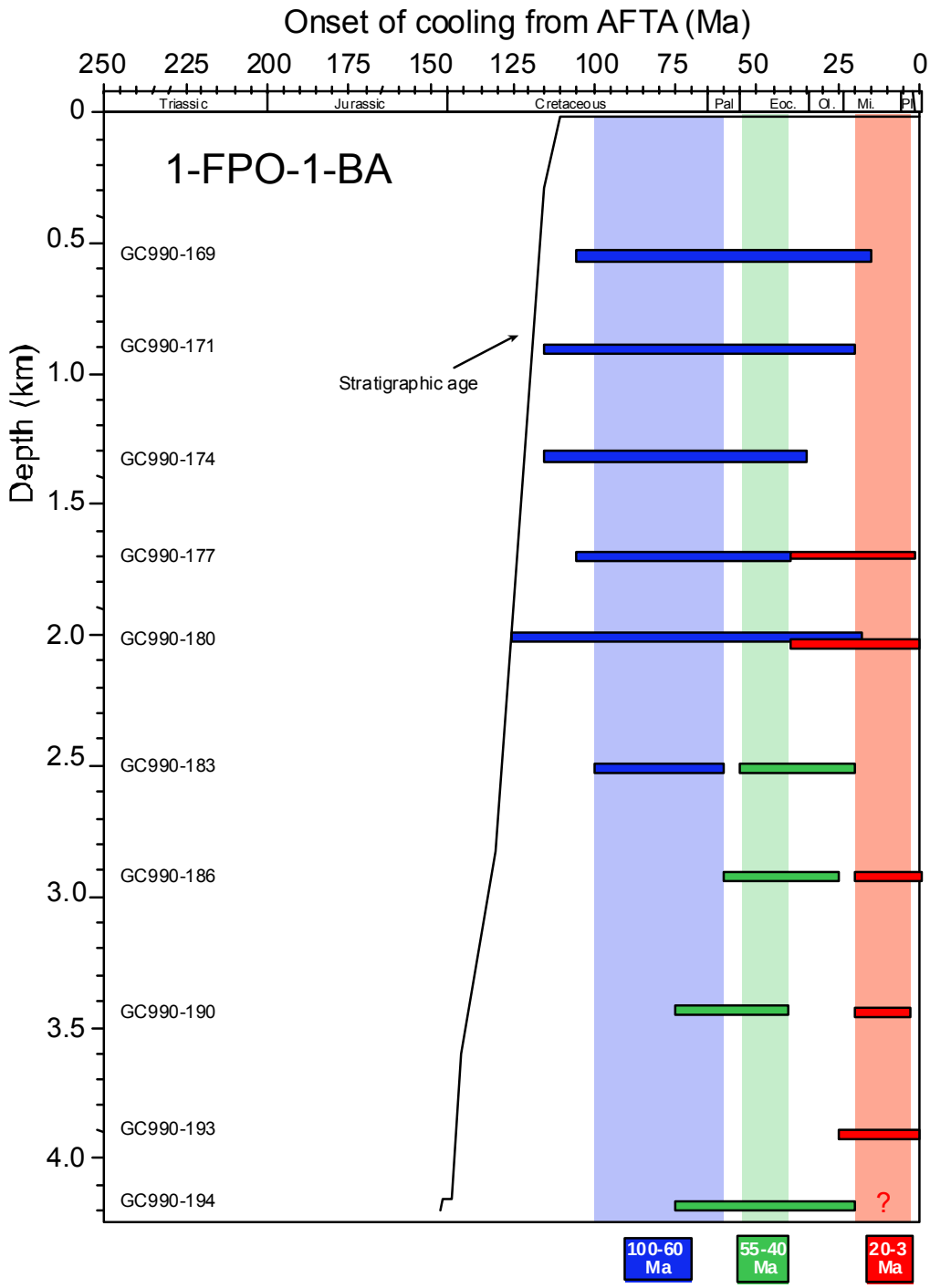

Figure 6.2: Timing constraints (from Table 6.3) on cooling episodes derived from AFTA data in samples from the **1-FPO-1-BA well, Recôncavo Basin, Onshore Brazil**. If the paleo-thermal effects identified in the AFTA data from these samples represent synchronous cooling episodes, then the results in all samples can be explained in terms of three post-depositional cooling episodes, as shown.

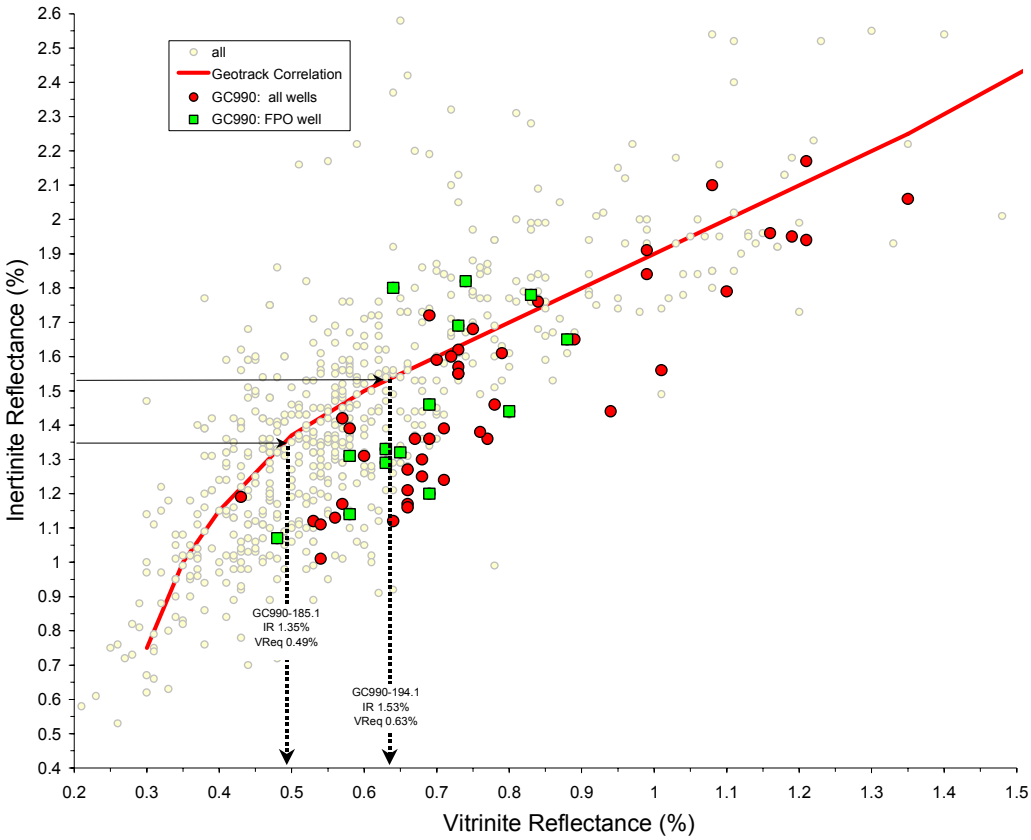

Figure 6.3: Using a compilation of mean Vitrinite Reflectance (VR) and Inertinite Reflectance (IR) values measured in samples from a wide range of settings around the world, mean IR values measured in samples from **the 1-FPO-1-BA well, Onshore Brasil**, from Table D.2 and the maceral descriptions in Appendix D, have been converted to equivalent VR values (VR_{eq}), as shown.

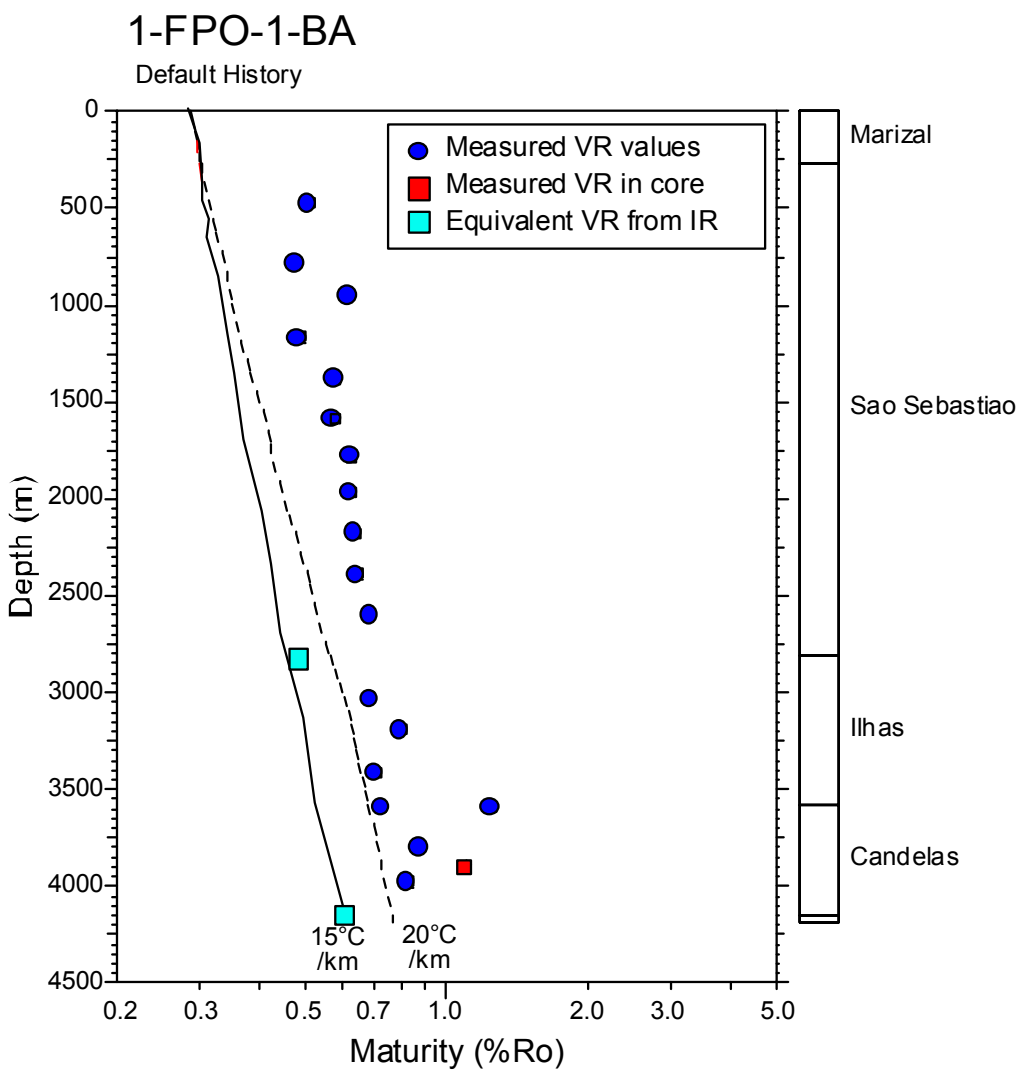

Figure 6.4: Mean vitrinite reflectance (VR) values in the **1-FPO-1-BA well**, from Table D.2, plotted against depth. The black lines shows the VR profiles predicted by two versions of the "Default History", i.e., the profile expected if samples throughout the section are currently at their maximum temperature since deposition (Section 2.1). The dashed line is based on a thermal gradient of 20.7°C/km as derived from corrected BHT values in this well (see Appendix A), while the solid line is based on a revised gradient of 15°C/km suggested by AFTA data from the deeper samples in the well. Both versions assume a surface temperature of 20°C. Measured VR values plot consistently above both predicted profiles, showing that the sampled units have been hotter than present temperatures at some time since deposition. See text for details.

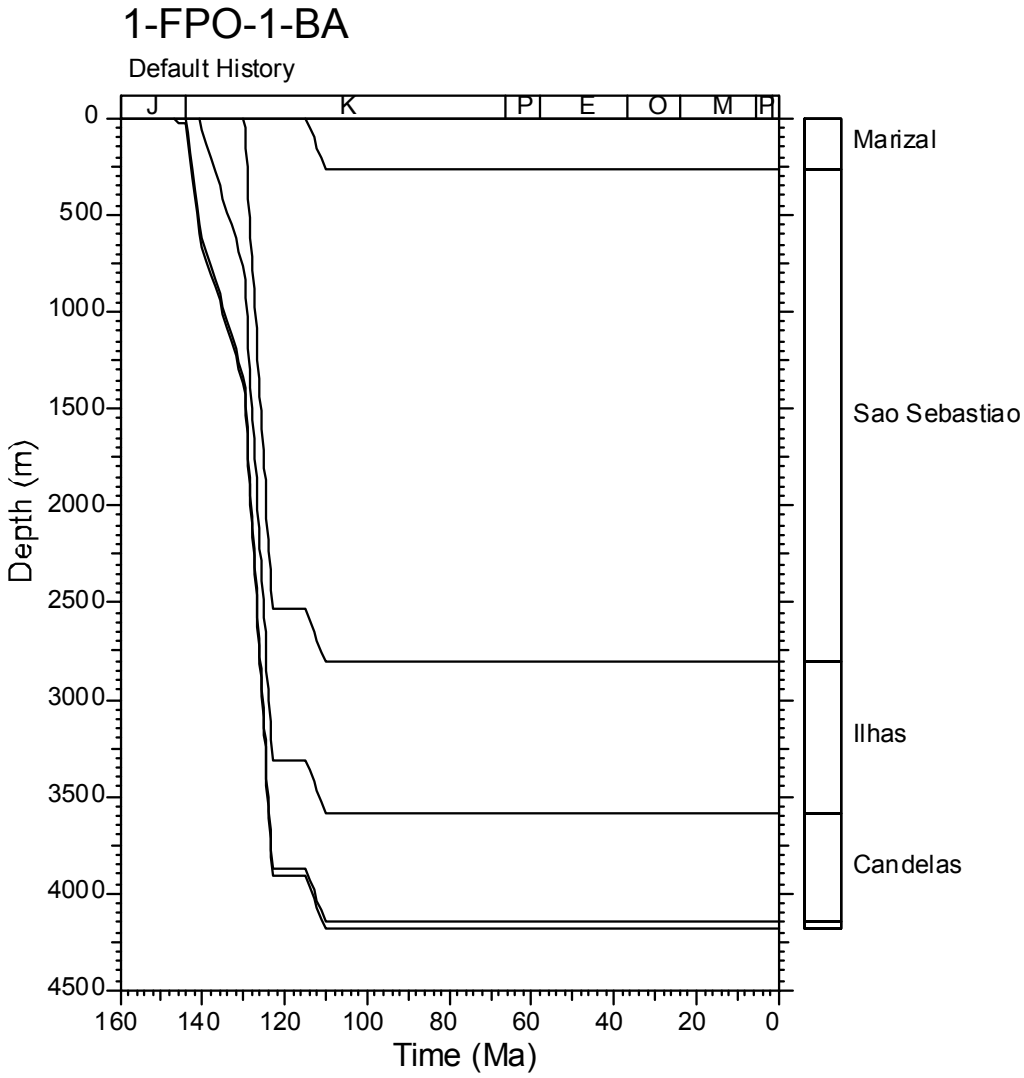

Figure 6.5: Burial history derived from the preserved section in the **1-FPO-1-BA well, Recôncavo Basin, Onshore Brazil**. This history, together with two values of present-day thermal gradient and a surface temperature of 20°C, has been used to predict the Default Thermal Histories for individual AFTA samples, as employed in the construction of Figure 6.1a and 6.1b, and for prediction of the maturity-depth profiles in Figure 6.4.

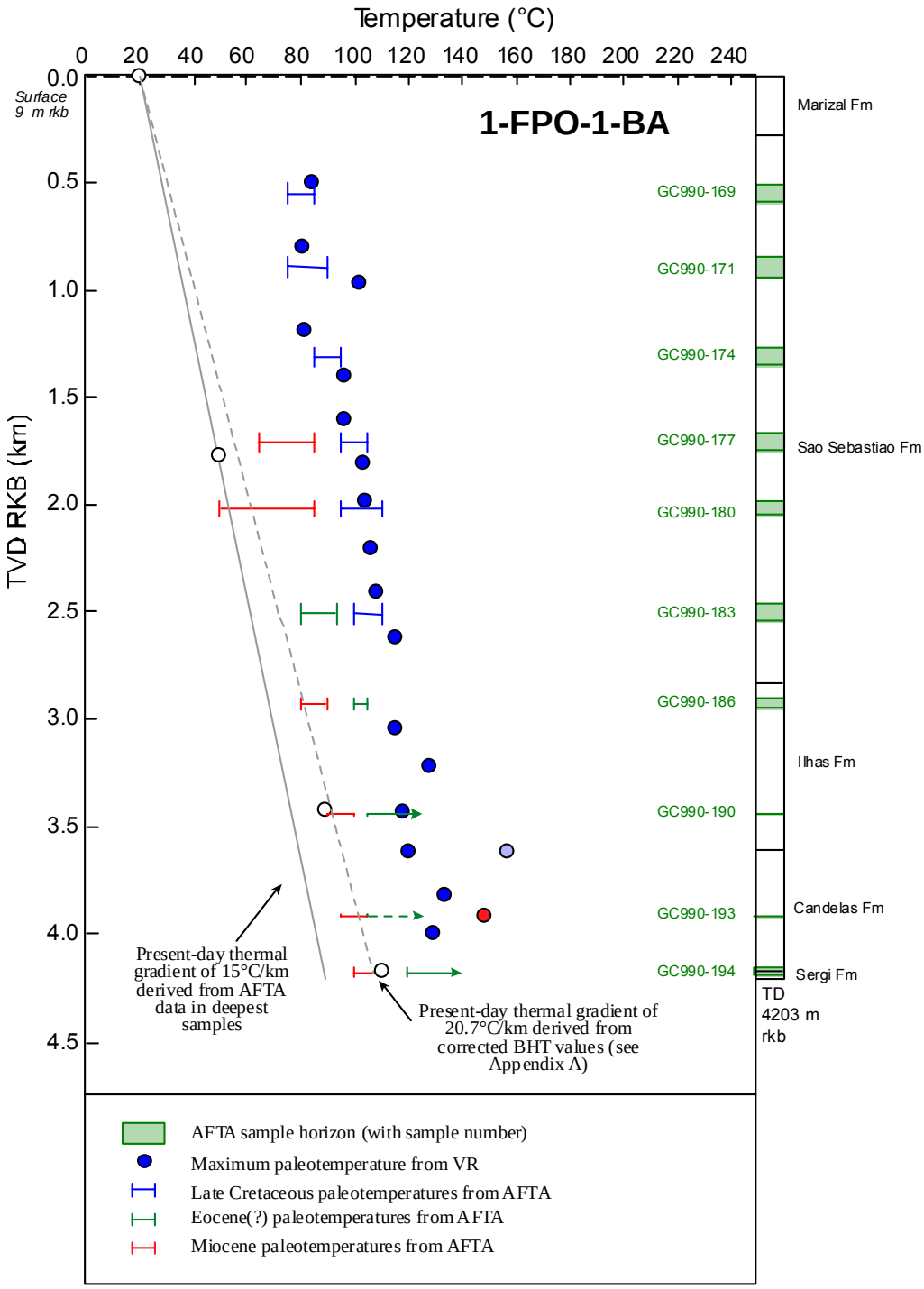

Figure 6.6: Paleotemperature constraints derived from AFTA data in the **1-FPO-1-BA well, Tucano Basin, Onshore Brazil**, plotted against depth (rkb). Present-day temperature profiles based on a thermal gradient of 20.7°C/km (derived from corrected BHT values as described in Appendix A) and a revised value of 15°C/km based on AFTA data from the deeper samples in this well (supported by data from Meister, 1973), plus a surface temperature of 20°C, are also shown. Note the high degree of consistency between maximum paleotemperatures derived from AFTA and VR in the Late Cretaceous episode (blue). See text for further details.

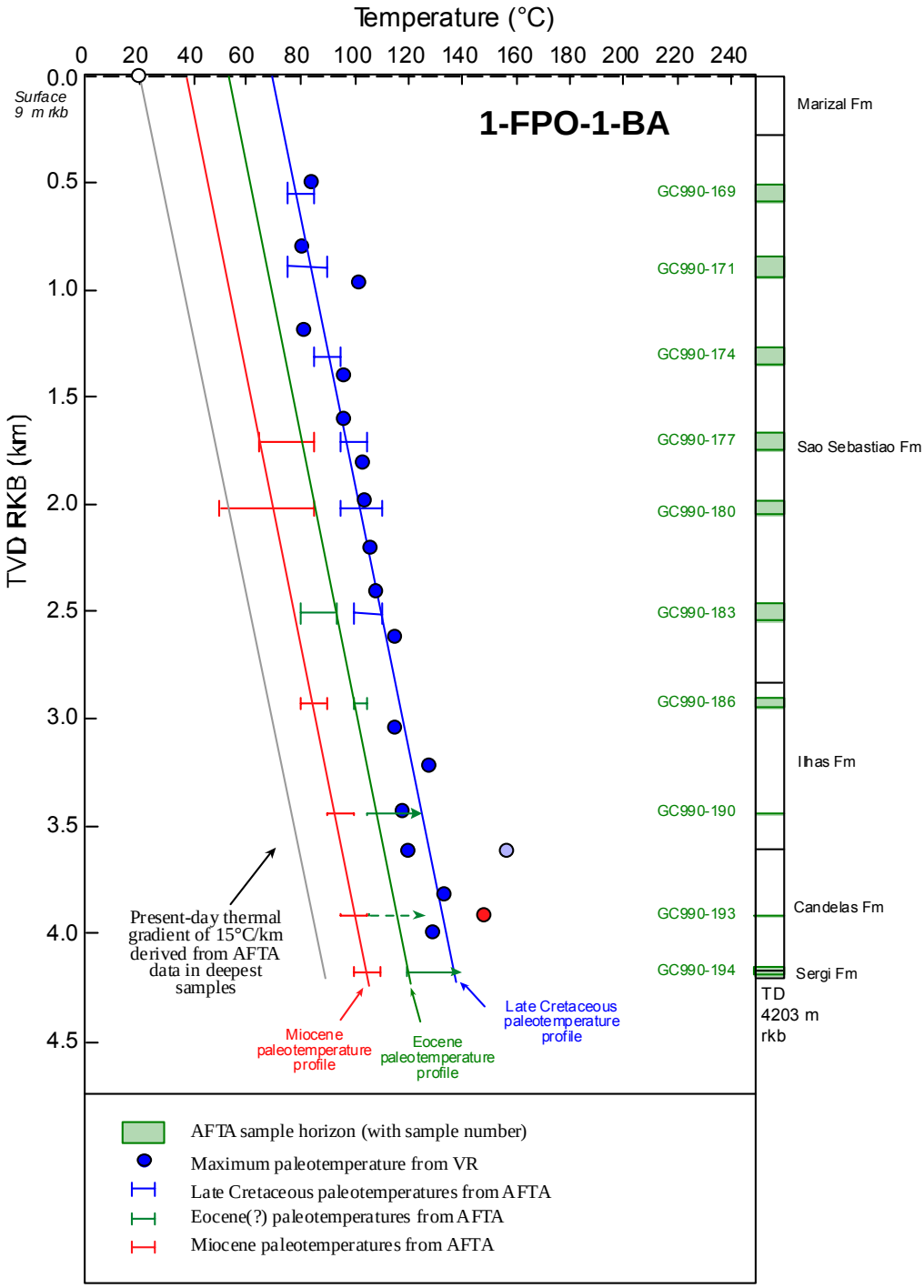

Figure 6.7: Interpreted paleotemperature profiles representing the constraints shown in Figure 6.5 for the **1-FPO-1-BA well, Tucano Basin, Onshore Brazil**. Paleotemperatures derived from AFTA and VR data in three paleo-thermal episodes define three linear sub-parallel profiles, as shown, suggesting little or no change in paleogeothermal gradient through time. See text for further details.

10. Thermal history interpretation of AFTA and VR data in the 6-MGP-34-BA well

10.1 Geological background

The 6-MGP-34-BA well intersected over 3600 m of an apparently conformable sequence of Early Cretaceous units including São Sebastião Formation (Barremian) at the ground surface, reaching TD in the latest Jurassic Sergi Formation at a depth of 3628 m (rkb). The detailed stratigraphic succession is summarised in Table A.2. A major unconformity occurs at the ground surface, representing the interval ~123 to 0 Ma.

A present-day thermal gradient of 32.0°C/km was initially calculated for this well, based on two corrected BHT values as described in Appendix A. This gradient, together with an assumed surface temperature of 20°C, has been used to calculate present-day temperatures for samples from this well, and in initial construction of Default Thermal Histories. But as explained in Section 10.2, AFTA data in deeper samples from the well suggest that present-day temperatures calculated in this way are too high, and suggest a revised present-day thermal gradient of ~20°C/km or less. Such a value is consistent with the map shown in Figure 2.3 from Meister (1973), in which this well lies within the region ascribed to gradients between 17 and 22°C/km. A gradient of 20°C/km has therefore been employed as a basis for final thermal history interpretation of the AFTA and VR data in this well, as described below.

10.2 Thermal history interpretation of AFTA data

Introduction

For this study, samples of cuttings from eight depth intervals were analysed by AFTA. Excellent yields of apatite were obtained from seven samples, with a poor yield in the remaining sample (GC990-251). Reliable thermal history constraints were obtained for all samples, as described below.

Fission track ages and mean track lengths in samples analysed from this well are summarised in Table 10.1 and plotted as a function of depth and present temperature in Figure 10.1a, where the fission track age data are contrasted with the variation of stratigraphic age through the section. The variation of fission track age and length vs depth predicted from the Default Thermal History (see Section 2.1) for this well using a thermal gradient of 32.0°C/km as derived from corrected BHT values are also

shown in Figure 10.1a, for selected apatite chlorine contents. Mean values predicted from the corresponding Default Thermal History for each sample are also summarised in Table 10.1. These values take explicit account of the distribution of wt% Cl within each sample.

Initial visual assessment of the AFTA parameters in Figure 10.1a shows that in the shallowest sample, the measured fission track age is much older than the depositional age of the host unit, and the AFTA data in this sample are clearly dominated by tracks formed prior to deposition. In contrast, the measured apatite fission track ages in samples from depths between 1 and 2 km are significantly younger than predicted from the Default Thermal History, immediately showing that the sampled units at these depths must have been hotter than present-day temperatures at some time after deposition. But in samples from depths greater than 2 km, the measured fission track ages are much older than the values predicted on the basis of the Default Thermal History. In these samples, the Default Thermal History calculated using a thermal gradient of 32.0°C/km predicts near total annealing in these samples, reflecting present-day temperatures of around 100°C or above in this scenario, in contrast to the measured fission track ages. In addition, the measured mean track lengths in these samples are much longer than the values predicted from the Default Thermal History. Thus, these deepest samples display a lower degree of annealing in the present-day thermal regime than expected using a thermal gradient of 32.0°C/km, suggesting that revision of the present-day thermal gradient is required before rigorous thermal history interpretation can begin.

More detailed assessment of the AFTA data in individual samples confirms this suggestion, but also reveals further complexities within the data, as discussed in the following Section.

Revision of present-day temperatures on the basis of AFTA, and evidence for contamination

Certain aspects of AFTA data are sensitive to the present-day thermal regime; in particular the longest tracks in each sample and the temperatures at which the fission track ages are progressively reduced towards zero. As discussed in Table 10.2, quantitative assessment of the AFTA data in several samples from this well are incompatible with the degree of annealing predicted by the Default Thermal History calculated using a present-day thermal gradient of 32.0°C/km derived from corrected BHT values as described in Appendix A, and require downward revision of the present-day thermal gradient.

As explained in Table 10.2, samples GC990-242 and -245 both contain a significant proportion of tracks which are much longer than those predicted from the respective Default Thermal Histories for these samples calculated using a present-day thermal gradient of 32.0°C/km. Modelling the length distributions in these samples for a range of scenarios and comparing with the measured data suggests that the present-day temperature of sample GC990-242 cannot be greater than 60°C, while for sample GC990-245 the corresponding upper limit is ~70°C.

Similarly, the Default Thermal Histories calculated for the three deepest samples, GC990-248, -251 and -254, using a present-day thermal gradient of 32.0°C/km predict near total or total annealing (i.e. near-zero or zero fission track ages) in contrast to the much older measured ages in these samples. Modelling the AFTA parameters in these samples as above through various scenarios provides an upper limit to the present-day temperature in each sample as summarised in Table 10.2.

Thus, data from the five deepest samples analysed from this well provide consistent evidence that the present-day thermal gradient of 32.0°C/km derived from corrected BHT values as described in Appendix A is too high. Note that the three shallower samples are from depths at which present-day temperatures are too low to exert a detectable influence on the measured data. The limits on present-day temperatures derived from the AFTA data in individual samples as above suggest a thermal gradient around 20°C/km or less is more appropriate. Such a value is consistent with the mapped values of thermal gradient shown in Figure 2.3 from Meister (1973), and we have therefore calculated a revised Default Thermal History scenario using a thermal gradient of 20°C/km, which has been used as a basis for extracting thermal history data from the AFTA and VR data in this study.

After revising the present-day thermal gradient in this way, the AFTA data in most of the deepest samples in this well reveal the presence of distinct populations of fission track ages which are older than other grains in common compositional groups, and as explained in Table 10.3 these grains are interpreted as contaminants. The influence of this contamination is demonstrated by the erratic variation in fission track age with depth in Figure 10.1a at depths greater than 2 km.

After excision of data from grains regarded as contaminants in the deepest samples, as discussed in Table 10.2, and also having revised the thermal gradient downwards to 20°C/km, as above, the pattern of AFTA parameters predicted from this scenario are compared with the edited data in Figure 10.1b, and corresponding values of fission track age and mean length are summarised for each sample in Table 10.1.

Measured fission track ages in all but the shallowest sample are now much less than predicted from the revised Default Thermal History, showing that the sampled units at depths greater than ~1 km have all been hotter in the past. Note that the variation of fission track age with depth in samples deeper than 1 km is now much smoother than in Figure 10.1a. In the shallowest sample, fission track age is still older than the depositional age, showing that the AFTA data in this sample is dominated by tracks formed prior to deposition of the host sediments.

Overall, the fission track age data in this well display the characteristic variation with depth of a rock sequence that has been hotter in the past, with a rapid decrease at shallow depths to values less than predicted from the Default Thermal History, then showing a "break-in-slope" (denoting the transition from partial to total annealing of tracks formed prior to the onset of cooling) below which the decrease with age is much slower, finally decreasing towards zero at greater depths due to annealing in the present-day thermal regime. Track length data show the characteristic sympathetic variation with first a decrease with depth and then an increase across the transition from partial to total annealing of tracks formed prior to the onset of cooling, before finally decreasing towards zero.

More detailed assessment of the AFTA data in individual samples is presented in the following Sections.

Evidence for elevated paleotemperatures from AFTA

Interpretation of the AFTA data in terms of evidence that the samples may have been hotter in the past is summarised in Table 10.2.

After downward revision of present-day temperatures and removal of contaminant grains as above, data in all eight samples show clear evidence that the samples must have been hotter than the revised present-day temperatures at some time since deposition. As explained in Table 10.2, for the shallowest sample, GC990-232, this evidence comes only from the track length data, which contains a dominant population of tracks which are shorter than expected from the (revised) Default Thermal History and cannot be explained by inheritance from sediment provenance terrains when considered in tandem with the fission track age data. The lack of significant reduction in fission track age in this sample suggests that the magnitude of paleo-thermal effects is not particularly severe.

In samples, GC990-237, -239 and -242, evidence for higher temperatures in the past comes from both the fission track age and track length data, while in the four deepest

samples, GC990-245. -248, -251 and -254, evidence comes from only the fission track age data, while track length data in these four samples are either dominated by the present-day thermal regime (although the revision of the present-day thermal gradient on the basis of track length data in these samples causes some uncertainty, since true present-day temperatures could be lower than those used in constructing revised Default Thermal Histories), or are insufficient to provide firm constraints. In the deepest sample, GC990-224, the AFTA data are dominated by the present-day thermal regime and provide no constraints on any possible paleo-thermal effects.

Magnitude of paleotemperatures and timing of cooling from AFTA

Following the strategy outlined in Section 2.1, estimates of the magnitude and timing of maximum paleotemperatures are summarised in Table 10.3.

AFTA data in the shallowest sample from this well, GC990-232, only clearly reveal a single episode of cooling from elevated paleotemperatures, which is required to explain the reduction in the length of the main mode of the track length distribution in this sample. In samples GC990-237 and -242, the AFTA data clearly require at least two episodes, with the earlier episode required to explain the fission track age reduction, while the later episode is defined by the reduction in length of tracks comprising the main mode in the track length distribution. And in the intervening sample GC990-239, the AFTA data require at least three discrete paleo-thermal episodes, with the two more recent episodes required to account for the full detail of the length distribution. In the four deepest samples, the AFTA clearly define only a single cooling episode in each case, controlled by the degree of fission track age reduction.

Timing constraints derived from the AFTA data in all eight samples are compared in Figure 10.2. If we assume that results from all samples represent the effects of synchronous cooling episodes throughout the section intersected in the well, then combining results from the eight samples shows that three dominant paleo-thermal episodes are required, involving cooling beginning in the intervals:

90 to 75 Ma	**Late Cretaceous**
48 to 38 Ma	**Eocene**
18 to 10 Ma	**Miocene**

(Stratigraphic assignments are based on the timescale of Gradstein et al., 2004).

Thermal history solutions derived from the AFTA data in each sample are summarised in Table viii.

Equivalent maturity values from AFTA

Estimates of maximum allowed paleotemperature from AFTA data in each sample have been converted to equivalent vitrinite reflectance values (using the Burnham and Sweeney, 1989, algorithm) which are summarised in Table 10.3. The quoted ranges increase from 0.42-0.48% in the shallowest sample (GC990-232) to >0.73% in the deepest sample (GC990-254). Integration of AFTA data with measured VR values from the well is discussed in Section 10.4.

10.3 Thermal history interpretation of VR data

Introduction

New VR analyses were undertaken for this study on cuttings material from seventeen depth intervals (Table D.2). These analyses were performed by Keiraville Konsultants (analyst: Alan Cook), and results are summarised in Table D.2 (Appendix D), while detailed maceral descriptions and histograms of reflectance measurements in each sample, together with a discussion of the results from this well, are also presented in Appendix D.

VR determinations were possible in most of the samples analysed, with variable quality (as expressed by the number of measurements) from sample to sample. Most samples only provided very small (typically <5) numbers of measurements, and the usual "target" of 25 fields was measured in only one sample, GC990-236.1. Nevertheless, the data define a consistent trend (see below) and the values are considered to provide reliable definition of maturity levels in this well.

In two samples (GC990-235.1 and -250.1), no vitrinite was present but reflectance could be measured in the inertinite maceral. Mean inertinite reflectance (IR) values obtained in these samples by Keiraville Konsultants are also summarised in Table D.2 (Appendix D). These have been converted to equivalent VR values (VR_{eq}) using the relationship between mean VR and IR shown in Figure 10.3, with the results summarised in Table 10.4. The relationship in Figure 10.3 is based on a compilation of results from a large number of previous studies (using data only from Keiraville Konsultants).

Both VR and VR_{eq} values are plotted against depth in Figure 10.4. Also shown in Figure 10.4 is the maturity profile predicted from two versions of Default Thermal History - i.e., the thermal history predicted for samples from this well if they are currently at their maximum post-depositional temperatures, as defined in Section 2.1 of this report. Predicted profiles based on present-day thermal gradients of 32.0°C/km as derived from corrected BHT values in this well (Appendix A) and 20°C/km as suggested by the AFTA data (Section 10.2) are shown in Figure 10.4. The burial history used in calculating these Default Thermal Histories, derived from the preserved stratigraphy in the well, is shown in Figure 10.5.

In contrast to other wells (e.g. 1-FPO-1-BA, Section 6), the deeper of the two mean VR_{eq} values (sample GC990-250.1) is consistent with the trend defined by the mean VR values in Figure 10.4, while the shallower value (sample GC990-235.1) plots well below the trend of the measured VR values. In other wells in this study, disparity between VR and VR_{eq} values is interpreted as reflecting the scatter in the relationship between VR and IR in Figure 10.3, with many of the IR values from this well plotting far below the correlation used to convert IR to VR_{eq}. This is thought to be due to provinciality in the relationship between the two parameters, as illustrated by the spread in individual datapoints in this plot, with the majority of data from this study appearing to define a distinct trend in Figure 10.3, separate from our usual correlation trend. But in this well, at least one of the two samples analysed clearly displays a relationship closer to the normal correlation. In quantitative analysis of paleotemperatures from this well, the VR_{eq} values listed in Table 10.4 for sample GC990-250.1 is considered to provide a reliable indication of the maturity level at the horizon of this sample, while the more disparate value in sample GC990-235.1 has not been used in quantitative analysis.

Evidence that samples have been hotter in the past

All of the measured Keiraville Konsultants VR values in Figure 10.4, as well as the deeper of the two VR_{eq} values derived from IR, plot well above both profiles predicted from the two versions of the Default Thermal History, confirming the indications from AFTA that the sampled units have been hotter in the past (whatever the precise value of present-day thermal gradient). Note that the trend defined by the data is sub-parallel to the profile predicted using a present-day thermal gradient of 20°C/km, suggesting that this value provides a more accurate description of the thermal regime in this well.

Magnitude of paleotemperatures from VR

Maximum paleotemperatures derived from the Keiraville Konsultants VR values in this well, calculated using the strategy outlined in Section 2.2, are summarised in Table 10.4. Values increase with depth from around 90°C in the shallowest samples to between 150 and 160°C in the deepest samples. Comparison of these paleotemperatures with those derived from AFTA, and the significance of these paleotemperatures in terms of the underlying heating mechanisms, are discussed in Section 10.4.

10.4 Integration of AFTA and VR data

Paleotemperature constraints from AFTA and VR are plotted against depth (TVD rkb) in Figure 10.6. Paleotemperature constraints from AFTA data representing the **Late Cretaceous** episode in samples GC990-237 and -239 are highly consistent with maximum paleotemperatures derived from VR data at similar depths. In contrast, the range of **Late Cretaceous** paleotemperatures defined by AFTA data in sample GC990-232 is lower than the maximum paleotemperatures indicated by VR data at bracketing depths. This is most likely to reflect the difficulty in resolving multiple episodes in AFTA data from samples which have only experienced moderate degrees of heating, as also discussed in the context of data from the 3-MB-3-BA well in Section 9. Thus the single paleo-thermal defined from AFTA data in sample GC990-232 most likely represents the unresolved effects of the three episodes that have affected the section in this well.

In samples deeper than 1.6 km, the older of two events revealed in the AFTA data is the **Eocene** episode, and samples GC990-242 and -245 only cooled to temperatures below ~110°C, at which tracks can be retained, in this event. But based on results from shallower samples, and also by analogy with results from other wells in this study, it is clear that in all samples from this well cooling from the paleo-thermal maximum took place during the **Late Cretaceous** episode. Therefore, VR data throughout the well can be interpreted as representing a **Late Cretaceous** paleo-thermal maximum, and paleotemperatures characterising this episode from the two techniques define a consistent linear profile throughout the well.

In contrast to the 1-BRN-1-BA and 1-FPO-1-BA wells discussed in Sections 4 and 6, respectively, no post-rift section is preserved in the 6-MGP-34-BA well. But as in those wells, the onset of cooling from the paleo-thermal maximum defined by the

AFTA and VR data in this well clearly post-dates deposition of the post-rift (Aptian) Marizal Formation, and no paleo-thermal effects attributed to the unconformity between this unit and the underlying syn-rift section are evident in this well.

10.5 Paleotemperature profiles and mechanisms of heating and cooling

As illustrated in Figure 10.7, **Late Cretaceous** paleotemperature constraints defined from AFTA and VR data in this well define a linear depth profile, sub-parallel to the present-day temperature profile and offset to higher temperatures by around 50°C. The nature of this profile suggests that the observed paleotemperatures can be explained solely in terms of heating due to additional depth of burial, with little or no change in basal heat flow. In this case, subsequent cooling would be due solely to uplift and erosion.

Eocene paleotemperatures defined from AFTA data are also consistent with a linear paleotemperature profile, although this episode is only expressed in three samples so the form of the profile is only loosely constrained. **Miocene** paleotemperatures are expressed in six of the seven deepest samples, and are these again highly consistent with a linear profile in Figure 10.7, sub-parallel to the present-day temperature profile and offset to higher temperatures by ~30°C. Thus an explanation of this episode in terms of deeper burial and subsequent exhumation appears reasonable. Given the nature of both the **Late Cretaceous** and **Miocene** paleotemperature profiles, extension of a similar conclusion to the intervening **Eocene** episode appears reasonable.

The preferred timing for the onset of cooling in each episode derived from the AFTA data, at **90 to 75 Ma**, **48 to 38 Ma** and **18 to 10 Ma**, all coincide with the post-Aptian unconformity forming the ground surface at the location of this well, representing the approximate interval 123 to 0 Ma. Thus an interpretation involving deeper burial on this unconformity provides a viable explanation of the observed **Late Cretaceous, Eocene** and **Miocene** paleotemperatures in this well.

Section 13 presents detailed evaluation of the range of values of paleogeothermal gradient and corresponding values of additional section required to explain the paleotemperatures in each event. Results from this well are discussed within the regional context. In Section 14 we develop thermal and burial/uplift history reconstructions for this well on the basis of the conclusions outlined above. The resulting maturation histories for units in this well are also discussed in Section 14.

Table 10.1: Summary of apatite fission track data in samples from the 6-MGP-3-BA well, Recôncavo Basin, Onshore Brazil (Geotrack Report #990)

Sample number	Average depth (m)	Present temp-erature[*1] (°C)	Stratigraphic age (Ma)	Mean track length (µm)	Predicted mean track length[*2] (µm)	Fission track age (Ma)	Predicted fission track age[*2] (Ma)
Default Thermal history calculated using a thermal gradient of 32°C/km from corrected BHT values							
GC990-232	504	36	130-123	12.46±0.14	13.9	229.9±24.1	120
GC990-237	1349	63	137-135	11.50±0.19	12.1	67.9±7.3	111
GC990-239	1536	69	137-135	11.22±0.31	11.5	46.0±5.3	106
GC990-242	1950	82	141-137	11.28±0.26	10.0	51.8±9.4	72
GC990-245	2370	96	141-137	12.16±0.19	9.9	69.3±7.9	21
GC990-248	2766	108	141-137	12.00±0.35	9.2	30.2±8.1	2
GC990-251	3012	116	141-137	-	7.4	47.0±25.2	0
GC990-254	3600	135	147-145	9.89±0.54	8.3	11.8±7.0	0
Default Thermal history calculated using a thermal gradient of 20°C/km from AFTA in deepest samples, also with summary AFTA parameters corrected for contamination in deeper samples							
GC990-232	504	30	130-123	12.46±0.14	14.1	229.9±24.1	123
GC990-237	1349	47	137-135	11.50±0.19	13.3	67.9±7.3	122
GC990-239	1536	51	137-135	11.22±0.31	13.0	46.0±5.3	120
GC990-242	1950	59	141-137	11.26±0.26	12.5	36.7±3.5	116
GC990-245	2370	67	141-137	12.35±0.19	12.1	42.3±11.7	111
GC990-248	2766	75	141-137	11.06±0.35	11.3	14.2±2.7	101
GC990-251	3012	80	141-137	-	10.1	14.7±6.6	82
GC990-254	3600	92	147-145	9.89±0.54	10.9	6.2±2.0	39

[*1] See Appendix A for discussion of present temperature data.

[*2] Values predicted from the Default Thermal History (Section 2.1); i.e. assuming that each sample is now at its maximum temperature since deposition. The values refer only to tracks formed after deposition. Samples may contain tracks inherited from sediment provenance areas. Calculations refer to apatites within the measured compositional range for each sample, as discussed in Appendix A. For this reason, predicted ages may not vary smoothly with depth.

Note: all depths quoted are TVD with respect to kb elevation.

Table 10.2: Evidence for higher temperatures in the past from AFTA data in samples from the 6-MGP-3-BA well (Geotrack Report #990)

Sample details **Sample No.** Depth Present temp Strat. age	Do AFTA data require any revision of present temperature?	Evidence of higher temperatures in the past from length data?	Evidence of higher temperatures in the past from fission track age data?	Conclusion
GC990-232 450-558 m 36°C (revised to 30°C on the basis of AFTA data – see text) 130-123 Ma	No [Present-day temperature is too low for AFTA data to provide any constraint.]	Yes [The mean track length is ~1.6 µm less than predicted from the (revised) Default Thermal History. Modelling the data through various scenarios shows that the discrepancy cannot be explained by inheritance of shorter tracks from sediment provenance terrains, and must be due to higher temperatures at some time after deposition.]	No [The Central fission track age is significantly older than the Default Thermal History, while single grain ages are consistent with or older than predicted on this basis.]	Track length data show that this sample has been hotter in the past, but paleo-thermal effects were not sufficiently severe to produce significant age reduction.
GC990-237 1320-1377 m 63°C (revised to 47°C on the basis of AFTA data – see text) 137-135 Ma	No [Track length data are consistent with the Default Thermal History calculated using a thermal gradient of 32°C/km. But based on results from deeper samples, this is interpreted as reflecting an erroneously high present-day temperature.]	Yes [Mean track length is ~1.8 µm less than that predicted from the (revised) Default Thermal History. Modelling AFTA parameters through likely thermal history scenarios shows that the shorter tracks within this sample cannot be explained by inheritance from sediment source terrains, and must be due to higher paleotemperatures at some time after deposition.]	Yes [Central fission track age and almost all the single grain ages are significantly less than the value predicted from the (revised) Default History.]	AFTA data show that this sample has been hotter in the past.

Note: Interpretation of AFTA data is based on comparison of measured AFTA parameters with values predicted from "Default Thermal History" (Section 2.1); i.e., assuming that each sample is now at its maximum temperature since deposition. The predicted values for each sample are summarised in Table 10.1, and refer only to tracks formed after deposition. Samples may also contain tracks inherited from sediment provenance areas, which must be allowed for in interpreting the data. Calculations refer to apatites with the compositional range appropriate to each sample, as explained in Appendix A.

Table 10.2: Continued (Geotrack Report #990)

Sample details **Sample No.** Depth Present temp Strat. age	Do AFTA data require any revision of present temperature?	Evidence of higher temperatures in the past from length data?	Evidence of higher temperatures in the past from fission track age data?	Conclusion
GC990-239 1500-1572 m 69°C (revised to 51°C on the basis of AFTA data – see text) 137-135 Ma	No [Track length data are consistent with the Default Thermal History calculated using a thermal gradient of 32°C/km. But based on results from deeper samples, this is interpreted as reflecting an erroneously high present-day temperature.]	Yes [Mean track length is ~1.8 µm less than that predicted from the (revised) Default Thermal History. Modelling AFTA parameters through likely thermal history scenarios shows that the shorter tracks within this sample cannot be explained by inheritance from sediment source terrains, and must be due to higher paleotemperatures at some time after deposition.]	Yes [Central fission track age and almost all the single grain ages are significantly less than the value predicted from the (revised) Default History.]	AFTA data show that this sample has been hotter in the past.
GC990-242 1899-2001 m 82°C (revised to 59°C on the basis of AFTA data – see text) 141-137 Ma	Yes [The mean track length measured in this sample is ~1.3 µm longer than the value predicted from the Default Thermal History calculated using a thermal gradient of 32°C/km, as derived from corrected BHT values. Thus, the AFTA data in this sample display a less severe degree of annealing than expected at a temperature of 82°C. Modelling AFTA parameters through various scenarios through suggests a lower present-day temperature around 60°C or less.]	Yes [Mean track length is ~1.1 µm less than that predicted from the (revised) Default Thermal History. Modelling AFTA parameters through likely thermal history scenarios shows that the shorter tracks within this sample cannot be explained by inheritance from sediment source terrains, and must be due to higher paleotemperatures at some time after deposition.]	Yes [Central fission track age and almost all the single grain ages are significantly less than the value predicted from the (revised) Default History.]	AFTA data show that this sample has been hotter in the past.

Note: Interpretation of AFTA data is based on comparison of measured AFTA parameters with values predicted from "Default Thermal History" (Section 2.1); i.e., assuming that each sample is now at its maximum temperature since deposition. The predicted values for each sample are summarised in Table 10.1, and refer only to tracks formed after deposition. Samples may also contain tracks inherited from sediment provenance areas, which must be allowed for in interpreting the data. Calculations refer to apatites with the compositional range appropriate to each sample, as explained in Appendix A.

Table 10.2: Continued (Geotrack Report #990)

Sample details **Sample No.** Depth Present temp Strat. age	Do AFTA data require any revision of present temperature?	Evidence of higher temperatures in the past from length data?	Evidence of higher temperatures in the past from fission track age data?	Conclusion
GC990-245 2340-2400 m 96°C (revised to 67°C on the basis of AFTA data – see text) 141-137 Ma	Yes [The mean track length measured in this sample is ~2.3 µm longer than the value predicted from the Default Thermal History calculated using a thermal gradient of 32°C/km, as derived from corrected BHT values, and apatites containing between 0.0 and 0.4 wt% Cl contain a component of long tracks which cannot be explained by this Default History. In addition, apatites containing <0.6 wt% Cl show a much lower degree of age reduction than predicted by this Default History. In summary, the AFTA data in this sample display a less severe degree of annealing than expected at a temperature of 96°C. Modelling AFTA parameters through various scenarios through suggests a lower present-day temperature around 70°C or less.]	No [Mean track length is consistent with the value predicted from the (revised) Default Thermal History.]	Yes [Central fission track age and most of the single grain ages are significantly less than the value predicted from the (revised) Default History.]	Fission track age data show that this sample has been hotter in the past. Track length data may be dominated by the present-day thermal regime, although this is uncertain due to the revision of present-day temperatures.

Note: Interpretation of AFTA data is based on comparison of measured AFTA parameters with values predicted from "Default Thermal History" (Section 2.1); i.e., assuming that each sample is now at its maximum temperature since deposition. The predicted values for each sample are summarised in Table 10.1, and refer only to tracks formed after deposition. Samples may also contain tracks inherited from sediment provenance areas, which must be allowed for in interpreting the data. Calculations refer to apatites with the compositional range appropriate to each sample, as explained in Appendix A.

Table 10.2: Continued (Geotrack Report #990)

Sample details **Sample No.** Depth Present temp Strat. age	Do AFTA data require any revision of present temperature?	Evidence of higher temperatures in the past from length data?	Evidence of higher temperatures in the past from fission track age data?	Conclusion
GC990-248 2730-2802 m 108°C (revised to 75°C on the basis of AFTA data – see text) 141-137 Ma	Yes [The Default Thermal History calculated using a thermal gradient of 32°C/km as derived from corrected BHT values, predicts total annealing in apatites containing up to 0.3 wt% Cl, whereas tracks are present in the corresponding compositional groups. In addition, apatites containing between 0.3 and 0.4 wt% Cl contain a component of long tracks which cannot be explained by this Default History, In summary, the AFTA data in this sample display a less severe degree of annealing than expected at a temperature of 108°C, and modelling AFTA parameters through various scenarios through suggests a lower present-day temperature around 70°C or less.]	No [Track length data are consistent with the predictions from the (revised) Default Thermal History.]	Yes [Central fission track age and most of the single grain ages are significantly less than the value predicted from the (revised) Default History.]	Fission track age data show that this sample has been hotter in the past. Track length data may be dominated by the present-day thermal regime, although this is uncertain due to the revision of present-day temperatures.

Note: Interpretation of AFTA data is based on comparison of measured AFTA parameters with values predicted from "Default Thermal History" (Section 2.1); i.e., assuming that each sample is now at its maximum temperature since deposition. The predicted values for each sample are summarised in Table 10.1, and refer only to tracks formed after deposition. Samples may also contain tracks inherited from sediment provenance areas, which must be allowed for in interpreting the data. Calculations refer to apatites with the compositional range appropriate to each sample, as explained in Appendix A.

Table 10.2: Continued (Geotrack Report #990)

Sample details **Sample No.** Depth Present temp Strat. age	Do AFTA data require any revision of present temperature?	Evidence of higher temperatures in the past from length data?	Evidence of higher temperatures in the past from fission track age data?	Conclusion
GC990-251 2973-3051 m 116°C (revised to 80°C on the basis of AFTA data – see text) 141-137 Ma	Yes [The Default Thermal History calculated using a thermal gradient of 32°C/km as derived from corrected BHT values, predicts total annealing in apatites containing up to 0.2 wt% Cl, whereas tracks are present in the corresponding compositional groups. So the AFTA data display a less severe degree of annealing than expected at a temperature of 116°C, and modelling AFTA parameters through various scenarios through suggests a lower present-day temperature around 95°C or less.]	No data [No track lengths were measured in this sample.]	Yes [Central fission track age and most of the single grain ages are significantly less than the value predicted from the (revised) Default History.]	Fission track age data show that this sample has been hotter in the past.
GC990-254 3573-3627 m 135°C (revised to 92°C on the basis of AFTA data – see text) 141-137 Ma	Yes [The Default Thermal History calculated using a thermal gradient of 32°C/km as derived from corrected BHT values, predicts total annealing in apatites containing up to 1 wt% Cl, whereas tracks are present in all compositional groups. So the AFTA data display a less severe degree of annealing than expected at a temperature of 135°C, and modelling AFTA parameters through various scenarios through suggests a lower present-day temperature around 110°C or less.]	No [Track length data are consistent with the predictions from the (revised) Default Thermal History.]	Yes [Central fission track age and most of the single grain ages are significantly less than the value predicted from the (revised) Default History.]	Fission track age data show that this sample has been hotter in the past. Track length data may be dominated by the present-day thermal regime, although this is uncertain due to the revision of present-day temperatures.

Note: Interpretation of AFTA data is based on comparison of measured AFTA parameters with values predicted from "Default Thermal History" (Section 2.1); i.e., assuming that each sample is now at its maximum temperature since deposition. The predicted values for each sample are summarised in Table 10.1, and refer only to tracks formed after deposition. Samples may also contain tracks inherited from sediment provenance areas, which must be allowed for in interpreting the data. Calculations refer to apatites with the compositional range appropriate to each sample, as explained in Appendix A.

Table 10.3: Estimates of timing and magnitude of elevated paleotemperatures from AFTA data in samples from the 6-MGP-3-BA well (Geotrack Report #990)

Sample Details	**Paleo-thermal constraints**			**Comments**
Sample No. Depth Present temp Strat. age	Event	Maximum paleo-temperature (°C)	Onset Of Cooling (Ma)	
GC990-232 450-558 m 36°C (revised to 30°C on the basis of AFTA data – see text) 130-123 Ma	1:	70-80	90-20	AFTA data can be explained in terms of a single paleo-thermal episode, as shown (left). Cooling from between 70 and 80°C beginning at some time between 90 and 20 Ma is required to explain the reduction of the main mode of the length distribution. No later episode can be resolved. Very high quality data (20 ages, 103 lengths) provide very good definition of this single dominant episode. The thermal history solution is therefore regarded as reliable within the stated uncertainty limits. **Equivalent $R_o$max: 0.42-0.48%.** Measured VR values of 0.60 and 0.53% from bracketing depths (Table D.2), equivalent to maximum paleotemperatures of 99 and 88°C (Table 10.4), respectively, are slightly higher than the range indicated by the interpretation of the AFTA data in this sample.
GC990-237 1320-1377 m 63°C (revised to 47°C on the basis of AFTA data – see text) 137-135 Ma	1: 2:	>105 80-90	110-75 20-0	AFTA data in this sample require at least two paleo-thermal episodes to explain all facets of the data. Cooling from a paleotemperature greater than 105°C, beginning some time between 110 and 75 Ma, is required to explain the fission track age reduction, while subsequent cooling from between 80 and 90°C beginning between 20 and 0 Ma is required to explain the shortening of the main mode in the length distribution. This result is based on good quality AFTA data (20 single grain ages and 33 track lengths), and the thermal history solution given here is regarded as reliable within stated limits. **Equivalent $R_o$max: >0.63%.** Measured VR values of 0.57% and 0.77% from bracketing depths (Table D.2), equivalent to maximum paleotemperatures of 94 and 124°C (Table 10.4), respectively, are consistent with the interpretation of the AFTA data in this sample (although the lower value is outside the range).

All thermal history constraints are based on assumed heating rates of 1°C/Myr and cooling rates of 10°C/Myr.

Events shown in italics are not required by the AFTA data, though they are allowed within the limits shown.

Table 10.3: Continued (Geotrack Report #990)

Sample Details	Paleo-thermal constraints			Comments
Sample No. Depth Present temp Strat. age	Event	Maximum paleo-temperature (°C)	Onset Of Cooling (Ma)	
GC990-239 1500-1572 m 69°C (revised to 51°C on the basis of AFTA data – see text) 137-135 Ma	1: 2: 3:	>100 90-105 60-95	90-50 48-7 20-0	AFTA data in this sample are best explained in terms of three discrete paleo-thermal episodes, as shown, to explain all facets of the data. Cooling from a paleotemperature greater than 100°C, beginning some time between 90 and 50 Ma, is required to explain the fission track age reduction. Later cooling from between 90 and 105°C beginning between 48 and 7 Ma, is required to explain the shorter tracks within the length distribution, while subsequent cooling from between 60 and 95°C in the interval 20 to 0 Ma is required to explain the lack of longer tracks in the length distribution. This result is based on good quality AFTA data (20 single grain ages and 28 track lengths), and the thermal history solution given here is regarded as reliable within stated limits. **Equivalent $R_o$max: >0.61%.** Measured VR values of 0.77% and 0.76% from bracketing depths (Table D.2), equivalent to maximum paleotemperatures of 124 and 123°C (Table 10.4), respectively, are consistent with the interpretation of the AFTA data in this sample.
GC990-242 1899-2001 m 82°C (revised to 59°C on the basis of AFTA data – see text) 141-137 Ma	1: 2:	>110 85-95	58-38 18-2	Two grains giving much older fission track ages around 200-250 Ma in the same compositional groups as much younger ages around 50 or less Ma (see Data Summary Sheet, Appendix B) are regarded as contaminants. After removing data in these grains, the remaining AFTA data in this sample require at least two paleo-thermal episodes to explain all facets of the data. Cooling from a paleotemperature greater than 110°C, beginning some time between 58 and 38 Ma, is required to explain the fission track age reduction, while subsequent cooling from between 85 and 95°C beginning between 18 and 2 Ma is required to explain the shortening of the main mode in the length distribution. This result is based on good quality AFTA data (20 single grain ages and 49 track lengths), and the thermal history solution given here is regarded as reliable within stated limits. **Equivalent $R_o$max: >0.67%.** Measured VR values of 0.78% and 0.84% from bracketing depths (Table D.2), equivalent to maximum paleotemperatures of 125 and 130°C (Table 10.4), respectively, are consistent with the interpretation of the AFTA data in this sample.

All thermal history constraints are based on assumed heating rates of 1°C/Myr and cooling rates of 10°C/Myr.

Events shown in italics are not required by the AFTA data, though they are allowed within the limits shown.

Table 10.3: Continued (Geotrack Report #990)

Sample Details	Paleo-thermal constraints			Comments
Sample No. Depth Present temp Strat. age	Event	Maximum paleo-temperature (°C)	Onset Of Cooling (Ma)	
GC990-245 2340-2400 m 96°C (revised to 67°C on the basis of AFTA data – see text) 141-137 Ma	1: 2:	>110	50-20	Apatites containing between 0.0 and 0.2 wt% Cl define two distinct groups, one with ages around 30 Ma and another with much older ages around 100 Ma or above. On the basis of comparison with adjacent samples, grains defining the older age grouping are regarded as contaminants, and have been excised from the dataset. The remaining AFTA data in this sample can be explained by a single paleo-thermal episode, involving cooling from a paleotemperature greater than 110°C beginning some time between 50 and 20 Ma. This is required to explain the fission track age reduction, while the track length data appear to be dominated by the present-day thermal regime. After removal of the contaminant data, the remaining AFTA data are of moderate quality (7 single grain ages and 47 track lengths), and although the suspected presence of contamination introduces additional uncertainty, the quoted interpretation is regarded as reliable within the stated uncertainty limits. **Equivalent $R_o$max: >0.63%.** Measured VR values of 0.75% and 0.94% from bracketing depths (Table D.2), equivalent to maximum paleotemperatures of 122 and 139°C (Table 10.4), respectively, are consistent with the interpretation of the AFTA data in this sample.
GC990-248 2730-2802 m 108°C (revised to 75°C on the basis of AFTA data – see text) 141-137 Ma	1:	>110	30-10	AFTA data in this sample contain some older fission track ages around 100 Ma in the same compositional groups as much younger ages around 20 to 30 Ma (see Data Summary Sheet, Appendix B). Similar features are seen in data from adjacent samples, and the grains giving these older ages are considered to be contaminants. After removal of the older ages, the AFTA data in this sample can be explained in terms of cooling from >110°C at some time between 30 and 10 Ma. This event is defined by the fission track age reduction in this sample. After removal of the contaminant data, the remaining age data are still of relatively high quality (16 ages giving a coherent trend with wt% Cl), and although the suspected presence of contamination introduces additional uncertainty, the quoted interpretation is regarded as reliable within the stated uncertainty limits. **Equivalent $R_o$max: >0.67%.** Measured VR values of 1.04% and 0.99% from bracketing depths (Table D.2), equivalent to maximum paleotemperatures of 144 and 142°C (Table 10.4), respectively, are consistent with the interpretation of the AFTA data in this sample.

All thermal history constraints are based on assumed heating rates of 1°C/Myr and cooling rates of 10°C/Myr.

Events shown in italics are not required by the AFTA data, though they are allowed within the limits shown.

Table 10.3: Continued (Geotrack Report #990)

Sample Details	Paleo-thermal constraints			Comments
Sample No. Depth Present temp Strat. age	Event	Maximum paleo-temperature (°C)	Onset Of Cooling (Ma)	
GC990-251 2973-3051 m 116°C (revised to 80°C on the basis of AFTA data – see text) 141-137 Ma	1:	>100	30-0	AFTA data in this sample contain one older fission track ages around 330 Ma in the same compositional groups as much younger ages (see Data Summary Sheet, Appendix B). Similar features are seen in data from shallower samples, and the grains giving these older ages are considered to be contaminants. After removal of the single older age in this sample, the AFTA data in this sample can be explained in terms of cooling from >100°C at some time between 30 and 0 Ma. This event is defined by the fission track age reduction in this sample. After removal of the contaminant data, the remaining age data are of lower quality than in other samples (8 ages , 0 lengths), but the quoted interpretation is regarded as reliable within the stated uncertainty limits. **Equivalent $R_o$max: >0.61%.** A measured VR_{eq} value of 0.99% from a slightly shallower depth (Table 7.4) and a measured VR value of 1.21% from slightly deeper in the well (Table D.2), equivalent to maximum paleotemperatures of 142 and 156°C (Table 10.4), respectively, are consistent with the interpretation of the AFTA data in this sample.
GC990-254 3573-3627 m 135°C (revised to 92°C on the basis of AFTA data – see text) 141-137 Ma	1: 2:	>120	50-0	AFTA data in this sample can be explained by a single paleo-thermal episodes, as shown. Cooling from a paleotemperature greater than 125°C, beginning some time between 50 and 0 Ma, is required to explain the fission track age reduction in this sample. Note that 20 of the 21 single grain ages show a very consistent trend with wt% Cl, with the exception being one grain with a much older age that is regarded as a contaminant. Despite the relative lack of track lengths (only 5 track lengths measured) the thermal history solution given here is regarded as reliable within stated limits. **Equivalent $R_o$max: >0.73%.** A measured VR value of 1.08% from the same depth interval (Table D.2), equivalent to a maximum paleotemperature of 147°C (Table 10.4), is highly consistent with the interpretation of the AFTA data in this sample.

All thermal history constraints are based on assumed heating rates of 1°C/Myr and cooling rates of 10°C/Myr.

Events shown in italics are not required by the AFTA data, though they are allowed within the limits shown.

Table 10.4: Maximum paleotemperatures from VR data in the 6-MGP-3-BA well (Geotrack Report #990)

Sample number	Average depth (m)	Present temp-erature[*1] (°C)	Strati-graphic Age (Ma)	Keiraville VR[*3]2 (%)	Equivalent VR from IR[*3] (%)	Maximum paleotemp-erature[*4] (°C)
GC990-231.1	405	33	130-123	0.64 (3)		99
GC990-233.1	594	39	130-123	0.60 (14)		88
GC990-234.5	816	46	135-130	0.53 (9)		90
GC990-235.1	1008	52	135-130	-	0.36 (3)	59
GC990-236.1	1197	58	135-130	0.57 (25)		94
GC990-238.1	1395	64	137-135	0.77 (7)		124
GC990-240.1	1608	71	137-135	0.76 (18)		123
GC990-241.1	1770	76	137-135	0.78 (9)		125
GC990-243.1	2004	84	141-137	0.84 (2)		130
GC990-244.1	2196	90	141-137	0.75 (1)		122
GC990-246.1	2409	97	141-137	0.94 (3)		139
GC990-247.1	2598	103	141-137	1.01 (1)		144
GC990-249.1	2832	110	141-137	0.99 (2)		142
GC990-250.1	2958	114	141-137	-	0.99 (7)	142
GC990-252.1	3189	122	141-137	1.21 (7)		156
GC990-253.1	3402	129	144-141	1.21 (1)		156
GC990-254.1	3585	134	146-145	1.08 (2)		147

*1 Present temperatures calculated as explained in Appendix A. Values in brackets are revised on the basis of AFTA data (see Table 10.2 and Section 10.2).

*2 From Table D.2. Numbers in brackets show the numbers of fields measured for each sample.

*3 Equivalent VR (VR_{eq}) derived from mean inertinite reflectance using Figure 10.2, as described in the text. Numbers in brackets refer to the numbers of inertinite fields measured for each sample.

*4 Estimates of maximum paleotemperature derived from mean VR or VR_{eq} using assumed heating and cooling rates of 1°C/Myr and 10°C/Myr, respectively.

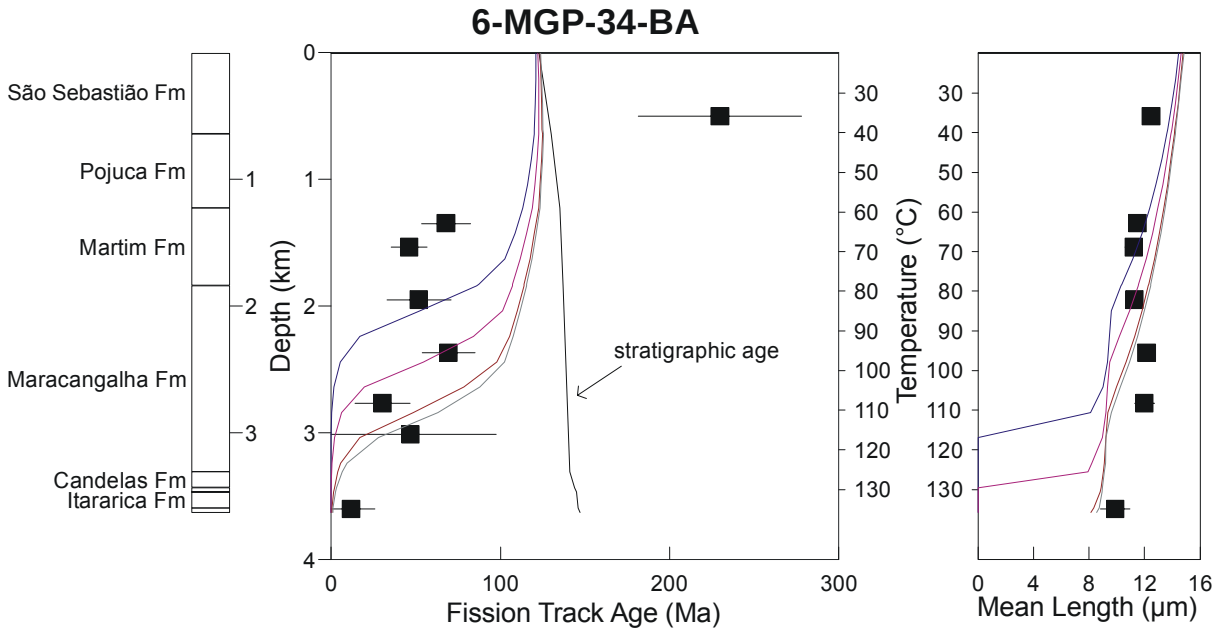

Figure 10.1a: AFTA parameters plotted against sample depth and present temperature for samples from the **6-MGP-34-B well, Recôncavo Basin, Onshore Brazil**. The variation of stratigraphic age with depth is also shown, as the solid black line in the central panel. Present-day temperatures shown here are based on a sea bed temperature of 20°C and a present-day thermal gradient of 32°C/km derived from corrected BHT values in this well (Appendix A). Coloured lines show the pattern of fission track age and mean track length predicted from the Default Thermal History (see Section 2.1) for apatites containing 0.0-0.1, 0.4-0.5, 0.9-1.0 and 1.5-1.6 wt% Cl. The Default Thermal History is based on the thermal structure reported above, combined with the burial history shown in Figure 10.5.

Initial visual assessment of these data shows that measured apatite fission track ages at depths between 1 and 2 km are significantly younger than predicted from the Default Thermal History, showing that these samples must have been hotter in the past. But in deeper samples, AFTA data show a lower degree of annealing (i.e longer lengths, less age reduction) than expected at the prevailing temperatures, suggesting that the present-day thermal gradient used in this construction is too high.

Detailed investigation of data in individual samples confirms this conclusion (Table 10.2). Figure 10.1b shows a revised version of this plot using a lower present-day gradient which is more compatible with the AFTA data in the deeper samples.

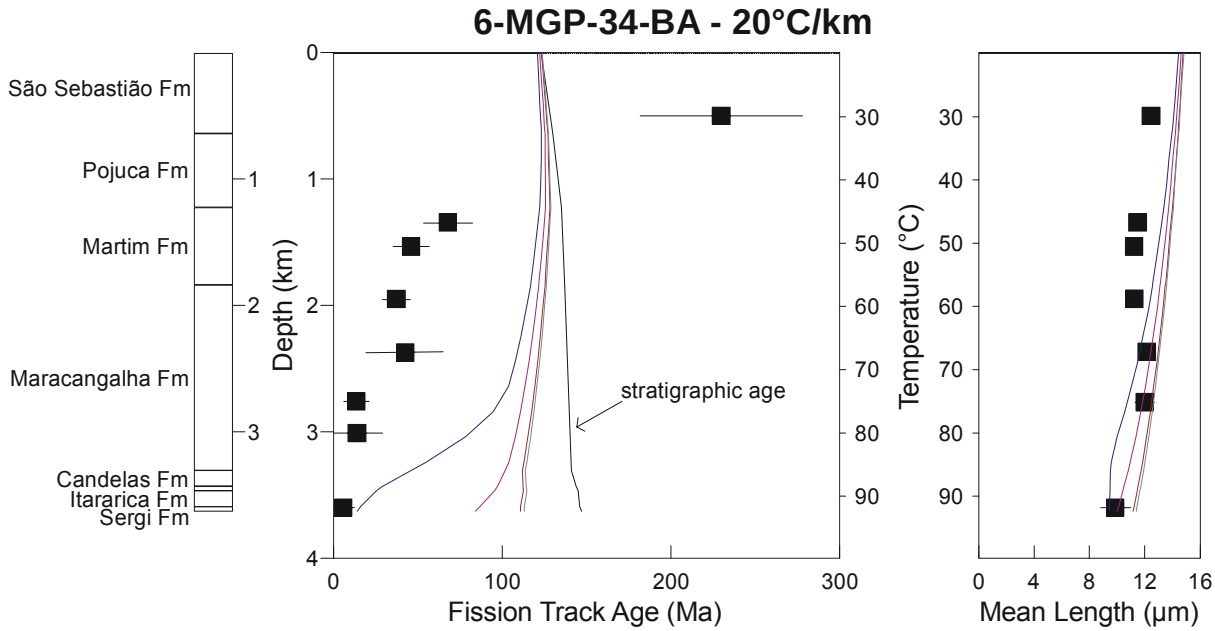

Figure 10.1b: AFTA parameters (after removal of data from contaminant grains) for samples from the **6-MGP-34-BA well, Recôncavo Basin, Onshore Brazil**, plotted against sample depth and present temperature as in Figure 10.1a. The variation of stratigraphic age with depth is again also shown, as the solid black line in the central panel. Present-day temperatures shown here are based on a surface temperature of 20°C and a revised present-day thermal gradient of 20°C/km based on AFTA data in deeper samples and also on data from Meister (l973) as discussed in Section 2.6. Coloured lines show the pattern of fission track age and mean track length predicted from the Default Thermal History (see Section 2.1) for apatites containing 0.0-0.1, 0.4-0.5, 0.9-1.0 and 1.5-1.6 wt% Cl. The Default Thermal History is based on the thermal structure reported above, combined with the burial history shown in Figure 10.5.

Initial visual assessment of these data now shows that measured apatite fission track ages in all except the shallowest sample are significantly younger than predicted from the Default Thermal History, while mean lengths in samples shallower than 2 km are less than predicted on this basis. These observations show that these samples must have been hotter in the past. Mean track length values measured in the three deepest samples are consistent with the values predicted from the Default Thermal History, suggesting that present-day temperatures in this construction are more reliable.

Detailed interpretation of data in individual samples, including extraction of formal thermal history solutions for each sample, is summarised in Tables10.2 and 10.3.

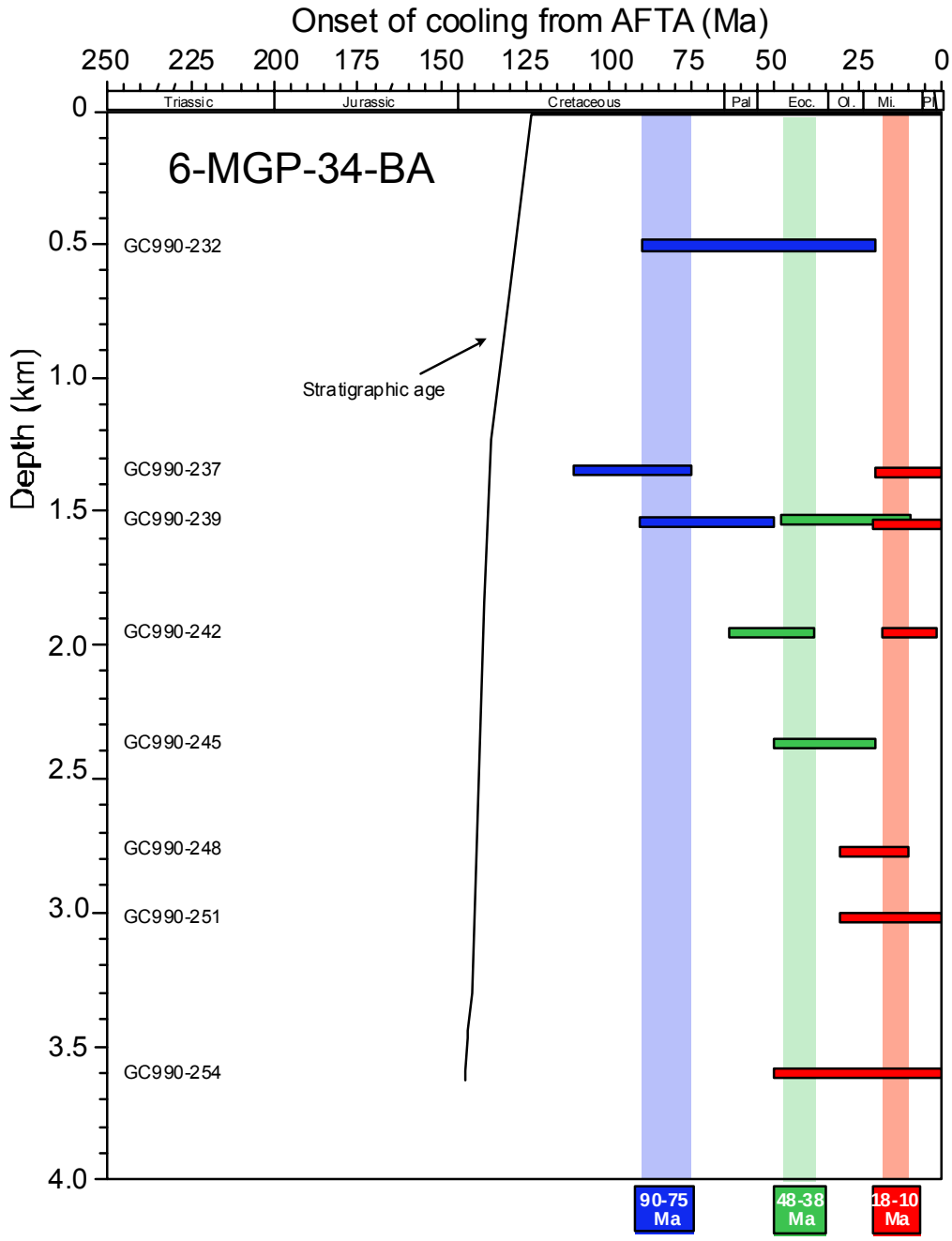

Figure 10.2: Timing constraints on cooling episodes derived from AFTA data in samples from the **6-MGP-34-BA well, Recôncavo Basin, Onshore Brazil** (from Table 10.3). If the paleo-thermal effects identified in the AFTA data from these samples represent synchronous cooling episodes, then the results in all samples can be explained in terms of three post-depositional cooling episodes, as shown.

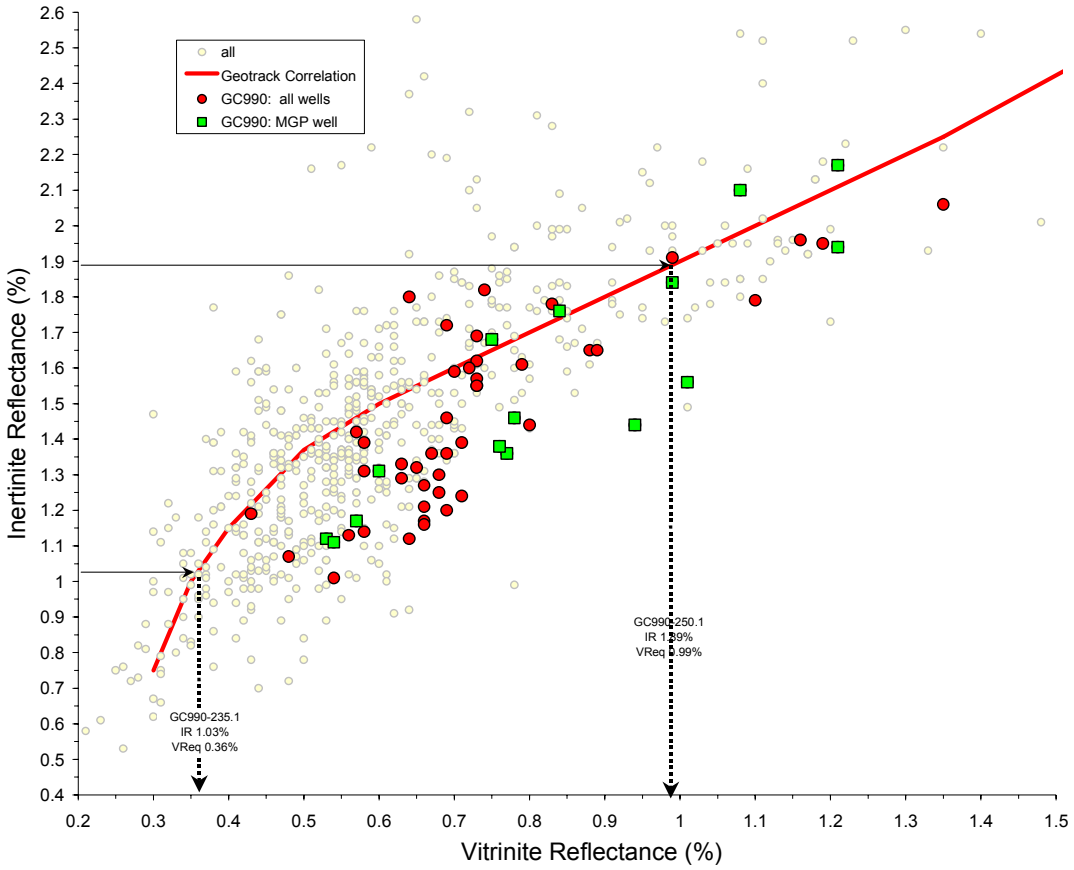

Figure 10.3: Using a compilation of mean Vitrinite Reflectance (VR) and Inertinite Reflectance (IR) values measured in samples from a wide range of settings around the world, mean IR values measured in samples from **the 3-MGP-34-BA well, Onshore Brasil**, from Table D.2 and the maceral descriptions in Appendix D, have been converted to equivalent VR values (VR_{eq}), as shown.

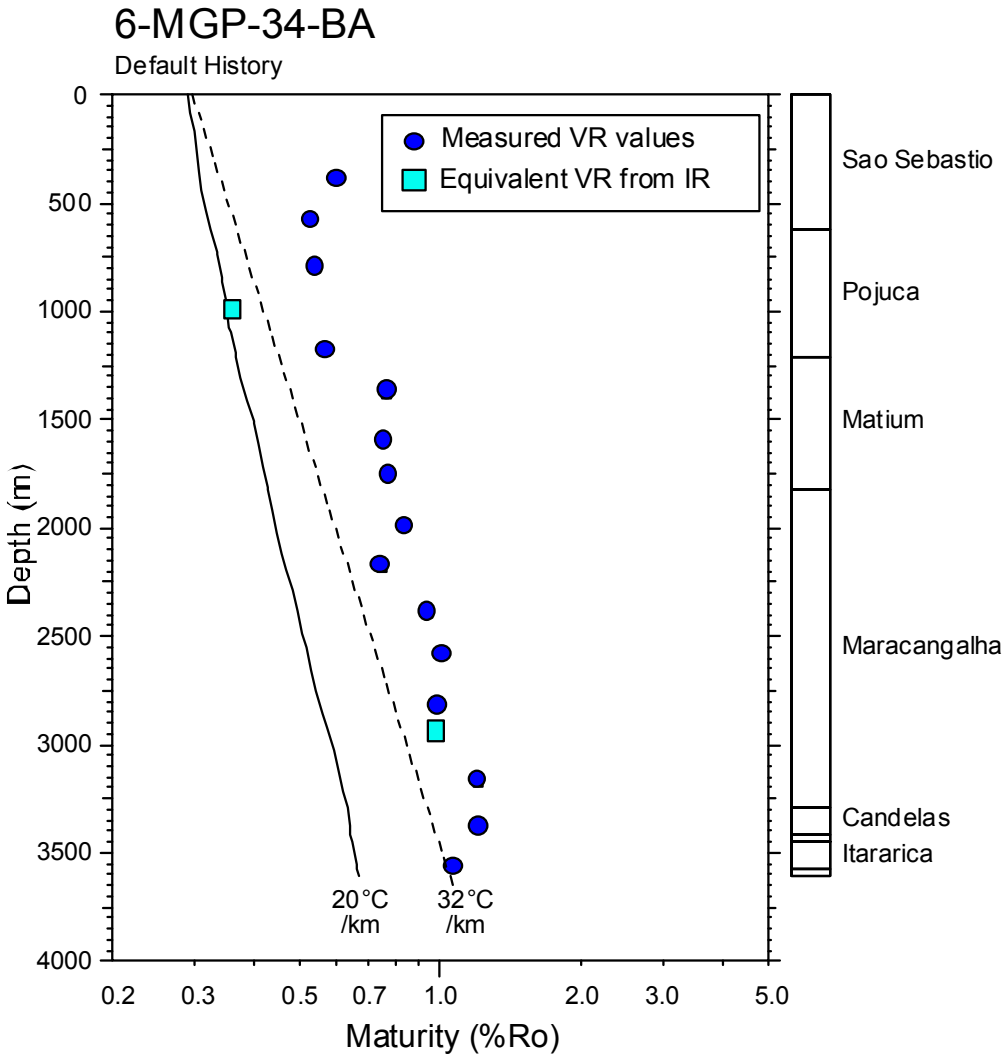

Figure 10.4: Mean vitrinite reflectance (VR) values in the **6-MGP-34-BA well**, from Table D.2, plotted against depth. The black lines shows the VR profiles predicted by two versions of the "Default History", i.e., the profile expected if samples throughout the section are currently at their maximum temperature since deposition (Section 2.1). The dashed line is based on a thermal gradient of 32.0°C/km as derived from corrected BHT values in this well (see Appendix A), while the solid line is based on a revised gradient of 20°C/km suggested by AFTA data from the deeper samples in the well. Both versions assume a surface temperature of 20°C. Measured VR values plot consistently above both predicted profiles, showing that the sampled units have been hotter than present temperatures at some time since deposition. See text for details.

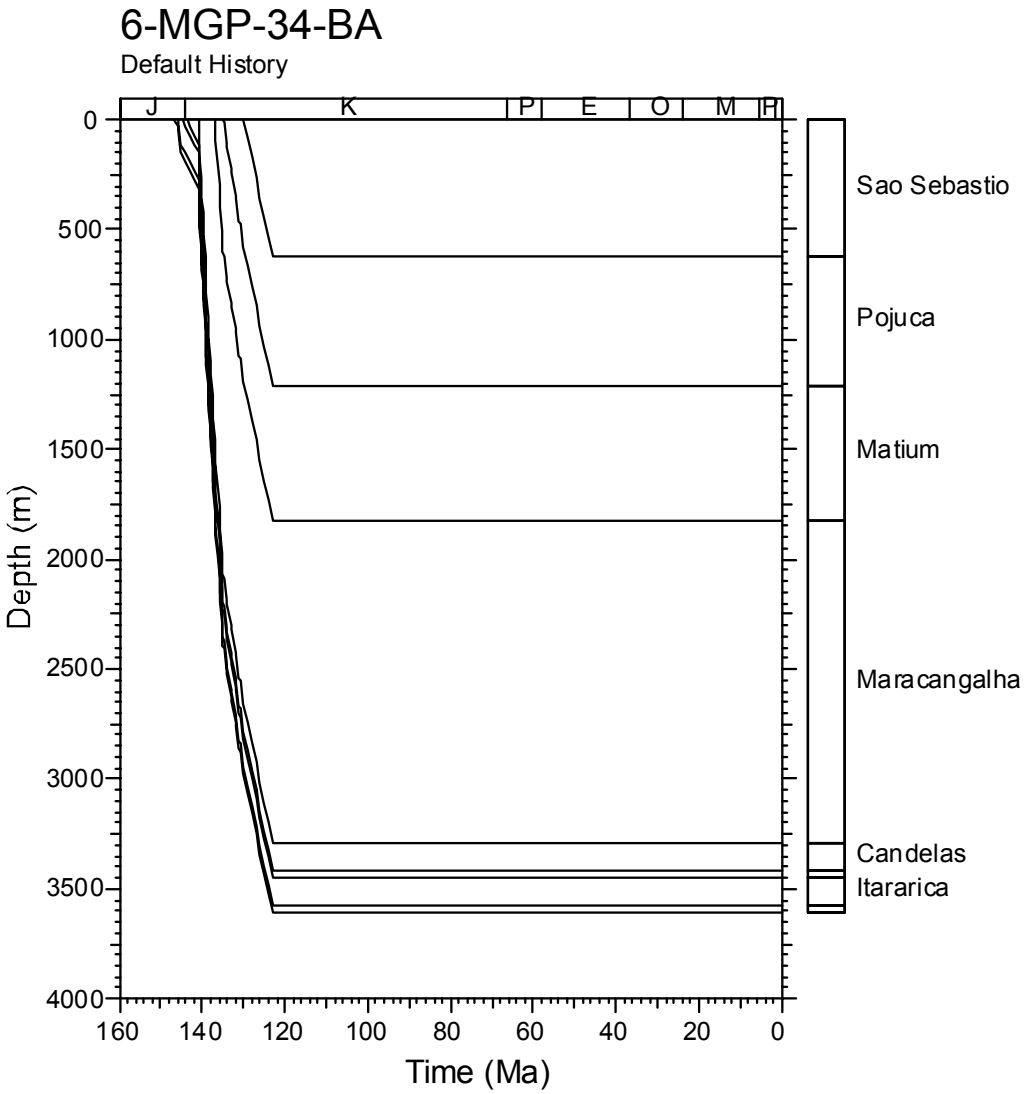

Figure 10.5: Burial history derived from the preserved section in the **6-MGP-34-BA well, Recôncavo Basin, Recôncavo Basin, Onshore Brazil**. This history, together with present-day thermal gradients of 32°C/km and 20°C/km and a surface temperature of 20°C, has been used to predict the Default Thermal Histories for individual AFTA samples, as employed in the construction of Figure 10.1, and for prediction of the maturity-depth profiles in Figure 10.4.

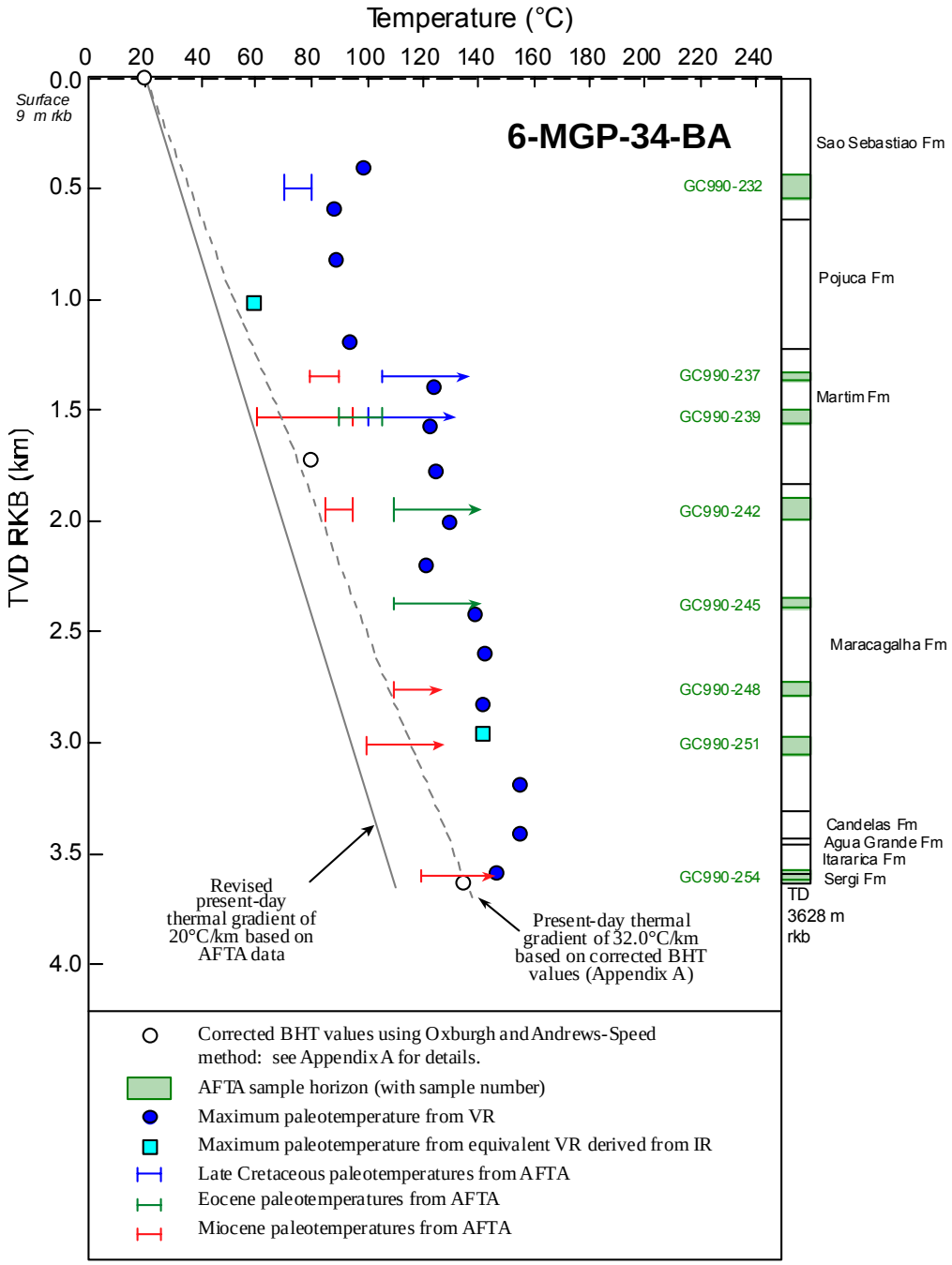

Figure 10.6: Paleotemperature constraints derived from AFTA data in the **6-MGP-34-BA well, Recôncavo Basin, Onshore Brazil**, plotted against depth (rkb). Present-day temperature profiles based on a thermal gradient of 32.0°C/km (derived from corrected BHT values as described in Appendix A) and a revised value of 20°C/km based on AFTA data from the deeper samples in this well, plus a surface temperature of 20°C, are also shown. Note the high degree of consistency between maximum paleotemperatures derived from AFTA and VR in the Late Cretaceous episode (blue). See text for further details

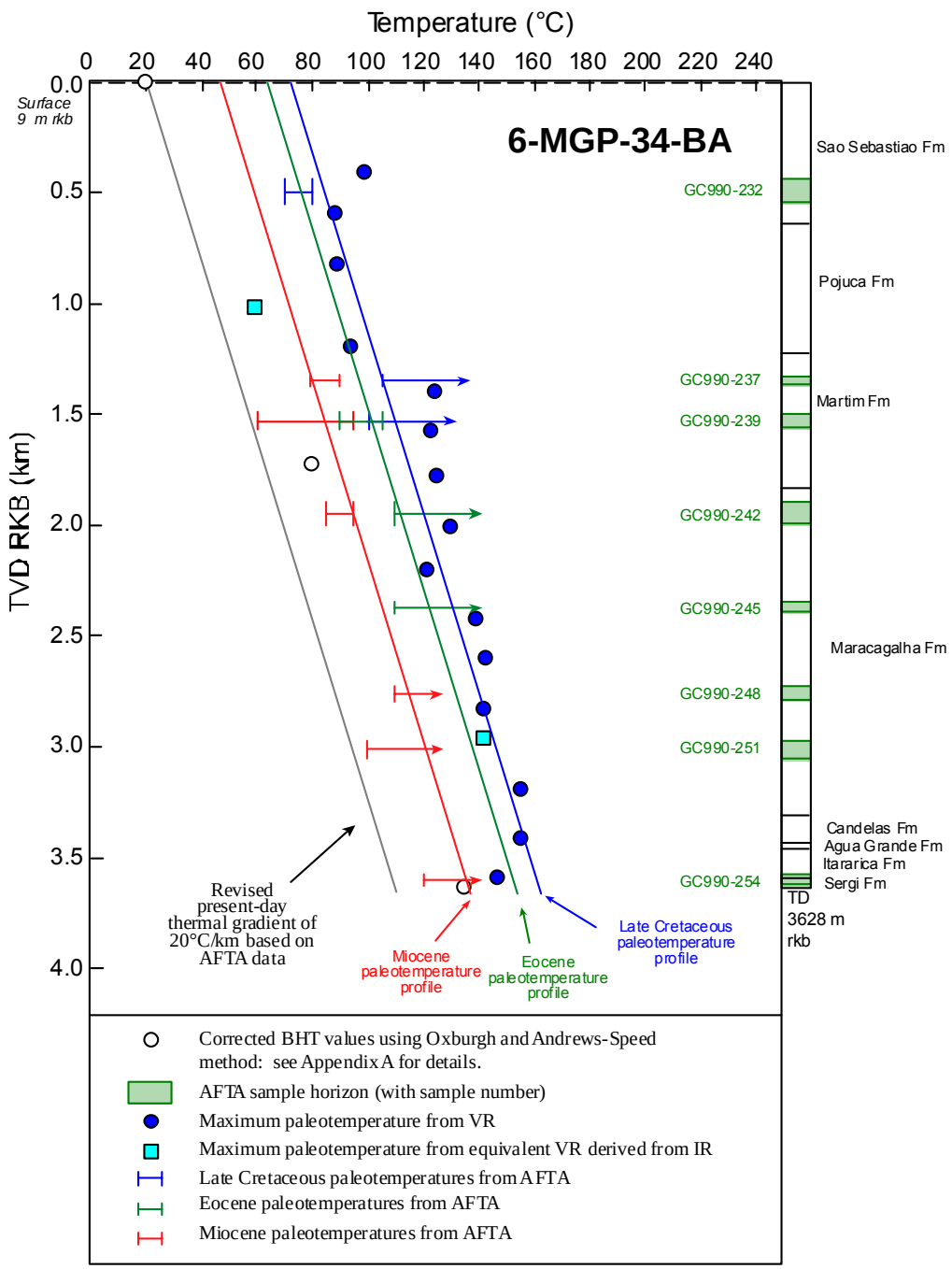

Figure 10.7: Interpreted paleotemperature profiles representing the constraints shown in Figure 6.5 for the **6-MGP-34-BA well, Recôncavo Basin, Onshore Brazil**. Paleotemperatures derived from AFTA and VR data in three paleo-thermal episodes define three linear sub-parallel profiles, as shown, suggesting little or no change in paleogeothermal gradient through time. See text for further details.

11. AFTA and VR data in outcrop samples from NE Brazil and associated thermal history interpretations

11.1 Introduction and sample locations

A total of 83 outcrop samples from NE Brazil were processed for AFTA, of which all but two yielded apatite suitable for analysis, mostly giving excellent yields (Table A.2). Details of all AFTA samples are summarised in Table A.2 (Appendix A) and results are presented in Appendix B. Five samples were also submitted for VR analyses by Keiraville Konsultants. Results of these analyses are presented in Appendix D.

Fission track age and mean track length data in the 81 samples that yielded apatite are summarised in Table 11.1, where they are compared with values predicted from the respective Default Thermal Histories. Sample locations are shown in Figure 11.1, which also shows the locations of samples from which AFTA data have been published by Turner et al. (2008). These samples are shown in green with either GC854- or JT- prefixes. Data in the GC854 samples have been reinterpreted for this study and are included with the new samples processed for this study in the following analysis. Also shown in Figure 11.1 are the locations of samples for which apatite fission track data were published by Harman et al. (1998). These and the JT samples from the Turner et al. (2008) study are included to provide a qualitative extension of the basic variation in fission track ages across the region, but are not used to provide quantitative thermal history solutions. Figure 11.1 also shows the locations of four elevation sections from which the AFTA data are employed in Section 11.8 to investigate the nature of key paleo-thermal episodes.

11.2 General features of the AFTA data

Figure 11.2 shows the relationship between mean track length and fission track age for the 81 samples analysed for this report. In Figure 11.3 these data are compared with other data from NE Brazil, including Turner et al. (2008), Harman et al. (1998) and Morais Neto et al. (2008). Samples from the Turner et al. (2008) study include both basement and sedimentary rock samples while those from the other two studies are of basement only. The Morais Neto et al. (2008) study involves samples from the Borborema Plateau, to the NE of the region shown in Figure 11.1. Locations of samples from these two published studies are shown in Figure 11.4.

The variation in measured apatite fission track ages across the region is shown in Figure 11.5, including data from Harman et al. (1998) and Turner et al. (2008). In some ways such a map can be misleading, because the measured fission track ages are sensitive to variation in the composition of apatites within each sample. regional variation is better addressed by investigating the regional variation of paleotemperatures in individual episodes, as will be discussed in a later Section. However, some broad generalisations are possible from Figure 11.5. In particular, some of the youngest ages between 75 and 130 Ma are measured in samples from coastal locations in the North of the region, from Salvador northwards. But such young ages are also measured in samples from the southwest in the Highland region. In contrast, samples from coastal locations south of Salvador give amongst the oldest ages in excess of 300 Ma. Many published studies suggest that the typical pattern of fission track ages along continental margins is to find youngest ages along the coast and oldest ages inland in highland locations. The results from this study stand in stark contrast to this pattern, and it is immediately clear that these data cannot be interpreted in terms of conventional models of rift-flank uplift etc, as suggested e.g. by Gallagher and Brown (1995).

AFTA parameters define a consistent trend in Figures 11.2 and 11.3, but display a complex pattern of variation. AFTA data in samples which have experienced varying maximum paleotemperatures prior to cooling in a single dominant episode show a characteristic “boomerang” trend in a plot of mean track length vs fission track age (Green et al., 1986). However, data in Figures 11.2 and 11.3 show a much more complex pattern of variation, in which reduction of fission track age from ~400 Ma is accompanied first by a progressive increase in mean track length from ~11.5 µm to a broadly defined maximum of ~12 µm at ages around 250 to 300 Ma, after which the mean length subsequently decreases once more reaching a minimum of around 11 µm at ages between 150 and 200 Ma, and then increasing towards the longest mean lengths around 13 µm samples with ages around 150 Ma. Further decrease in fission track age is accompanied by a decrease in mean track length to ~12 µm at ages around 100 Ma, and finally mean lengths show a suggestion of an increase in samples with ages less than 100 Ma.

The pattern of variation in Figures 11.2 and 11.3 shows that the thermal history framework for the region is much more complex than a single dominant paleo-thermal event, and detailed assessment of thermal history solutions from individual samples is required before any rigorous conclusions can be reached. Nevertheless, the consistent trend shown by the data in Figures 11.2 and 11.3 suggests that all samples (or at least the great majority) have undergone a similar overall style of

thermal history, suggesting a history involving a series of regionally synchronous cooling episodes, with different samples having experienced differing paleotemperatures in the different episodes. Extraction of thermal history information from the AFTA data and subsequent synthesis has therefore been carried out on this basis.

Note that there is no appreciable difference in Figures 11.2 and 11.3 between samples of sedimentary rock and basement, with data from both types of sample defining a common trend. This implies that a common history style of thermal history applies to both accessory apatites in basement samples and to detrital apatites from sedimentary units.

Note also that no measured fission track ages over 400 Myr have been measured in these samples, and the majority of samples give ages less than 300 Ma (Figure 11.2). despite many of the samples being of Precambrian basement with formation ages up to 2600 Ma or more. Mean track lengths are generally between 11 and 14 μm, with only a very small number outside this range. These values immediately show that the AFTA data in these samples of Precambrian basement are dominated by Phanerozoic events, and preserve little or no information on the earlier (Precambrian) history. For this reason, extraction of thermal histories from Precambrian basement samples has been carried out using Default Thermal Histories (Section 2.1) based on the assumption that these samples have resided at or near to surface temperatures throughout Phanerozoic times (i.e since the end of the Precambrian at 542 Ma). Note that we do not suggest that this history is in anyway realistic. Instead this history simply provides a starting point for extracting thermal history solutions, while not in any way biassing the outcome of the interpretation.

Detailed thermal history interpretation of the AFTA data is provided in Tables 11.2 and 11.11. Qualitative interpretation of the AFTA data, in terms of evidence that the samples may have been hotter in the past, is summarised in Table 11.2. Following the strategy outlined in Section 2.1, quantitative interpretation of the AFTA data is summarised in Table 11.3.

11.3 Evidence for elevated paleotemperatures from AFTA

As explained in Table 11.2, AFTA data in all but two of the samples which yielded apatite show clear evidence of higher temperatures in the past. In all basement samples, this evidence comes from both the fission track age and track length data,

both of which show a greater degree of reduction than expected from the Default Thermal History. In many samples of Cretaceous sedimentary rocks, evidence for higher temperatures after deposition comes only from the track length data, while the lack of significant fission track age reduction suggests that maximum paleo-temperatures in these samples were generally less than 100°C. But in some samples of Cretaceous sedimentary rocks, together with most samples from older sedimentary units both the track length data and fission track age data show consistent evidence of higher temperatures after deposition.

Of the two samples which do not provide definite evidence of higher temperatures after deposition, data in sample GC990-20 are not of sufficient quality to provide a rigorous interpretation, while in the case of sample GC990-40 the depositional age is so young that the data are dominated by tracks formed prior to deposition.

11.4 Magnitude of paleotemperatures and timing of cooling from AFTA

Table 11.3 presents details of the thermal history interpretation of AFTA data from this study, in terms of the maximum paleotemperature and the timing of cooling in a number of discrete episodes derived from the AFTA data in each sample. As explained in Section 2.1 and Appendix C, these estimates are obtained for each sample using proprietary software which compares the AFTA parameters (fission track age and track length distribution and their variation with Cl content) predicted for a range of likely thermal history scenarios with the measured values, defining the range of conditions for which predictions are consistent with the measured data within 95% confidence limits.

In each basement sample analysed for this report, as well as samples of Paleozoic sedimentary rocks, the AFTA data clearly require a history involving at least two episodes of heating and cooling, while in some samples, three episodes are required to explain all facets of the data. Definition of two paleo-thermal episodes represents the usual level of resolution that can be achieved from AFTA (typically the earlier episode would be defined by the fission track age data and possibly the shorter track lengths while the more recent episode would be defined by the shortening of the main mode of the track length distribution). But where the paleotemperatures in each episode are sufficiently well separated, three episodes can be resolved. The most obvious case is where the earliest episode produces total annealing of all tracks, a subsequent event leads to shortening of tracks formed after the initial cooling to lengths around 10-11 μm, and a later event then shortens tracks formed subsequent to

the second episode to lengths around 13 µm. The ability to resolve three episodes often depends on the quality of the data, with 100 tracks normally required in order to provide a confident conclusion. In most samples from this study, data quality is similar. Nevertheless, random fluctuation in measurements and sampling can lead to the failure to identify three episodes in some samples while nearby samples provide clear resolution. Thus, in some cases, the quoted thermal history solutions may represent the combined effects of unresolved multiple cooling episodes. This is also particularly important at low temperatures (<70°C), where differences in track length may be insufficient to allow multiple episodes to be resolved.

In contrast, in many samples from Mesozoic sedimentary units, the AFTA data only define a single episode with confidence, while a second (earlier) episode may be tentatively suggested by the data, but could alternatively represent the presence of shorter tracks formed in sediment provenance terrains.

In fact, synthesis of all data, as discussed in Section 11.4 (below), suggests that at least eight cooling episodes are required to explain the results from all samples analysed for this study. This emphasises the fact that since AFTA data in individual samples even in the most favourable circumstances allow resolution of only three discrete episodes, and more typically only two, results from any particular sample will define those events which dominate the data in that sample. This will be a function of the magnitude of each episode, the quality of the resulting AFTA data and the spread of compositions present (often the highest Cl contents may reveal an earlier episode, evidence for which has been overprinted by later events in the more sensitive, low-Cl apatites).

11.5 Identification of paleo-thermal episodes

Estimates of the timing of discrete cooling episode derived from AFTA data in individual samples from Table 11.3 show a considerable range. Timing estimates for individual cooling episodes in all samples are compared in Figures 11.6, 11.7 and 11.8, referring to samples from discrete geographic areas defined in the inset to each Figure. Figure 11.6 also includes results for basement samples from locations to the Northeast of Figure 11.1 originally published by Turner et al. (2008) and reinterpreted for this study (samples with GC854- prefixes, Tables 11.2, 11.3). Based on the consistent trend defined by the data in Figures 11.2 and 11.3, we have sought to define the minimum number of regionally synchronous cooling episodes which can explain all of the results across the region. In doing so, attention has been

paid to ensuring that events of similar magnitude in adjacent samples represent common episodes, and the final timing has been designed to match the most precise timing constraints wherever possible.

As illustrated in Figures 11.6, 11.7 and 11.8, timing constraints for the onset of cooling derived from AFTA in samples across the entire region of NE Brazil in Figure 11.1 can be explained in terms of eight discrete cooling episodes, viz:

460 to 410 Ma	**Ordovician -Devonian**
320 to 300 Ma	**Carboniferous**
230 to 220 Ma	**Triassic**
180 to 170 Ma	**Jurassic**
~120 Ma	**Early Cretaceous**
110 to 90 Ma	**mid-Cretaceous**
80 to 70 Ma	**Late Cretaceous**
20 to 15 Ma	**Miocene**

These intervals are illustrated by the vertical coloured (cross-hatched) bands common to Figures 11.6, 11.7 and 11.8. Timing constraints in individual samples are attributed to specific events in these Figures by colour. Data in all samples can be explained in terms of combinations of these episodes.

Cautionary comments

Note that the intervals quoted in Table 11.3 and plotted in Figures 11.6, 11.7 and 11.8 represent the times at which cooling began, and we do not suggest that cooling was restricted to these intervals.

We should stress that attempting to explain the data in terms of the smallest number of regionally synchronous cooling episodes may mask a more complex regional thermal history framework. In addition, as discussed in Section 11.4 it is important to remember that AFTA data in individual samples only reveal two or at best three dominant episodes, and in at least some of the samples described here, it is clear that the results must represent the unresolved effects of a larger number of episodes. Therefore definition of these episodes should best be regarded as providing an general indication of the overall style of likely thermal history, rather than providing a precise definition of events.

11.6 Regional variation in the magnitude of individual cooling episodes

Maps of paleotemperatures characterising the eight paleo-thermal episodes identified in Section 11.5 are shown in Figures 11.9 through 11.16. These maps show that some events are localised while others have affected much of the region. Below we discuss general trends within the data while regional variation in thermal history trends and their significance in terms of the underlying mechanisms and processed are discussed in more detail elsewhere.

The **Ordovician to Devonian** episode is recognised across an E-W axis in the south of the region (Figure 11.9), with maximum paleotemperatures in excess of 100°C in all samples in which this episode is recognised. Since this is the earliest of the paleo-thermal episodes recognised across the region, it is only recorded in areas where paleotemperatures in subsequent episodes have remained sufficiently low as to not overprint evidence of this episode. Those locations in Figure 11.9 recording this episode therefore represent the most stable areas of the study region which have undergone less denudation (based on discussion in Section 13 to 16) than surrounding regions.

The **Carboniferous** episode is recognised along the western flanks of the Tucano and Recôncavo Basins and along the coast south of Salvador (Figure 11.10), with maximum paleotemperatures in excess of 100°C in most of the samples in which this episode is recognised. Again, this early episode is only recorded in areas where paleotemperatures in subsequent episodes have remained sufficiently low as to not overprint evidence of this episode, and those locations in Figure 11.10 recording this episode are clearly amongst the most stable areas of the study region, which have undergone less denudation (based on discussion in Section 13 to 16) than surrounding regions.

The **Triassic** episode is recognised only in the centre of the region, west of Salvador (Figure 11.11), while the **Jurassic** episode is recognised in two areas north and south of this region (Figure 11.12). Many of the locations recording the **Triassic** episode cooled from maximum paleotemperatures in excess of 100°C in this episode, and any evidence of previous episodes would have been overprinted by this episode. **Jurassic** paleotemperatures in some samples are >100°C but in others are slightly lower, and sample GC990-105 preserves evidence of the **Ordovician-Devonian episode**. Given the spatial relations between these four earliest episodes, it seems most likely that all four affected the entire region, with different parts of the region undergoing different degrees of cooling (probably reflecting different degrees of denudation) in different episodes.

In contrast to these earlier episodes, the **Early Cretaceous** episode is identified in basement samples across the entire region (Figure 11.13). Several samples in the north and south of the region cooled from paleotemperatures in excess of 100°C in this episode, but a noteable feature of the paleotemperature map in Figure 11.13 is a "saddle" of low values generally in the range 80 to 100°C in the centre of the region. Comparison with the map of fission track ages in Figure 11.5 suggests that this Early Cretaceous episode exerts a first-order control on the regional variation of fission track ages across the region.

Of all the episodes identified in this study, the **mid-Cretaceous** episode (Figure 11.14) appears to be the most localised, only being identified in samples to the Northeast of the study area. Taking all available data at face value, this episode is clearly later than the **Early Cretaceous** episode discussed above, and may be evidence of a shift in the focus of cooling to the north through early to mid-Cretaceous times. This is supported by the recognition of major cooling at a similar time in the study by Morais Neto et al. (2008) in the Borborema Plateau, further to the northeast.

Late Cretaceous cooling is ubiquitous across most of the study region (Figure 11.15), with paleotemperatures typically around 70 to 80°C but with some variation in the magnitude of paleotemperatures across the region. As will be discussed in more detail in Section 13, this episode is also recognised in AFTA data from wells in the Tucano and Recôncavo Basin, in which it dominates the AFTA and VR data and represents the timing of maximum paleo-burial, and the switch from burial of exhumation. But significantly, this episode is recognised not only in these basins but also in adjacent basement terrain, and on the basis of results from the wells discussed in Sections 3 to 10, this episode clearly represents a major phase of exhumation which has affected the entire region.

Miocene cooling is also recognised in samples across the entire region (Figure 11.16), with peak paleotemperatures generally around 50 to 60°C. Again based on results from the onshore wells, an explanation of this episode in terms of regional exhumation appears likely.

Further discussion regarding the comparison of the paleo-thermal episodes identified in Bahia with those in other regions is provided in Section 13. The variation in paleotemperatures with elevation in the four elevation transects and the implications for paleogeothermal gradients and amounts of removed section are discussed in Section 14. And likely burial and uplift histories for the region are discussed in Section 15.

Further cautionary comments

The cautionary comments provided at the end of in Section 11.5 in relation to the difficulty of resolving multiple paleo-thermal episodes in individual samples is particularly relevant to the two most recent episodes identified in this study, due to the relatively low paleotemperatures involved. Peak **Late Cretaceous** paleotemperatures in individual samples are typically around 70 to 80°C, and with **Miocene** paleotemperatures around 50 to 60°C, in most cases it will not be possible to resolve these two episodes unless data are of extremely high quality. Even then, in many cases confident resolution may not be possible, e.g. in samples of Early Cretaceous sedimentary rocks in which the AFTA data are dominated by tracks formed prior to deposition.

Therefore, while the data do appear to define the **Late Cretaceous** and **Miocene** episodes with confidence, and this is strongly supported by results from wells 1-BRN-1-BA, 1-FPO-1-BA, 1-FVM-1-BA and 6-MGP-34-BA, the allocation of results to individual episodes in Figures 11.6, 11.7 and 11.8 is in some cases equivocal. Where the two events are not resolved with confidence, it is possible that the peak paleotemperature and the timing of cooling defined from AFTA may represent a mixture of both episodes. Therefore the paleotemperature maps for these episodes in Figures 11.15 and 11.16 are best regarded as providing a broad representation of these episodes, rather than attributing too much significance to variation from one sample to another.

11.7 VR data

As detailed in Appendix D, of the five samples submitted for analysis, only one sample provided any data, and in this sample (GC990-44.1), only a single field of vitrinite was measured. These data have not been considered further.

11.8 Vertical variation in paleotemperatures in four elevation sections

Four locations where samples were collected along transects over a range of vertical elevations are shown in Figure 11.1. If all samples in a vertical transect form a coherent rock section that has undergone several paleo-thermal episodes, we would expect to see a coherent pattern of variation in these transects, with paleotemperatures in each episode increasing with depth, and the magnitude of each

episode at a particular depth increasing with the timing of the episode until total annealing is reached. The rate of increase of paleotemperatures with depth in each episode would then provide constraints on paleogeothermal gradients and the amounts of section removed by erosion since the onset of cooling in each episode. However, in general the results from this study do not show such a pattern. We review data from each transect in turn, before discussing the implications.

Locations of samples from the **Mucuge transect** are shown in more detail in Figure 11.18 and the paleotemperatures defined in these samples are plotted against elevation (above sea level) in Figure 11.18. With only three samples from this transect yielding apatite, and only a low yield in sample GC990-66 defining only a single episode, the amount of information that can be derived from these data is limited. While the Miocene paleotemperatures in samples GC990-64 and -64 are similar, and may be consistent with a progressive increase with depth, paleotemperatures in earlier events show considerable scatter, and no coherent pattern is evident.

Locations of samples from the **Jussiape transect** are shown in Figure 11.20 and the paleotemperatures defined in these samples are plotted against elevation (asl) in Figure 11.21. As illustrated in the Figure, results from this transect would be consistent with a simple pattern in which paleotemperatures increase with depth in each of the four episodes recognised in this well. However, with three of the four episodes revealed in only two samples from this transect, and only minimum paleotemperatures available for two of the four episodes, these data will provide no rigorous constraints on paleogeothermal gradients or amounts of additional section. In contrast, the Late Cretaceous paleotemperatures from this section do appear to define a coherent sequence increasing with depth in the section.

Locations of samples from the **Rio de Contas transect** are shown in Figure 11.21 and the paleotemperatures defined in these samples are plotted against elevation (asl) in Figure 11.22. The earlier episodes in this transect are only recognised in isolated samples, while Miocene paleotemperature constraints are available in three samples but are so broad that they provide no real constraint on the paleogeothermal gradient, assuming that the section is coherent. Late Cretaceous paleotemperatures show erratic variation suggesting the possibility of a tectonic offset between samples GC990-79, -81 and -80. So again results from this transect offer little in the way of rigorous constraint on paleogeothermal gradients or amounts of additional section.

Finally, locations of samples from the **Vitoria da Conquista transect** are shown in more detail in Figure 11.23 and the paleotemperatures defined in these samples are

plotted against elevation (above sea level) in Figure 11.24. Although results are available in seven samples from this transect, paleotemperatures in individual episodes show considerable scatter through the section, and no coherent pattern can be discerned in these results which can be interpreted in terms of paleogeothermal gradients.

In summary, results from these elevation transects offer little in the way of rigorous insight into the magnitude of paleogeothermal gradients in any of the paleo-thermal episodes identified from AFTA data in this study. However, one key observation that can be made from these results is that all samples, whatever their elevation, require considerable Miocene cooling. As illustrated by the notional profiles drawn through the Miocene paleotemperatures in Figures 11.18, 11.20, 11.22 and 11.24, even samples from the highest present-day elevations have cooled by at least ~20°C since the onset of cooling in the Miocene (beginning between 20 to 15 Ma based on results presented here), suggesting that several hundred metres of section have been removed by erosion in the last 20 Myr in this region of NE Brazil.

The erratic variation in paleotemperatures with elevation in at least some events in these transects could be explained by the presence of major tectonic offsets between different samples. That is, different samples may have been exhumed (cooled) by different amounts since the onset of cooling in these episodes, suggesting that major fault offsets exist throughout the region. However, landscape analysis in a parallel study suggests that major fault offsets are unlikely. Given that results over a wider area (Section 12) suggest that an Eocene cooling episode has also affected the region, it is possible that some of the scatter in Miocene paleotemperaturs in Figures 11.18, 11.20, 11.22 and 11.24 coudl be due to the unresolved effects of multiple episodes.

The implications of these conclusions are considered further in Section 13.

Table 11.1: Summary of apatite fission track data in outcrop samples from Bahia State, Onshore Brazil (Geotrack Report #990)

Sample number	Source number	Present temp-erature*1 (°C)	Stratigraphic age (Ma)	Mean track length (µm)	Predicted mean track length*2 (µm)	Fission track age (Ma)	Predicted fission track age*2 (Ma)
GC990-5	BRFT06-11	20	>2600	11.20±0.24	14.14	274.7±26.1	2491
GC990-14	514401	20	>2600	13.14±0.15	13.92	117.6±6.8	2451
GC990-15	514402	20	200-146	12.68±0.16	14.47	285.1±27.0	170
GC990-16	514403	20	>2600	13.00±0.15	13.92	122.1±5.9	2452
GC990-17	514404	20	>2600	12.00±0.26	14.10	261.5±15.5	2482
GC990-18	514405	20	150-144	12.01±0.20	14.48	271.6±25.3	144
GC990-20	514408	20	150-144	11.12±1.26	14.44	232.1±177.0	146
GC990-21	514409	20	290-250	11.58±0.23	14.41	251.6±25.3	264
GC990-22	514410	20	>1600	11.32±0.16	14.00	386.2±23.8	1519
GC990-23	514411	20	>1600	11.13±0.19	14.00	336.3±30.0	1518
GC990-24	514412	20	136-127	11.55±0.18	14.48	331.4±31.6	129
GC990-25	514413	20	115-112	11.57±0.23	14.54	254.0±30.7	112
GC990-26	514414	20	115-112	11.65±0.34	14.51	150.0±26.1	112
GC990-27	514415	20	115-112	11.75±0.17	14.51	213.4±19.9	112
GC990-28	514416	20	115-112	11.80±0.19	14.50	228.6±25.5	112
GC990-29	514417	20	115-112	11.66±0.17	14.50	208.7±13.2	112
GC990-30	514418	20	150-144	11.44±0.23	14.48	199.2±25.6	144
GC990-31	514419	20	150-144	10.99±0.22	14.46	357.2±37.7	144
GC990-32	514420	20	>250	11.75±0.24	14.41	186.3±25.3	244
GC990-33	514421	20	>250	11.81±0.20	14.36	246.3±29.5	243
GC990-34	514422	20	>500	10.91±0.20	14.29	213.9±27.9	485
GC990-35	514423	20	150-144	12.14±0.31	14.49	110.8±25.4	144
GC990-36	514424	20	115-112	11.76±0.39	14.52	263.6±57.2	112
GC990-37	514425	20	115-112	11.00±0.45	14.56	222.5±37.5	112
GC990-38	514426	20	115-112	11.74±0.24	14.59	255.2±14.6	112
GC990-39	514427	20	>2600	12.95±0.16	13.90	120.4±7.4	2449
GC990-40	514428	20	5-2	11.88±0.18	15.05	348.8±21.5	4
GC990-41	514429	20	>2600	12.56±0.26	14.11	242.9±13.3	2482
GC990-42	514430	20	145-125	11.50±0.14	14.48	339.9±37.4	133
GC990-43	514431	20	140-120	11.51±0.16	14.53	152.1±18.8	128
GC990-45	514434	20	150-144	12.69±0.38	14.49	86.3±9.5	144
GC990-46	514436	20	>1600	11.43±0.21	14.00	188.0±14.7	1518
GC990-47	514437	20	>1600	11.65±0.15	14.15	255.7±12.1	1533
GC990-48	514438	20	132-120	11.94±0.32	14.47	102.2±9.5	124
GC990-49	514439	20	132-120	12.03±0.26	14.47	129.0±17.1	124
GC990-57	514447	20	>1600	11.19±0.21	14.00	191.7±17.3	1518
GC990-58	514448	20	>1600	12.65±0.17	14.10	202.4±16.1	1531
GC990-60	514450	20	>1600	10.98±0.17	14.05	235.1±36.4	1525
GC990-61	514451	20	>1600	13.53±0.19	14.11	214.7±31.7	1527
GC990-62	514452	20	1000-540	12.53±0.56	14.23	172.7±42.7	741
GC990-64	514454	20	1600-1000	11.87±0.16	14.08	301.6±33.7	1241
GC990-66	514456	20	1600-1000	13.23±0.39	14.14	75.3±28.2	1240
GC990-68	514458	20	1600-1000	13.17±0.36	14.06	137.9±25.7	1238

Continued....\.

Table 11.1: Continued (Geotrack Report #990)

Sample number	Source number	Present temp-erature*1 (°C)	Stratigraphic age (Ma)	Mean track length (µm)	Predicted mean track length*2 (µm)	Fission track age (Ma)	Predicted fission track age*2 (Ma)
GC990-72	514466	20	1600-1000	13.00±0.38	14.06	133.2±26.3	1238
GC990-73	514467	20	1600-1000	13.93±0.40	14.16	283.7±51.4	1242
GC990-74	514468	20	1600-1000	12.95±0.22	14.04	150.7±23.2	1239
GC990-75	514469	20	>1600	±12.420.20	14.00	102.0±8.9	1518
GC990-76	514470	20	>1600	12.23±0.20	14.00	102.4±7.8	1518
GC990-77	514471	20	1600-1000	-	-	-	-
GC990-78	514472	20	1600-1000	12.03±0.68	14.05	248.5±42.9	1242
GC990-79	514473	20	1600-1000	11.46±0.34	14.21	311.1±21.7	1252
GC990-80	514474	20	1800-1600	13.95±0.78	14.02	144.1±16.3	1612
GC990-81	514475	20	1600-1000	12.68±0.61	14.04	127.2±21.2	1237
GC990-82	514476	20	>1600	11.45±0.58	14.00	121.1±15.4	1520
GC990-84	514478	20	>1600	12.50±0.32	14.00	131.7±14.4	1520
GC990-85	514479	20	>1600	12.53±0.36	14.00	139.9±11.2	1518
GC990-86	514480	20	>1600	-	14.00	107.9±10.0	1518
GC990-87	514481	20	>1600	11.98±0.58	14.01	105.5±11.9	1519
GC990-88	514482	20	>1600	12.58±0.20	14.00	159.8±15.8	1518
GC990-93	514487	20	>1600	12.21±0.21	14.00	80.3±7.3	1518
GC990-94	514488	20	>1600	11.95±0.21	14.01	103.7±7.7	1522
GC990-95	514489	20	>1600	13.21±0.46	14.02	145.6±17.0	1519
GC990-97	514491	20	>1600	12.90±0.17	14.00	75.8±4.7	1518
GC990-99	514493	20	>1600	12.89±0.14	14.00	99.7±8.3	1518
GC990-101	514495	20	>1600	12.54±0.22	14.00	114.6±9.4	1519
GC990-103	514497	20	>1600	11.48±0.96	14.20	176.2±14.9	1518
GC990-105	514499	20	>1600	12.91±0.16	14.37	340.1±22.0	1558
GC990-106	514550	20	>1600	12.51±0.23	14.18	163.8±.6	1536
GC990-107	514551	20	>1600	11.54±0.20	14.08	225.4±12.7	1527
GC990-108	514552	20	154-135	11.47±0.15	14.53	341.7±26.8	142
GC990-109	514553	20	>1600	11.73±0.16	14.07	365.2±16.7	1526
GC990-110	514554	20	>1600	12.13±0.15	14.12	333.2±21.8	1531
GC990-111	514555	20	154-135	12.19±0.29	14.50	308.1±34.3	142
GC990-113	514557	20	154-135	11.35±0.24	14.48	327.8±41.9	142
GC990-115	514559	20	>1600	11.51±0.18	14.13	324.2±19.3	1538
GC990-116	514560	20	154-135	10.94±0.46	14.45	285.8±24.0	142
GC990-119	514564	20	>570	12.67±0.25	14.20	87.8±8.1	549
GC990-120	514565	20	>570	12.67±0.19	14.20	140.3±15.7	549
GC990-122	514567	20	>570	12.70±0.16	14.20	121.6±7.5	549
GC990-123	514568	20	150-120	11.65±0.17	14.47	231.9±32.2	132
GC990-125	514570	20	435-345	11.71±0.22	14.33	338.3±25.8	378
GC990-126	514571	20	>570	12.50±0.18	14.20	109.6±7.4	549
GC990-128	514573	20	>570	13.44±0.20	14.37	119.0±8.7	556

Continued....\.

Table 11.1: Continued (Geotrack Report #990)

Sample number	Source number	Present temp-erature[*1] (°C)	Stratigraphic age (Ma)	Mean track length (µm)	Predicted mean track length[*2] (µm)	Fission track age (Ma)	Predicted fission track age[*2] (Ma)
Additional samples from Turner et al. (2008)							
GC854-1	02/01	20	>600	11.64±0.20	14.46	235.6±14.5	589
GC854-2	02/02	20	>600	12.29±0.20	14.42	274.8±13.8	587
GC854-5	02/05	20	>600	11.41±0.23	14.38	283.5±20.3	585
GC854-7	02/07	20	141-125	12.08±0.31	14.65	244.4±21.7	132
GC854-11	02/11	20	141-125	11.67±0.13	14.65	327.9±41.7	132
GC854-14	02/14	20	>600	13.46±0.17	14.38	81.3±6.8	585
GC854-16	02/16	20	>600	13.49±0.35	14.39	140.7±22.6	586
GC854-17	02/17	20	>600	12.19±0.44	14.39	97.1±13.9	585
GC854-19	02/19	20	>600	12.45±0.41	14.43	108.4±7.7	587
GC854-20	02/20	20	>600	13.27±0.13	14.38	86.5±6.0	585

[*1] See Appendix A for discussion of present temperature data.

[*2] Values predicted from the Default Thermal History (Section 2.1); i.e. assuming that each sample is now at its maximum temperature since deposition. The values refer only to tracks formed after deposition. Samples may contain tracks inherited from sediment provenance areas. Calculations refer to apatites within the measured compositional range for each sample, as discussed in Appendix A. For this reason, predicted ages may not vary smoothly with depth.

Table 11.2: Evidence for higher temperatures in the past from AFTA data in outcrop samples from Bahia State, Onshore Brazil (Geotrack Report #990)

Sample details **Sample No.** Source number Elevation Strat. Age	Evidence of higher temperatures in the past from length data?	Evidence of higher temperatures in the past from fission track age data?	Conclusion
GC990-5 BRFT06-11 0 m >2600 Ma	Yes [Mean track length is ~3.2 µm less than predicted by the Default Thermal History. Since this sample is of Precambrian basement, the discrepancy cannot be explained by inheritance of short tracks from sediment source terrains, so the sample must have been hotter at some time since the beginning of the Phanerozoic.	Yes [The central fission track age and most of the single grain ages are significantly younger than predicted on the basis of the Default Thermal History.]	This sample has been hotter than the present-day temperature during the Phanerozoic.
GC990-14 514401 0 m >2600 Ma	Yes [Mean track length is ~1.1 µm less than predicted by the Default Thermal History. Since this sample is of Precambrian basement, the discrepancy cannot be explained by inheritance of short tracks from sediment source terrains, so the sample must have been hotter at some time since the beginning of the Phanerozoic.	Yes [The Pooled fission track age is significantly younger than predicted on the basis of the Default Thermal History.]	This sample has been hotter than the present-day temperature during the Phanerozoic.
GC990-15 514402 0 m 200-146 Ma	Yes [Mean track length is ~1.8 µm less than predicted by the Default Thermal History. Modelling AFTA parameters through likely thermal history scenarios shows that the shorter tracks within this sample cannot be explained by inheritance from sediment source terrains, and must be due to higher paleotemperatures at some time after deposition.]	No [The Central fission track age is significantly older than predicted on the basis of the Default Thermal History. Single grain ages are close to or older than predicted from the Default Thermal History. No grains give fission track ages which are significantly younger than expected on this basis.]	This sample has been hotter than the present-day temperature after deposition, but heating was not sufficiently severe to produce significant age reduction. ***Note the uncertainty regarding the precise stratigraphic age of this sample.***

Note: Interpretation of AFTA data is based on comparison of measured AFTA parameters with values predicted from "Default Thermal History" (Section 2.1); i.e., assuming that each sample is now at its maximum temperature since deposition. The predicted values for each sample are summarised in Table 11.1, and refer only to tracks formed after deposition. Samples may also contain tracks inherited from sediment provenance areas, which must be allowed for in interpreting the data. Calculations refer to apatites with the compositional range appropriate to each sample, as explained in Appendix A.

Table 11.2: Continued (Geotrack Report #990)

Sample details **Sample No.** Source number Elevation Strat. Age	Evidence of higher temperatures in the past from length data?	Evidence of higher temperatures in the past from fission track age data?	Conclusion
GC990-16 514403 0 m >2600 Ma	Yes [Mean track length is ~1.2 µm less than predicted by the Default Thermal History. Since this sample is of Precambrian basement, the discrepancy cannot be explained by inheritance of short tracks from sediment source terrains, so the sample must have been hotter at some time since the beginning of the Phanerozoic.	Yes [The Pooled fission track age is significantly younger than predicted on the basis of the Default Thermal History.]	This sample has been hotter than the present-day temperature during the Phanerozoic.
GC990-17 514404 0 m >2600 Ma	Yes [Mean track length is ~2.4 µm less than predicted by the Default Thermal History. Since this sample is of Precambrian basement, the discrepancy cannot be explained by inheritance of short tracks from sediment source terrains, so the sample must have been hotter at some time since the beginning of the Phanerozoic.	Yes [The central fission track age and all of the single grain ages are significantly younger than predicted on the basis of the Default Thermal History.]	This sample has been hotter than the present-day temperature during the Phanerozoic.
GC990-18 514405 96 m 150-144 Ma	Yes [Mean track length is ~2.5 µm less than predicted by the Default Thermal History. Modelling AFTA parameters through likely thermal history scenarios shows that the shorter tracks within this sample cannot be explained by inheritance from sediment source terrains, and must be due to higher paleotemperatures at some time after deposition.]	No [The Central fission track age is significantly older than predicted on the basis of the Default Thermal History. Single grain ages are close to or older than predicted from the Default Thermal History. No grains give fission track ages which are significantly younger than expected on this basis.]	This sample has been hotter than the present-day temperature after deposition, but heating was not sufficiently severe to produce significant age reduction.

Note: Interpretation of AFTA data is based on comparison of measured AFTA parameters with values predicted from "Default Thermal History" (Section 2.1); i.e., assuming that each sample is now at its maximum temperature since deposition. The predicted values for each sample are summarised in Table 11.1, and refer only to tracks formed after deposition. Samples may also contain tracks inherited from sediment provenance areas, which must be allowed for in interpreting the data. Calculations refer to apatites with the compositional range appropriate to each sample, as explained in Appendix A.

Table 11.2: Continued (Geotrack Report #990)

Sample details **Sample No.** Source number Elevation Strat. Age	Evidence of higher temperatures in the past from length data?	Evidence of higher temperatures in the past from fission track age data?	Conclusion
GC990-20 514408 159 m 150-144 Ma	Equivocal [Mean track length is ~3.3 µm less than predicted by the Default Thermal History. Modelling AFTA parameters through likely thermal history scenarios shows that the shorter tracks within this sample can be explained either by inheritance of shorter tracks from sediment source terrains or by higher paleotemperatures at some time after deposition.]	No [The Central fission track age is significantly older than predicted on the basis of the Default Thermal History. Only two grain ages were measured in this sample, and these data are not of sufficient quality to provide a rigorous interpretation.]	AFTA data show no evidence that the sample has been hotter in the past, and are not of sufficient quality to provide a rigorous interpretation
GC990-21 514409 137 m 290-256 Ma	Yes [Mean track length is ~2.8 µm less than predicted by the Default Thermal History. Modelling AFTA parameters through likely thermal history scenarios shows that the shorter tracks within this sample cannot be explained by inheritance of shorter tracks from sediment source terrains, and must be due to higher paleotemperatures at some time after deposition.]	No [The Central fission track age is consistent with the value predicted on the basis of the Default Thermal History. No single grain ages are significantly younger than predicted on this basis.]	This sample has been hotter than the present-day temperature after deposition, but heating was not sufficiently severe to produce significant age reduction.
GC990-22 514410 136 m >1600 Ma	Yes [Mean track length is ~2.8 µm less than predicted by the Default Thermal History. Since this sample is of Precambrian basement, the discrepancy cannot be explained by inheritance of short tracks from sediment source terrains, so the sample must have been hotter at some time since the beginning of the Phanerozoic.	Yes [The Pooled fission track age is significantly younger than predicted on the basis of the Default Thermal History.]	This sample has been hotter than the present-day temperature during the Phanerozoic.

Note: Interpretation of AFTA data is based on comparison of measured AFTA parameters with values predicted from "Default Thermal History" (Section 2.1); i.e., assuming that each sample is now at its maximum temperature since deposition. The predicted values for each sample are summarised in Table 11.1, and refer only to tracks formed after deposition. Samples may also contain tracks inherited from sediment provenance areas, which must be allowed for in interpreting the data. Calculations refer to apatites with the compositional range appropriate to each sample, as explained in Appendix A.

Table 11.2: Continued (Geotrack Report #990)

Sample details **Sample No.** Source number Elevation Strat. Age	Evidence of higher temperatures in the past from length data?	Evidence of higher temperatures in the past from fission track age data?	Conclusion
GC990-23 514411 377m >1600 Ma	Yes [Mean track length is ~3 µm less than predicted by the Default Thermal History. Since this sample is of Precambrian basement, the discrepancy cannot be explained by inheritance of short tracks from sediment source terrains, so the sample must have been hotter at some time since the beginning of the Phanerozoic.	Yes [The central fission track age and most of the single grain ages are significantly younger than predicted on the basis of the Default Thermal History.]	This sample has been hotter than the present-day temperature during the Phanerozoic.
GC990-24 514412 175m 136-127 Ma	Yes [Mean track length is ~2.9 µm less than predicted by the Default Thermal History. Modelling AFTA parameters through likely thermal history scenarios shows that the shorter tracks within this sample cannot be explained by inheritance from sediment source terrains, and must be due to higher paleotemperatures at some time after deposition.]	No [The Central fission track age is significantly older than predicted on the basis of the Default Thermal History. Single grain ages are close to or older than predicted from the Default Thermal History. No grains give fission track ages which are significantly younger than expected on this basis.]	This sample has been hotter than the present-day temperature after deposition, but heating was not sufficiently severe to produce significant age reduction.
GC990-25 514413 220 m 115-112 Ma	Yes [Mean track length is ~3 µm less than predicted by the Default Thermal History. Modelling AFTA parameters through likely thermal history scenarios shows that the shorter tracks within this sample cannot be explained by inheritance from sediment source terrains, and must be due to higher paleotemperatures at some time after deposition.]	No [The Central fission track age is significantly older than predicted on the basis of the Default Thermal History. Single grain ages are close to or older than predicted from the Default Thermal History. No grains give fission track ages which are significantly younger than expected on this basis.]	This sample has been hotter than the present-day temperature after deposition, but heating was not sufficiently severe to produce significant age reduction.

Note: Interpretation of AFTA data is based on comparison of measured AFTA parameters with values predicted from "Default Thermal History" (Section 2.1); i.e., assuming that each sample is now at its maximum temperature since deposition. The predicted values for each sample are summarised in Table 11.1, and refer only to tracks formed after deposition. Samples may also contain tracks inherited from sediment provenance areas, which must be allowed for in interpreting the data. Calculations refer to apatites with the compositional range appropriate to each sample, as explained in Appendix A.

Table 11.2: Continued (Geotrack Report #990)

Sample details **Sample No.** Source number Elevation Strat. Age	Evidence of higher temperatures in the past from length data?	Evidence of higher temperatures in the past from fission track age data?	Conclusion
GC990-26 514414 340 mm 115-112 Ma	Yes [Mean track length is ~2.9 µm less than predicted by the Default Thermal History. Modelling AFTA parameters through likely thermal history scenarios shows that the shorter tracks within this sample cannot be explained by inheritance from sediment source terrains, and must be due to higher paleotemperatures at some time after deposition.]	No [The Central fission track age is significantly older than predicted on the basis of the Default Thermal History. Single grain ages are close to or older than predicted from the Default Thermal History. No grains give fission track ages which are significantly younger than expected on this basis.]	This sample has been hotter than the present-day temperature after deposition, but heating was not sufficiently severe to produce significant age reduction.
GC990-27 514415 440 m 115-112 Ma	Yes [Mean track length is ~2.8 µm less than predicted by the Default Thermal History. Modelling AFTA parameters through likely thermal history scenarios shows that the shorter tracks within this sample cannot be explained by inheritance from sediment source terrains, and must be due to higher paleotemperatures at some time after deposition.]	No [The Central fission track age is significantly older than predicted on the basis of the Default Thermal History. Single grain ages are close to or older than predicted from the Default Thermal History. No grains give fission track ages which are significantly younger than expected on this basis.]	This sample has been hotter than the present-day temperature after deposition, but heating was not sufficiently severe to produce significant age reduction.
GC990-28 514416 439 m 115-112 Ma	Yes [Mean track length is ~2.7 µm less than predicted by the Default Thermal History. Modelling AFTA parameters through likely thermal history scenarios shows that the shorter tracks within this sample cannot be explained by inheritance from sediment source terrains, and must be due to higher paleotemperatures at some time after deposition.]	No [The Central fission track age is significantly older than predicted on the basis of the Default Thermal History. Single grain ages are close to or older than predicted from the Default Thermal History. No grains give fission track ages which are significantly younger than expected on this basis.]	This sample has been hotter than the present-day temperature after deposition, but heating was not sufficiently severe to produce significant age reduction.

Note: Interpretation of AFTA data is based on comparison of measured AFTA parameters with values predicted from "Default Thermal History" (Section 2.1); i.e., assuming that each sample is now at its maximum temperature since deposition. The predicted values for each sample are summarised in Table 11.1, and refer only to tracks formed after deposition. Samples may also contain tracks inherited from sediment provenance areas, which must be allowed for in interpreting the data. Calculations refer to apatites with the compositional range appropriate to each sample, as explained in Appendix A.

Table 11.2: Continued (Geotrack Report #990)

Sample details **Sample No.** Source number Elevation Strat. Age	Evidence of higher temperatures in the past from length data?	Evidence of higher temperatures in the past from fission track age data?	Conclusion
GC990-29 514417 363 m 115-112 Ma	Yes [Mean track length is ~2.8 µm less than predicted by the Default Thermal History. Modelling AFTA parameters through likely thermal history scenarios shows that the shorter tracks within this sample cannot be explained by inheritance from sediment source terrains, and must be due to higher paleotemperatures at some time after deposition.]	No [The Pooled fission track age is significantly older than predicted on the basis of the Default Thermal History.]	This sample has been hotter than the present-day temperature after deposition, but heating was not sufficiently severe to produce significant age reduction.
GC990-30 514418 273 m 150-144 Ma	Yes [Mean track length is ~3 µm less than predicted by the Default Thermal History. Modelling AFTA parameters through likely thermal history scenarios shows that the shorter tracks within this sample cannot be explained by inheritance from sediment source terrains, and must be due to higher paleotemperatures at some time after deposition.]	No [The Central fission track age is significantly older than predicted on the basis of the Default Thermal History. Single grain ages are close to or older than predicted from the Default Thermal History. No grains give fission track ages which are significantly younger than expected on this basis.]	This sample has been hotter than the present-day temperature after deposition, but heating was not sufficiently severe to produce significant age reduction.
GC990-31 514419 303 m 150-144 Ma	Yes [Mean track length is ~3.5 µm less than predicted by the Default Thermal History. Modelling AFTA parameters through likely thermal history scenarios shows that the shorter tracks within this sample cannot be explained by inheritance from sediment source terrains, and must be due to higher paleotemperatures at some time after deposition.]	No [The Central fission track age is significantly older than predicted on the basis of the Default Thermal History. Single grain ages are close to or older than predicted from the Default Thermal History. No grains give fission track ages which are significantly younger than expected on this basis.]	This sample has been hotter than the present-day temperature after deposition, but heating was not sufficiently severe to produce significant age reduction.

Note: Interpretation of AFTA data is based on comparison of measured AFTA parameters with values predicted from "Default Thermal History" (Section 2.1); i.e., assuming that each sample is now at its maximum temperature since deposition. The predicted values for each sample are summarised in Table 11.1, and refer only to tracks formed after deposition. Samples may also contain tracks inherited from sediment provenance areas, which must be allowed for in interpreting the data. Calculations refer to apatites with the compositional range appropriate to each sample, as explained in Appendix A.

Table 11.2: Continued (Geotrack Report #990)

Sample details **Sample No.** Source number Elevation Strat. Age	Evidence of higher temperatures in the past from length data?	Evidence of higher temperatures in the past from fission track age data?	Conclusion
GC990-32 514420 294 m >250 Ma	Yes [Mean track length is ~2.6 µm less than predicted by the Default Thermal History. Modelling AFTA parameters through likely thermal history scenarios shows that the shorter tracks within this sample cannot be explained by inheritance from sediment source terrains, and must be due to higher paleotemperatures at some time after deposition.]	Yes [The Central fission track age is significantly younger than predicted on the basis of the Default Thermal History. Inspection of the single grain age vs wt% Cl trend in the Data Summary Sheet (Appendix B) shows that the most sensitive apatites (0.0-0.1 wt% Cl) give much younger ages than those with higher Cl contents, suggesting that heating was sufficient to partially reset the ages in the lowest Cl grains.]	This sample has been hotter than the present-day temperature after deposition, and heating was sufficient to partially reset fission track ages in the most sensitive grains.
GC990-33 514421 302 m >250 Ma	Yes [Mean track length is ~2.5 µm less than predicted by the Default Thermal History. Modelling AFTA parameters through likely thermal history scenarios shows that the shorter tracks within this sample cannot be explained by inheritance from sediment source terrains, and must be due to higher paleotemperatures at some time after deposition.]	No [The Central fission track age is consistent with the value predicted on the basis of the Default Thermal History. Single grain ages are close to or older than predicted from the Default Thermal History. No grains give fission track ages which are significantly younger than expected on this basis.]	This sample has been hotter than the present-day temperature after deposition, but heating was not sufficiently severe to produce significant age reduction.
GC990-34 514422 265 m >500 Ma	Yes [Mean track length is ~2.3 µm less than predicted by the Default Thermal History. Since this sample is of Precambrian basement, the discrepancy cannot be explained by inheritance of short tracks from sediment source terrains, so the sample must have been hotter at some time since the beginning of the Phanerozoic.	Yes [The central fission track age and many of the single grain ages are significantly younger than predicted on the basis of the Default Thermal History.]	This sample has been hotter than the present-day temperature during the Phanerozoic.

Note: Interpretation of AFTA data is based on comparison of measured AFTA parameters with values predicted from "Default Thermal History" (Section 2.1); i.e., assuming that each sample is now at its maximum temperature since deposition. The predicted values for each sample are summarised in Table 11.1, and refer only to tracks formed after deposition. Samples may also contain tracks inherited from sediment provenance areas, which must be allowed for in interpreting the data. Calculations refer to apatites with the compositional range appropriate to each sample, as explained in Appendix A.

Table 11.2: Continued (Geotrack Report #990)

Sample details **Sample No.** Source number Elevation Strat. Age	Evidence of higher temperatures in the past from length data?	Evidence of higher temperatures in the past from fission track age data?	Conclusion
GC990-35 514423 324 m 150-144 Ma	Yes [After removal of anomalously young ages (see right), the mean track length is ~2.3 µm less than predicted by the Default Thermal History. Modelling AFTA parameters through likely thermal history scenarios shows that the shorter tracks within this sample cannot be explained by inheritance from sediment source terrains, and must be due to higher paleotemperatures at some time after deposition.]	Possibly [a great spread of single grain ages is present in this sample, including a group of very young (<50 Ma) ages which appear to be anomalous when compared to data from other nearby samples. These young ages may possibly represent the effect of local movement of hot ground waters. After removal of these ages, the remaining grains define a Central fission track age which is significantly older than predicted on the basis of the Default Thermal History.]	This sample has been hotter than the present-day temperature after deposition. It is possible that local heating has affected some parts of this sample, but away from such effects heating was not sufficiently severe to produce significant age reduction.
GC990-36 514424 304 m 115-112 Ma	Yes (tentative) [Mean track length is ~2.7 µm less than predicted by the Default Thermal History. Modelling AFTA parameters through likely thermal history scenarios shows that the shorter tracks within this sample are best explained by higher paleotemperatures at some time after deposition, although an alternative explanation in terms of inheritance of shorter tracks from sediment source terrains cannot be entirely ruled out.]	No [The Central fission track age is significantly older than predicted on the basis of the Default Thermal History. One single grain ages is significantly younger than expected on this basis but this appears to be anomalous, as the grain contains a higher Cl content than other grains with much older ages. Other grains give ages which are close to or older than predicted from the Default Thermal History.]	This sample may have been hotter than the present-day temperature after deposition, but evidence is tentative
GC990-37 514425 251 m 115-112 Ma	Yes [Mean track length is ~3.6 µm less than predicted by the Default Thermal History. Modelling AFTA parameters through likely thermal history scenarios shows that the shorter tracks within this sample cannot be explained by inheritance from sediment source terrains, and must be due to higher paleotemperatures at some time after deposition.]	No [The Central fission track age is significantly older than predicted on the basis of the Default Thermal History. Single grain ages are close to or older than predicted from the Default Thermal History. No grains give fission track ages which are significantly younger than expected on this basis.]	This sample has been hotter than the present-day temperature after deposition, but heating was not sufficiently severe to produce significant age reduction.

Note: Interpretation of AFTA data is based on comparison of measured AFTA parameters with values predicted from "Default Thermal History" (Section 2.1); i.e., assuming that each sample is now at its maximum temperature since deposition. The predicted values for each sample are summarised in Table 11.1, and refer only to tracks formed after deposition. Samples may also contain tracks inherited from sediment provenance areas, which must be allowed for in interpreting the data. Calculations refer to apatites with the compositional range appropriate to each sample, as explained in Appendix A.

Table 11.2: Continued (Geotrack Report #990)

Sample details **Sample No.** Source number Elevation Strat. Age	Evidence of higher temperatures in the past from length data?	Evidence of higher temperatures in the past from fission track age data?	Conclusion
GC990-38 514426 188 m 115-112 Ma	Yes [Mean track length is ~2.9 µm less than predicted by the Default Thermal History. Modelling AFTA parameters through likely thermal history scenarios shows that the shorter tracks within this sample cannot be explained by inheritance from sediment source terrains, and must be due to higher paleotemperatures at some time after deposition.]	No [The Pooled fission track age is significantly older than predicted on the basis of the Default Thermal History.]	This sample has been hotter than the present-day temperature after deposition, but heating was not sufficiently severe to produce significant age reduction.
GC990-39 514427 204 m >2600 Ma	Yes [Mean track length is ~1.2 µm less than predicted by the Default Thermal History. Since this sample is of Precambrian basement, the discrepancy cannot be explained by inheritance of short tracks from sediment source terrains, so the sample must have been hotter at some time since the beginning of the Phanerozoic.]	Yes [The Pooled fission track age is significantly younger than predicted on the basis of the Default Thermal History.]	This sample has been hotter than the present-day temperature during the Phanerozoic.
GC990-40 514428 160 m 5-2 Ma	No [Mean track length is ~2.3 µm less than predicted by the Default Thermal History. Modelling AFTA parameters through likely thermal history scenarios shows that the shorter tracks within this sample can easily be explained by inheritance from sediment source terrains.]	No [The Pooled fission track age is significantly older than predicted on the basis of the Default Thermal History.]	AFTA data provide no evidence to suggest that this sample has ever been hotter than the present-day temperature.

Note: Interpretation of AFTA data is based on comparison of measured AFTA parameters with values predicted from "Default Thermal History" (Section 2.1); i.e., assuming that each sample is now at its maximum temperature since deposition. The predicted values for each sample are summarised in Table 11.1, and refer only to tracks formed after deposition. Samples may also contain tracks inherited from sediment provenance areas, which must be allowed for in interpreting the data. Calculations refer to apatites with the compositional range appropriate to each sample, as explained in Appendix A.

Table 11.2: Continued (Geotrack Report #990)

Sample details **Sample No.** Source number Elevation Strat. Age	Evidence of higher temperatures in the past from length data?	Evidence of higher temperatures in the past from fission track age data?	Conclusion
GC990-41 514429 35 m >2600 Ma	Yes [Mean track length is ~1.8 µm less than predicted by the Default Thermal History. Since this sample is of Precambrian basement, the discrepancy cannot be explained by inheritance of short tracks from sediment source terrains, so the sample must have been hotter at some time since the beginning of the Phanerozoic.]	Yes [The Pooled fission track age is significantly younger than predicted on the basis of the Default Thermal History.]	This sample has been hotter than the present-day temperature during the Phanerozoic.
GC990-42 514430 0 m 145-125 Ma	Yes [Mean track length is ~2.9 µm less than predicted by the Default Thermal History. Modelling AFTA parameters through likely thermal history scenarios shows that the shorter tracks within this sample cannot be explained by inheritance from sediment source terrains, and must be due to higher paleotemperatures at some time after deposition.]	No [The Central fission track age is significantly older than predicted on the basis of the Default Thermal History. Single grain ages are close to or older than predicted from the Default Thermal History. No grains give fission track ages which are significantly younger than expected on this basis.]	This sample has been hotter than the present-day temperature after deposition, but heating was not sufficiently severe to produce significant age reduction.
GC990-43 514431 0 m 140-120 Ma	Yes [Mean track length is ~3.0 µm less than predicted by the Default Thermal History. Modelling AFTA parameters through likely thermal history scenarios shows that the shorter tracks within this sample cannot be explained by inheritance from sediment source terrains, and must be due to higher paleotemperatures at some time after deposition.]	No [The Central fission track age is significantly older than predicted on the basis of the Default Thermal History. Single grain ages are close to or older than predicted from the Default Thermal History. No grains give fission track ages which are significantly younger than expected on this basis.]	This sample has been hotter than the present-day temperature after deposition, but heating was not sufficiently severe to produce significant age reduction.

Note: Interpretation of AFTA data is based on comparison of measured AFTA parameters with values predicted from "Default Thermal History" (Section 2.1); i.e., assuming that each sample is now at its maximum temperature since deposition. The predicted values for each sample are summarised in Table 11.1, and refer only to tracks formed after deposition. Samples may also contain tracks inherited from sediment provenance areas, which must be allowed for in interpreting the data. Calculations refer to apatites with the compositional range appropriate to each sample, as explained in Appendix A.

Table 11.2: Continued (Geotrack Report #990)

Sample details **Sample No.** Source number Elevation Strat. Age	Evidence of higher temperatures in the past from length data?	Evidence of higher temperatures in the past from fission track age data?	Conclusion
GC990-45 514434 0 m 150-144 Ma	Yes [Mean track length is ~1.8 µm less than predicted by the Default Thermal History. Modelling AFTA parameters through likely thermal history scenarios shows that the shorter tracks within this sample cannot be explained by inheritance from sediment source terrains, and must be due to higher paleotemperatures at some time after deposition.]	Yes [The Pooled fission track age is significantly younger than predicted on the basis of the Default Thermal History.]	This sample has been hotter than the present-day temperature after deposition.
GC990-46 514436 27 m >1600 Ma	Yes [Mean track length is ~2.8 µm less than predicted by the Default Thermal History. Since this sample is of Precambrian basement, the discrepancy cannot be explained by inheritance of short tracks from sediment source terrains, so the sample must have been hotter at some time since the beginning of the Phanerozoic.	Yes [The central fission track age and all of the single grain ages are significantly younger than predicted on the basis of the Default Thermal History.]	This sample has been hotter than the present-day temperature during the Phanerozoic.
GC990-47 514437 100 m >1600 Ma	Yes [Mean track length is ~2.5 µm less than predicted by the Default Thermal History. Since this sample is of Precambrian basement, the discrepancy cannot be explained by inheritance of short tracks from sediment source terrains, so the sample must have been hotter at some time since the beginning of the Phanerozoic.]	Yes [The Pooled fission track age is significantly younger than predicted on the basis of the Default Thermal History.]	This sample has been hotter than the present-day temperature during the Phanerozoic.

Note: Interpretation of AFTA data is based on comparison of measured AFTA parameters with values predicted from "Default Thermal History" (Section 2.1); i.e., assuming that each sample is now at its maximum temperature since deposition. The predicted values for each sample are summarised in Table 11.1, and refer only to tracks formed after deposition. Samples may also contain tracks inherited from sediment provenance areas, which must be allowed for in interpreting the data. Calculations refer to apatites with the compositional range appropriate to each sample, as explained in Appendix A.

Table 11.2: Continued (Geotrack Report #990)

Sample details **Sample No.** Source number Elevation Strat. Age	Evidence of higher temperatures in the past from length data?	Evidence of higher temperatures in the past from fission track age data?	Conclusion
GC990-48 514438 50 m 132-120 Ma	Yes [Mean track length is ~2.5 µm less than predicted by the Default Thermal History. Modelling AFTA parameters through likely thermal history scenarios shows that the shorter tracks within this sample cannot be explained by inheritance from sediment source terrains, and must be due to higher paleotemperatures at some time after deposition.]	Yes [The Central fission track age and most of the single grain ages are significantly younger than predicted on the basis of the Default Thermal History.]	This sample has been hotter than the present-day temperature after deposition.
GC990-49 514439 42 m 132-120 Ma	Yes [Mean track length is ~2.4 µm less than predicted by the Default Thermal History. Modelling AFTA parameters through likely thermal history scenarios shows that the shorter tracks within this sample cannot be explained by inheritance from sediment source terrains, and must be due to higher paleotemperatures at some time after deposition.]	Yes [Although the Central fission track age is consistent with the value predicted by the Default Thermal History, most of the single grain ages in the most sensitive apatites, i.e those containing less than 0.1 wt% Cl, are significantly younger than predicted on this basis.]	This sample has been hotter than the present-day temperature after deposition.
GC990-57 514447 288 m >1600 Ma	Yes [Mean track length is ~2.8 µm less than predicted by the Default Thermal History. Since this sample is of Precambrian basement, the discrepancy cannot be explained by inheritance of short tracks from sediment source terrains, so the sample must have been hotter at some time since the beginning of the Phanerozoic.	Yes [The central fission track age and all of the single grain ages are significantly younger than predicted on the basis of the Default Thermal History.]	This sample has been hotter than the present-day temperature during the Phanerozoic.

Note: Interpretation of AFTA data is based on comparison of measured AFTA parameters with values predicted from "Default Thermal History" (Section 2.1); i.e., assuming that each sample is now at its maximum temperature since deposition. The predicted values for each sample are summarised in Table 11.1, and refer only to tracks formed after deposition. Samples may also contain tracks inherited from sediment provenance areas, which must be allowed for in interpreting the data. Calculations refer to apatites with the compositional range appropriate to each sample, as explained in Appendix A.

Table 11.2: Continued (Geotrack Report #990)

Sample details **Sample No.** Source number Elevation Strat. Age	Evidence of higher temperatures in the past from length data?	Evidence of higher temperatures in the past from fission track age data?	Conclusion
GC990-58 514448 167 m >1600 Ma	Yes [Mean track length is ~1.5 µm less than predicted by the Default Thermal History. Since this sample is of Precambrian basement, the discrepancy cannot be explained by inheritance of short tracks from sediment source terrains, so the sample must have been hotter at some time since the beginning of the Phanerozoic.	Yes [The central fission track age and all of the single grain ages are significantly younger than predicted on the basis of the Default Thermal History.]	This sample has been hotter than the present-day temperature during the Phanerozoic.
GC990-60 514450 250 m >1600 Ma	Yes [Mean track length is ~1.5 µm less than predicted by the Default Thermal History. Since this sample is of Precambrian basement, the discrepancy cannot be explained by inheritance of short tracks from sediment source terrains, so the sample must have been hotter at some time since the beginning of the Phanerozoic.	Yes [The central fission track age and all of the single grain ages are significantly younger than predicted on the basis of the Default Thermal History. In detail, the sample contains a number of grains giving very young (<100 Ma) ages, which appear anomalous within the context of the remaining ages, and these have been eliminated from the dataset prior to extraction of a thermal history solution. These grains may reflect further complication to the thermal history of this sample.]	This sample has been hotter than the present-day temperature during the Phanerozoic.
GC990-61 514451 600 m >1600 Ma	Yes [Mean track length is ~0.6 µm less than predicted by the Default Thermal History. Since this sample is of Precambrian basement, the discrepancy cannot be explained by inheritance of short tracks from sediment source terrains, so the sample must have been hotter at some time since the beginning of the Phanerozoic.	Yes [The central fission track age and all of the single grain ages are significantly younger than predicted on the basis of the Default Thermal History.]	This sample has been hotter than the present-day temperature during the Phanerozoic.

Note: Interpretation of AFTA data is based on comparison of measured AFTA parameters with values predicted from "Default Thermal History" (Section 2.1); i.e., assuming that each sample is now at its maximum temperature since deposition. The predicted values for each sample are summarised in Table 11.1, and refer only to tracks formed after deposition. Samples may also contain tracks inherited from sediment provenance areas, which must be allowed for in interpreting the data. Calculations refer to apatites with the compositional range appropriate to each sample, as explained in Appendix A.

Table 11.2: Continued (Geotrack Report #990)

Sample details **Sample No.** Source number Elevation Strat. Age	Evidence of higher temperatures in the past from length data?	Evidence of higher temperatures in the past from fission track age data?	Conclusion
GC990-62 514452 330 m 1000-540 Ma	Yes [Mean track length is ~1.7 µm less than predicted by the Default Thermal History. Since this sample is of Precambrian basement, the discrepancy cannot be explained by inheritance of short tracks from sediment source terrains, so the sample must have been hotter at some time since the beginning of the Phanerozoic.	Yes [The central fission track age and all of the single grain ages are significantly younger than predicted on the basis of the Default Thermal History.]	This sample has been hotter than the present-day temperature during the Phanerozoic.
GC990-64 514454 800 m 1600-1000 Ma	Yes [Mean track length is ~2.2 µm less than predicted by the Default Thermal History. Since this sample is of Precambrian basement, the discrepancy cannot be explained by inheritance of short tracks from sediment source terrains, so the sample must have been hotter at some time since the beginning of the Phanerozoic.	Yes [The central fission track age and almost all of the single grain ages are significantly younger than predicted on the basis of the Default Thermal History. In detail, the sample contains a number of grains giving younger (<100 Ma) ages which appear anomalous within the context of the remaining ages, and these have been eliminated from the dataset prior to extraction of a thermal history solution. These grains may reflect further complication to the thermal history of this sample.]	This sample has been hotter than the present-day temperature during the Phanerozoic.
GC990-66 514456 498 m 1600-1000 Ma	Yes [Mean track length is ~0.9 µm less than predicted by the Default Thermal History. Since this sample is of Precambrian basement, the discrepancy cannot be explained by inheritance of short tracks from sediment source terrains, so the sample must have been hotter at some time since the beginning of the Phanerozoic.	Yes [The central fission track age and all of the single grain ages are significantly younger than predicted on the basis of the Default Thermal History.]	This sample has been hotter than the present-day temperature during the Phanerozoic.

Note: Interpretation of AFTA data is based on comparison of measured AFTA parameters with values predicted from "Default Thermal History" (Section 2.1); i.e., assuming that each sample is now at its maximum temperature since deposition. The predicted values for each sample are summarised in Table 11.1, and refer only to tracks formed after deposition. Samples may also contain tracks inherited from sediment provenance areas, which must be allowed for in interpreting the data. Calculations refer to apatites with the compositional range appropriate to each sample, as explained in Appendix A.

Table 11.2: Continued (Geotrack Report #990)

Sample details **Sample No.** Source number Elevation Strat. Age	Evidence of higher temperatures in the past from length data?	Evidence of higher temperatures in the past from fission track age data?	Conclusion
GC990-68 514458 1212 m 1600-1000 Ma	Yes [Mean track length is ~0.9 µm less than predicted by the Default Thermal History. Since this sample is of Precambrian basement, the discrepancy cannot be explained by inheritance of short tracks from sediment source terrains, so the sample must have been hotter at some time since the beginning of the Phanerozoic.]	Yes [The central fission track age and all of the single grain ages are significantly younger than predicted on the basis of the Default Thermal History.]	This sample has been hotter than the present-day temperature during the Phanerozoic.
GC990-72 514466 1033 m 1600-1000 Ma	Yes [Mean track length is ~1.0 µm less than predicted by the Default Thermal History. Since this sample is of Precambrian basement, the discrepancy cannot be explained by inheritance of short tracks from sediment source terrains, so the sample must have been hotter at some time since the beginning of the Phanerozoic.]	Yes [The central fission track age and all of the single grain ages are significantly younger than predicted on the basis of the Default Thermal History.]	This sample has been hotter than the present-day temperature during the Phanerozoic.
GC990-73 514467 1312 m 1600-1000 Ma	No [Mean track length is consistent with the value predicted by the Default Thermal History.]	Yes [The Pooled fission track age is significantly younger than predicted on the basis of the Default Thermal History.]	This sample has been hotter than the present-day temperature during the Phanerozoic.
GC990-74 514468 1025 m 1600-1000 Ma	Yes [Mean track length is ~1.0 µm less than predicted by the Default Thermal History. Since this sample is of Precambrian basement, the discrepancy cannot be explained by inheritance of short tracks from sediment source terrains, so the sample must have been hotter at some time since the beginning of the Phanerozoic.]	Yes [The central fission track age and all of the single grain ages are significantly younger than predicted on the basis of the Default Thermal History.]	This sample has been hotter than the present-day temperature during the Phanerozoic.

Note: Interpretation of AFTA data is based on comparison of measured AFTA parameters with values predicted from "Default Thermal History" (Section 2.1); i.e., assuming that each sample is now at its maximum temperature since deposition. The predicted values for each sample are summarised in Table 11.1, and refer only to tracks formed after deposition. Samples may also contain tracks inherited from sediment provenance areas, which must be allowed for in interpreting the data. Calculations refer to apatites with the compositional range appropriate to each sample, as explained in Appendix A.

Table 11.2: Continued (Geotrack Report #990)

Sample details **Sample No.** Source number Elevation Strat. Age	Evidence of higher temperatures in the past from length data?	Evidence of higher temperatures in the past from fission track age data?	Conclusion
GC990-75 514469 741 m >1600 Ma	Yes [Mean track length is ~1.6 µm less than predicted by the Default Thermal History. Since this sample is of Precambrian basement, the discrepancy cannot be explained by inheritance of short tracks from sediment source terrains, so the sample must have been hotter at some time since the beginning of the Phanerozoic.]	Yes [The central fission track age and all of the single grain ages are significantly younger than predicted on the basis of the Default Thermal History.]	This sample has been hotter than the present-day temperature during the Phanerozoic.
GC990-76 514470 529 m >1600 Ma	Yes [Mean track length is ~1.8 µm less than predicted by the Default Thermal History. Since this sample is of Precambrian basement, the discrepancy cannot be explained by inheritance of short tracks from sediment source terrains, so the sample must have been hotter at some time since the beginning of the Phanerozoic.]	Yes [The central fission track age and all of the single grain ages are significantly younger than predicted on the basis of the Default Thermal History.]	This sample has been hotter than the present-day temperature during the Phanerozoic.
GC990-77 514471 1575 m 1600-1000 Ma	-	-	No apatite
GC990-78 514472 1309 m 1600-1000 Ma	Yes [Mean track length is ~1.8 µm less than predicted by the Default Thermal History. Since this sample is of Precambrian basement, the discrepancy cannot be explained by inheritance of short tracks from sediment source terrains, so the sample must have been hotter at some time since the beginning of the Phanerozoic.]	Yes [The central fission track age and all of the single grain ages are significantly younger than predicted on the basis of the Default Thermal History. In detail, the sample contains one grain giving a much younger age (~11 Ma) which appears anomalous within the context of the other ages, and this has been eliminated from the dataset prior to extraction of a thermal history solution.]	This sample has been hotter than the present-day temperature during the Phanerozoic.

Note: Interpretation of AFTA data is based on comparison of measured AFTA parameters with values predicted from "Default Thermal History" (Section 2.1); i.e., assuming that each sample is now at its maximum temperature since deposition. The predicted values for each sample are summarised in Table 11.1, and refer only to tracks formed after deposition. Samples may also contain tracks inherited from sediment provenance areas, which must be allowed for in interpreting the data. Calculations refer to apatites with the compositional range appropriate to each sample, as explained in Appendix A.

Table 11.2: Continued (Geotrack Report #990)

Sample details **Sample No.** Source number Elevation Strat. Age	Evidence of higher temperatures in the past from length data?	Evidence of higher temperatures in the past from fission track age data?	Conclusion
GC990-79 514473 1040 m 1600-1000 Ma	Yes [Mean track length is ~2.7 µm less than predicted by the Default Thermal History. Since this sample is of Precambrian basement, the discrepancy cannot be explained by inheritance of short tracks from sediment source terrains, so the sample must have been hotter at some time since the beginning of the Phanerozoic.]	Yes [The Pooled fission track age is significantly younger than predicted on the basis of the Default Thermal History.]	This sample has been hotter than the present-day temperature during the Phanerozoic.
GC990-80 514474 543 m 1800-1600 Ma	No [Mean track length is consistent with the value predicted by the Default Thermal History.]	Yes [The central fission track age and all of the single grain ages are significantly younger than predicted on the basis of the Default Thermal History.]	This sample has been hotter than the present-day temperature during the Phanerozoic.
GC990-81 514475 891 m 1600-1000 Ma	Yes [Mean track length is ~1.3 µm less than predicted by the Default Thermal History. Since this sample is of Precambrian basement, the discrepancy cannot be explained by inheritance of short tracks from sediment source terrains, so the sample must have been hotter at some time since the beginning of the Phanerozoic.]	Yes [The central fission track age and all of the single grain ages are significantly younger than predicted on the basis of the Default Thermal History.]	This sample has been hotter than the present-day temperature during the Phanerozoic.
GC990-82 514476 404 m >1600 Ma	Yes [Mean track length is ~2.5 µm less than predicted by the Default Thermal History. Since this sample is of Precambrian basement, the discrepancy cannot be explained by inheritance of short tracks from sediment source terrains, so the sample must have been hotter at some time since the beginning of the Phanerozoic.]	Yes [The central fission track age and all of the single grain ages are significantly younger than predicted on the basis of the Default Thermal History.]	This sample has been hotter than the present-day temperature during the Phanerozoic.

Note: Interpretation of AFTA data is based on comparison of measured AFTA parameters with values predicted from "Default Thermal History" (Section 2.1); i.e., assuming that each sample is now at its maximum temperature since deposition. The predicted values for each sample are summarised in Table 11.1, and refer only to tracks formed after deposition. Samples may also contain tracks inherited from sediment provenance areas, which must be allowed for in interpreting the data. Calculations refer to apatites with the compositional range appropriate to each sample, as explained in Appendix A.

Table 11.2: Continued (Geotrack Report #990)

Sample details **Sample No.** Source number Elevation Strat. Age	Evidence of higher temperatures in the past from length data?	Evidence of higher temperatures in the past from fission track age data?	Conclusion
GC990-84 514478 744 m >1600 Ma	Yes [Mean track length is ~1.5 µm less than predicted by the Default Thermal History. Since this sample is of Precambrian basement, the discrepancy cannot be explained by inheritance of short tracks from sediment source terrains, so the sample must have been hotter at some time since the beginning of the Phanerozoic.]	Yes [The central fission track age and all of the single grain ages are significantly younger than predicted on the basis of the Default Thermal History.]	This sample has been hotter than the present-day temperature during the Phanerozoic.
GC990-85 514479 377 m >1600 Ma	Yes [Mean track length is ~1.5 µm less than predicted by the Default Thermal History. Since this sample is of Precambrian basement, the discrepancy cannot be explained by inheritance of short tracks from sediment source terrains, so the sample must have been hotter at some time since the beginning of the Phanerozoic.]	Yes [The Pooled fission track age is significantly younger than predicted on the basis of the Default Thermal History.]	This sample has been hotter than the present-day temperature during the Phanerozoic.
GC990-86 514480 594 m >1600 Ma	- [No track lengths.]	Yes [The Pooled fission track age is significantly younger than predicted on the basis of the Default Thermal History.]	This sample has been hotter than the present-day temperature during the Phanerozoic.
GC990-87 514481 806 m >1600 Ma	Yes [Mean track length is ~2.0 µm less than predicted by the Default Thermal History. Since this sample is of Precambrian basement, the discrepancy cannot be explained by inheritance of short tracks from sediment source terrains, so the sample must have been hotter at some time since the beginning of the Phanerozoic.]	Yes [The central fission track age and all of the single grain ages are significantly younger than predicted on the basis of the Default Thermal History.]	This sample has been hotter than the present-day temperature during the Phanerozoic.

Note: Interpretation of AFTA data is based on comparison of measured AFTA parameters with values predicted from "Default Thermal History" (Section 2.1); i.e., assuming that each sample is now at its maximum temperature since deposition. The predicted values for each sample are summarised in Table 11.1, and refer only to tracks formed after deposition. Samples may also contain tracks inherited from sediment provenance areas, which must be allowed for in interpreting the data. Calculations refer to apatites with the compositional range appropriate to each sample, as explained in Appendix A.

Table 11.2: Continued (Geotrack Report #990)

Sample details **Sample No.** Source number Elevation Strat. Age	Evidence of higher temperatures in the past from length data?	Evidence of higher temperatures in the past from fission track age data?	Conclusion
GC990-88 514482 1055 m >1600 Ma	Yes [Mean track length is ~1.4 µm less than predicted by the Default Thermal History. Since this sample is of Precambrian basement, the discrepancy cannot be explained by inheritance of short tracks from sediment source terrains, so the sample must have been hotter at some time since the beginning of the Phanerozoic.]	Yes [The central fission track age and all of the single grain ages are significantly younger than predicted on the basis of the Default Thermal History.]	This sample has been hotter than the present-day temperature during the Phanerozoic.
GC990-93 514487 737 m >1600 Ma	Yes [Mean track length is ~1.8 µm less than predicted by the Default Thermal History. Since this sample is of Precambrian basement, the discrepancy cannot be explained by inheritance of short tracks from sediment source terrains, so the sample must have been hotter at some time since the beginning of the Phanerozoic.]	Yes [The Pooled fission track age is significantly younger than predicted on the basis of the Default Thermal History.]	This sample has been hotter than the present-day temperature during the Phanerozoic.
GC990-94 514488 500 m >1600 Ma	Yes [Mean track length is ~2 µm less than predicted by the Default Thermal History. Since this sample is of Precambrian basement, the discrepancy cannot be explained by inheritance of short tracks from sediment source terrains, so the sample must have been hotter at some time since the beginning of the Phanerozoic.]	Yes [The Pooled fission track age is significantly younger than predicted on the basis of the Default Thermal History.]	This sample has been hotter than the present-day temperature during the Phanerozoic.
GC990-95 514489 349 m >1600 Ma	No [Mean track length is consistent with the value predicted by the Default Thermal History.]	Yes [The Pooled fission track age is significantly younger than predicted on the basis of the Default Thermal History.]	This sample has been hotter than the present-day temperature during the Phanerozoic.

Note: Interpretation of AFTA data is based on comparison of measured AFTA parameters with values predicted from "Default Thermal History" (Section 2.1); i.e., assuming that each sample is now at its maximum temperature since deposition. The predicted values for each sample are summarised in Table 11.1, and refer only to tracks formed after deposition. Samples may also contain tracks inherited from sediment provenance areas, which must be allowed for in interpreting the data. Calculations refer to apatites with the compositional range appropriate to each sample, as explained in Appendix A.

Table 11.2: Continued (Geotrack Report #990)

Sample details **Sample No.** Source number Elevation Strat. Age	Evidence of higher temperatures in the past from length data?	Evidence of higher temperatures in the past from fission track age data?	Conclusion
GC990-97 514491 244 m >1600 Ma	Yes [Mean track length is ~1.1 µm less than predicted by the Default Thermal History. Since this sample is of Precambrian basement, the discrepancy cannot be explained by inheritance of short tracks from sediment source terrains, so the sample must have been hotter at some time since the beginning of the Phanerozoic.]	Yes [The central fission track age and all of the single grain ages are significantly younger than predicted on the basis of the Default Thermal History.]	This sample has been hotter than the present-day temperature during the Phanerozoic.
GC990-99 514493 222 m >1600 Ma	Yes [Mean track length is ~1.1 µm less than predicted by the Default Thermal History. Since this sample is of Precambrian basement, the discrepancy cannot be explained by inheritance of short tracks from sediment source terrains, so the sample must have been hotter at some time since the beginning of the Phanerozoic.]	Yes [The central fission track age and all of the single grain ages are significantly younger than predicted on the basis of the Default Thermal History.]	This sample has been hotter than the present-day temperature during the Phanerozoic.
GC990-101 514495 109 m >1600 Ma	Yes [Mean track length is ~1.5 µm less than predicted by the Default Thermal History. Since this sample is of Precambrian basement, the discrepancy cannot be explained by inheritance of short tracks from sediment source terrains, so the sample must have been hotter at some time since the beginning of the Phanerozoic.]	Yes [The Pooled fission track age is significantly younger than predicted on the basis of the Default Thermal History.]	This sample has been hotter than the present-day temperature during the Phanerozoic.

Note: Interpretation of AFTA data is based on comparison of measured AFTA parameters with values predicted from "Default Thermal History" (Section 2.1); i.e., assuming that each sample is now at its maximum temperature since deposition. The predicted values for each sample are summarised in Table 11.1, and refer only to tracks formed after deposition. Samples may also contain tracks inherited from sediment provenance areas, which must be allowed for in interpreting the data. Calculations refer to apatites with the compositional range appropriate to each sample, as explained in Appendix A.

Table 11.2: Continued (Geotrack Report #990)

Sample details **Sample No.** Source number Elevation Strat. Age	Evidence of higher temperatures in the past from length data?	Evidence of higher temperatures in the past from fission track age data?	Conclusion
GC990-103 514497 9 m >1600 Ma	Yes [Mean track length is ~2.7 µm less than predicted by the Default Thermal History. Since this sample is of Precambrian basement, the discrepancy cannot be explained by inheritance of short tracks from sediment source terrains, so the sample must have been hotter at some time since the beginning of the Phanerozoic.]	Yes [The Pooled fission track age is significantly younger than predicted on the basis of the Default Thermal History.]	This sample has been hotter than the present-day temperature during the Phanerozoic.
GC990-105 514499 0 m >1600 Ma	Yes [Mean track length is ~1.4 µm less than predicted by the Default Thermal History. Since this sample is of Precambrian basement, the discrepancy cannot be explained by inheritance of short tracks from sediment source terrains, so the sample must have been hotter at some time since the beginning of the Phanerozoic.]	Yes [The Pooled fission track age is significantly younger than predicted on the basis of the Default Thermal History.]	This sample has been hotter than the present-day temperature during the Phanerozoic.
GC990-106 514550 109 m >1600 Ma	Yes [Mean track length is ~1.7 µm less than predicted by the Default Thermal History. Since this sample is of Precambrian basement, the discrepancy cannot be explained by inheritance of short tracks from sediment source terrains, so the sample must have been hotter at some time since the beginning of the Phanerozoic.]	Yes [The Pooled fission track age is significantly younger than predicted on the basis of the Default Thermal History.]	This sample has been hotter than the present-day temperature during the Phanerozoic.

Note: Interpretation of AFTA data is based on comparison of measured AFTA parameters with values predicted from "Default Thermal History" (Section 2.1); i.e., assuming that each sample is now at its maximum temperature since deposition. The predicted values for each sample are summarised in Table 11.1, and refer only to tracks formed after deposition. Samples may also contain tracks inherited from sediment provenance areas, which must be allowed for in interpreting the data. Calculations refer to apatites with the compositional range appropriate to each sample, as explained in Appendix A.

Table 11.2: Continued (Geotrack Report #990)

Sample details **Sample No.** Source number Elevation Strat. Age	Evidence of higher temperatures in the past from length data?	Evidence of higher temperatures in the past from fission track age data?	Conclusion
GC990-107 514551 82 m >1600 Ma	Yes [Mean track length is ~2.6 µm less than predicted by the Default Thermal History. Since this sample is of Precambrian basement, the discrepancy cannot be explained by inheritance of short tracks from sediment source terrains, so the sample must have been hotter at some time since the beginning of the Phanerozoic.]	Yes [The central fission track age and all of the single grain ages are significantly younger than predicted on the basis of the Default Thermal History.]	This sample has been hotter than the present-day temperature during the Phanerozoic.
GC990-108 514552 19 m 154-135 Ma	Yes [Mean track length is ~3 µm less than predicted by the Default Thermal History. Modelling AFTA parameters through likely thermal history scenarios shows that the shorter tracks within this sample cannot be explained by inheritance from sediment source terrains, and must be due to higher paleotemperatures at some time after deposition.]	No [The Central fission track age is significantly older than predicted on the basis of the Default Thermal History. Single grain ages are close to or older than predicted from the Default Thermal History. No grains give fission track ages which are significantly younger than expected on this basis.]	This sample has been hotter than the present-day temperature after deposition, but heating was not sufficiently severe to produce significant age reduction.
GC990-109 514553 18 m >1600 Ma	Yes [Mean track length is ~2.3 µm less than predicted by the Default Thermal History. Since this sample is of Precambrian basement, the discrepancy cannot be explained by inheritance of short tracks from sediment source terrains, so the sample must have been hotter at some time since the beginning of the Phanerozoic.]	Yes [The Pooled fission track age is significantly younger than predicted on the basis of the Default Thermal History.]	This sample has been hotter than the present-day temperature during the Phanerozoic.

Note: Interpretation of AFTA data is based on comparison of measured AFTA parameters with values predicted from "Default Thermal History" (Section 2.1); i.e., assuming that each sample is now at its maximum temperature since deposition. The predicted values for each sample are summarised in Table 11.1, and refer only to tracks formed after deposition. Samples may also contain tracks inherited from sediment provenance areas, which must be allowed for in interpreting the data. Calculations refer to apatites with the compositional range appropriate to each sample, as explained in Appendix A.

Table 11.2: Continued (Geotrack Report #990)

Sample details **Sample No.** Source number Elevation Strat. Age	Evidence of higher temperatures in the past from length data?	Evidence of higher temperatures in the past from fission track age data?	Conclusion
GC990-110 514554 10 m >1600 Ma	Yes [Mean track length is ~2 µm less than predicted by the Default Thermal History. Since this sample is of Precambrian basement, the discrepancy cannot be explained by inheritance of short tracks from sediment source terrains, so the sample must have been hotter at some time since the beginning of the Phanerozoic.]	Yes [The Pooled fission track age is significantly younger than predicted on the basis of the Default Thermal History.]	This sample has been hotter than the present-day temperature during the Phanerozoic.
GC990-111 514555 20 m 154-135 Ma	Yes [Mean track length is ~2.3 µm less than predicted by the Default Thermal History. Modelling AFTA parameters through likely thermal history scenarios shows that the shorter tracks within this sample cannot be explained by inheritance from sediment source terrains, and must be due to higher paleotemperatures at some time after deposition.]	No [The Central fission track age is significantly older than predicted on the basis of the Default Thermal History. Single grain ages are close to or older than predicted from the Default Thermal History. No grains give fission track ages which are significantly younger than expected on this basis.]	This sample has been hotter than the present-day temperature after deposition, but heating was not sufficiently severe to produce significant age reduction.
GC990-113 514557 17 m 154-135 Ma	Yes [Mean track length is ~3.1 µm less than predicted by the Default Thermal History. Modelling AFTA parameters through likely thermal history scenarios shows that the shorter tracks within this sample cannot be explained by inheritance from sediment source terrains, and must be due to higher paleotemperatures at some time after deposition.]	No [The Central fission track age is significantly older than predicted on the basis of the Default Thermal History. Single grain ages are close to or older than predicted from the Default Thermal History. No grains give fission track ages which are significantly younger than expected on this basis.]	This sample has been hotter than the present-day temperature after deposition, but heating was not sufficiently severe to produce significant age reduction.

Note: Interpretation of AFTA data is based on comparison of measured AFTA parameters with values predicted from "Default Thermal History" (Section 2.1); i.e., assuming that each sample is now at its maximum temperature since deposition. The predicted values for each sample are summarised in Table 11.1, and refer only to tracks formed after deposition. Samples may also contain tracks inherited from sediment provenance areas, which must be allowed for in interpreting the data. Calculations refer to apatites with the compositional range appropriate to each sample, as explained in Appendix A.

Table 11.2: Continued (Geotrack Report #990)

Sample details **Sample No.** Source number Elevation Strat. Age	Evidence of higher temperatures in the past from length data?	Evidence of higher temperatures in the past from fission track age data?	Conclusion
GC990-115 514559 22 m >1600 Ma	Yes [Mean track length is ~2.6 µm less than predicted by the Default Thermal History. Since this sample is of Precambrian basement, the discrepancy cannot be explained by inheritance of short tracks from sediment source terrains, so the sample must have been hotter at some time since the beginning of the Phanerozoic.]	Yes [The Pooled fission track age is significantly younger than predicted on the basis of the Default Thermal History.]	This sample has been hotter than the present-day temperature during the Phanerozoic.
GC990-116 514560 16 m 154-135 Ma	Yes [Mean track length is ~3.5 µm less than predicted by the Default Thermal History. Modelling AFTA parameters through likely thermal history scenarios shows that the shorter tracks within this sample cannot be explained by inheritance from sediment source terrains, and must be due to higher paleotemperatures at some time after deposition.]	No [The Central fission track age is significantly older than predicted on the basis of the Default Thermal History. Single grain ages are close to or older than predicted from the Default Thermal History. No grains give fission track ages which are significantly younger than expected on this basis.]	This sample has been hotter than the present-day temperature after deposition, but heating was not sufficiently severe to produce significant age reduction.
GC990-119 514564 316 m >570 Ma	Yes [Mean track length is ~1.7 µm less than predicted by the Default Thermal History. Since this sample is of Precambrian basement, the discrepancy cannot be explained by inheritance of short tracks from sediment source terrains, so the sample must have been hotter at some time since the beginning of the Phanerozoic.]	Yes [The Pooled fission track age is significantly younger than predicted on the basis of the Default Thermal History.]	This sample has been hotter than the present-day temperature during the Phanerozoic.

Note: Interpretation of AFTA data is based on comparison of measured AFTA parameters with values predicted from "Default Thermal History" (Section 2.1); i.e., assuming that each sample is now at its maximum temperature since deposition. The predicted values for each sample are summarised in Table 11.1, and refer only to tracks formed after deposition. Samples may also contain tracks inherited from sediment provenance areas, which must be allowed for in interpreting the data. Calculations refer to apatites with the compositional range appropriate to each sample, as explained in Appendix A.

Table 11.2: Continued (Geotrack Report #990)

Sample details **Sample No.** Source number Elevation Strat. Age	Evidence of higher temperatures in the past from length data?	Evidence of higher temperatures in the past from fission track age data?	Conclusion
GC990-120 514565 57 m >570 Ma	Yes [Mean track length is ~1.5 µm less than predicted by the Default Thermal History. Since this sample is of Precambrian basement, the discrepancy cannot be explained by inheritance of short tracks from sediment source terrains, so the sample must have been hotter at some time since the beginning of the Phanerozoic.]	Yes [The central fission track age and all of the single grain ages are significantly younger than predicted on the basis of the Default Thermal History.]	This sample has been hotter than the present-day temperature during the Phanerozoic.
GC990-122 514567 253 m >570 Ma	Yes [Mean track length is ~1.5 µm less than predicted by the Default Thermal History. Since this sample is of Precambrian basement, the discrepancy cannot be explained by inheritance of short tracks from sediment source terrains, so the sample must have been hotter at some time since the beginning of the Phanerozoic.]	Yes [The central fission track age and all of the single grain ages are significantly younger than predicted on the basis of the Default Thermal History.]	This sample has been hotter than the present-day temperature during the Phanerozoic.
GC990-123 514568 359 m 150-120 Ma	Yes [Mean track length is ~2.8 µm less than predicted by the Default Thermal History. Modelling AFTA parameters through likely thermal history scenarios shows that the shorter tracks within this sample cannot be explained by inheritance from sediment source terrains, and must be due to higher paleotemperatures at some time after deposition.]	No [The Central fission track age is significantly older than predicted on the basis of the Default Thermal History. Single grain ages are close to or older than predicted from the Default Thermal History. No grains give fission track ages which are significantly younger than expected on this basis.]	This sample has been hotter than the present-day temperature after deposition, but heating was not sufficiently severe to produce significant age reduction.

Note: Interpretation of AFTA data is based on comparison of measured AFTA parameters with values predicted from "Default Thermal History" (Section 2.1); i.e., assuming that each sample is now at its maximum temperature since deposition. The predicted values for each sample are summarised in Table 11.1, and refer only to tracks formed after deposition. Samples may also contain tracks inherited from sediment provenance areas, which must be allowed for in interpreting the data. Calculations refer to apatites with the compositional range appropriate to each sample, as explained in Appendix A.

Table 11.2: Continued (Geotrack Report #990)

Sample details **Sample No.** Source number Elevation Strat. Age	Evidence of higher temperatures in the past from length data?	Evidence of higher temperatures in the past from fission track age data?	Conclusion
GC990-125 514570 282 m 435-345 Ma	Yes [Mean track length is ~2.6 µm less than predicted by the Default Thermal History. Modelling AFTA parameters through likely thermal history scenarios shows that the shorter tracks within this sample cannot be explained by inheritance from sediment source terrains, and must be due to higher paleotemperatures at some time after deposition.]	Yes [The Central fission track age and many of the single grain ages (particularly in the more sensitive compositions containing <0.1 wt% Cl) are significantly younger than predicted on the basis of the Default Thermal History.]	This sample has been hotter than the present-day temperature after deposition.
GC990-126 514571 204 m >570 Ma	Yes [Mean track length is ~1.7 µm less than predicted by the Default Thermal History. Since this sample is of Precambrian basement, the discrepancy cannot be explained by inheritance of short tracks from sediment source terrains, so the sample must have been hotter at some time since the beginning of the Phanerozoic.]	Yes [The central fission track age and all of the single grain ages are significantly younger than predicted on the basis of the Default Thermal History.]	This sample has been hotter than the present-day temperature during the Phanerozoic.
GC990-128 514573 162 m >570 Ma	Yes [Mean track length is ~1 µm less than predicted by the Default Thermal History. Since this sample is of Precambrian basement, the discrepancy cannot be explained by inheritance of short tracks from sediment source terrains, so the sample must have been hotter at some time since the beginning of the Phanerozoic.]	Yes [The Pooled fission track age is significantly younger than predicted on the basis of the Default Thermal History.]	This sample has been hotter than the present-day temperature during the Phanerozoic.

Note: Interpretation of AFTA data is based on comparison of measured AFTA parameters with values predicted from "Default Thermal History" (Section 2.1); i.e., assuming that each sample is now at its maximum temperature since deposition. The predicted values for each sample are summarised in Table 11.1, and refer only to tracks formed after deposition. Samples may also contain tracks inherited from sediment provenance areas, which must be allowed for in interpreting the data. Calculations refer to apatites with the compositional range appropriate to each sample, as explained in Appendix A.

Table 11.2: Continued (Geotrack Report #990)

Sample details **Sample No.** Source number Elevation Strat. Age	Evidence of higher temperatures in the past from length data?	Evidence of higher temperatures in the past from fission track age data?	Conclusion
GC854-1 12/01 - >600 Ma	Yes [The mean length is ~2.4µm less than that predicted on the basis of the Default Thermal History. Since this sample is of Precambrian basement, the discrepancy cannot be explained by inheritance of short tracks from sediment source terrains, so the sample must have been hotter at some time since the beginning of the Phanerozoic.]	Yes [The central fission track age of this sample and most single grain ages are less than that predicted by the Default Thermal History, indicating the sample has been hotter in the past.]	This sample has been hotter than the present-day temperature during the Phanerozoic.
GC854-2 12/02 - >600 Ma	Yes [The mean length is ~1.7µm less than that predicted on the basis of the Default Thermal History. Since this sample is of Precambrian basement, the discrepancy cannot be explained by inheritance of short tracks from sediment source terrains, so the sample must have been hotter at some time since the beginning of the Phanerozoic.]	Yes [The central fission track age of this sample and most single grain ages are less than that predicted by the Default Thermal History, indicating the sample has been hotter in the past.]	This sample has been hotter than the present-day temperature during the Phanerozoic.
GC854-5 12/03 - >600 Ma	Yes [The mean length is ~2.4µm less than that predicted on the basis of the Default Thermal History. Since this sample is of Precambrian basement, the discrepancy cannot be explained by inheritance of short tracks from sediment source terrains, so the sample must have been hotter at some time since the beginning of the Phanerozoic.]	Yes [The pooled fission track age of this sample is less than that predicted by the Default Thermal History, indicating the sample has been hotter in the past.]	This sample has been hotter than the present-day temperature during the Phanerozoic.

Note: Interpretation of AFTA data is based on comparison of measured AFTA parameters with values predicted from "Default Thermal History" (Section 2.1); i.e., assuming that each sample is now at its maximum temperature since deposition. The predicted values for each sample are summarised in Table 11.1, and refer only to tracks formed after deposition. Samples may also contain tracks inherited from sediment provenance areas, which must be allowed for in interpreting the data. Calculations refer to apatites with the compositional range appropriate to each sample, as explained in Appendix A.

Table 11.2: Continued (Geotrack Report #990)

Sample details **Sample No.** Source number Elevation Strat. Age	Evidence of higher temperatures in the past from length data?	Evidence of higher temperatures in the past from fission track age data?	Conclusion
GC854-7 12/07 - 141-125 Ma	Yes, tentatively [The mean length is 2.3 µm less than that predicted on the basis of the Default Thermal History. Modelling the AFTA parameters through likely thermal history scenarios shows that post-depositional heating is required to explain the age-length-compositional relationships.]	No [The pooled fission track age of this sample is greater than that predicted by the Default Thermal History.]	Sample has been hotter in the past, but paleo-heating was not sufficient to cause severe age reduction.
GC854-11 12/11 - 141-125 Ma	Yes [The mean length is ~2.7µm less than that predicted on the basis of the Default Thermal History. Modelling the AFTA parameters through likely thermal history scenarios shows that track length data in this sample cannot be explained by pre-depositional heating only.]	No [The central fission track age of this sample and most single grain ages are greater than that predicted by the Default Thermal History. No single grain ages are less than predicted.]	There is clear evidence that the sample has been hotter in the past, from the length data. The data also show any paleo-heating was not sufficient to cause severe age reduction.
GC854-14 12/14 - >600 Ma	Yes [The mean length is ~0.5 µm less than that predicted on the basis of the Default Thermal History. Since this sample is of Precambrian basement, the discrepancy cannot be explained by inheritance of short tracks from sediment source terrains, so the sample must have been hotter at some time since the beginning of the Phanerozoic.]	Yes [The pooled fission track age of this sample is less than that predicted by the Default Thermal History, indicating the sample has been hotter in the past.]	This sample has been hotter than the present-day temperature during the Phanerozoic.

Note: Interpretation of AFTA data is based on comparison of measured AFTA parameters with values predicted from "Default Thermal History" (Section 2.1); i.e., assuming that each sample is now at its maximum temperature since deposition. The predicted values for each sample are summarised in Table 11.1, and refer only to tracks formed after deposition. Samples may also contain tracks inherited from sediment provenance areas, which must be allowed for in interpreting the data. Calculations refer to apatites with the compositional range appropriate to each sample, as explained in Appendix A.

Table 11.2: Continued (Geotrack Report #990)

Sample details **Sample No.** Source number Elevation Strat. Age	Evidence of higher temperatures in the past from length data?	Evidence of higher temperatures in the past from fission track age data?	Conclusion
GC854-16 12/16 - >600 Ma	Yes [The mean length is 0.5 µm less than that predicted on the basis of the Default Thermal History. Since this sample is of Precambrian basement, the discrepancy cannot be explained by inheritance of short tracks from sediment source terrains, so the sample must have been hotter at some time since the beginning of the Phanerozoic.]	Yes [The central fission track age of this sample and most single grain ages are less than that predicted by the Default Thermal History, indicating the sample has been hotter in the past.]	This sample has been hotter than the present-day temperature after deposition.
GC854-17 12/17 - >600 Ma	Yes [The mean length is ~1.8 µm less than that predicted on the basis of the Default Thermal History. Since this sample is of Precambrian basement, the discrepancy cannot be explained by inheritance of short tracks from sediment source terrains, so the sample must have been hotter at some time since the beginning of the Phanerozoic.]	Yes [The central fission track age of this sample and most single grain ages are less than that predicted by the Default Thermal History, indicating the sample has been hotter in the past.]	This sample has been hotter than the present-day temperature during the Phanerozoic.
GC854-19 12/19 - >600 Ma	Yes [The mean length is ~1.5 µm less than that predicted on the basis of the Default Thermal History. Since this sample is of Precambrian basement, the discrepancy cannot be explained by inheritance of short tracks from sediment source terrains, so the sample must have been hotter at some time since the beginning of the Phanerozoic.]	Yes [The pooled fission track age of this sample is less than that predicted by the Default Thermal History, indicating the sample has been hotter in the past.]	This sample has been hotter than the present-day temperature during the Phanerozoic.

Note: Interpretation of AFTA data is based on comparison of measured AFTA parameters with values predicted from "Default Thermal History" (Section 2.1); i.e., assuming that each sample is now at its maximum temperature since deposition. The predicted values for each sample are summarised in Table 11.1, and refer only to tracks formed after deposition. Samples may also contain tracks inherited from sediment provenance areas, which must be allowed for in interpreting the data. Calculations refer to apatites with the compositional range appropriate to each sample, as explained in Appendix A.

Table 11.2: Continued (Geotrack Report #990)

Sample details **Sample No.** Source number Elevation Strat. Age	Evidence of higher temperatures in the past from length data?	Evidence of higher temperatures in the past from fission track age data?	Conclusion
GC854-20 12/20 - >600 Ma	Yes [The mean length is ~0.7 µm less than that predicted on the basis of the Default Thermal History. Since this sample is of Precambrian basement, the discrepancy cannot be explained by inheritance of short tracks from sediment source terrains, so the sample must have been hotter at some time since the beginning of the Phanerozoic.]	Yes [The central fission track age of this sample and all single grain ages are less than that predicted by the Default Thermal History, indicating the sample has been hotter in the past.]	This sample has been hotter than the present-day temperature during the Phanerozoic.

Note: Interpretation of AFTA data is based on comparison of measured AFTA parameters with values predicted from "Default Thermal History" (Section 2.1); i.e., assuming that each sample is now at its maximum temperature since deposition. The predicted values for each sample are summarised in Table 11.1, and refer only to tracks formed after deposition. Samples may also contain tracks inherited from sediment provenance areas, which must be allowed for in interpreting the data. Calculations refer to apatites with the compositional range appropriate to each sample, as explained in Appendix A.

Table 11.3: Estimates of timing and magnitude of elevated paleotemperatures from AFTA data in outcrop samples from Bahia State, Onshore Brazil (Geotrack Report #990)

Sample Details	**Paleo-thermal constraints**			**Comments**
Sample No. Source no. Elevation Strat. age	Event	Maximum paleo-temperature (°C)	Onset Of Cooling (Ma)	
GC990-5 BRFT06-11 0 m >2600 Ma	1: 2:	95-110 40-90	210-70 90-0	AFTA data from this sample can be explained by two episodes of heating and cooling, as shown (left). The earliest episode is required in order to explain the reduction in fission track age and the shorter tracks within the noteably broad track length distribution. The later episode is defined by the reduction in length of the longer peak within the track length distribution. The earlier history of the sample cannot be resolved, due to the dominance of the first episode defined from AFTA. High data quality in this sample (20 ages, 110 lengths) provide a very reliable interpretation. **Equivalent $R_o$max: 0.57-0.67%** (in overlying sediments). No VR values are available for comparison.
GC990-14 514401 0 m >2600 Ma	1: 2: 3:	>105 70-90 <70	155-115 140-40 <60	AFTA data from this sample require at least two episodes of heating and cooling, as shown (left), and possibly a third. Cooling from >105°C in the interval 155 to 115 Ma is defined by the fission track age data, while subsequent cooling from between 70 and 90°C at some time between 140 and 40 Ma is required to explain the shortening of the main mode of the track length distribution. A later episode involving cooling from a lower paleotemperature provides an improved match to the observed length distribution at longer lengths but cannot be resolved with confidence. High data quality in this sample (20 ages, 100 lengths) provide a very reliable interpretation. **Equivalent $R_o$max: >0.63%** (in overlying sediments). No VR values are available for comparison.
GC990-15 514402 0 m 200-146 Ma	1:	60-75	95-0	Assuming that this sample is from a Jurassic sandstone unit, then the AFTA data can be explained in terms of a single post-depositional paleo-thermal episode, in which the sample cooled from between 60 and 75°C some time in the last 95 Ma. Note that if the parent sample is younger than Jurassic, this constraint still remains valid. High data quality in this sample (20 ages, 101 lengths) provide a very reliable interpretation, despite the uncertainty in depositional age. **Equivalent $R_o$max: 0.37-0.44%** (for post-depositional heating). No VR values are available for comparison.

All thermal history constraints are based on assumed heating rates of 1°C/Myr and cooling rates of 10°C/Myr.

Events shown in italics are not required by the AFTA data, though they are allowed within the limits shown.

Table 11.3: Continued (Geotrack Report #990)

Sample Details	Paleo-thermal constraints			Comments
Sample No. Source no. Elevation Strat. age	Event	Maximum paleo-temperature (°C)	Onset Of Cooling (Ma)	
GC990-16 514403 0 m >2600 Ma	1: 2:	95-105 50-65	130-90 45-0	AFTA data from this sample can be explained by two episodes of heating and cooling, as shown (left). The earliest episode is required in order to explain the reduction in fission track age and the shorter tracks within the track length distribution. The later episode is defined by the shortening of the mode of the track length distribution. The earlier history of the sample cannot be resolved, due to the dominance of the first episode defined from AFTA. High data quality in this sample (20 ages, 111 lengths) provide a very reliable interpretation. **Equivalent $R_o$max: 0.57-0.63%** (in overlying sediments). No VR values are available for comparison.
GC990-17 514404 0 m >2600 Ma	1: 2:	95-105 55-85	245-130 120-0	AFTA data from this sample can be explained by two episodes of heating and cooling, as shown (left). The earliest episode is required in order to explain the reduction in fission track age and the shorter tracks within the noteably broad track length distribution. The later episode is defined by the reduction in length of the longer peak within the track length distribution. The earlier history of the sample cannot be resolved, due to the dominance of the first episode defined from AFTA. High data quality in this sample (20 ages, 103 lengths) provide a very reliable interpretation. **Equivalent $R_o$max: 0.57-0.63%** (in overlying sediments). No VR values are available for comparison.
GC990-18 514405 96 m 150-144 Ma	1:	80-90	130-55	AFTA data in this sample can be explained in terms of a single post-depositional paleo-thermal episode, in which the sample cooled from between 80 and 90°C beginning between 130 and 55 Ma. High data quality in this sample (20 ages, 101 lengths) provide a very straightforward interpretation, which is considered highly reliable. **Equivalent $R_o$max: 0.48-0.54%**. No VR values are available for comparison.
GC990-20 514408 159 m 150-144 Ma	Limit:	<100	post-deposition	With only two single grain ages measured, the AFTA data from this sample are not of sufficient quality to provide a rigorous interpretation, but a broad upper limit of 100°C can be placed on the maximum post-depositional paleotemperature.

All thermal history constraints are based on assumed heating rates of 1°C/Myr and cooling rates of 10°C/Myr.

Events shown in italics are not <u>required</u> by the AFTA data, though they are <u>allowed</u> within the limits shown.

Table 11.3: Continued (Geotrack Report #990)

Sample Details	Paleo-thermal constraints			Comments
Sample No. Source no. Elevation Strat. age	Event	Maximum paleo-temperature (°C)	Onset Of Cooling (Ma)	
GC990-21 514409 137 m 290-256 Ma	1: 2:	85-100 60-80	245-80 40-0	AFTA data from this sample can be explained by two episodes of heating and cooling, as shown (left). The earliest episode is required in order to explain the shorter tracks within the track length distribution, while the later episode is defined by the shortening of the main mode of the track length distribution. High data quality in this sample (18 ages, 93 lengths) provide a very reliable interpretation. **Equivalent $R_o$max: 0.51-0.61**%. No VR values are available for comparison.
GC990-22 514410 136 m >1600 Ma	1: 2:	90-105 80-90	525-145 80-10	AFTA data from this sample can be explained by two episodes of heating and cooling, as shown (left). The earliest episode is required in order to explain the reduction in fission track age and the shorter tracks within the length distribution. The later episode is defined by the shortening of the main mode of the track length distribution. The earlier history of the sample cannot be resolved, due to the dominance of the first episode defined from AFTA. High data quality in this sample (20 ages, 104 lengths) provide a very reliable interpretation. **Equivalent $R_o$max: 0.54-0.63%** (in overlying sediments). No VR values are available for comparison.
GC990-23 514411 377m >1600 Ma	1: 2: 3:	95-100 *75-90* 60-80	380-190 *150-20* 60-0	AFTA data from this sample require at least two and probably three episodes of heating and cooling, as shown (left), to explain all aspects of the data. The earliest episode is required in order to explain the reduction in fission track age and the shortest tracks within the length distribution. Two later episodes are required to explain the precise form of the track length distribution, although the earlier of these two episodes cannot be rigorously resolved in detail. The earlier history of the sample also cannot be resolved, due to the dominance of the first episode defined from AFTA. High data quality in this sample (20 ages, 108 lengths) provide a very reliable interpretation. **Equivalent $R_o$max: 0.57-0.61%** (in overlying sediments). No VR values are available for comparison.

All thermal history constraints are based on assumed heating rates of 1°C/Myr and cooling rates of 10°C/Myr.

Events shown in italics are not required by the AFTA data, though they are allowed within the limits shown.

Table 11.3: Continued (Geotrack Report #990)

Sample Details	Paleo-thermal constraints			Comments
Sample No. Source no. Elevation Strat. age	Event	Maximum paleo-temperature (°C)	Onset Of Cooling (Ma)	
GC990-24 514412 175m 136-127 Ma	1: 2:	*80-100* 50-75	*>50* 40-0	AFTA data from this sample are best explained in terms of two episodes of heating and cooling after deposition, as shown (left), although the earlier of the two episodes could alternatively represent heating of the apatites prior to deposition in sediment provenance terrains. The earlier episode is required in order to explain the shorter tracks within the track length distribution, while the later episode is defined by the shortening of the main mode of the track length distribution. High data quality in this sample (20 ages, 104 lengths) provide a very reliable interpretation. **Equivalent $R_o$max: 0.48-0.61**% (assuming the earlier event represents the post-depositional paleo-thermal maximum). No VR values are available for comparison.
GC990-25 514413 220 m 115-112 Ma	1: 2:	*85-110* 45-80	*>60* 50-0	AFTA data from this sample are best explained in terms of two episodes of heating and cooling after deposition, as shown (left), although the earlier of the two episodes could alternatively represent heating of the apatites prior to deposition in sediment provenance terrains. The earlier episode is required in order to explain the shorter tracks within the track length distribution, while the later episode is defined by the shortening of the main mode of the track length distribution. High data quality in this sample (18 ages, 75 lengths) provide a very reliable interpretation. **Equivalent $R_o$max: 0.51-0.67**% (assuming the earlier event represents the post-depositional paleo-thermal maximum). No VR values are available for comparison.
GC990-26 514414 340 mm 115-112 Ma	1: 2:	*75-105* <85	*>10* 35-0	AFTA data from this sample are best explained in terms of two episodes of heating and cooling after deposition, as shown (left), although the earlier of the two episodes could alternatively represent heating of the apatites prior to deposition in sediment provenance terrains. The earlier episode is required in order to explain the shorter tracks within the track length distribution, while the later episode is defined by the shortening of the main mode of the track length distribution. Lower quality data in this sample (7 ages, 35 lengths) still provide a very reliable interpretation, within the stated uncertainty limits. **Equivalent $R_o$max: 0.44-0.63**% (assuming the earlier event represents the post-depositional paleo-thermal maximum). No VR values are available for comparison.

All thermal history constraints are based on assumed heating rates of 1°C/Myr and cooling rates of 10°C/Myr.

Events shown in italics are not required by the AFTA data, though they are allowed within the limits shown.

Table 11.3: Continued (Geotrack Report #990)

Sample Details	Paleo-thermal constraints			Comments
Sample No. Source no. Elevation Strat. age	Event	Maximum paleo-temperature (°C)	Onset Of Cooling (Ma)	
GC990-27 514415 440 m 115-112 Ma	1: 2:	*80-100* 25-80	*>25* 40-0	AFTA data from this sample are best explained in terms of two episodes of heating and cooling after deposition, as shown (left), although the earlier of the two episodes could alternatively represent heating of the apatites prior to deposition in sediment provenance terrains. The earlier episode is required in order to explain the shorter tracks within the track length distribution, while the later episode is defined by the shortening of the main mode of the track length distribution. High data quality in this sample (20 ages, 109 lengths) provide a very reliable interpretation. **Equivalent $R_o$max: 0.48-0.61**% (assuming the earlier event represents the post-depositional paleo-thermal maximum). No VR values are available for comparison.
GC990-28 514416 439 m 115-112 Ma	1: 2:	*80-105* 40-75	*>50* 40-0	AFTA data from this sample are best explained in terms of two episodes of heating and cooling after deposition, as shown (left), although the earlier of the two episodes could alternatively represent heating of the apatites prior to deposition in sediment provenance terrains. The earlier episode is required in order to explain the shorter tracks within the track length distribution, while the later episode is defined by the shortening of the main mode of the track length distribution. High data quality in this sample (20 ages, 109 lengths) provide a very reliable interpretation. **Equivalent $R_o$max: 0.48-0.63**% (assuming the earlier event represents the post-depositional paleo-thermal maximum). No VR values are available for comparison.
GC990-29 514417 363 m 115-112 Ma	1: 2:	*70-100* <80	*>10* 40-0	AFTA data from this sample are best explained in terms of two episodes of heating and cooling after deposition, as shown (left), although the earlier of the two episodes could alternatively represent heating of the apatites prior to deposition in sediment provenance terrains. The earlier episode is required in order to explain the shorter tracks within the track length distribution, while the later episode is defined by the shortening of the main mode of the track length distribution. High data quality in this sample (20 ages, 103 lengths) provide a very reliable interpretation. **Equivalent $R_o$max: 0.42-0.61**% (assuming the earlier event represents the post-depositional paleo-thermal maximum). No VR values are available for comparison.

All thermal history constraints are based on assumed heating rates of 1°C/Myr and cooling rates of 10°C/Myr.

Events shown in italics are not required by the AFTA data, though they are allowed within the limits shown.

Table 11.3: Continued (Geotrack Report #990)

Sample Details	Paleo-thermal constraints			Comments
Sample No. Source no. Elevation Strat. age	Event	Maximum paleo-temperature (°C)	Onset Of Cooling (Ma)	
GC990-30 514418 273 m 150-144 Ma	1: 2:	*90-110* 65-85	*>70* 55-10	AFTA data from this sample are best explained in terms of two episodes of heating and cooling after deposition, as shown (left), although the earlier of the two episodes could alternatively represent heating of the apatites prior to deposition in sediment provenance terrains. The earlier episode is required in order to explain the shorter tracks within the track length distribution, while the later episode is defined by the shortening of the main mode of the track length distribution. High data quality in this sample (20 ages, 85 lengths) provide a very reliable interpretation. **Equivalent $R_o$max: 0.54-0.67**% (assuming the earlier event represents the post-depositional paleo-thermal maximum). No VR values are available for comparison.
GC990-31 514419 303 m 150-144 Ma	1: 2:	85-105 30-80	145-40 70-0	AFTA data from this sample require two episodes of heating and cooling after deposition, as shown (left), to explain all aspects of the data. The earlier episode is required in order to explain the dominant short mode within the track length distribution, while the later episode is defined by the reduction in length of the longer tracks within the length distribution. High data quality in this sample (20 ages, 102 lengths) provide a very reliable interpretation. **Equivalent $R_o$max: 0.51-0.63**%. No VR values are available for comparison.
GC990-32 514420 294 m >250 Ma	1: 2:	100-105 60-80	135-60 45-0	AFTA data from this sample require two episodes of heating and cooling after deposition, as shown (left), to explain all aspects of the data. The earlier episode is required in order to explain the shorter tracks within the length distribution and the age reduction in the most sensitive apatites, while the later episode is defined by the shortening of the main mode of the length distribution. High data quality in this sample (20 ages, 103 lengths) provide a very reliable interpretation. **Equivalent $R_o$max: 0.61-0.63**% (assuming the earlier event represents the post-depositional paleo-thermal maximum). No VR values are available for comparison.

All thermal history constraints are based on assumed heating rates of 1°C/Myr and cooling rates of 10°C/Myr.

Events shown in italics are not required by the AFTA data, though they are allowed within the limits shown.

Table 11.3: Continued (Geotrack Report #990)

Sample Details	Paleo-thermal constraints			Comments
Sample No. Source no. Elevation Strat. age	Event	Maximum paleo-temperature (°C)	Onset Of Cooling (Ma)	
GC990-33 514421 302 m >250 Ma	1: 2:	80-90 40-65	155-70 50-0	AFTA data from this sample require two episodes of heating and cooling after deposition, as shown (left), to explain all aspects of the data. The earlier episode is required in order to explain the shorter tracks within the noteable broad track length distribution, while the later episode is defined by the shortening the longer tracks within the length distribution (with both components combining to produce a very broad distribution). High data quality in this sample (20 ages, 104 lengths) provide a very reliable interpretation. **Equivalent $R_o$max: 0.48-0.54**% (assuming the earlier event represents the post-depositional paleo-thermal maximum). No VR values are available for comparison.
GC990-34 514422 265 m >500 Ma	1: 2:	95-100 70-85	220-80 30-0	AFTA data from this sample can be explained by two episodes of heating and cooling, as shown (left). The earliest episode is required in order to explain the reduction in fission track age and the shorter tracks within the noteably broad track length distribution. The later episode is defined by the reduction in length of the longer peak within the track length distribution. The earlier history of the sample cannot be resolved, due to the dominance of the first episode defined from AFTA. High data quality in this sample (20 ages, 107 lengths) provide a very reliable interpretation. **Equivalent $R_o$max: 0.57-0.61%** (in overlying sediments). No VR values are available for comparison.
GC990-35 514423 324 m 150-144 Ma	1:	60-80	95-15	After removal of anomalously young ages (see Table 11.2), AFTA data in this sample can be explained in terms of a single post-depositional paleo-thermal episode, in which the sample cooled from between 60 and 80°C beginning between 95 and 15 Ma. Moderate data quality in this sample (11 ages, 63 lengths) provide an apparently straightforward interpretation, but because of the presence of the anomalously young ages this should possibly treated with caution. **Equivalent $R_o$max: 0.37-0.48%**. No VR values are available for comparison.

All thermal history constraints are based on assumed heating rates of 1°C/Myr and cooling rates of 10°C/Myr.

Events shown in italics are not required by the AFTA data, though they are allowed within the limits shown.

Table 11.3: Continued (Geotrack Report #990)

Sample Details	Paleo-thermal constraints			Comments
Sample No. Source no. Elevation Strat. age	Event	Maximum paleo-temperature (°C)	Onset Of Cooling (Ma)	
GC990-36 514424 304 m 115-112 Ma	1: 2:	*65-105* <90	*>45* 70-0	AFTA data from this sample can be explained by post-depositional heating, as shown (left), but precise conditions cannot be defined with confidence. Cooling from between 65 and 105°C at some time prior to 45 Ma can explain the shorter tracks within the track length distribution, but these can alternatively be explained in terms of heating prior to deposition in sediment provenance terrains. Following any such episode, the sample has remained below 90°C. Lower quality data compared to other samples (11 ages, 34 lengths) provide an equivocal interpretation. **Equivalent $R_o$max: 0.39-0.63%** (assuming post-depositional heating). No VR values are available for comparison.
GC990-37 514425 251 m 115-112 Ma	1:	90-105	105-20	AFTA data in this sample can be explained in terms of a single post-depositional paleo-thermal episode, in which the sample cooled from between 90 and 105°C beginning between 105 and 20 Ma. Despite lower quality data compared to other samples (9 ages, 36 lengths), the data provide an apparently straightforward interpretation, which is considered highly reliable. **Equivalent $R_o$max: 0.54-0.63%**. No VR values are available for comparison.
GC990-38 514426 188 m 115-112 Ma	1:	60-85	90-15	AFTA data in this sample can be explained in terms of a single post-depositional paleo-thermal episode, in which the sample cooled from between 60 and 85°C beginning between 90 and 15 Ma. High quality data (20 ages, 111 lengths) provide a straightforward interpretation, which is considered highly reliable. **Equivalent $R_o$max: 0.37-0.52%**. No VR values are available for comparison.
GC990-39 514427 204 m >2600 Ma	1: 2: 3:	>100 85-110 50-80	180-140 145-80 70-0	AFTA data from this sample require at least three episodes of heating and cooling, as shown (left), to explain all aspects of the data. Cooling from >100°C in the interval 180 to 140 Ma is defined primarily by the fission track age data, while the two subsequent cooling episodes are required to explain the detailed form of the track length distribution. High data quality in this sample (20 ages, 107 lengths) provide a very reliable interpretation. **Equivalent $R_o$max: >0.61%** (in overlying sediments). No VR values are available for comparison.

All thermal history constraints are based on assumed heating rates of 1°C/Myr and cooling rates of 10°C/Myr.

Events shown in italics are not required by the AFTA data, though they are allowed within the limits shown.

Table 11.3: Continued (Geotrack Report #990)

Sample Details	**Paleo-thermal constraints**			**Comments**
Sample No. Source no. Elevation Strat. age	Event	Maximum paleo-temperature (°C)	Onset Of Cooling (Ma)	
GC990-40 514428 160 m 5-2 Ma	Prov-en-ance:	90-100 60-80	350-180 80-0	AFTA data in this sample of latest Miocene to Pliocene sandstone shows no evidence of post-depositional heating, but contains significant information on the history of the sediment provenance terrain, showing reliable of two paleo-thermal episodes, as shown (left).
GC990-41 514429 35 m >2600 Ma	1: 2: 3:	115-120 70-90 <90	235-170 150-70 70-0	AFTA data from this sample can be explained by two episodes of heating and cooling, while also placing limits on the later stages of the history, as shown (left). The earliest of the quoted episodes is required in order to explain the reduction in fission track age and the shorter tracks within the noteably broad track length distribution. The later episode is defined by the reduction in length of the longer peak within the track length distribution. The earlier history of the sample cannot be resolved, due to the dominance of the first episode defined from AFTA. High data quality in this sample (14 ages, 120 lengths) provide a reliable interpretation. **Equivalent $R_o$max: 0.69-0.73%** (in overlying sediments). No VR values are available for comparison.
GC990-42 514430 0 m 145-125 Ma	1: 2:	*80-100* 50-75	*>20* 20-0	AFTA data from this sample are best explained in terms of two episodes of heating and cooling after deposition, as shown (left), although the earlier of the two episodes could alternatively represent heating of the apatites prior to deposition in sediment provenance terrains. The earlier episode is required in order to explain the shorter tracks within the track length distribution, while the later episode is defined by the shortening of the main mode of the track length distribution. High data quality in this sample (20 ages, 106 lengths) provide a very reliable interpretation. **Equivalent $R_o$max: 0.48-0.61**% (assuming the earlier event represents the post-depositional paleo-thermal maximum). No VR values are available for comparison.

All thermal history constraints are based on assumed heating rates of 1°C/Myr and cooling rates of 10°C/Myr.

Events shown in italics are not <u>required</u> by the AFTA data, though they are <u>allowed</u> within the limits shown.

Table 11.3: Continued (Geotrack Report #990)

Sample Details	Paleo-thermal constraints			Comments
Sample No. Source no. Elevation Strat. age	Event	Maximum paleo-temperature (°C)	Onset Of Cooling (Ma)	
GC990-43 514431 0 m 140-120 Ma	1: 2:	85-95 40-80	100-15 40-0	AFTA data from this sample require two episodes of heating and cooling after deposition, as shown (left), to explain all aspects of the data. The earlier episode is required in order to explain the shorter tracks within the track length distribution, while the later episode is defined by the shortening the longer tracks within the length distribution (with both components combining to produce a broad distribution). High data quality in this sample (20 ages, 85 lengths) provide a very reliable interpretation. **Equivalent $R_o$max: 0.52-0.58**%. No VR values are available for comparison.
GC990-45 514434 0 m 150-144 Ma	1: 2:	>100 55-85	135-65 55-0	AFTA data from this sample require two episodes of heating and cooling after deposition, as shown (left), to explain all aspects of the data. The earlier episode is required in order to explain the reduction in fission track age, while the later episode is defined by the shortening of the main mode of the length distribution. Despite much lower data quality compared to other samples (4 ages, 7 lengths), results from this sample appear to provide a straightforward interpretation, which is considered reliable . **Equivalent $R_o$max: >0.61**%. No VR values are available for comparison.
GC990-46 514436 27 m >1600 Ma	1: 2:	>100 75-85	265-170 40-0	AFTA data from this sample can be explained in terms of two episodes of heating and cooling, as shown (left). Cooling from >100°C in the interval 265-170 Ma is defined primarily by the fission track age data, while the subsequent cooling episode is required to explain the shortening of the main mode of the track length distribution. High data quality in this sample (20 ages, 37 lengths) provide a very reliable interpretation. **Equivalent $R_o$max: >0.61%** (in overlying sediments). No VR values are available for comparison.
GC990-47 514437 100 m >1600 Ma	1: 2: 3:	>110 85-95 50-80	365-290 170-50 35-0	AFTA data from this sample require three episodes of heating and cooling, as shown (left), to explain all aspects of the results. The earliest of the quoted episodes is required in order to explain the reduction in fission track age. The subsequent episodes are required in order to explain the detailed form of the track length distribution. High data quality in this sample (20 ages, 100 lengths) provide a reliable interpretation. **Equivalent $R_o$max: >0.67%** (in overlying sediments). No VR values are available for comparison.

All thermal history constraints are based on assumed heating rates of 1°C/Myr and cooling rates of 10°C/Myr.

Events shown in italics are not required by the AFTA data, though they are allowed within the limits shown.

Table 11.3: Continued (Geotrack Report #990)

Sample Details	Paleo-thermal constraints			Comments
Sample No. Source no. Elevation Strat. age	Event	Maximum paleo-temperature (°C)	Onset Of Cooling (Ma)	
GC990-48 514438 50 m 132-120 Ma	1: 2:	80-95 40-75	100-35 30-0	AFTA data from this sample can be explained in terms of two episodes of heating and cooling, as shown (left). Cooling from between 80 and 95°C in the interval 100-35 Ma is required to explain the shorter tracks within the length distribution, while subsequent cooling from between 40 and 75°C beginning in the interval 30-0 Ma is required to explain the shortening of the main mode of the track length distribution. High data quality in this sample (20 ages, 45 lengths) provide a very reliable interpretation. **Equivalent $R_o$max: 0.48-0.57%**. No VR values are available for comparison.
GC990-49 514439 42 m 132-120 Ma	1: 2:	90-100 45-65	85-40 30-0	AFTA data from this sample can be explained in terms of two episodes of heating and cooling, as shown (left). Cooling from between 90 and 100°C in the interval 85-40 Ma is required to explain the age reduction in the most sensitive apatites plus the shorter tracks within the length distribution, while subsequent cooling from between 45 and 65°C beginning in the interval 30-0 Ma is required to explain the shortening of the main mode of the track length distribution. High data quality in this sample (20 ages, 83 lengths) provide a very reliable interpretation. **Equivalent $R_o$max: 0.54-0.61%**. No VR values are available for comparison.
GC990-57 514447 288 m >1600 Ma	1: 2: 3:	100-105 85-95 55-80	210-90 160-40 35-0	AFTA data from this sample require three episodes of heating and cooling, as shown (left), to explain all aspects of the results. The earliest of the quoted episodes is required in order to explain the reduction in fission track age. The subsequent episodes are required in order to explain the detailed form of the track length distribution. High data quality in this sample (20 ages, 109 lengths) provide a reliable interpretation, although the earlier history remains unconstrained. **Equivalent $R_o$max: >0.67%** (in overlying sediments). No VR values are available for comparison.

All thermal history constraints are based on assumed heating rates of 1°C/Myr and cooling rates of 10°C/Myr.

Events shown in italics are not required by the AFTA data, though they are allowed within the limits shown.

Table 11.3: Continued (Geotrack Report #990)

Sample Details	Paleo-thermal constraints			Comments
Sample No. Source no. Elevation Strat. age	Event	Maximum paleo-temperature (°C)	Onset Of Cooling (Ma)	
GC990-58 514448 167 m >1600 Ma	1: 2: 3:	>115 80-95 45-65	260-220 180-85 40-0	AFTA data from this sample require three episodes of heating and cooling, as shown (left), to explain all aspects of the results. The earliest of the quoted episodes is required in order to explain the reduction in fission track age. The subsequent episodes are required in order to explain the detailed form of the track length distribution. High data quality in this sample (11 ages, 72 lengths) provide a reliable interpretation. **Equivalent $R_o$max: >0.69%** (in overlying sediments). No VR values are available for comparison.
GC990-60 514450 250 m >1600 Ma	1: 2:	95-100 65-85	275-80 40-0	AFTA data from this sample can be explained by two episodes of heating and cooling, as shown (left). The earliest episode is required in order to explain the reduction in fission track age and the shorter tracks within the noteably broad track length distribution. The later episode is defined by the reduction in length of the main mode of the track length distribution. The earlier history of the sample cannot be resolved, due to the dominance of the first episode defined from AFTA. High data quality in this sample (20 ages, 116 lengths) provide a very reliable interpretation, although the presence of the anomalously young ages (Table 11.2) remains unexplained. **Equivalent $R_o$max: 0.57-0.61%** (in overlying sediments). No VR values are available for comparison.
GC990-61 514451 600 m >1600 Ma	1: 2:	105-115 25-90	265-145 190-0	AFTA data from this sample can be explained by two episodes of heating and cooling, as shown (left). The earliest episode is required in order to explain the reduction in fission track age while the later episode is defined by the reduction in length of the main mode of the track length distribution. Because of the small number of track lengths, only broad constraints are possible on this later episode. The earlier history of the sample cannot be resolved, due to the dominance of the first episode defined from AFTA. Despite lower data quality in this sample compared to others (7 ages, 9 lengths), the data provide a straightforward interpretation, which is considered reliable within the stated uncertainty limits. **Equivalent $R_o$max: 0.63-0.69%** (in overlying sediments). No VR values are available for comparison.

All thermal history constraints are based on assumed heating rates of 1°C/Myr and cooling rates of 10°C/Myr.

Events shown in italics are not required by the AFTA data, though they are allowed within the limits shown.

Table 11.3: Continued (Geotrack Report #990)

Sample Details	Paleo-thermal constraints			Comments
Sample No. Source no. Elevation Strat. age	Event	Maximum paleo-temperature (°C)	Onset Of Cooling (Ma)	
GC990-62 514452 330 m 1000-540 Ma	1: 2:	>120 60-90	280-180 175-0	AFTA data from this sample can be explained by two episodes of heating and cooling, as shown (left). The earliest episode is required in order to explain the reduction in fission track age while the later episode is defined by the reduction in length of the main mode of the track length distribution. Because of the small number of track lengths, only broad constraints are possible on this later episode. Despite lower data quality in this sample compared to others (5 ages, 8 lengths), the data provide a straightforward interpretation, which is considered reliable within the stated uncertainty limits. **Equivalent $R_o$max: >0.73%** (in overlying sediments). No VR values are available for comparison.
GC990-64 514454 800 m 1600-1000 Ma	1: 2: 3:	>120 85-95 55-70	500-390 300-140 50-0	AFTA data from this sample require three episodes of heating and cooling, as shown (left), to explain all aspects of the results. The earliest of the quoted episodes is required in order to explain the reduction in fission track age. The subsequent episodes are required in order to explain the detailed form of the track length distribution. High data quality in this sample (20 ages, 116 lengths) provide a reliable interpretation, although the presence of the anomalously young ages (Table 11.2) remains unexplained. **Equivalent $R_o$max: >0.73%** (in overlying sediments). No VR values are available for comparison.
GC990-66 514456 498 m 1600-1000 Ma	1:	100-105	80-15	AFTA data from this sample can be explained by a single paleo-thermal episode, as shown (left). This episode explains the reduction in fission track age and the track length distribution, although since only 7 lengths were measured, constraints on the more recent history are poor. The earlier history of the sample also cannot be resolved, due to the dominance of the first episode defined from AFTA. Lower data quality in this sample compared to others (12 ages, 7 lengths) provide a less reliable interpretation. **Equivalent $R_o$max: 0.61-0.63%** (in overlying sediments). No VR values are available for comparison.

All thermal history constraints are based on assumed heating rates of 1°C/Myr and cooling rates of 10°C/Myr.

Events shown in italics are not required by the AFTA data, though they are allowed within the limits shown.

Table 11.3: Continued (Geotrack Report #990)

Sample Details	Paleo-thermal constraints			Comments
Sample No. Source no. Elevation Strat. age	Event	Maximum paleo-temperature (°C)	Onset Of Cooling (Ma)	
GC990-68 514458 1212 m 1600-1000 Ma	1: 2:	100-110 50-80	160-85 75-0	AFTA data from this sample can be explained by two episodes of heating and cooling, as shown (left). The earliest episode is required in order to explain the reduction in fission track age while the later episode is defined by the reduction in length of the main mode of the track length distribution. Because of the small number of track lengths, only broad constraints are possible on this later episode. The earlier history of the sample cannot be resolved, due to the dominance of the first episode defined from AFTA. Despite lower data quality in this sample compared to others (9 ages, 16 lengths), the data provide a straightforward interpretation, which is considered reliable within the stated uncertainty limits. **Equivalent $R_o$max: 0.61-0.67%** (in overlying sediments). No VR values are available for comparison.
GC990-72 514466 1033 m 1600-1000 Ma	1: 2:	>100 65-90	230-120 130-20	AFTA data from this sample can be explained by two episodes of heating and cooling, as shown (left). The earliest episode is required in order to explain the reduction in fission track age while the later episode is defined by the reduction in length of the main mode of the track length distribution. Because of the small number of track lengths, only broad constraints are possible on this later episode. Despite lower data quality in this sample compared to others (7 ages, 20 lengths), the data provide a straightforward interpretation, which is considered reliable within the stated uncertainty limits. **Equivalent $R_o$max: >0.61%** (in overlying sediments). No VR values are available for comparison.
GC990-73 514467 1312 m 1600-1000 Ma	1: 2:	>100 <100	490-200 200-0	AFTA data from this sample can be explained by a single paleo-thermal episode, as shown (left), which explains the reduction in fission track age. Due to the lack of track lengths (only 3 lengths measured), no rigorous constraints are possible on the more recent history. Despite the low data quality in this sample compared to others (2 ages, 3 lengths) the thermal history solution is considered reliable within the stated uncertainty limits. **Equivalent $R_o$max: >0.61%** (in overlying sediments). No VR values are available for comparison.

All thermal history constraints are based on assumed heating rates of 1°C/Myr and cooling rates of 10°C/Myr.

Events shown in italics are not required by the AFTA data, though they are allowed within the limits shown.

Table 11.3: Continued (Geotrack Report #990)

Sample Details	Paleo-thermal constraints			Comments
Sample No. Source no. Elevation Strat. age	Event	Maximum paleo-temperature (°C)	Onset Of Cooling (Ma)	
GC990-74 514468 1025 m 1600-1000 Ma	1: 2:	>105 70-85	275-210 130-35	AFTA data from this sample can be explained by two episodes of heating and cooling, as shown (left). The earliest episode is required in order to explain the reduction in fission track age while the later episode is defined by the reduction in length of the main mode of the track length distribution. High quality data in this sample (20 ages, 51 lengths) provide a straightforward interpretation, which is considered reliable within the stated uncertainty limits. **Equivalent $R_o$max: >0.63%** (in overlying sediments). No VR values are available for comparison.
GC990-75 514469 741 m >1600 Ma	1: 2: 3:	>105 85-105 55-75	140-100 115-55 35-0	AFTA data from this sample require three episodes of heating and cooling, as shown (left), to explain all aspects of the results. The earliest of the quoted episodes is required in order to explain the reduction in fission track age. The subsequent episodes are required in order to explain the detailed form of the track length distribution. High data quality in this sample (20 ages, 61 lengths) provide a reliable interpretation. **Equivalent Romax: >0.63%** (in overlying sediments). No VR values are available for comparison.
GC990-76 514470 529 m >1600 Ma	1: 2: 3:	>100 80-110 55-75	130-100 120-50 20-0	AFTA data from this sample require three episodes of heating and cooling, as shown (left), to explain all aspects of the results. The earliest of the quoted episodes is required in order to explain the reduction in fission track age. The subsequent episodes are required in order to explain the detailed form of the track length distribution. High data quality in this sample (20 ages, 50 lengths) provide a reliable interpretation. **Equivalent Romax: >0.61%** (in overlying sediments). No VR values are available for comparison.
GC990-77 514471 1575 m 1600-1000 Ma	-	-	-	No apatite

All thermal history constraints are based on assumed heating rates of 1°C/Myr and cooling rates of 10°C/Myr.

Events shown in italics are not required by the AFTA data, though they are allowed within the limits shown.

Table 11.3: Continued (Geotrack Report #990)

Sample Details	Paleo-thermal constraints			Comments
Sample No. Source no. Elevation Strat. age	Event	Maximum paleo-temperature (°C)	Onset Of Cooling (Ma)	
GC990-78 514472 1309 m 1600-1000 Ma	1: 2:	>100 75-90	750-200 200-0	AFTA data from this sample can be explained by two episodes of heating and cooling, as shown (left). The earliest episode is required in order to explain the reduction in fission track age while the later episode is required to explain the shorter tracks within the track length distribution. Despite the lower quality data compared to other samples (9 ages, 8 lengths), results from this sample are considered to provide a reliable interpretation within the stated uncertainty limits. **Equivalent $R_o$max: >0.61%** (in overlying sediments). No VR values are available for comparison.
GC990-79 514473 1040 m 1600-1000 Ma	1: 2:	>120 80-90	480-350 100-0	AFTA data from this sample can be explained by two episodes of heating and cooling, as shown (left). The earliest episode is required in order to explain the reduction in fission track age while the later episode is required to explain the shortening of the main mode of the track length distribution. Despite the lower quality data compared to other samples (14 ages, 23 lengths), results from this sample are considered to provide a reliable interpretation within the stated uncertainty limits. **Equivalent $R_o$max: >0.73%** (in overlying sediments). No VR values are available for comparison.
GC990-80 514474 543 m 1800-1600 Ma	1:	>100	150-50	AFTA data from this sample can be explained in terms of a single episode of heating and cooling, as shown (left), involving cooling from >100°C at some time between 150 and 50 Ma. This is required to explain the fission track age data. The lack of track length data (only 3 track lengths measured) precludes resolution of further detail in the cooling history. Despite lower data quality compared to other samples (16 ages, 3 lengths) the interpretation is regarded as reliable within the stated limits of uncertainty. **Equivalent Romax: >0.61%** (in overlying sediments). No VR values are available for comparison.

All thermal history constraints are based on assumed heating rates of 1°C/Myr and cooling rates of 10°C/Myr.

Events shown in italics are not required by the AFTA data, though they are allowed within the limits shown.

Table 11.3: Continued (Geotrack Report #990)

Sample Details	Paleo-thermal constraints			Comments
Sample No. Source no. Elevation Strat. age	Event	Maximum paleo-temperature (°C)	Onset Of Cooling (Ma)	
GC990-81 514475 891 m 1600-1000 Ma	1: 2:	100-105 45-90	140-40 80-0	AFTA data from this sample can be explained by two episodes of heating and cooling, as shown (left). The earliest episode is required in order to explain the reduction in fission track age while the later episode is defined by the reduction in length of the main mode of the track length distribution. Because of the small number of track lengths, only broad constraints are possible on this later episode. The earlier history of the sample cannot be resolved, due to the dominance of the first episode defined from AFTA. Despite lower data quality in this sample compared to others (13 ages, 10 lengths), the interpretation is considered reliable within the stated uncertainty limits. **Equivalent $R_o$max: 0.61-0.63%** (in overlying sediments). No VR values are available for comparison.
GC990-82 514476 404 m >1600 Ma	1: 2:	>110 60-90	250-120 90-0	AFTA data from this sample can be explained by two episodes of heating and cooling, as shown (left). The earliest episode is required in order to explain the reduction in fission track age while the later episode is required to explain the shortening of the main mode of the track length distribution. Despite the lower quality data compared to other samples (20 ages, 4 lengths), results from this sample are considered to provide a reliable interpretation within the stated uncertainty limits. **Equivalent $R_o$max: >0.67%** (in overlying sediments). No VR values are available for comparison.
GC990-84 514478 744 m >1600 Ma	1: 2: 3:	>105 70-100 30-75	185-130 140-45 60-0	AFTA data from this sample require three episodes of heating and cooling, as shown (left), to explain all aspects of the results. The earliest of the quoted episodes is required in order to explain the reduction in fission track age. The subsequent episodes are required in order to explain the detailed form of the track length distribution. High data quality in this sample (20 ages, 36 lengths) provide a reliable interpretation. **Equivalent Romax: >0.63%** (in overlying sediments). No VR values are available for comparison.

All thermal history constraints are based on assumed heating rates of 1°C/Myr and cooling rates of 10°C/Myr.

Events shown in italics are not required by the AFTA data, though they are allowed within the limits shown.

Table 11.3: Continued (Geotrack Report #990)

Sample Details	Paleo-thermal constraints			Comments
Sample No. Source no. Elevation Strat. age	Event	Maximum paleo-temperature (°C)	Onset Of Cooling (Ma)	
GC990-85 514479 377 m >1600 Ma	1: 2: 3:	>105 80-100 40-70	210-120 160-55 45-0	AFTA data from this sample require three episodes of heating and cooling, as shown (left), to explain all aspects of the results. The earliest of the quoted episodes is required in order to explain the reduction in fission track age. The subsequent episodes are required in order to explain the detailed form of the track length distribution. Moderate quality data in this sample (20 ages, 20 lengths) provide a reliable interpretation. **Equivalent Romax: >0.63%** (in overlying sediments). No VR values are available for comparison.
GC990-86 514480 594 m >1600 Ma	1:	>100	150-55	AFTA data from this sample can be explained in terms of a single episode of heating and cooling, as shown (left), involving cooling from >100°C at some time between 150 and 55 Ma. This is required to explain the fission track age data. The lack of track length data (no track lengths measured) precludes resolution of further detail in the cooling history. Despite lower data quality compared to other samples (13 ages, 0 lengths) the interpretation is regarded as reliable within the stated limits of uncertainty. **Equivalent Romax: >0.61%** (in overlying sediments). No VR values are available for comparison.
GC990-87 514481 806 m >1600 Ma	1: 2:	>105 75-90	140-85 65-0	AFTA data from this sample can be explained by two episodes of heating and cooling, as shown (left). The earliest episode is required in order to explain the reduction in fission track age while the later episode is required to explain the shorter peak within the track length distribution. Despite the lower quality data compared to other samples (21 ages, 10 lengths), results from this sample are considered to provide a reliable interpretation within the stated uncertainty limits. **Equivalent $R_o$max: >0.63%** (in overlying sediments). No VR values are available for comparison.

All thermal history constraints are based on assumed heating rates of 1°C/Myr and cooling rates of 10°C/Myr.

Events shown in italics are not required by the AFTA data, though they are allowed within the limits shown.

Table 11.3: Continued (Geotrack Report #990)

Sample Details	Paleo-thermal constraints			Comments
Sample No. Source no. Elevation Strat. age	Event	Maximum paleo-temperature (°C)	Onset Of Cooling (Ma)	
GC990-88 514482 1055 m >1600 Ma	1: 2: 3:	>100 75-115 45-75	200-140 185-45 40-0	AFTA data from this sample require three episodes of heating and cooling, as shown (left), to explain all aspects of the results. The earliest of the quoted episodes is required in order to explain the reduction in fission track age. The subsequent episodes are required in order to explain the detailed form of the track length distribution. High quality data in this sample (20 ages, 48 lengths) provide a reliable interpretation. **Equivalent Romax: >0.61%** (in overlying sediments). No VR values are available for comparison.
GC990-93 514487 737 m >1600 Ma	1: 2: 3:	>100 80-100 30-70	120-65 90-35 30-0	AFTA data from this sample require three episodes of heating and cooling, as shown (left), to explain all aspects of the results. The earliest of the quoted episodes is required in order to explain the reduction in fission track age. The subsequent episodes are required in order to explain the detailed form of the track length distribution. High quality data in this sample (20 ages, 103 lengths) provide a reliable interpretation. **Equivalent Romax: >0.61%** (in overlying sediments). No VR values are available for comparison.
GC990-94 514488 500 m >1600 Ma	1: 2: 3:	>105 90-100 60-75	160-100 115-60 35-0	AFTA data from this sample require three episodes of heating and cooling, as shown (left), to explain all aspects of the results. The earliest of the quoted episodes is required in order to explain the reduction in fission track age. The subsequent episodes are required in order to explain the detailed form of the track length distribution. High quality data in this sample (20 ages, 102 lengths) provide a reliable interpretation. **Equivalent Romax: >0.63%** (in overlying sediments). No VR values are available for comparison.
GC990-95 514489 349 m >1600 Ma	1: 2:	>105 60-95	215-115 135-15	AFTA data from this sample can be explained by two episodes of heating and cooling, as shown (left). The earliest episode is required in order to explain the reduction in fission track age while the later episode is required to explain the shorter tracks within the track length distribution. It is possible that the broad limits on the later episode (due to the small number of track lengths measured) may encompass two separate events, but no further resolution is possible. Despite the lower quality data compared to other samples (19 ages, 18 lengths), results from this sample are considered to provide a reliable interpretation within the stated uncertainty limits. **Equivalent $R_o$max: >0.63%** (in overlying sediments). No VR values are available for comparison.

All thermal history constraints are based on assumed heating rates of 1°C/Myr and cooling rates of 10°C/Myr.

Events shown in italics are not required by the AFTA data, though they are allowed within the limits shown.

Table 11.3: Continued (Geotrack Report #990)

Sample Details	Paleo-thermal constraints			Comments
Sample No. Source no. Elevation Strat. age	Event	Maximum paleo-temperature (°C)	Onset Of Cooling (Ma)	
GC990-97 514491 244 m >1600 Ma	1: 2:	95-105 50-75	85-45 35-0	AFTA data from this sample can be explained by two episodes of heating and cooling, as shown (left). The earliest episode is required in order to explain the reduction in fission track age and the shorter tracks within the length distribution, while the later episode is defined by the reduction in length of the main mode of the track length distribution. An earlier episode of cooling from >100°C is suggested by the data but cannot be definitely resolved due to the dominance of the first episode defined from AFTA (left). High quality data (20 ages, 102 lengths) provide a reliable interpretation, although some aspects remain uncertain. **Equivalent $R_o$max: 0.57-0.63%** (in overlying sediments) or **>0.63%** if indications of an earlier event are correct. No VR values are available for comparison.
GC990-99 514493 222 m >1600 Ma	1: 2:	>100 60-70	125-90 30-5	AFTA data from this sample can be explained by two episodes of heating and cooling, as shown (left). The earliest episode is required in order to explain the reduction in fission track age, while the later episode is defined by the reduction in length of the main mode of the track length distribution. The data provide some indication of an intermediate episode between the two quoted (left), but such an event can not be resolved with confidence. High quality data (20 ages, 102 lengths) provide a reliable interpretation, although some uncertainty remains concerning a possible intermediate event. **Equivalent $R_o$max: >0.61%** (in overlying sediments). No VR values are available for comparison.
GC990-101 514495 109 m >1600 Ma	1: 2: 3:	>100 *80-110* 40-80	160-100 *120-50* 55-0	AFTA data from this sample are best explained in terms of three episodes of heating and cooling, as shown (left), although the intermediate event cannot be defined with 100% confidence. The earliest of the quoted episodes is required in order to explain the reduction in fission track age. The subsequent episodes are required in order to explain the detailed form of the track length distribution. High quality data in this sample (20 ages, 90 lengths) provide a reliable interpretation. **Equivalent Romax: >0.61%** (in overlying sediments). No VR values are available for comparison.

All thermal history constraints are based on assumed heating rates of 1°C/Myr and cooling rates of 10°C/Myr.

Events shown in italics are not required by the AFTA data, though they are allowed within the limits shown.

Table 11.3: Continued (Geotrack Report #990)

Sample Details	Paleo-thermal constraints			Comments
Sample No. Source no. Elevation Strat. age	Event	Maximum paleo-temperature (°C)	Onset Of Cooling (Ma)	
GC990-103 514497 9 m >1600 Ma	1: 2:	>120 65-90	260-160 100-0	AFTA data from this sample can be explained by two episodes of heating and cooling, as shown (left). The earliest episode is required in order to explain the reduction in fission track age, while the later episode is defined by the reduction in length of the main mode of the track length distribution. Due to the small number of track lengths measured (10), constraints on the later episode are only broad and further detail cannot be resolved. Good quality age data (20 ages showing a consistent trend with wt% Cl) provide reliable definition of the earlier episode. **Equivalent $R_o$max: >0.73%** (in overlying sediments). No VR values are available for comparison.
GC990-105 514499 0 m >1600 Ma	1: 2: 3:	>125 95-105 50-80	460-320 330-170 130-0	AFTA data from this sample require three episodes of heating and cooling, as shown (left), to explain all aspects of the results. The earliest of the quoted episodes is required in order to explain the reduction in fission track age. The subsequent episodes are required in order to explain the detailed form of the track length distribution. High quality data in this sample (20 ages, 104 lengths) provide a reliable interpretation. Note the higher Cl contents in this sample result in the recognition of an earlier episode than seen in nearby samples. **Equivalent Romax: >0.78%** (in overlying sediments). No VR values are available for comparison.
GC990-106 514550 109 m >1600 Ma	1: 2: 3:	>115 90-100 45-70	240-165 160-70 40-0	AFTA data from this sample require three episodes of heating and cooling, as shown (left), to explain all aspects of the results. The earliest of the quoted episodes is required in order to explain the reduction in fission track age. The subsequent episodes are required in order to explain the detailed form of the track length distribution. High quality data in this sample (19 ages, 55 lengths) provide a reliable interpretation. **Equivalent Romax: >0.69%** (in overlying sediments). No VR values are available for comparison.

All thermal history constraints are based on assumed heating rates of 1°C/Myr and cooling rates of 10°C/Myr.

Events shown in italics are not required by the AFTA data, though they are allowed within the limits shown.

Table 11.3: Continued (Geotrack Report #990)

Sample Details	Paleo-thermal constraints			Comments
Sample No. Source no. Elevation Strat. age	Event	Maximum paleo-temperature (°C)	Onset Of Cooling (Ma)	
GC990-107 514551 82 m >1600 Ma	1: 2: 3:	>110 90-100 50-70	340-270 150-65 30-0	AFTA data from this sample require three episodes of heating and cooling, as shown (left), to explain all aspects of the results. The earliest of the quoted episodes is required in order to explain the reduction in fission track age. The subsequent episodes are required in order to explain the detailed form of the track length distribution. High quality data in this sample (20 ages, 100 lengths) provide a reliable interpretation. **Equivalent Romax: >0.67%** (in overlying sediments). No VR values are available for comparison.
GC990-108 514552 19 m 154-135 Ma	1: 2:	*80-105* 45-80	*>20* 25-0	AFTA data from this sample are best explained in terms of two episodes of heating and cooling after deposition, as shown (left), although the earlier of the two episodes could alternatively represent heating of the apatites prior to deposition in sediment provenance terrains. The earlier episode is required in order to explain the shorter tracks within the track length distribution, while the later episode is defined by the shortening of the main mode of the track length distribution. High quality data in this sample (20 ages, 102 lengths) provide a very reliable interpretation, although some uncertainty remains surrounding the possible earlier episode. **Equivalent $R_o$max: 0.48-0.63**% (assuming the earlier event represents the post-depositional paleo-thermal maximum). No VR values are available for comparison.
GC990-109 514553 18 m >1600 Ma	1: 2: 3:	>110 80-95 35-80	500-410 400-50 70-0	AFTA data from this sample require three episodes of heating and cooling, as shown (left), to explain all aspects of the results. The earliest of the quoted episodes is required in order to explain the reduction in fission track age. The subsequent episodes are required in order to explain the detailed form of the track length distribution. High quality data in this sample (20 ages, 112 lengths) provide a reliable interpretation. **Equivalent Romax: >0.67%** (in overlying sediments). No VR values are available for comparison.

All thermal history constraints are based on assumed heating rates of 1°C/Myr and cooling rates of 10°C/Myr.

Events shown in italics are not required by the AFTA data, though they are allowed within the limits shown.

Table 11.3: Continued (Geotrack Report #990)

Sample Details	Paleo-thermal constraints			Comments
Sample No. Source no. Elevation Strat. age	Event	Maximum paleo-temperature (°C)	Onset Of Cooling (Ma)	
GC990-110 514554 10 m >1600 Ma	1: 2: 3:	>110 90-110 70-85	480-330 400-180 90-20	AFTA data from this sample require three episodes of heating and cooling, as shown (left), to explain all aspects of the results. The earliest of the quoted episodes is required in order to explain the reduction in fission track age. The subsequent episodes are required in order to explain the detailed form of the track length distribution. High quality data in this sample (20 ages, 104 lengths) provide a reliable interpretation. **Equivalent Romax: >0.67%** (in overlying sediments). No VR values are available for comparison.
GC990-111 514555 20 m 154-135 Ma	1:	60-90	140-10	AFTA data from this sample can be explained in terms of a single episode of heating and cooling, as shown (left), involving cooling from a maximum paleotemperature between 60 and 90°C at some time between 140 and 10 Ma. This is required to explain the shortening of the main mode of the track length distribution. At the upper limit, the defined range for the onset of cooling overlaps with the younger limit for the depositional age, suggesting that the data could possibly be interpreted as reflecting inheritance of short tracks from sediment source terrains. But comparison with data from adjacent samples suggests that post-depositional heating provides a more consistent explanation, and this is the preferred scenario. Moderate to good quality data (13 ages, 66 lengths) provide a reliable interpretation within the stated limits of uncertainty. **Equivalent Romax: 0.37-0.54%** (in overlying sediments). No VR values are available for comparison.
GC990-113 514557 17 m 154-135 Ma	1: 2:	*80-105* 30-85	*>20* 50-0	AFTA data from this sample are best explained in terms of two episodes of heating and cooling after deposition, as shown (left), although the earlier of the two episodes could alternatively represent heating of the apatites prior to deposition in sediment provenance terrains. The earlier episode is required in order to explain the shorter tracks within the track length distribution, while the later episode is defined by the shortening of the main mode of the track length distribution. Moderate quality data in this sample (9 ages, 48 lengths) provide a reliable interpretation, although some uncertainty remains surrounding the possible earlier episode. **Equivalent $R_o$max: 0.48-0.63**% (assuming the earlier event represents the post-depositional paleo-thermal maximum). No VR values are available for comparison.

All thermal history constraints are based on assumed heating rates of 1°C/Myr and cooling rates of 10°C/Myr.

Events shown in italics are not required by the AFTA data, though they are allowed within the limits shown.

Table 11.3: Continued (Geotrack Report #990)

Sample Details	Paleo-thermal constraints			Comments
Sample No. Source no. Elevation Strat. age	Event	Maximum paleo-temperature (°C)	Onset Of Cooling (Ma)	
GC990-115 514559 22 m >1600 Ma	1: 2:	>115 85-95	475-350 80-20	AFTA data from this sample can be explained by two episodes of heating and cooling, as shown (left). The earliest episode is required in order to explain the reduction in fission track age, while the later episode is defined by the reduction in length of the main mode of the track length distribution. High quality age data (20 ages, 111 lengths) provide reliable definition of the earlier episode. **Equivalent $R_o$max: >0.67%** (in overlying sediments) . No VR values are available for comparison.
GC990-116 514560 16 m 154-135 Ma	1:	80-90	100-5	AFTA data from this sample can be explained in terms of a single episode of heating and cooling, as shown (left), involving cooling from a maximum paleotemperature between 80 and 90°C at some time between 100 and 5 Ma. This is required to explain the shortening of the main mode of the track length distribution. Moderate quality data (10 ages, 22 lengths) provide a reliable interpretation within the stated limits of uncertainty. **Equivalent Romax: 0.48-0.54%** (in overlying sediments). No VR values are available for comparison.
GC990-119 514564 316 m >570 Ma	1: 2: 3:	*>110?* 90-105 40-80	*100-150?* 100-45 60-0	AFTA data from this sample are best explained in terms of three episodes of heating and cooling, as shown (left), to explain all aspects of the results. However, the earliest of the three episodes is difficult to define with confidence because of the dominance of the intermediate episode. The combination of the two earlier episodes is required in order to explain the reduction in fission track age and the shorter tracks within the length distribution. The most recent episode is required in order to explain the shortening of the main mode of the track length distribution. High quality data in this sample (20 ages, 100 lengths) provide a reliable interpretation. **Equivalent Romax: >0.67%** (in overlying sediments), for the earliest of the three episodes. No VR values are available for comparison.

All thermal history constraints are based on assumed heating rates of 1°C/Myr and cooling rates of 10°C/Myr.

Events shown in italics are not required by the AFTA data, though they are allowed within the limits shown.

Table 11.3: Continued (Geotrack Report #990)

Sample Details	Paleo-thermal constraints			Comments
Sample No. Source no. Elevation Strat. age	Event	Maximum paleo-temperature (°C)	Onset Of Cooling (Ma)	
GC990-120 514565 57 m >570 Ma	1: 2: 3:	*>110?* 80-105 30-80	*>100* 145-55 65-0	AFTA data from this sample are best explained in terms of three episodes of heating and cooling, as shown (left), to explain all aspects of the results. However, the earliest of the three episodes cannot be rigorously defined because of the dominance of the intermediate episode. The combination of the two earlier episodes is required in order to explain the reduction in fission track age and the shorter tracks within the length distribution. The most recent episode is required in order to explain the shortening of the main mode of the track length distribution. High quality data in this sample (20 ages, 73 lengths) provide a reliable interpretation. **Equivalent Romax: >0.67%** (in overlying sediments), for the earliest of the three episodes. No VR values are available for comparison.
GC990-122 514567 253 m >570 Ma	1: 2: 3:	>105 75-90 40-65	160-120 120-45 40-0	AFTA data from this sample require three episodes of heating and cooling, as shown (left), to explain all aspects of the results. The earliest of the quoted episodes is required in order to explain the reduction in fission track age. The subsequent episodes are required in order to explain the detailed form of the track length distribution. High quality data in this sample (20 ages, 102 lengths) provide a reliable interpretation. **Equivalent Romax: >0.63%** (in overlying sediments). No VR values are available for comparison.
GC990-123 514568 359 m 150-120 Ma	1: 2:	*75-105* 20-80	*>25* 50-0	AFTA data from this sample are best explained in terms of two episodes of heating and cooling after deposition, as shown (left), although the earlier of the two episodes could alternatively represent heating of the apatites prior to deposition in sediment provenance terrains. The earlier episode is required in order to explain the shorter tracks within the track length distribution, while the later episode is defined by the shortening of the main mode of the track length distribution. High quality data in this sample (20 ages, 103 lengths) provide a reliable interpretation within the stated limits of uncertainty, although due to the moderate degree of heating, some aspects of the history cannot be defined with full confidence. **Equivalent $R_o$max: 0.45-0.63**% (assuming the earlier event represents the post-depositional paleo-thermal maximum). No VR values are available for comparison.

All thermal history constraints are based on assumed heating rates of 1°C/Myr and cooling rates of 10°C/Myr.

Events shown in italics are not required by the AFTA data, though they are allowed within the limits shown.

Table 11.3: Continued (Geotrack Report #990)

Sample Details	Paleo-thermal constraints			Comments
Sample No. Source no. Elevation Strat. age	Event	Maximum paleo-temperature (°C)	Onset Of Cooling (Ma)	
GC990-125 514570 282 m 435-345 Ma	1: 2:	90-100 40-85	270-115 150-0	AFTA data from this sample can be explained by two episodes of heating and cooling, as shown (left). The earliest episode is required in order to explain the reduction in fission track age and the shorter lengths in the track length distribution, while the later episode is defined by the reduction in length of the longer mode in the noteably broad track length distribution. High quality age data (21 ages, 104 lengths) provide reliable definition of the earlier episode. **Equivalent $R_o$max: 0.54-0.61%.** No VR values are available for comparison.
GC990-126 514571 204 m >570 Ma	1: 2: 3:	*>110?* 95-105 65-80	*200-100?* 140-70 50-15	AFTA data from this sample are best explained in terms of three episodes of heating and cooling, as shown (left), to explain all aspects of the results. However, the earliest of the three episodes cannot be rigorously defined because of the dominance of the intermediate episode. The combination of the two earlier episodes is required in order to explain the reduction in fission track age and the shorter tracks within the length distribution. The most recent episode is required in order to explain the shortening of the main mode of the track length distribution. High quality data in this sample (20 ages, 105 lengths) provide a reliable interpretation. **Equivalent Romax: >0.67%** (in overlying sediments), for the earliest of the three episodes. No VR values are available for comparison.
GC990-128 514573 162 m >570 Ma	1: 2:	>115 65-85	150-100 80-25	AFTA data from this sample can be explained by two episodes of heating and cooling, as shown (left). The earliest episode is required in order to explain the reduction in fission track age, while the later episode is defined by the reduction in length of the main mode of the track length distribution. High quality age data (20 ages, 100 lengths) provide reliable definition of the earlier episode. **Equivalent $R_o$max: >0.69%** (in overlying sediments) . No VR values are available for comparison.

All thermal history constraints are based on assumed heating rates of 1°C/Myr and cooling rates of 10°C/Myr.

Events shown in italics are not required by the AFTA data, though they are allowed within the limits shown.

Table 11.3: Continued (Geotrack Report #990)

Sample Details	Paleo-thermal constraints			Comments
Sample No. Source no. Elevation Strat. age	Event	Maximum paleo-temperature (°C)	Onset Of Cooling (Ma)	
GC854-1 12/01 - >600 Ma	1: 2:	>115 90-95 50-70	320-275 150-70 50-0	AFTA data from this sample are of very good quality, with 25 age grains and 100 confined track lengths. The AFTA data *require* higher temperatures in the past, with modelling indicating the sample must have cooled from a paleotemperature >115°C sometime between 310 and 270 Ma. Two subsequent events are also required by the data, with this 3-event solution providing a very good fit to the data. **Equivalent $R_o$max >0.69%**. This maturity estimate derived from AFTA is relevant to any sedimentary cover that experienced the same history. No measured VR values are available for comparison.
GC854-2 12/02 - >600 Ma	1: 2: 3:	>105 85-100 <80	370-300 270-100 150-0	AFTA data from this sample are of very good quality, with 20 age grains and 101 confined track lengths. The AFTA data *require* higher temperatures in the past, with modelling indicating the sample must have experienced two events (see left), with a third later event *possible*. The earliest event is particularly well defined. **Equivalent $R_o$max >0.63%**. This maturity estimate derived from AFTA is relevant to any sedimentary cover that experienced the same history. No measured VR values are available for comparison.
GC854-5 12/03 - >600 Ma	1: 2: 3:	>110? 85-95 50-75	>250? 230-60 55-0	AFTA data from this sample are of very good quality, with 21 age grains and 101 confined track lengths. All analysed grains fall into the 0.0-0.1 wt% Cl group (in contrast to the range of Cl represented in the two previous basement samples). The AFTA data are consistent with a 3-event solution, as shown to the left, although the earliest event cannot be defined with confidence. But the data provide relatively tight control on paleotemperatures during two subsequent events, as shown. **Equivalent $R_o$max >0.66% (for earliest event).** This maturity estimate derived from AFTA is relevant to any sedimentary cover that experienced the same history. No measured VR values are available for comparison.

All thermal history constraints are based on assumed heating rates of 1°C/Myr and cooling rates of 10°C/Myr.

Events shown in italics are not required by the AFTA data, though they are allowed within the limits shown.

Table 11.3: Continued (Geotrack Report #990)

Sample Details	Paleo-thermal constraints			Comments
Sample No. Source no. Elevation Strat. age	Event	Maximum paleo-temperature (°C)	Onset Of Cooling (Ma)	
GC854-7 12/07 - 141-125 Ma	1:	70-100	120-10	AFTA data from this sample are of moderate quality, with 9 age grains and 25 confined track lengths. The AFTA data can be explained by cooling from a maximum paleotemperature in the range 70-100°C commencing sometime between 120 and 10 Ma. **Equivalent $R_o$max 0.42-0.61%.** No measured VR values are available for comparison.
GC854-11 12/11 - 141-125 Ma	1: 2:	*70-100* 70-80	*post-deposition* 55-0	AFTA data from this sample are of good quality, with 20 age grains and 102 confined track lengths. The AFTA data are best explained in terms of cooling from a maximum paleotemperature in the range 70 to 100°C commencing sometime after deposition, but within the resolution of the data it is possible that this represents the effects of heating in sediment source terrains. A subsequent cooling event is clearly required after deposition, as shown. **Equivalent $R_o$max 0.42-0.61%** (for post-depositional heating). No measured VR values are available for comparison.
GC854-14 12/14 - >600 Ma	1: 2:	>100 45-75	110-70 65-0	AFTA data from this sample are of very good quality, with 20 age grains and 52 confined track lengths. Modelling the AFTA data shows the data can be explained by two events (see left). The earlier event (110-70 Ma) is particularly well defined, and sufficiently intense as to "erase" any evidence for any prior heating. **Equivalent $R_o$max >0.61%.** This maturity estimate derived from AFTA is relevant to any sedimentary cover that experienced the same history. No measured VR values are available for comparison.

All thermal history constraints are based on assumed heating rates of 1°C/Myr and cooling rates of 10°C/Myr.

Events shown in italics are not required by the AFTA data, though they are allowed within the limits shown.

Table 11.3: Continued (Geotrack Report #990)

Sample Details	Paleo-thermal constraints			Comments
Sample No. Source no. Elevation Strat. age	Event	Maximum paleo-temperature (°C)	Onset Of Cooling (Ma)	
GC854-16 12/16 - >600 Ma	1: 2:	100-105 <80	150-70 120-0	Results from this basement sample (17 age grains and 13 confined track lengths) show a clear requirement for paleo-heating, but only broad quantitative constraint on the description of the events, as shown (left). Modelling shows the sample cooled from maximum paleotemperatures in the range of 100 to 105°C commencing sometime between 150 and 70 Ma. Other events (as shown) are allowed, but not required, and in particular the earlier history cannot be defined with confidence. **Equivalent $R_o$max 0.61-0.63%.** This maturity estimate derived from AFTA is relevant to any sedimentary cover that experienced the same history. No measured VR values are available for comparison.
GC854-17 12/17 - >600 Ma	1: 2:	>100 70-95	165-85 75-15	Results from this basement sample (13 age grains and 22 confined track lengths) show a clear requirement for paleo-heating, with total overprinting (>100°C) prior to the onset of cooling in the 165-85 Ma event (as shown). Modelling shows the sample subsequently cooled from maximum paleotemperatures in the range of 70 to 95°C beginning sometime between 75 and 15 Ma. **Equivalent $R_o$max >0.61%.** This maturity estimate derived from AFTA is relevant to any sedimentary cover that experienced the same history. No measured VR values are available for comparison.
GC854-19 12/19 - >600 Ma	1: 2:	>105 55-80	155-90 50-0	Results from this basement sample (18 age grains and 10 confined track lengths) show a clear requirement for paleo-heating, with total overprinting (>105°C) prior to the onset of cooling in the 155-90 Ma event (as shown). Subsequent cooling from between 55 and 80°C is required to explain the length reduction. Despite the limited number of confined track lengths, this later event is well defined. **Equivalent $R_o$max >0.63%**. This maturity estimate derived from AFTA is relevant to any sedimentary cover that experienced the same history. No measured VR values are available for comparison..

All thermal history constraints are based on assumed heating rates of 1°C/Myr and cooling rates of 10°C/Myr.

Events shown in italics are not required by the AFTA data, though they are allowed within the limits shown.

Table 11.3: Continued (Geotrack Report #990)

Sample Details	**Paleo-thermal constraints**			**Comments**
Sample No. Source no. Elevation Strat. age	Event	Maximum paleo-temperature (°C)	Onset Of Cooling (Ma)	
GC854-20 12/20 - >600 Ma	1: 2:	>100 60-70	110-85 45-5	High quality AFTA data in this sample (20 age grains, and 100 confined track lengths) provide a very well-defined solution. Modelling the AFTA parameters provides very tight definition of the earlier episode, in which the sample cooled below 100°C sometime between 110 and 85 Ma. Subsequent cooling from between 60 and 70°C is required to explain the length reduction. Despite the limited number of confined track lengths, this later event is well defined. **Equivalent $R_o$max >0.63%**. This maturity estimate derived from AFTA is relevant to any sedimentary cover that experienced the same history. No measured VR values are available for comparison.

All thermal history constraints are based on assumed heating rates of 1°C/Myr and cooling rates of 10°C/Myr.

Events shown in italics are not required by the AFTA data, though they are allowed within the limits shown.

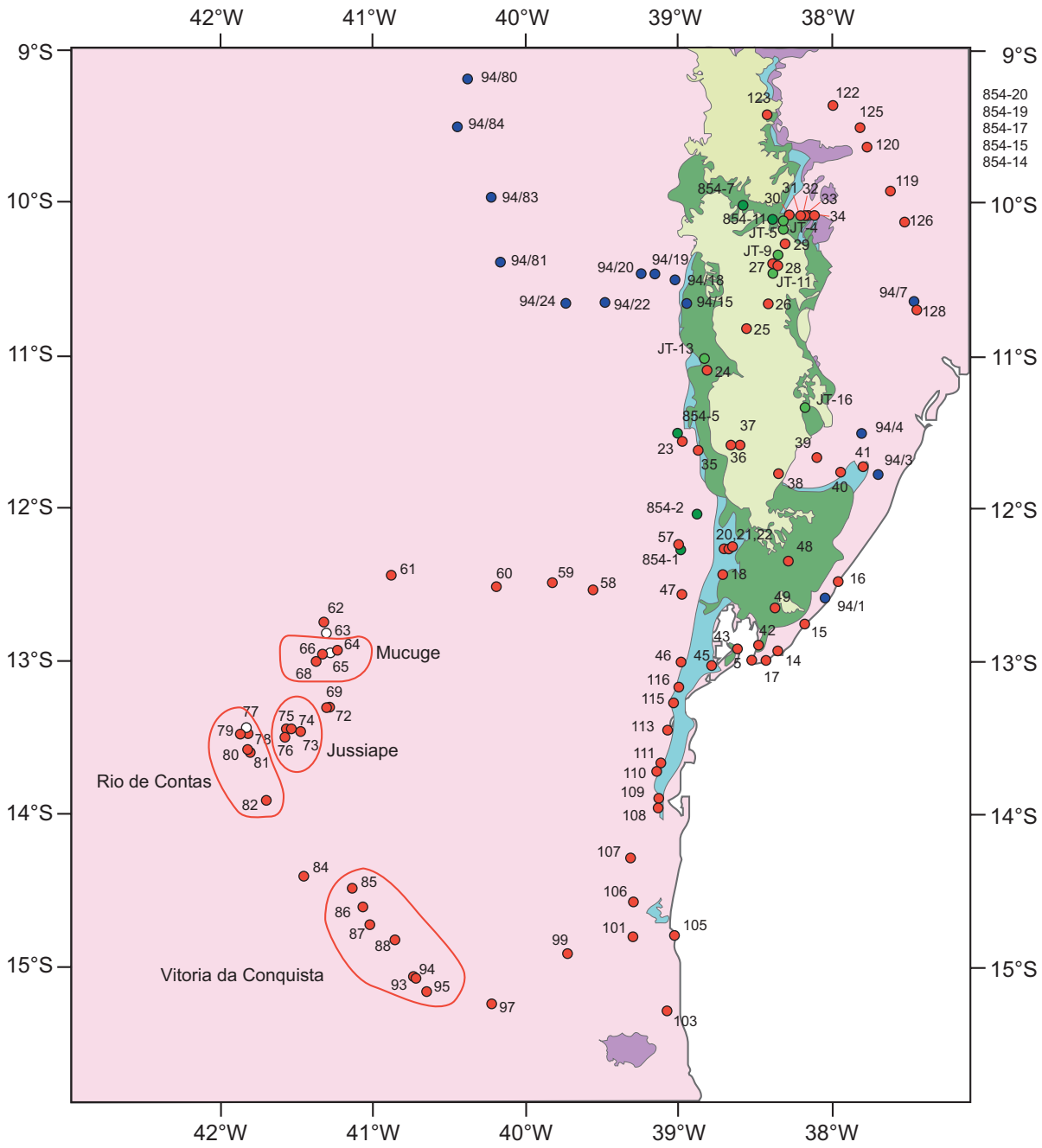

Figure 11.1: Location map showing **outcrop samples from Bahia, NE Brazil,** for which AFTA data are discussed in this Section. Samples shown with green symbols refer to published data from Turner et al. (2008). Those shown with 854 prefixes have been reinterpreted for this study and details are included in Tables 11.2 and 11.3. Samples shown with blue symbols are from Harman et al. (1998), and are included only to extend the map of fission track ages shown in Figure 11.5. Locations of four elevation sections discussed in Section 11.8 are also shown (red outlines).

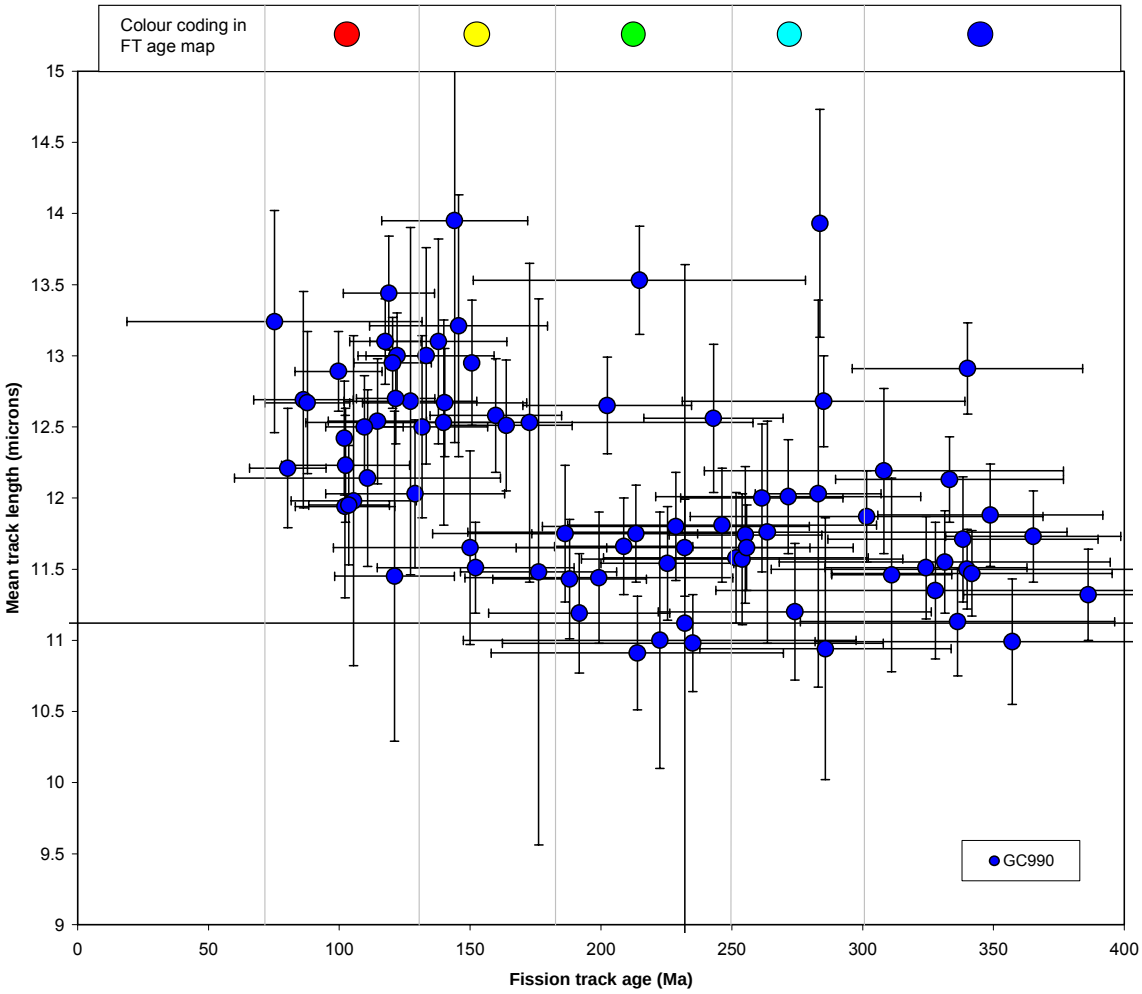

Figure 11.2: Mean track length vs fission track age for **outcrop samples from Bahia**. The data define a coherent trend but in detail the trend is not the simple "boomerang" trend characteristic of a single dominant paleo-thermal episode. Instead, these results suggest a more complex thermal history framework, involving multiple paleo-thermal episodes.

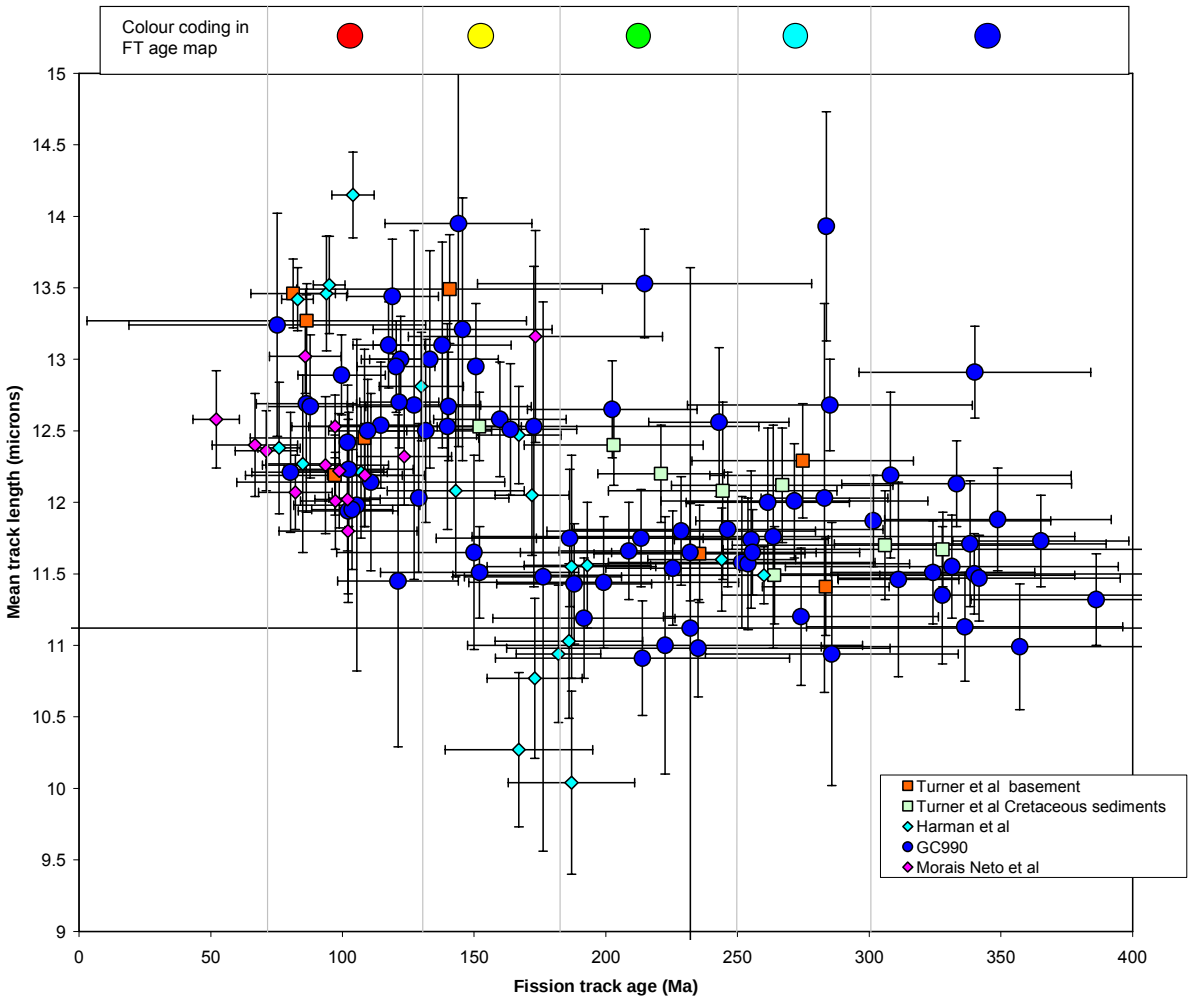

Figure 11.3: Mean track length vs fission track age for **outcrop samples from Bahia**, as in Figure 11.2, together with data from published studies of NE Brazil (Harman et al. 1998; Turner et al. 2008; Morais Neto et al. 2008). The different datasets are generally consistent, although note that data from Morais Neto et al (2008) plot at the limit of the trend, suggesting a specific history for those samples.

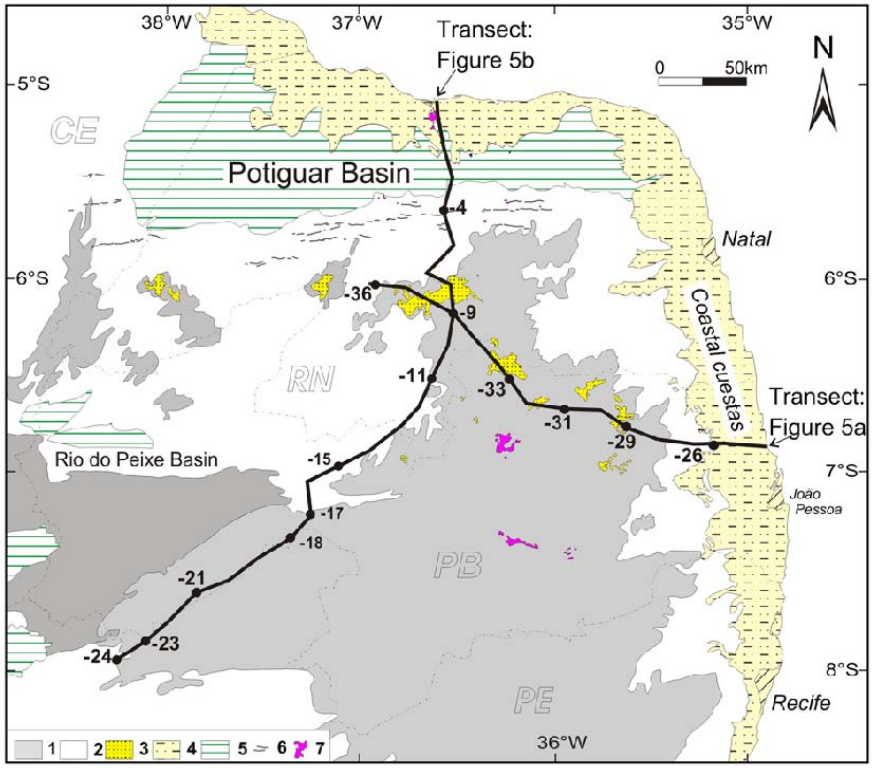

Figure 11.4a: Locations of samples analysed by Morais Neto et al. (2008) included in Figure 11.3.

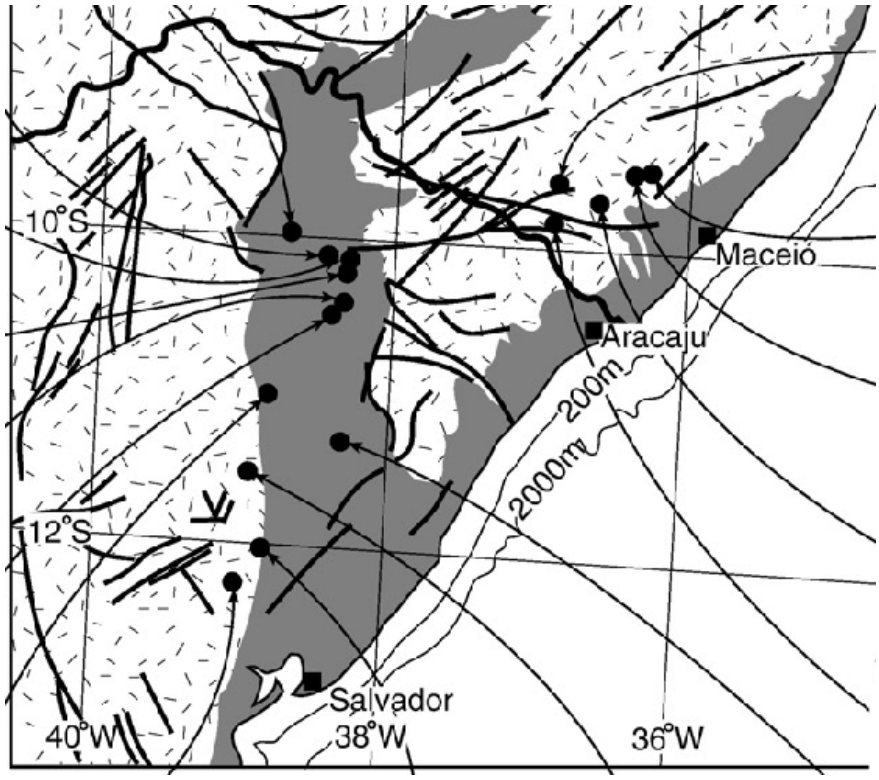

Figure 11.4b: Locations of samples analysed by Turner et al. (2008), included in Figure 11.3, showing in particular the locations of samples to the NE of the region shown in Figure 11.1.

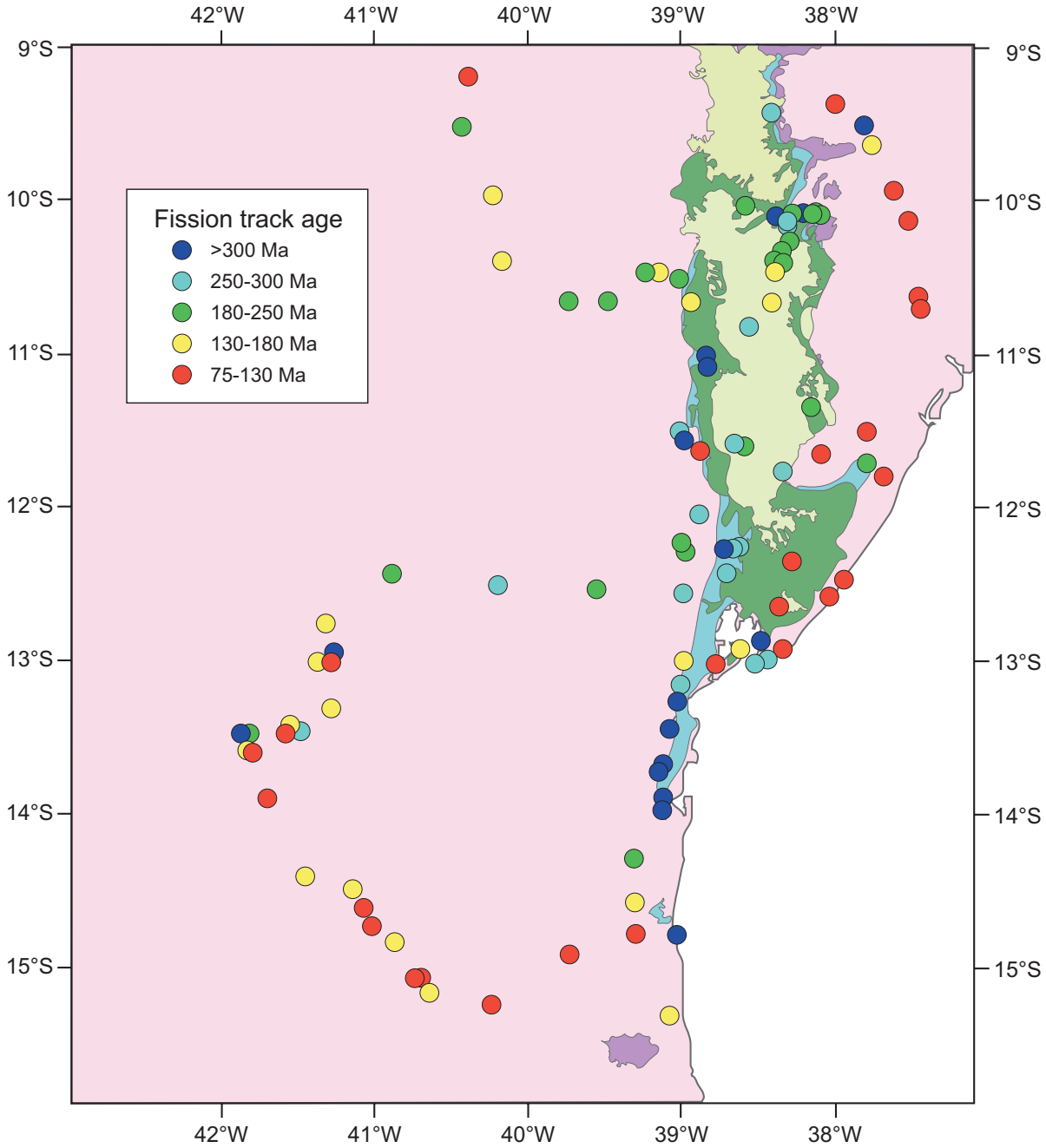

Figure 11.5: Fission track ages in individual **outcrop samples from Bahia**, from locations shown in Figure 11.1, colour coded as shown in Figures 11.2 and 11.3. Values for individual samples are listed in Table 11.1 and more details of the data are provided in the Data Summary Sheets in Appendix B.

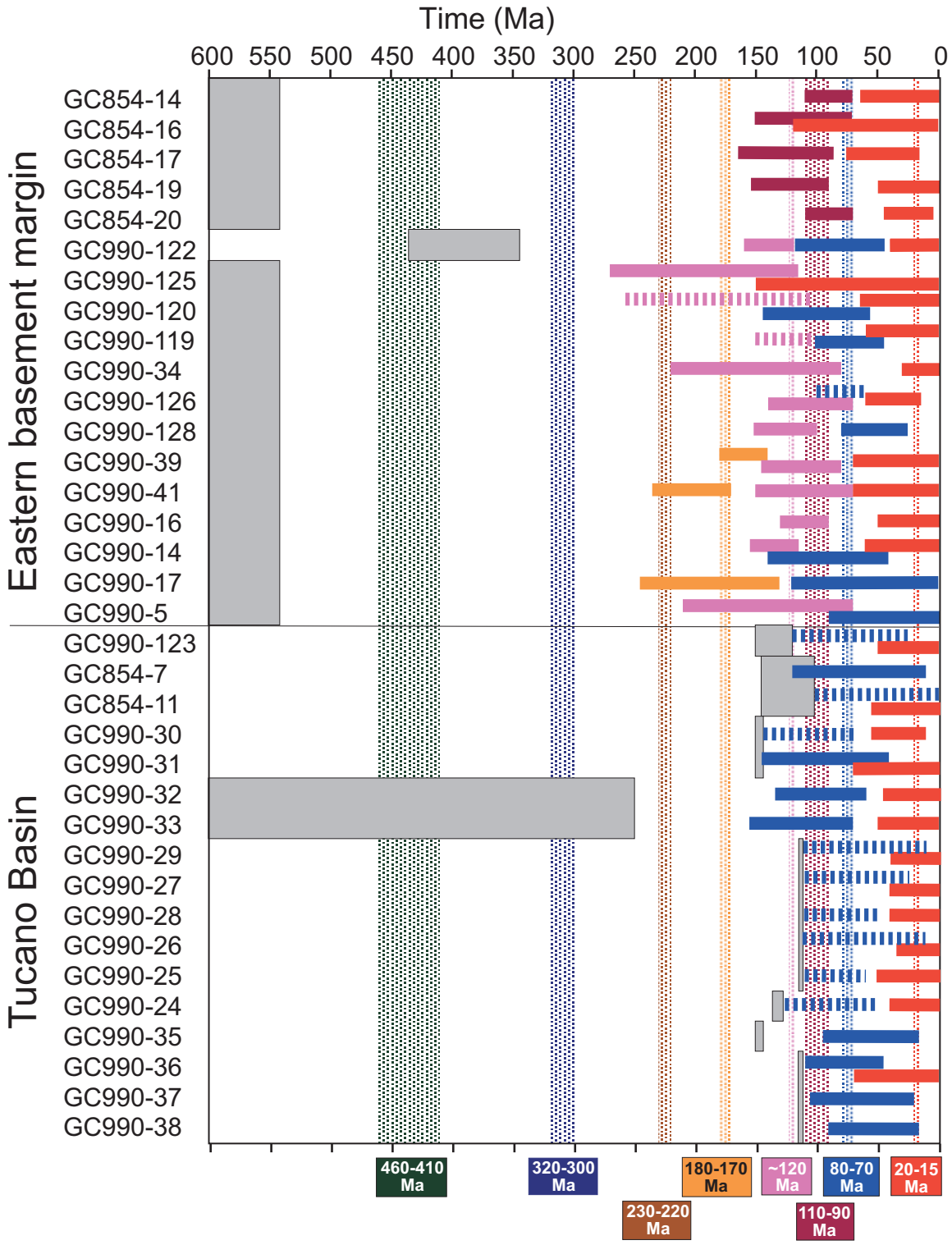

Figure 11.6: Timing constraints derived from AFTA data in individual outcrop samples from the **Northeast** of the study region shown in Figure 11.1. Values for individual samples are listed in Table 11.3. Vertical coloured columns denote the timing of regional cooling episodes derived from the AFTA data, as discussed in Section 11.5. Grey boxes denote depositional ages (Precambrian samples are allocated a minimum age of 542 Ma). Dashed lines represent episodes that are only tentatively identified from the AFTA data.

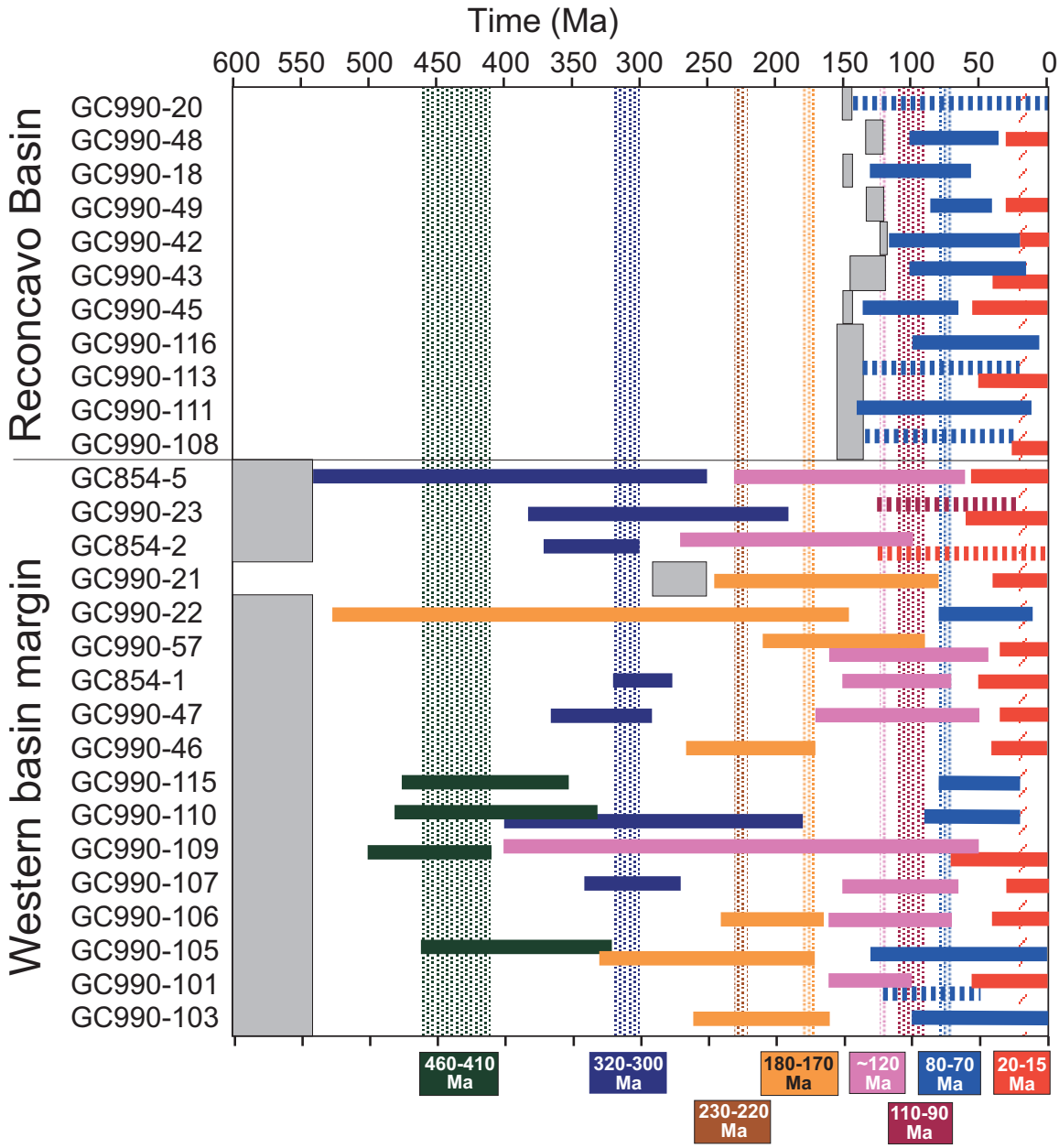

Figure 11.7: Timing constraints derived from AFTA data in individual outcrop samples from the **Recôncavo Basin and its western margin**, as shown in Figure 11.1. Values for individual samples are listed in Table 11.3. Other details are as described for Figure 11.6.

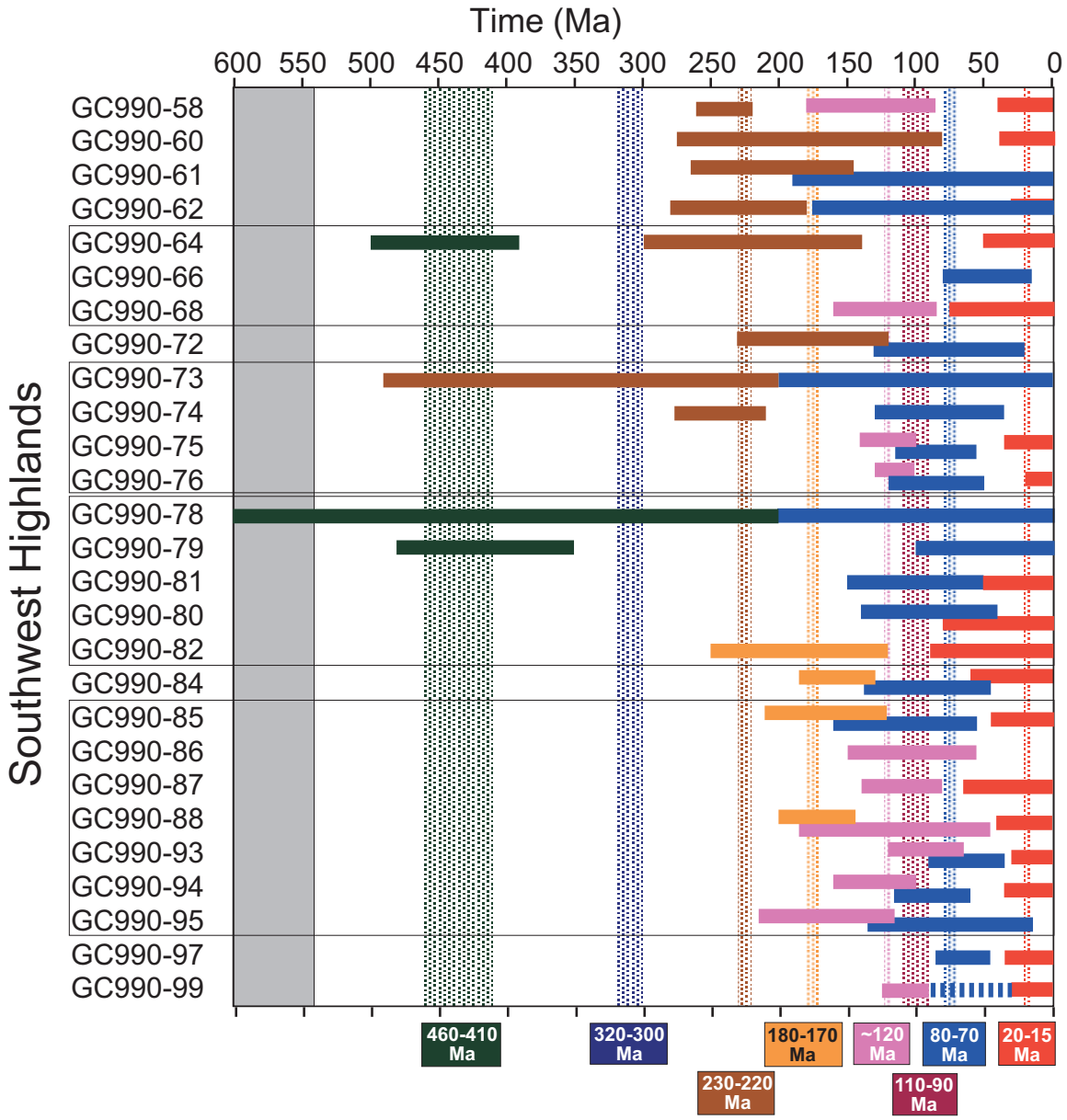

Figure 11.8: Timing constraints derived from AFTA data in individual outcrop samples from the **Southwest** of the study region shown in Figure 11.1. Values for individual samples are listed in Table 11.3. Other details are as described for Figure 11.6. Samples from four elevation transects are denoted by boxes.

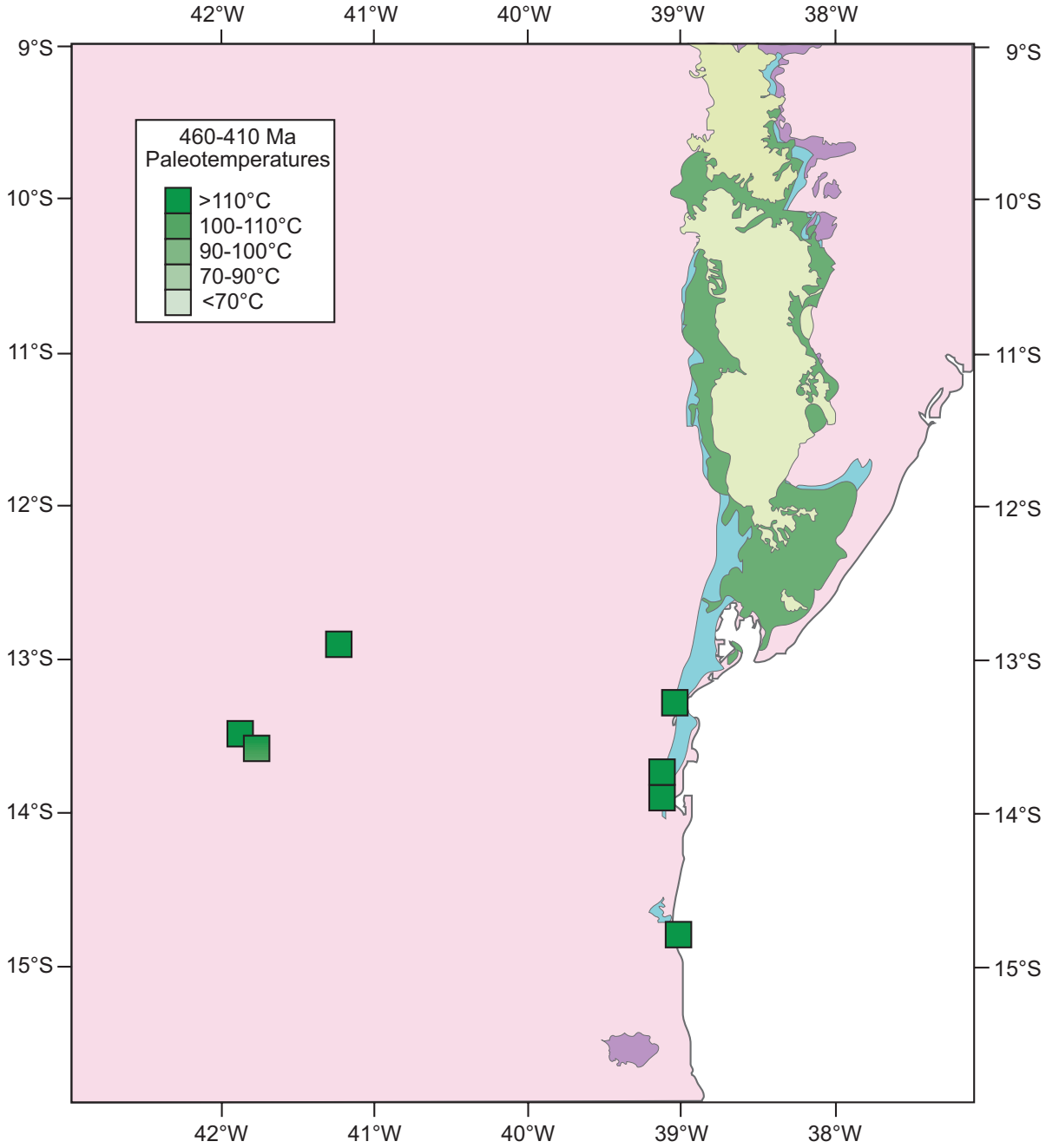

Figure 11.9: **Ordovician to Devonian (460-410 Ma)** paleotemperatures derived from AFTA data in **outcrop samples from Bahia**, from locations shown in Figure 11.1. Values for individual samples analysed for this report are listed in Table 11.3 and attributed to individual paleo-thermal episodes in Figures 11.6, 11.7 and 11.8.

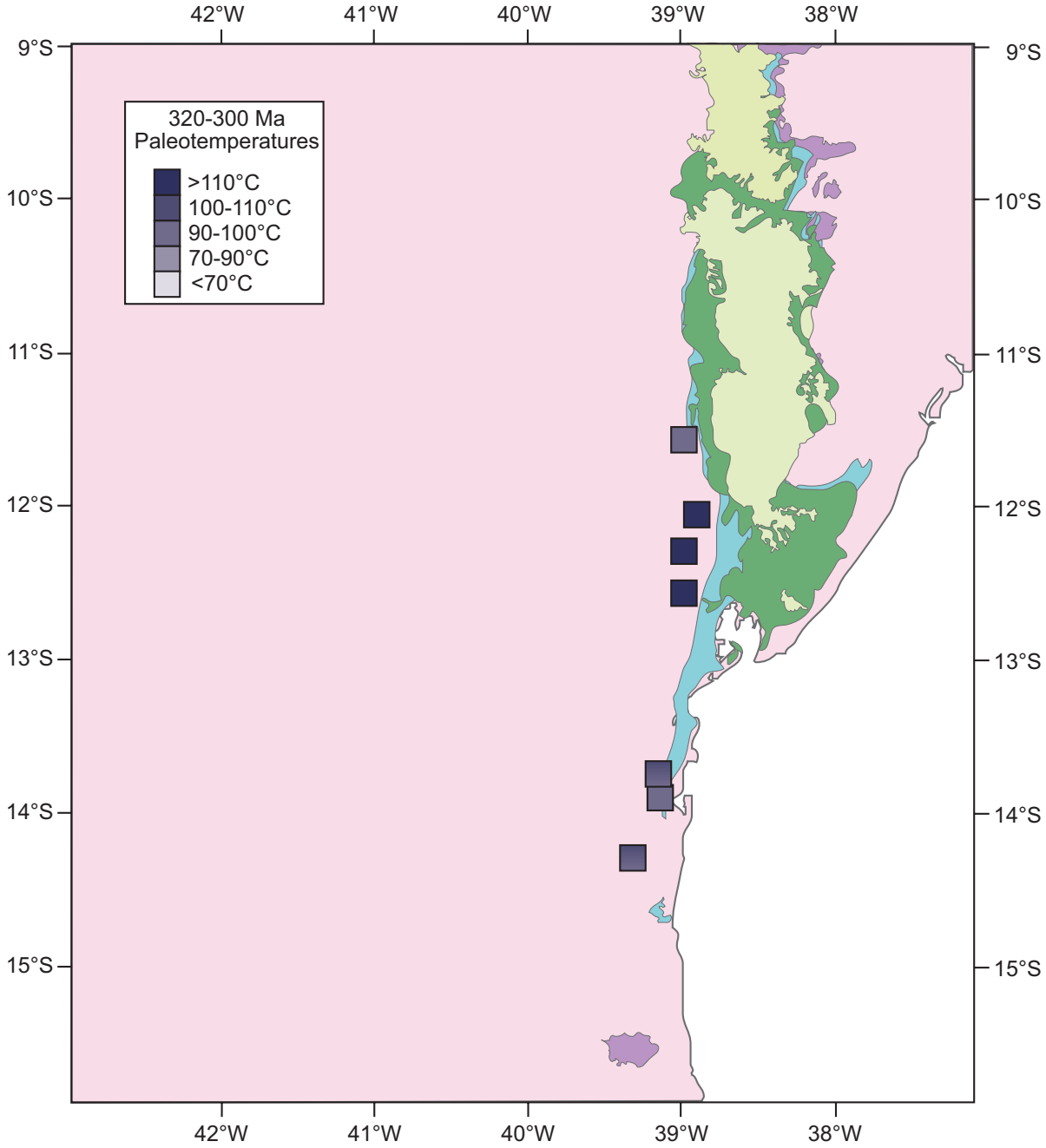

Figure 11.10: Carboniferous (320-300 Ma) paleotemperatures derived from AFTA data in **outcrop samples from Bahia**, from locations shown in Figure 11.1. Values for individual samples analysed for this report are listed in Table 11.3 and attributed to individual paleo-thermal episodes in Figures 11.6, 11.7 and 11.8.

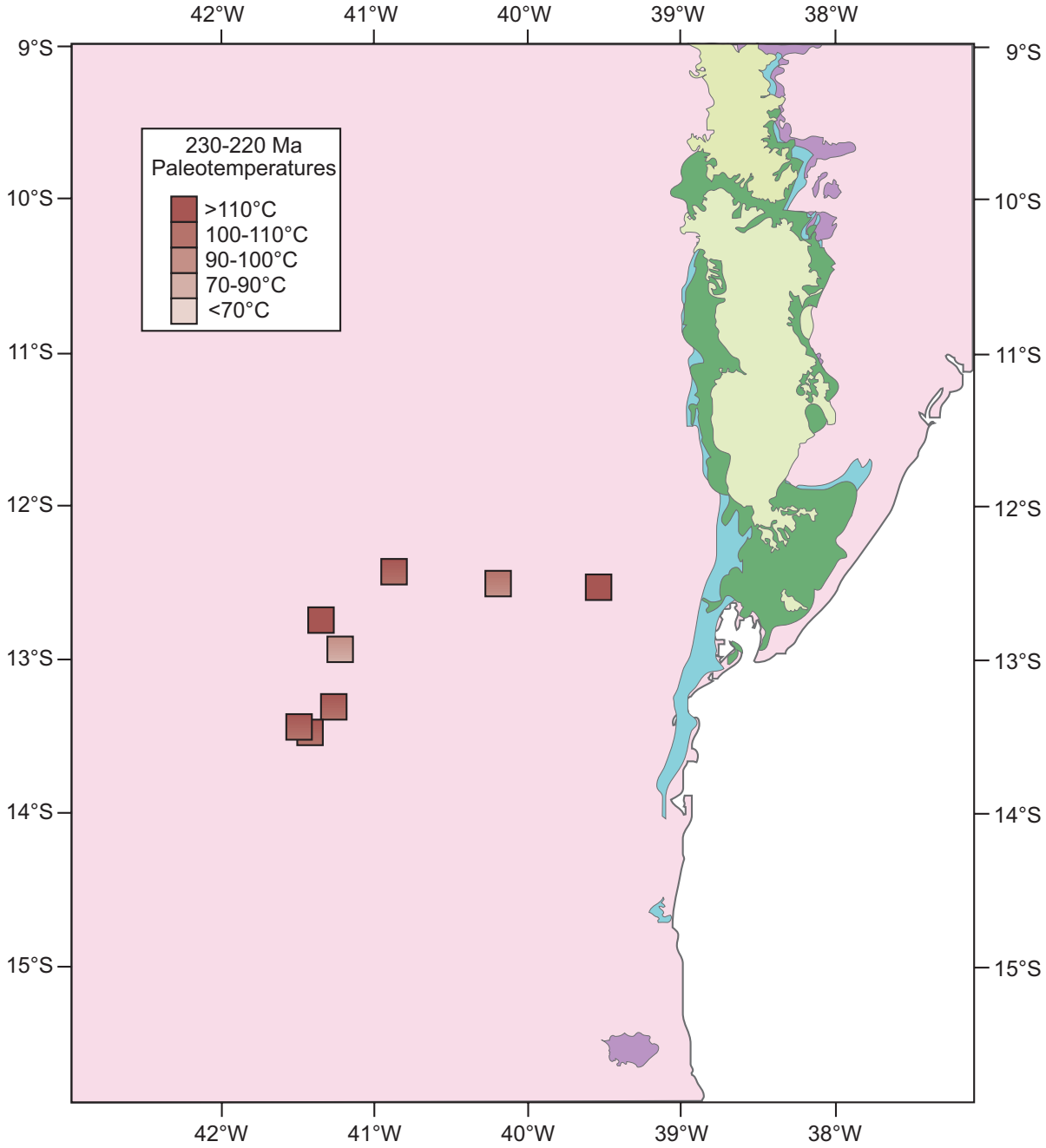

Figure 11.11: Triassic (230-220 Ma) paleotemperatures derived from AFTA data in **outcrop samples from Bahia**, from locations shown in Figure 11.1. Values for individual samples analysed for this report are listed in Table 11.3 and attributed to individual paleo-thermal episodes in Figures 11.6, 11.7 and 11.8.

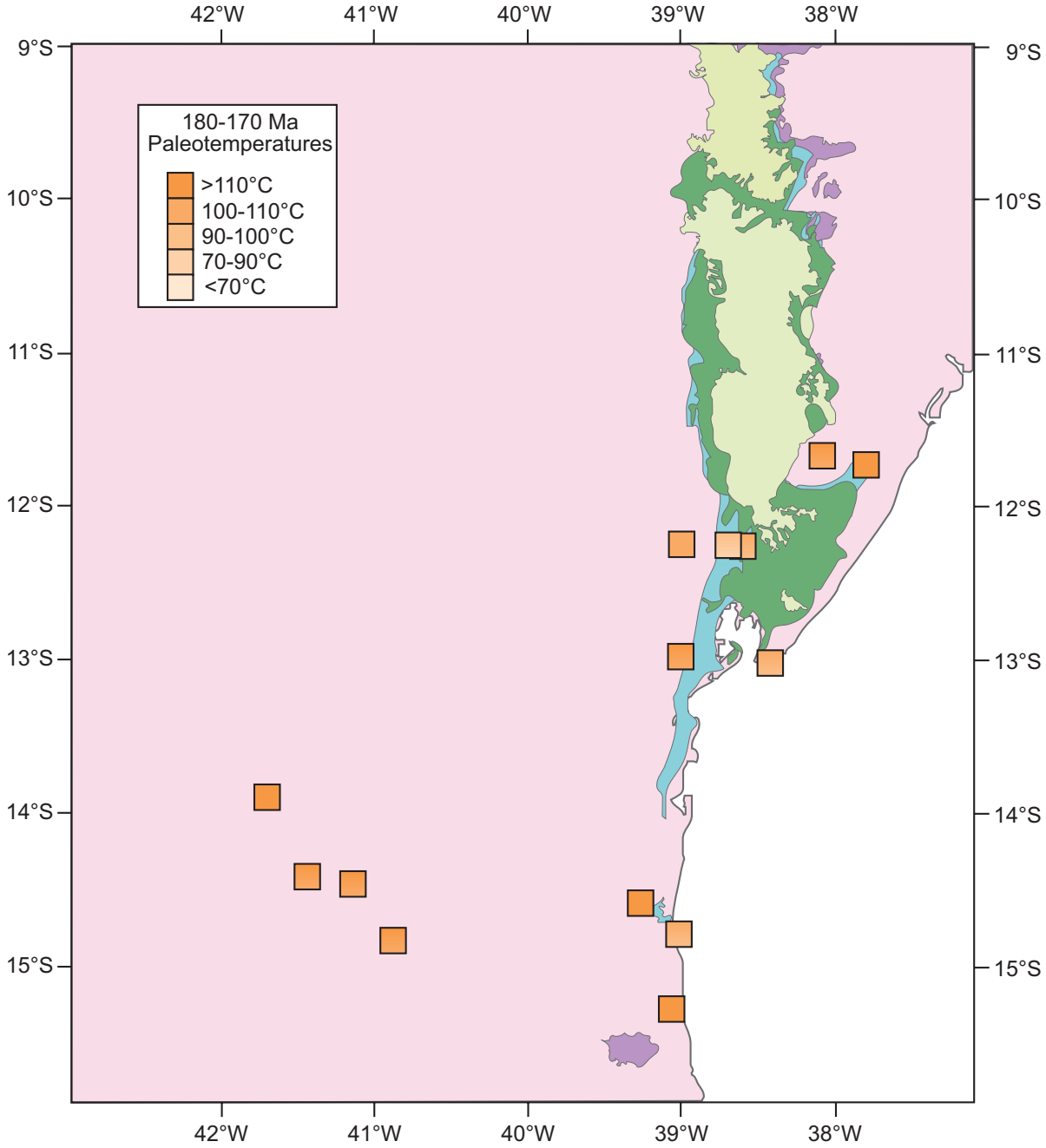

Figure 11.12: Jurassic (180-170 Ma) paleotemperatures derived from AFTA data in **outcrop samples from Bahia**, from locations shown in Figure 11.1. Values for individual samples analysed for this report are listed in Table 11.3 and attributed to individual paleo-thermal episodes in Figures 11.6, 11.7 and 11.8.

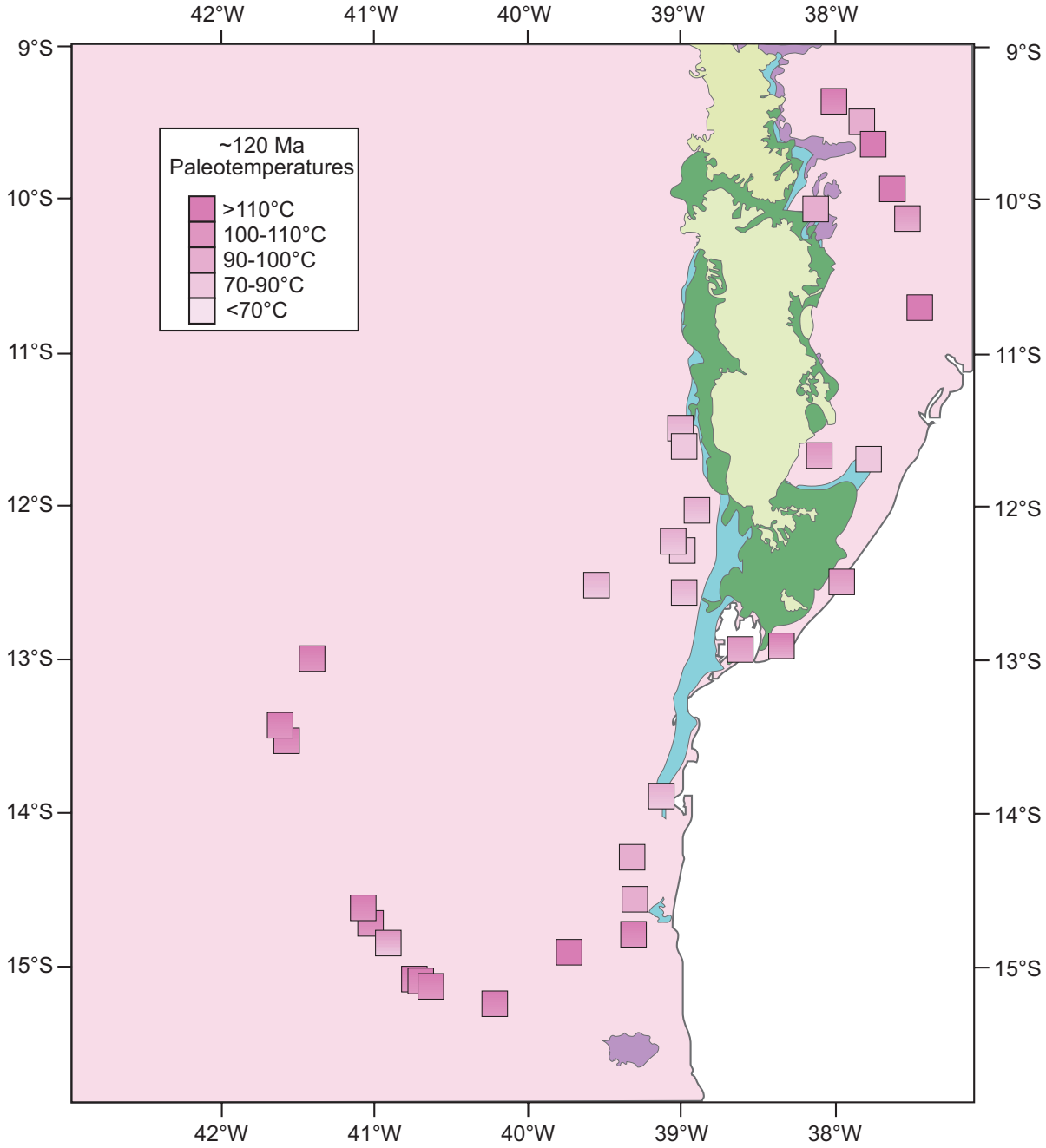

Figure 11.13: Early Cretaceous (~120 Ma) paleotemperatures derived from AFTA data in **outcrop samples from Bahia**, from locations shown in Figure 11.1. Values for individual samples analysed for this report are listed in Table 11.3 and attributed to individual paleo-thermal episodes in Figures 11.6, 11.7 and 11.8.

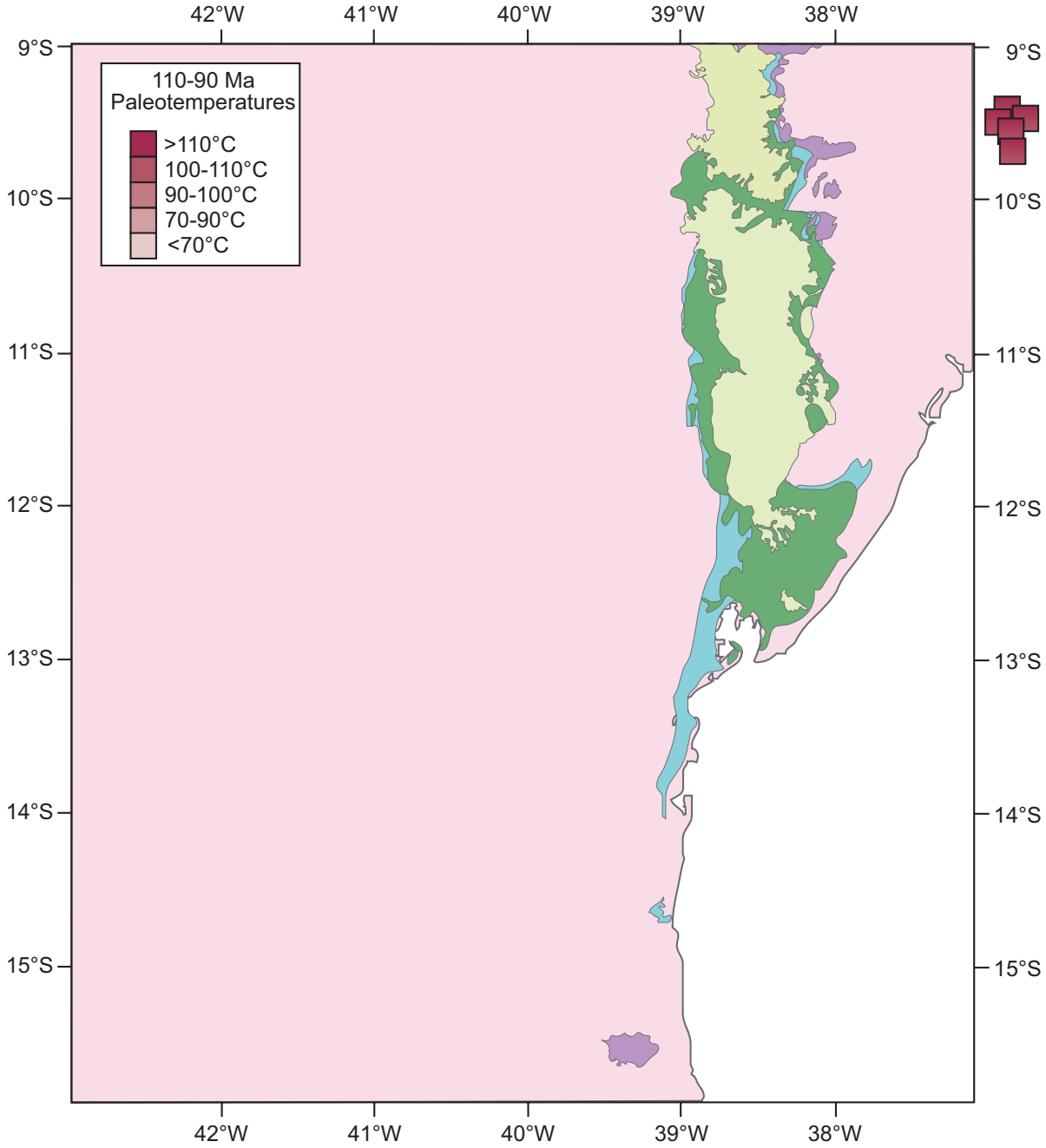

Figure 11.14: Mid-Cretaceous (110-90 Ma) paleotemperatures derived from AFTA data in **outcrop samples from Bahia**, from locations shown in Figure 11.1. Values for individual samples analysed for this report are listed in Table 11.3 and attributed to individual paleo-thermal episodes in Figures 11.6, 11.7 and 11.8.

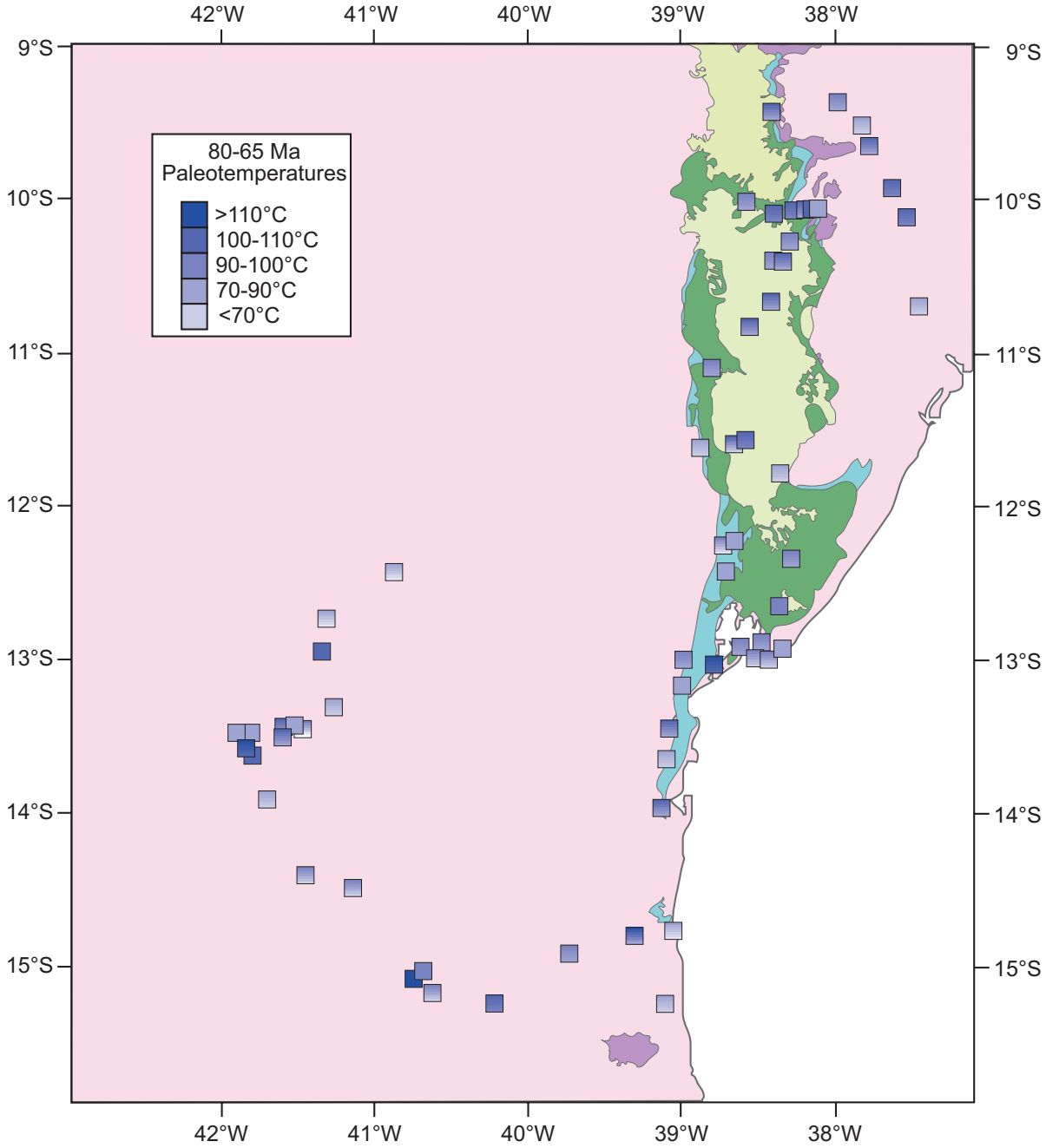

Figure 11.15: Late Cretaceous (80-65 Ma) paleotemperatures derived from AFTA data in **outcrop samples from Bahia**, from locations shown in Figure 11.1. Values for individual samples analysed for this report are listed in Table 11.3 and attributed to individual paleo-thermal episodes in Figures 11.6, 11.7 and 11.8.

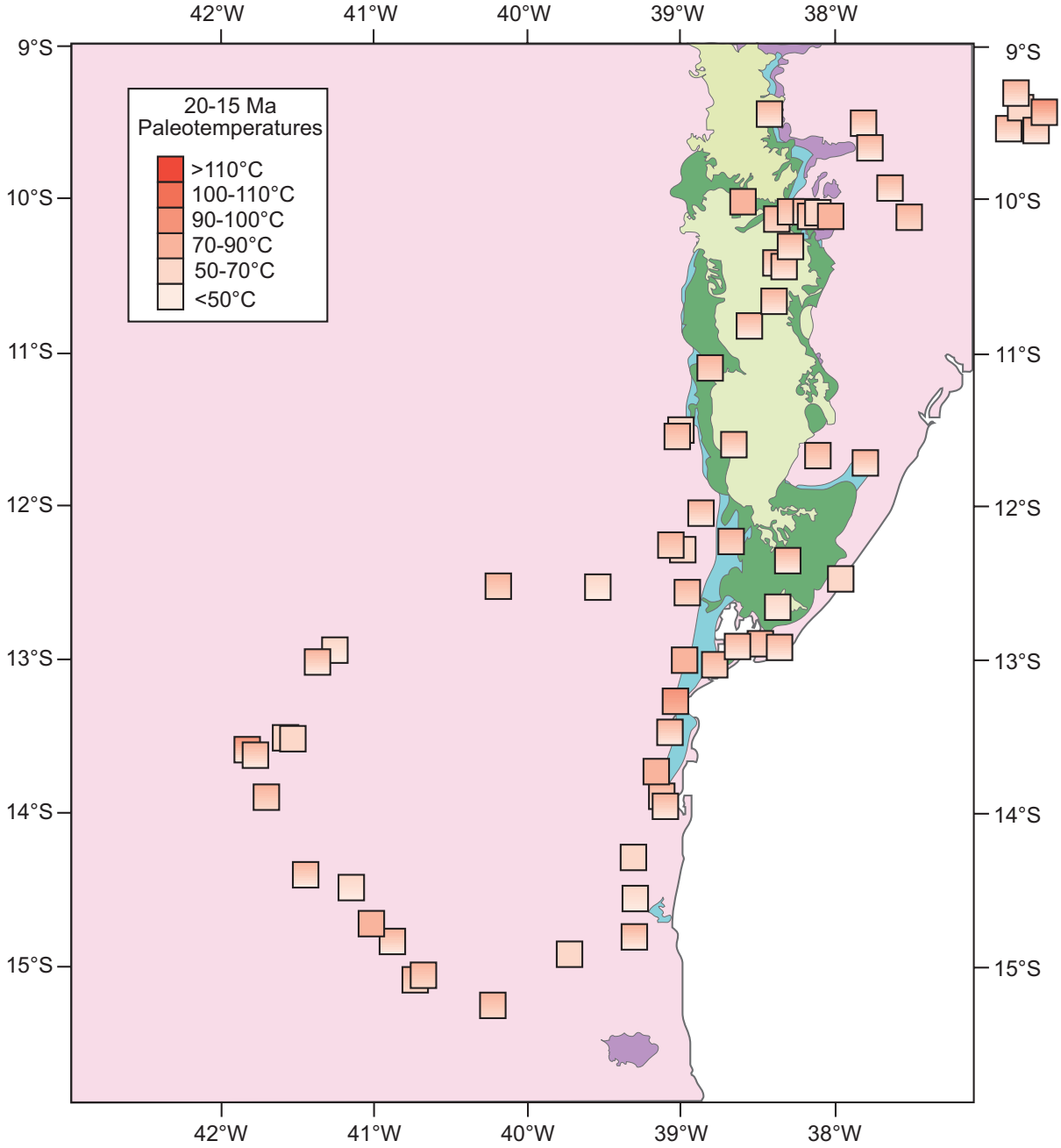

Figure 11.16: Miocene (20-15 Ma) paleotemperatures derived from AFTA data in **outcrop samples from Bahia**, from locations shown in Figure 11.1. Values for individual samples analysed for this report are listed in Table 11.3 and attributed to individual paleo-thermal episodes in Figures 11.6, 11.7 and 11.8.

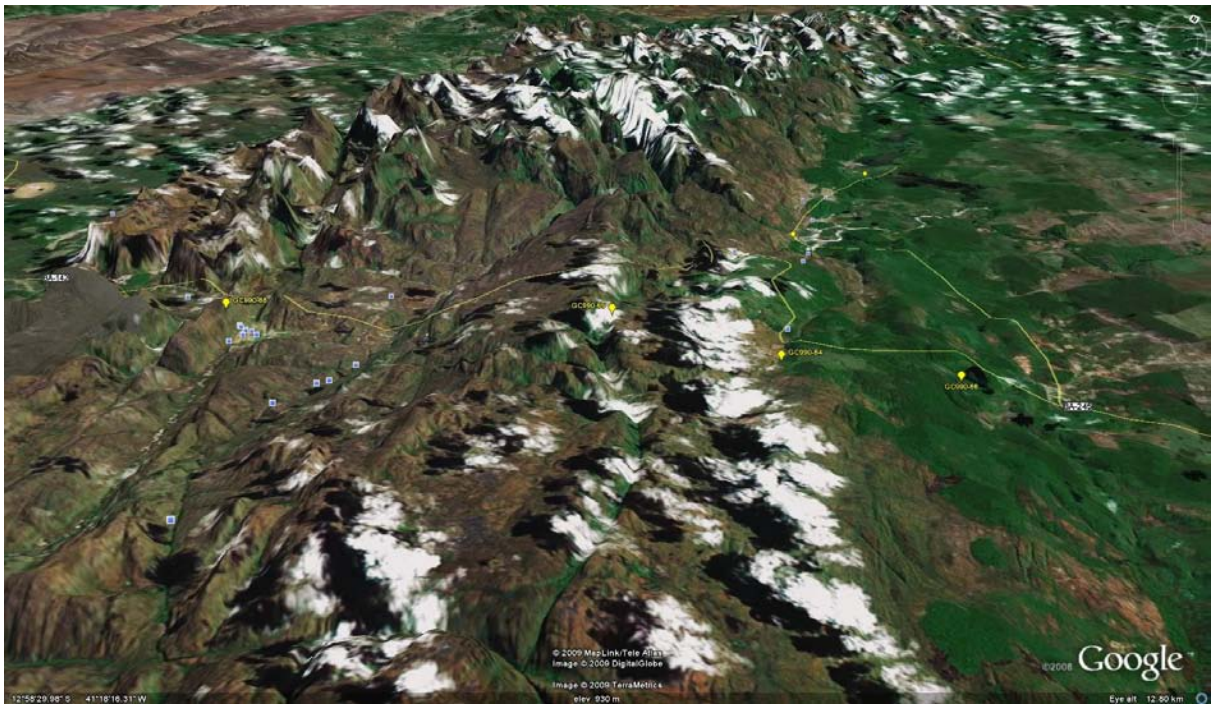

Figure 11.17: Google Earth view of samples GC990-64, -66 and -68 comprising an elevation section near **Mucugê**, Bahia.

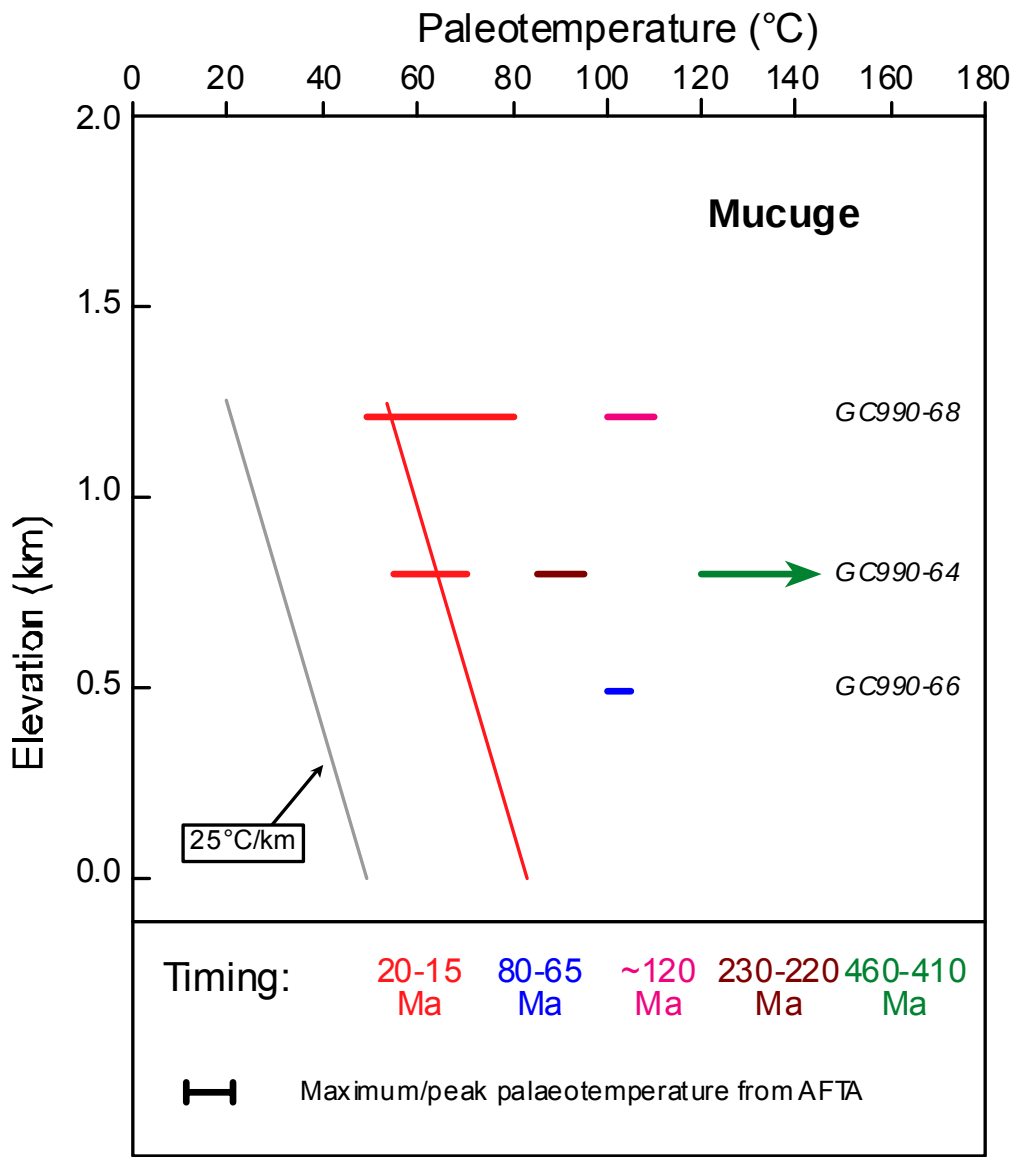

Figure 11.18: Paleotemperatures in discrete paleo-thermal episodes derived from AFTA data in **samples from an elevation section at Mucugê** (Figure 11.17), plotted against elevation (asl). Paleotemperatures in each episode for individual samples are listed in Table ix. Also shown is a notional present-day thermal gradient of 25°C/km from the local summit level of ~1250 m. The variation of paleotemperature with elevation allows insight into the mechanisms of heating and cooling in each episodes (Section 2). As shown here, the Miocene paleotemperatures from this section can be explained in terms of a paleotemperature profile parallel to the present-day temperature profile, suggesting that these paleotemperatures can be explained solely to additional burial, and cooling can be explained solely by exhumation. However, this is not true of other paleotemperatures, suggesting tectonic offsets exist between these samples. See text for further discussion.

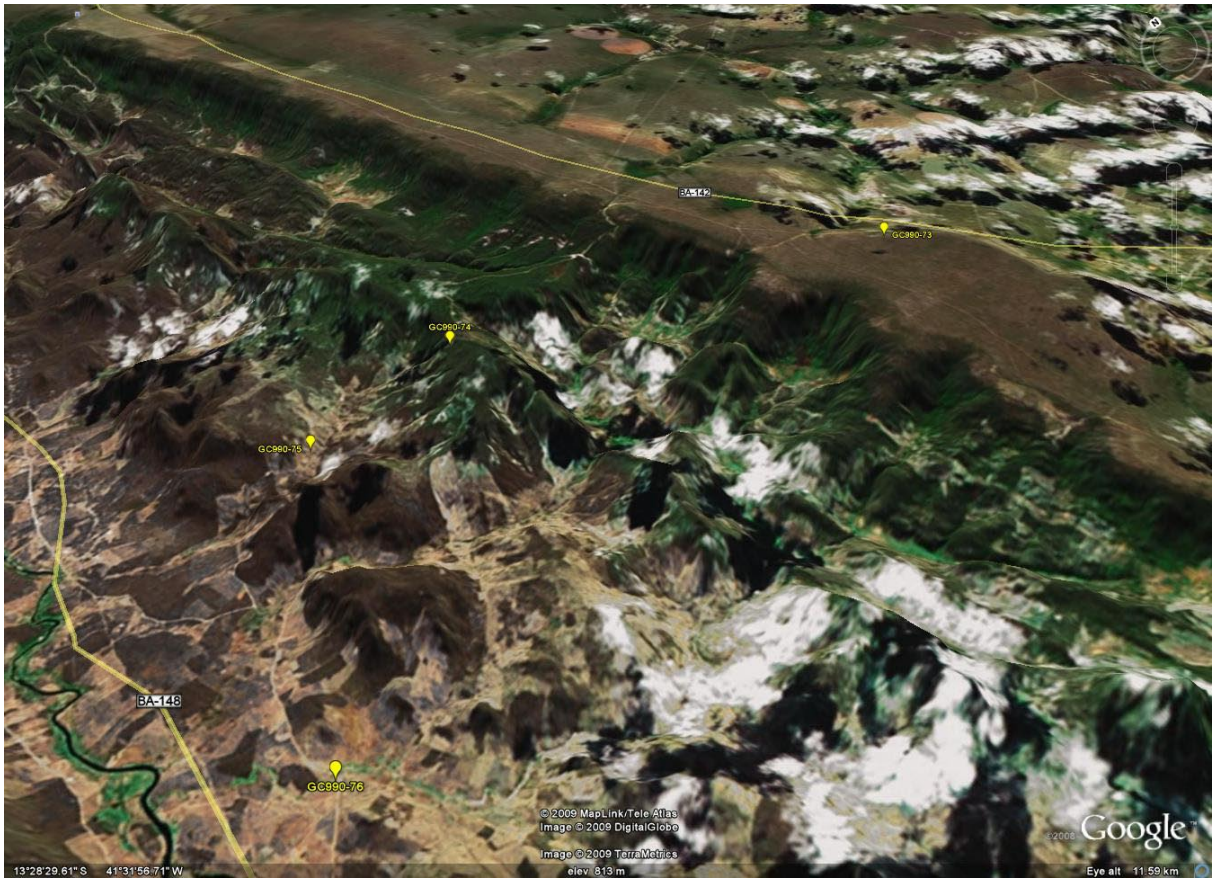

Figure 11.19: Google Earth view of samples GC990-73, -74, -75 and -76 comprising an elevation section near **Jussiape**, Bahia.

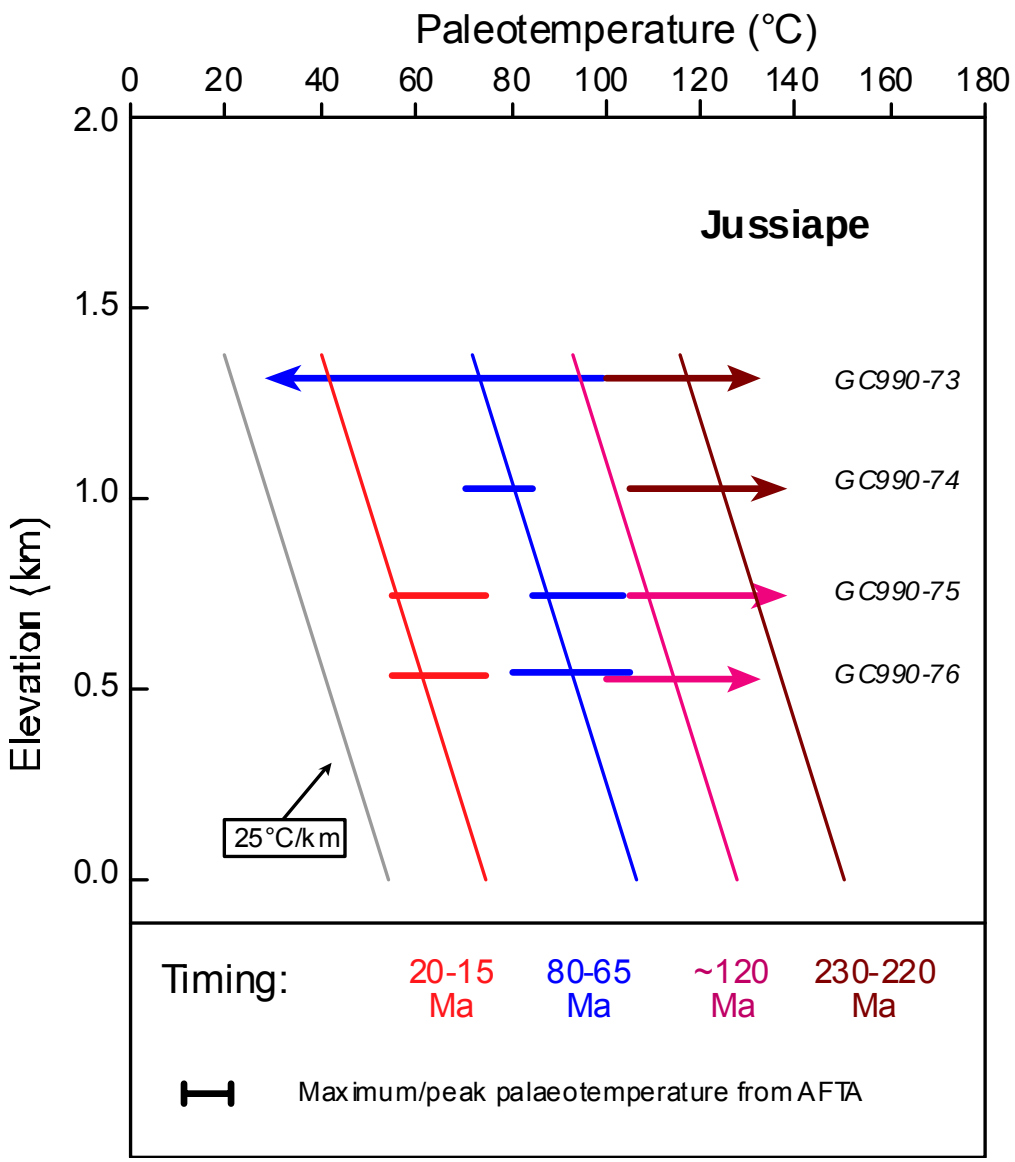

Figure 11.20: Paleotemperatures in discrete paleo-thermal episodes derived from AFTA data in **samples from an elevation section at Jussiape** (Figure 11.19), plotted against elevation (asl). Paleotemperatures in each episode for individual samples are listed in Table ix. Also shown is a notional present-day thermal gradient of 25°C/km from the local summit level of ~1375 m. The variation of paleotemperature with elevation allows insight into the mechanisms of heating and cooling in each episodes (Section 2). As shown here, the results from this section can all be explained in terms of paleotemperature profiles parallel to the present-day temperature profile, suggesting that these paleotemperatures can be explained solely to additional burial, and cooling can be explained solely by exhumation. See text for further discussion.

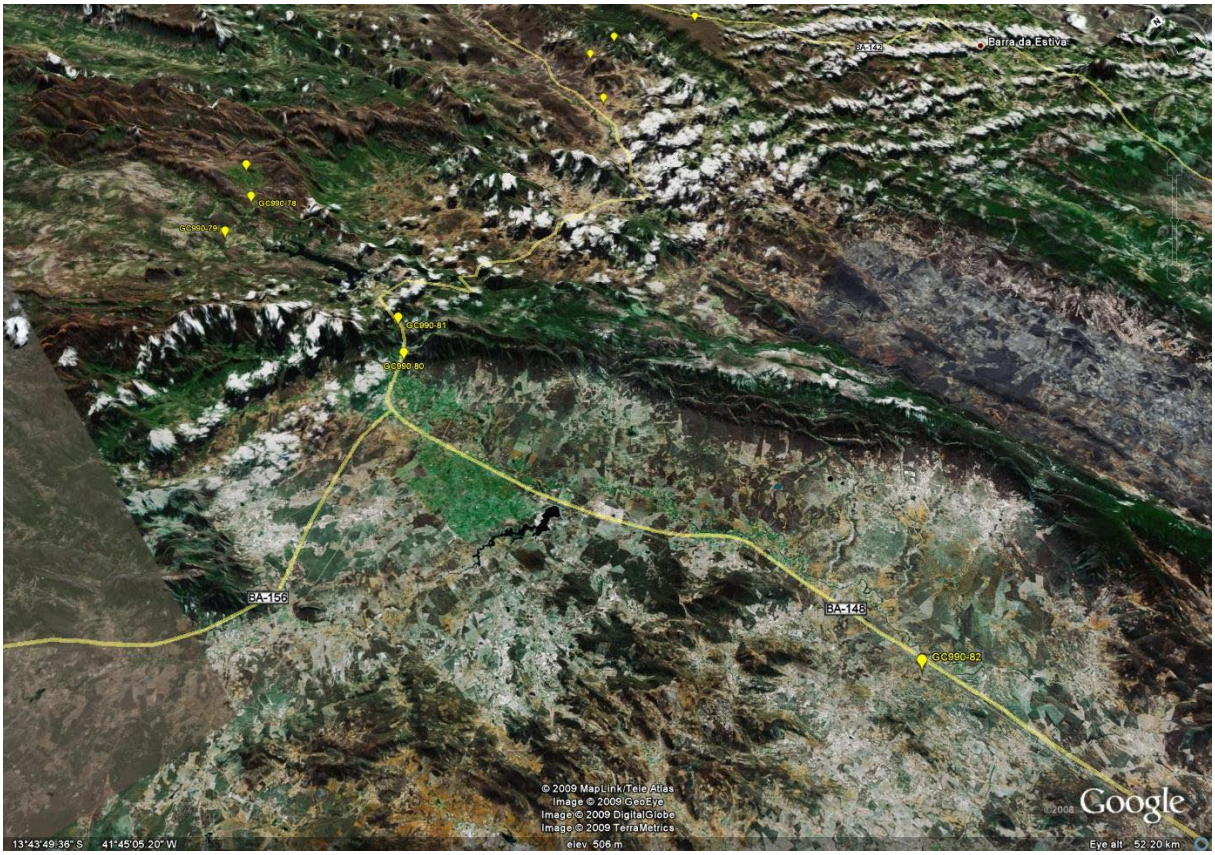

Figure 11.21: Google Earth view of samples GC990-78, 79, -80, -81 and -82 comprising an elevation section near **Rio de Contas**, Bahia.

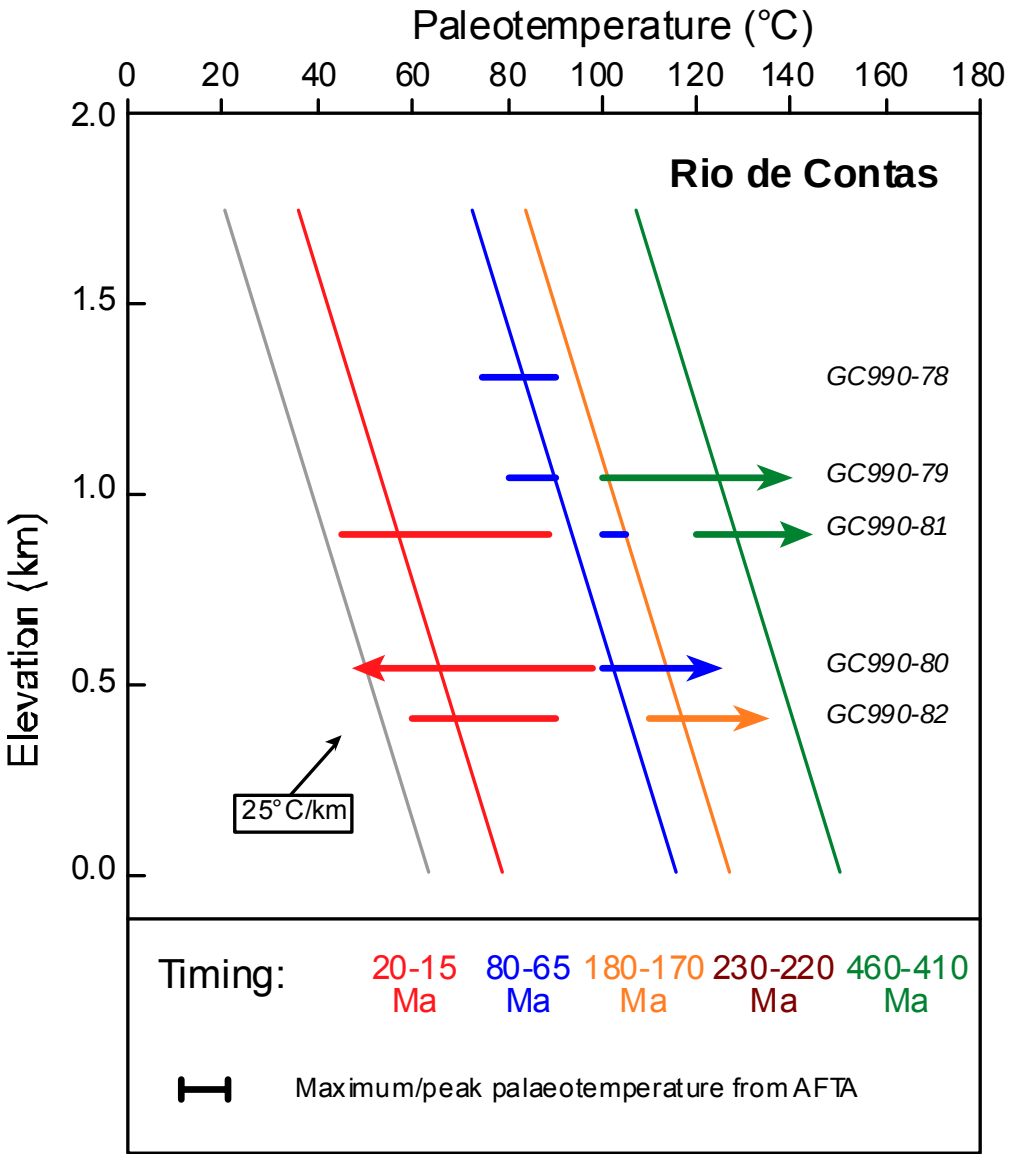

Figure 11.22: Paleotemperatures in discrete paleo-thermal episodes derived from AFTA data in **samples from an elevation section at Rio de Contas**, plotted against elevation (asl). Paleotemperatures in each episode for individual samples are listed in Table ix. Also shown is a notional present-day thermal gradient of 25°C/km from the local summit level of ~1750 m. The variation of paleotemperature with elevation allows insight into the mechanisms of heating and cooling in each episodes (Section 2). As shown here, with the exception of perhaps sample GC990-81, the results from this section can all be explained in terms of paleotemperature profiles parallel to the present-day temperature profile, suggesting that these paleotemperatures can be explained solely to additional burial, and cooling can be explained solely by exhumation. However, more complex interpretations are also possible. See text for further discussion.

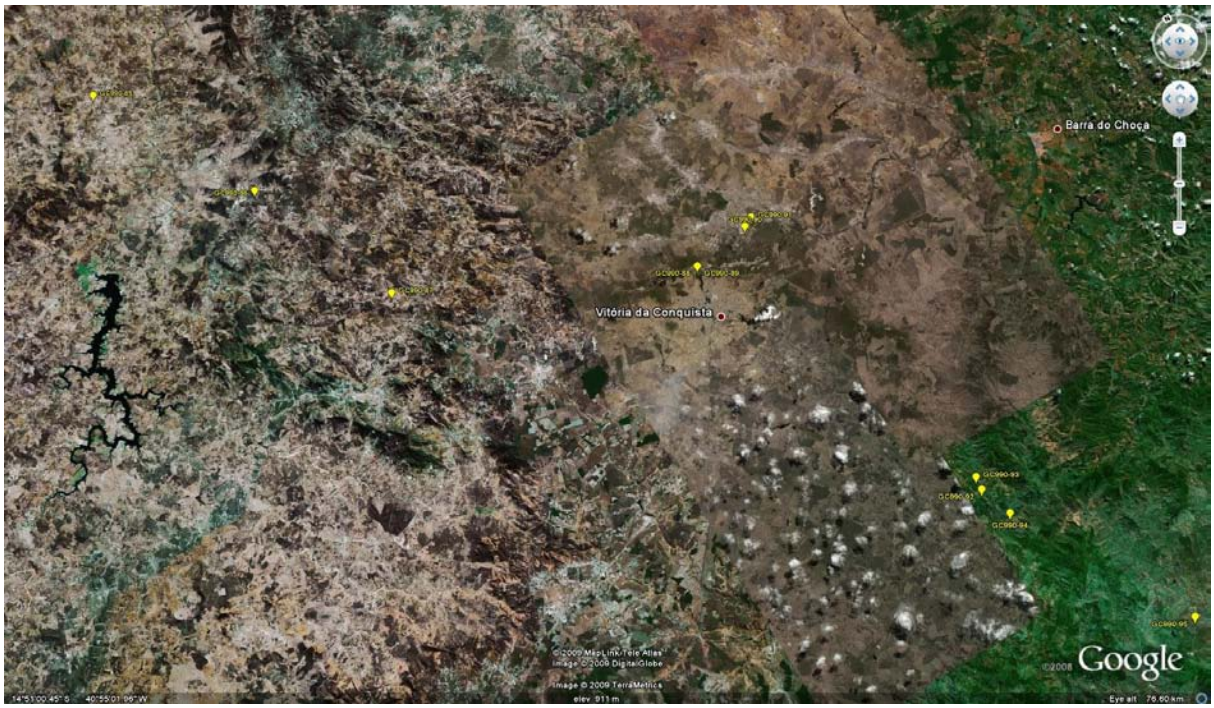

Figure 11.23: Google Earth view of samples GC990-85, 86, -87. -88, -93, -94 and -95 comprising an elevation section near **Vitoria da Conquista**, Bahia.

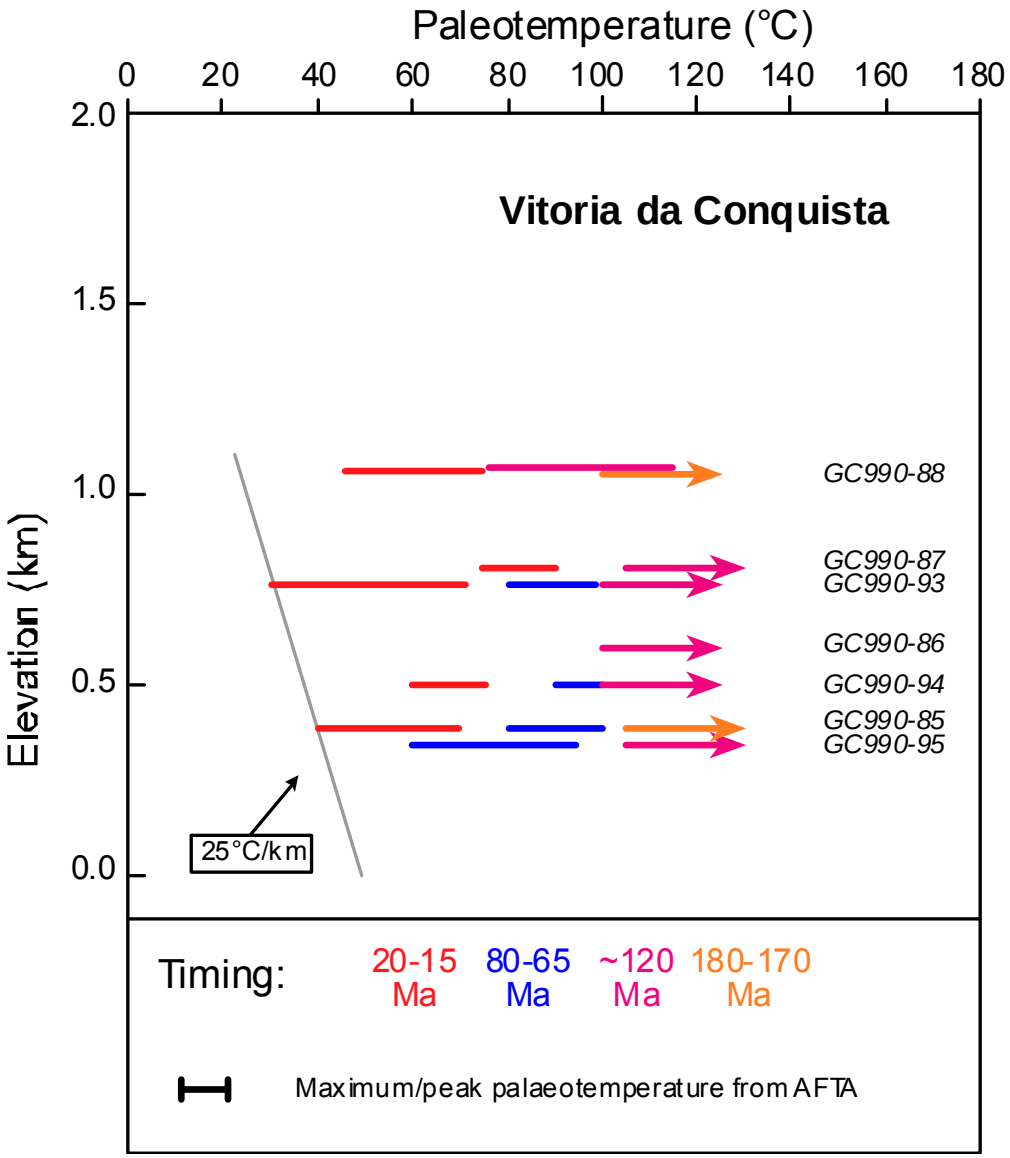

Figure 11.24: Paleotemperatures in discrete paleo-thermal episodes derived from AFTA data in **samples from an elevation section at Vitoria da Conquista**, plotted against elevation (asl). Paleotemperatures in each episode for individual samples are listed in Table ix. Also shown is a notional present-day thermal gradient of 25°C/km from the local summit level of ~1100 m. The variation of paleotemperature with elevation allows insight into the mechanisms of heating and cooling in each episodes (Section 2). As shown here, paleotemperatures in individual episodes from this section do not define consistent paleotemperature profiles, suggesting that significant offsets exist between individual sample locations. See text for further discussion.

13. Regional synthesis: definition of major regional paleo-thermal episodes, mechanisms of heating and cooling, and regional variation

13.1 Introduction

In this Section, we integrate the results presented in Sections to produce a regional synthesis describing the major paleo-thermal events that have affected NE Brazil and adjacent regions, with particular emphasis on the hinterland to the Camamu and Almada basins, which are the prime focus of the larger study of which this Report forms part (Figure 13.1). We begin by comparing evidence for the timing of major paleo-thermal episodes identified across the region to define the significant regional events. We then briefly compare these events with regional geological information to gain insights into the possible mechanisms underlying these episodes. We then analyse the variation of paleotemperatures with depth (in boreholes) or elevation (in outcrop sections) to obtain rigorous constraints on paleogeothermal gradients and amounts of additional section required to explain the observed paleotemperatures in different episodes. Finally we integrate all this information into a regional synthesis describing the tectonic and paleo-thermal evolution of the region.

13.2 Timing of significant regional paleo-thermal episodes

Figure 13.2 provides a comparison of the timing of cooling defined from AFTA data in the eight boreholes and two outcrop datasets analysed for this study. Also included in Figure 13.2 are timing constraints on three episodes of cooling identified in the 1-BAS-113-BA well, from the offshore counterpart to this study, Geotrack Report GC1013. There is clearly a strong consistency in the timing of **Late Cretaceous** and **Miocene** cooling events in all datasets, with all results consistent with a series of regional cooling episodes beginning in the following intervals:

450 to 410 Ma	**Ordovician-Devonian**
320 to 300 Ma	**Carboniferous**
230 to 220 Ma	**Triassic**
180 to 170 Ma	**Jurassic**
~120 Ma	**Aptian**
110 to 105 Ma	**Albian**
80 to 75 Ma	**Campanian**
48 to 45 Ma	**Eocene**
18 to 15 Ma	**Miocene**

The timing of the earlier of two cooling episodes identified in the 1-FLU-1-BA well overlaps with both the 460 to 410 Ma and 320 to 300 Ma cooling episode identified in the outcrop samples from Bahia. In Figure 13.2, the event in the 1-FLU-1-BA well is correlated with the earlier of these two episodes because this dominates the early history in the west of the region (Figure 11.9) closer to the well location, while the 300 to 320 Ma episode is seen only in coastal basement outcrops (Figure 11.10). Thus the timing of the **Ordovician-Devonian** episode is refined to the interval **450 to 410 Ma**.

The **Carboniferous**, **Triassic** and **Jurassic** episodes are recognised only in the outcrop samples from Bahia, and the onset of cooling in each of these episodes remain unchanged from Section 11. All of these earlier episodes are recognised only in restricted areas (Figures 11.10 through 11.12). As discussed in Section 11, the most likely explanation of this is that only in these areas are the magnitude of later events (particularly the Aptian event, as discussed below) low enough to preserve evidence of these earlier episodes.

The timing of the **Latest Jurassic-Early Cretaceous** episode (cooling beginning between **170 and 120 Ma**) identified from AFTA data in samples from the highest elevations in the Serra do Mar and around Rio de Janeiro (Section 12) matches the timing of the **Early Cretaceous** cooling episode (cooling beginning at **~120 Ma**) recognised in the outcrop samples from Bahia (Section 11). While this correlation is less strong than for other episodes discussed below, it seems reasonable to assume a common timing of **~120 Ma** (**Aptian**) for the onset of cooling in both areas, given the regional nature of this episode as evidenced by the widespread recognition of this episode in the outcrop samples from Bahia (Figure 11.13). In fact, if we accept the correlation between these two areas, the Aptian cooling episode is recognised across the whole region considered in this study.

The **mid-Cretaceous** episode (cooling beginning at **110 to 105 Ma**) identified in samples from the Serra do Mar correlates well with the mid-Cretaceous cooling (cooling beginning at **110 to 90 Ma**) identified in AFTA from the northeast of the main study area in samples originally from the Turner et al. (2008) study (Figure 11.14). Combining timing constraints from both region suggests a refined interval of **110 to 105 Ma** (**Albian**) could apply to both regions. But in contrast to the Aptian episode (above), evidence for the Albian episode is not present in samples from the main outcrop dataset from Bahia (Figure 11.14). Further discussion on this issue is presented in the regional synthesis in Section 13.5.

From the synthesis in Figure 13.2, it is clear that cooling during the **Late Cretaceous** is identified across the whole of the study region, including the offshore shelf (well 1-BAS-113-BA), with timing constraints from AFTA data in all outcrop areas and all wells consistent with cooling beginning in the interval **80 to 75 Ma** (**Campanian**). This episode dominates the AFTA data from all seven wells drilled in the Early Cretaceous rift basins, (also being recognised in the 1-FLU-1 BA well drilled in a Paleoproterozoic sedimentary section) as well as the AFTA data in outcrop samples across these Basins, and is also recognised in surrounding basement regions (Figure 11.15). This event is also particularly strongly expressed in data from the Serra do Mar and around Rio de Janeiro (Section 12). As with the Aptian event discussed above, the Campanian cooling episode clearly represents a profound cooling event of regional extent. One clear difference between the two episodes, however, is the absence of any evidence of Aptian cooling is samples from sedimentary units within the basins (note comments on the lack of detectable events on the Aptian-Albian unconformities in the 1-BRN-1-BA, 1-FPO-1-BA, 1-FVM-1-BA and 6-MGP-34-BA wells discussed in Sections 4, 6, 7 and 10, respectively).

Evidence for **Eocene** cooling is seen consistently in the four wells in which the largest vertical spread of samples is available (1-BRN-1-BA, 1-FPO-1-BA, 1-FVM-1-BA and 6-MGP-34-BA), as well as in outcrop samples from the Serra do Mar (Section 12), and all these datasets are consistent with cooling beginning **between 48 and 45 Ma**. In contrast, evidence for this episode is absent in outcrop samples from Bahia (Section 11) and wells that penetrate only ~2 km or less of section. The most likely reason for this is that Eocene paleotemperatures were not of sufficient magnitude in outcrop samples across Bahia to be resolved from those during the Campanian and Miocene episodes. (Note that in many outcrop samples it is not possible to resolve these two episodes so resolution of Eocene effects is particularly unlikely.) Only in well samples which are sufficiently deep today to have attained paleotemperatures around 90°C or more during the Eocene episode, and in those areas of the Serra do Mar where this episode is very strongly expressed, can these be confidently resolved. Thus it seems likely that Eocene cooling probably affected at least most of the Bahia region. However the absence of Eocene cooling in samples from the Serra do Mar around Teresopolis and the Graben region to the south, when contrasted with the major Eocene cooling identified only 25 km or less to the west around Metropolis, suggests that structural controls do exist on the occurrence of this episode. This raises the possibility that Eocene cooling may not have been synchronous across the region, although any differences must be small (Figure 13.2). This aspect of the study is discussed further in Section 13.5.

Figure 13.2 illustrates that **Miocene** cooling effects are also recognised in all datasets. Almost all data are consistent with an onset of cooling between **18 and 15 Ma**, although samples from the **Serra do Mar** suggest an earlier onset of **25 to 20 Ma**. This is controlled by two samples (GC990-8 and -9) which require an onset of cooling prior to 20 Ma. Both of these samples also show firm evidence of Eocene cooling (Figure 12.5) so this cannot be explained by a lack of resolution of multiple episodes. One possible explanation of this slight disparity could simply be normal statistical fluctuations outside 95% confidence limits, given the large number of samples analysed or this study. Or the onset of Miocene cooling could possibly have been slightly earlier in the Serra do Mar compared with regions to the northeast (remembering that treatment of the data in terms of synchronous cooling episodes is undoubtedly a necessary simplification). In the following discussion, we pursue an overall interpretation involving a single Miocene cooling episode which began between 18 and 15 Ma, but the qualifications presented here and possible alternatives should be borne in mind.

13.3 Comparison with regional geological framework

The timing of the nine cooling episodes identified from AFTA data in this study (Figure 13.2) are compared with a summary of the regional geological and stratigraphic framework around the Recôncavo-Tucano-Jatobá rift, from Magnavita et al. (1994) in Figure 13.3. This illustrates that most of the paleo-thermal episodes show a strong correlation with regional unconformities, suggesting that exhumation during the intervals represented by these unconformities makes a major contribution to the observed cooling in each episode.

The **Ordovician-Devonian** episode (beginning **450-410 Ma**) episode correlates well with the regional unconformity between Precambrian and Carboniferous-Devonian sedimentary units. Similarly, the **Carboniferous** episode (beginning **320-300** Ma) correlates with the unconformity between Carboniferous-Devonian and Permian-Triassic sedimentary units, while the **Triassic** and **Jurassic** episodes (beginning **230-220 Ma** and **180 to 170 Ma**) correlate with the regional unconformity between Permian-Triassic and Late Jurassic sedimentary units.

The **Aptian** episode (**~120 Ma**) is just slightly younger than the unconformity shown in Figure 13.3 between Barremian and Aptian section. These timings may be close enough to justify correlating the cooling episode with this unconformity, particularly bearing in mind the spread is individual sample estimates for the onset of cooling in

this episode in Figures 11.6, 11.7 and 11.8. However, since the Aptian cooling episode is not recognised in the sedimentary basins, such an association is not straightforward. Since Aptian cooling is focussed in the basement terrains surrounding the basins, it seems more likely that this episode represents uplift and erosion of these basement areas, providing sediment input to the rift basins. In this regard, it should be borne in mind that the breakdown of the results into discrete cooling episodes denoted by a single interval is clearly a broad approximation to the true history, and it is possible that our Aptian episode could in fact represent cooling due to uplift and erosion through the Early Cretaceous, to provide the sedimentary fill of the basins. This would help to explain the lack of total consistency in timing estimates for the onset of cooling in this episode (Figures 11.6, 11.7 and 11.8).

Both the **Campanian** (beginning **80 to 70 Ma**) and **Eocene** (beginning **48 to 45 Ma**) cooling episodes fall within the interval represented by a long period of erosion in Figure 13.3 from Albian to Miocene times. And the **Miocene** episode (beginning **18 to 15 Ma**) correlates closely in Figure 13.3 with unconformity between the Sabia Formation and the Barreiras group, although this aspect of the stratigraphy remains highly uncertain, as will be discussed in greater detail in the Final Synthesis Report for this study.

In contrast to the above discussion, the **Albian** cooling episode (beginning between 110 and 105 Ma) does not correlate with a regional unconformity in Figure 13.3. Given the lack of definition of this episode in the region around the Recôncavo-Tucano-Jatobá rift, this is probably not significant. Although Albian-aged dolerite dykes are indicated in Figure 13.3, these have clearly not had any detectable effect on the thermal history of samples analysed for this study.

In conclusion, comparison of the timing of the dominant paleo-thermal episodes identified from AFTA in NE Brazil with the regional stratigraphic framework shows a strong correlation with major unconformities, suggesting that uplift and erosion during the intervals corresponding to these unconformities contributes a significant proportion of the observed cooling in these episodes.

13.4 Paleogeothermal gradients and amounts of removed section

In this section, we consider the constraints that can be obtained on paleogeothermal gradients and removed section from paleotemperatures over a range of depths in the wells discussed in Sections 3 through 10. In detail, samples from sufficient samples

to provide useful constraints are only available in five wells, while only one or two samples were analysed from the 1-FLU-1-BA, 1-RSO-1-BA and 3-MB-3-BA wells and these provide no useful constraints on paleogeothermal gradients. As discussed in Sections 11 and 12, we consider the results from outcrop transects involving a range of elevations are likely to be affected either by tectonic offsets or by problems due to unresolved multiple episodes, and these have not been used to provide quantitative estimates of paleogeothermal gradients or amounts of removed section.

This being so, formal estimation of these parameters is only possible for the **Campanian**, **Eocene** and **Miocene** episodes as recognised in the **1-AO-1-BA**, **1-BRN-1-BA**, **1-FPO-1-BA**, **1-FVM-1-BA** and **6-MGP-34-BA** wells. In each well, maximum paleotemperatures derived from VR data, representing the Campanian episode, have been used as upper limits to the paleotemperature during Eocene and Miocene episodes. And in samples where all three episodes are not identified, paleotemperature constraints have been derived based on those during other episodes. For example, in samples which reveal Campanian paleotemperatures but not subsequent episodes, the Campanian values have been used as upper limits for Eocene and Miocene paleotemperatures.

Paleogeothermal gradients

Using the approach outlined in Section 2.4 and methods explained in Appendix C (Section C.9), we have determined the range of paleogeothermal gradients consistent with the **Campanian**, **Eocene** and **Miocene** paleotemperature constraints from AFTA data and VR values in each of the five wells listed above, from Tables i, ii, iv, v and viii, assuming that the paleotemperatures in each episode can be represented by a linear profile. Maximum likelihood estimates of paleogeothermal gradient for the three episodes in the five wells are summarised. together with 95% confidence limits (equivalent to the $\pm 2\sigma$ uncertainty level), in Table 13.1. The corresponding likelihood profile from which these constraints are taken are shown in Figures 13.4 through 13.19 (top left plots in each Figure).

Likelihood profiles for **Campanian** paleogeothermal gradients in the 1-BRN-1-BA, 1-FPO-1-BA, 1-FVM-1-BA and 6-MGP-34-BA wells all show well-defined quadratic forms, characteristic of well-defined datasets, with a well defined maximum likelihood estimate in each case. In all four wells, the range of allowed values is very narrow, due to the availability of consistent paleotemperatures over depths of up to 5km. Note that two analyses are presented of the Late Cretaceous paleotemperatures in the 1-BRN-1-BA well, one based on AFTA and VR data, and another based on AFTA alone. This has been done because of the slight but

consistent disparity in paleotemperatures indicated by the two techniques in this well (Section 4.4). In contrast to results from the other four wells, results from the 1-AO-1-BA well give a much broader profile (Figure 13.4), due to availability of constraints at only four depths in this well, over a much narrower depth range.

Likelihood profiles for **Eocene** paleogeothermal gradients in all wells tend to be less well-defined than for other episodes, because of the usually wider paleotemperature constraints over most of the depth range in each well. The likelihood profile for the 1-AO-1-BA well in Figure 13.5 is particularly poorly defined, because this episode is not recognised in this well and paleotemperature constraints have been derived from the limiting values in the Campanian and Miocene episodes. In contrast, the likelihood profile for Eocene paleo-gradients in the 1-FPO-1-BA well (Figure 13.12) is quite well defined, as a result of reliable constraints on this episode.

In similar fashion, likelihood profiles for **Miocene** paleogeothermal gradients tend to be less well-defined than for the Campanian episode, but better defined than for the Eocene episode. But in general, results from all five wells provide good definition of the range of allowed paleogeothermal gradients in the three key paleo-thermal episodes (Table 13.1).

Maximum likelihood paleogeothermal gradients together with the corresponding 95% confidence limits are compared in Figure 13.20 with the estimated present-day gradients in the five wells. Also shown in this Figure are results from the 1-BAS-113-1-BA well, analysed for the Offshore counterpart of this study, described in Geotrack Report #1013 (using the preferred Campanian value of 26°C/km based on AFTA and selected VR data). A present-day thermal gradient of 15°C/km is preferred for the three Tucano Basin wells, based primarily on AFTA data from these wells, as discussed in Sections 4.2, 6.2 and 7.2, but also deriving support from the compilation of Meister (1973). A value of 20°C/km was preferred for Recôncavo Basin well 6-MGP-34 in Section 10, but a higher value of 25°C/km was used for the 1-AO-1-BA well in Section 3 and for the 1-BAS-113-BA well in Geotrack Report #1013. Data from the vicinity of these wells from Meister (1973) show rapid variations over narrow distances, and the value appropriate to each well is less clear. A value in the range 20 to 25°C/km is clearly appropriate for these wells, but the precise value remains somewhat uncertain.

Nevertheless, the comparison in Figure 13.20 provides a strong indication that geothermal gradients have remained at or close to present-day values since at least the Campanian, suggesting that the main process contributing to the heating expressed in the Campanian, Eocene and Miocene paleotemperatures in the five

wells was deeper burial, with little or no change in basal heat flow through time. By extension, these observations suggest that the main process responsible for cooling in the three episodes was exhumation (i.e. uplift and erosion).

Estimating amounts of removed section

In this Section, we calculate the amount of additional section that must have been deposited and subsequently removed by uplift and erosion in order to explain the observed Campanian, Eocene and Miocene paleotemperatures in the five wells, given the constraints on paleogeothermal gradients established during each episode in Section 3.6. While such an interpretation seems likely, based on prior discussion, other possible explanations are possible (e.g. long-term heating as a result of hot fluid flow at a shallow level), but the calculations presented here provide a quantitative framework in which these aspects of the results can be assessed.

Assuming that the paleogeothermal gradient was linear throughout the entire section at the time of maximum paleotemperatures, extrapolation of the fitted linear profile from the appropriate unconformity to an assumed paleo-surface temperature provides an estimate of the amount by which that unconformity surface was more deeply buried, and hence the amount of section that has since been removed by erosion.

As emphasised in Section 2.5, estimation of amounts of removed section from paleotemperature data depends critically on various key assumptions. The principal difficulty lies with definition of the paleogeothermal gradient through the removed section (Figure 13.21), which cannot be constrained by direct measurement and must therefore always be assumed. In deriving estimates of removed section for each of the paleo-thermal episodes recognised in the well, the paleogeothermal gradient through the removed section is assumed to have been linear and equal to the value through the preserved section. This assumption may be invalid if the elevated paleotemperatures are caused by processes involving lateral or local introduction of heat, such as by confined fluid flow or igneous intrusions, or if major differences in lithology caused severely non-linear paleotemperature profiles (Figure 13.21).

Estimates of the amount of additional section required to explain **Campanian**, **Eocene** and **Miocene** paleotemperatures in the five wells have been calculated with respect to the top-Early Cretaceous unconformity at the ground surface at each well location, representing the approximate interval 110 Ma to 0 Ma for the three Tucano Basin wells and slightly longer for the Recôncavo Basin wells (Table A.2). Estimates have been derived assuming a paleo-surface temperature of 20°C during all three episodes.

Given all the assumptions which underlie this analysis, application of the methods described in Section 2.5 gives estimates of the amounts of removed section required to explain the observed paleotemperatures as summarised in Table 13.2. Estimates are quoted corresponding to the maximum likelihood estimate of paleogeothermal gradient and associated ±95% confidence limits for each episode, derived from the likelihood profiles shown in the upper right positions in Figures 13.4 through 13.19. In addition, ranges of removed section (again corresponding to ±95% confidence limits) are quoted in Table 13.2 for various specified values of paleogeothermal gradient within the allowed range of values. These are taken from the lower plots in Figures 13.4 through 13.19, which illustrate the correlation between values of paleogeothermal gradient and removed section allowed by the paleotemperature constraints characterising each episode within ±95% confidence limits. That is, any set of paired values inside the contoured region of the plot are compatible with the corresponding paleotemperature data at 95% confidence limits, with higher paleogeothermal gradients requiring correspondingly less removed section, and vice versa.

In most cases, the range of allowed values of removed section derived from the combined constraints from AFTA and VR data is quite broad, reflecting the extrapolation of the fitted paleogeothermal gradients required by the estimation, exaggerated further by the generally low gradients involved. Even the Campanian paleotemperatures in the four deep wells allow a range of over 1500 metres for the amount of removed section, despite the wide range of depths over which paleotemperatures are available. But for fixed values of paleogeothermal gradient, the range of values of removed section are narrower (Table 13.2). For example, in the Tucano Basin wells, for a paleogeothermal gradient of 15°C/km, the range of allowed values of additional burial required to explain the observed paleotemperatures is typically around 500 metres or less (Table 13.2).

Additional burial vs removed section

Note that values of “removed section” shown in Figures 13.4 through 13.19 refer to the total amount of section removed since the onset of cooling (exhumation) in each episode, up to the present-day. Following the discussion in Section 2.5 (see also Figure 2.2), since all these episodes occur within the time interval represented by the top-Early Cretaceous unconformity in these wells, the history between the separate episodes is not constrained (since the data constrain only the paleotemperature peak, and not the prior history during heating to that peak). Therefore it is not clear what proportion of the total amount of section removed since the onset of cooling in the

Campanian episode was removed prior to the onset of any reburial leading to the Eocene peak. Similar comments apply for the period between the onset of Eocene and Miocene exhumation. This aspect of the results is discussed in more detail in Section 14.

Changes in paleo-surface temperature

The magnitude of removed section required to explain the observed paleotemperatures can be easily adjusted to an alternative paleo-surface temperature by subtracting or adding the difference in depth equivalent to the change in paleo-surface temperature, for the appropriate paleo-gradient, as described in Section 2.5. For example, increasing the paleo-surface temperature by 10°C, for a paleogeothermal gradient of ~20°C/km, would require a reduction of 500 metres in the amount of removed section needed to explain the observed paleotemperatures.

Comparison of results in all wells

Figure 13.22 shows constraints on Campanian, Eocene and Miocene paleogeothermal gradients and removed section in the five wells in which formal estimation is possible, plotted on a common scale to facilitate comparison. Figure 13.23 shows a similar comparison of constraints in each episode from the five wells. Results from the 1-AO-1-BA well are clearly not as well constrained as in the other four wells, but are consistent with the conclusions derived from these four wells discussed below.

These plots emphasise the extremely high level of consistency between the results from different wells in this study. Results from the three Tucano Basin wells illustrate that late Cretaceous paleogeothermal gradients much in excess of 15°C/km can be ruled out. While slightly higher values would be allowed for the Eocene episode, the Miocene constraints again rule out paleo-gradients in excess of 20°C/km in the Tucano Basin. In Figure 13.23, a consistent difference between Tucano Basin and Recôncavo Basin wells is evident, with the higher paleo-gradients around 20to 25°C/km indicated in the Recôncavo Basin wells echoing the general pattern indicated by present-day gradients from Meister (1973) as shown in Figure 12.3.

Based on a constant paleogeothermal gradient of 15°C/km, estimates of the amounts of additional section required to explain the Campanian episode in the three Tucano Basin wells are also highly consistent, viz:

1-BRN-1-BA	2800-3400 m
1-FPO-1-BA	3350-3750 m
1-FVM-1-BA	3100-3600 m

Using 20°C for the Recôncavo Basin wells, corresponding values are:

1-AO-1-BA	2900-3500 m
6-MGP-34-BA	3000-3500 m

Thus, results from all five wells are consistent with around 3350 to 3400 metres of removed section, suggesting that the total amount of section removed in both basins since the onset of exhumation Campanian could be similar across the region (although a range of alternative scenarios are also possible, within the constraints in Figure 13.22). This is of interest because Magnavita et al. (1994) reported that the depth to the top of the oil window at the present day is less in the Recôncavo Basin than in the Tucano Basin. Magnavita et al. (1994) interpreted this in terms of a greater degree of uplift and erosion in the Recôncavo Basin compared to the Tucano Basin. But the results presented here and summarised in Figures 13.22 and 13.23 suggest that this difference could simply reflect the higher thermal gradients in the Recôncavo Basin, with similar amounts of section removed across the entire region.

Comparison of estimates of additional section required to explain Eocene and Miocene paleotemperatures in the five wells from Figures 13.22 and 13.23 show similar features to those discussed for the Campanian episode above, suggesting a similar post-Campanian evolution across the region. However we should emphasise that a range of alternative scenarios are also possible, as summarised in Table 13.2.

13.5 Regional synthesis

Based on the information presented in this and preceding Sections, the nature of the dominant paleo-thermal episodes (Section 13.2) that have affected the onshore region adjacent to the Camamu and Almada Basins is now clear. A close match between the timing of most of the paleo-thermal episodes with regional unconformities (Section 13.3) suggests that uplift and erosion played a major role in causing the cooling identified from AFTA. This is confirmed for the three most recent episodes from analysis of paleogeothermal gradients and removed section (Section 13.4). The restriction of Aptian cooling to basement regions and the absence of this event within the basin, coupled with a spread in estimates for the onset of cooling in this episode, all combine to suggest that this episode represents uplift and erosion of basement regions providing sedimentary fill to the basins, most likely associated with rifting along the Atlantic margin.

Thus, the evolution of the region involves progressive episodes of uplift and erosion through the Paleozoic and into the Mesozoic, culminating in a major phase during the rifting of the continental margin in the early Cretaceous, producing sedimentary fill for the rift basins. While heat flow may have been higher during the pre-Cretaceous episodes, there is no evidence of elevated basal heat flow during rifting. Following rifting, a further 3 km of section was deposited, most likely covering much of the region. Deposition of this post-rift sequence terminated during the Campanian, between 80 and 75 Ma, at which time subsidence and burial turned to uplift and erosion. The ~3 km of post-Aptian section was removed, in three dominant episodes in the Campanian, Eocene and Miocene.

In the context of the above summary, it is worthwhile considering the meaning of the cooling episodes identified from AFTA. In extracting thermal history information from AFTA, histories involving rapid episodic cooling are employed as a convenient framework for defining paleo-thermal maxima, and we then seek to identify the minimum number of synchronous events that can explain all observations. But compared to real geological thermal histories this undoubtedly represents an oversimplification, and in reality cooling will obviously be protracted to some degree. One manifestation of this may be the lack of total consistency in the timing of the Aptian cooling episode, as discussed above. However, the overall consistency in the timing of cooling for most of the episodes, particularly the three most recent episodes, suggests that the syntheses presented here provides a reasonable representation of the overall regional history.

Results from basement terrains where samples are available over a range of elevation suggests that significant offsets may exist across major structures (although in SW Bahia, landscape analysis suggests this is unlikely, and problems with unresolved multiple episodes are probably responsible for erratic paleotemperature profiles). The clearest manifestation of this is seen in results from the Serra do Mar, where samples around Petropolis are dominated by Eocene cooling while samples from ~25 km to the east at Teresopolis show no evidence of this episode. In addition, paleotemperatures in samples around Petropolis show a clear offset (Figure 12.6). Samples from locations around Rio de Janeiro also show clear evidence of major tectonic offsets in Figure 12.6. Results from the Serra do Mar and around Rio reveal major Miocene cooling (as well as 4 earlier episodes) which is interpreted as representing exhumation associated with development of the present-day fault scarp morphology of the region as suggested by Zalan and Oliveira (2005) as shown in Figure 13.24.

Table 13.1: Paleogeothermal gradient estimates: Tucano and Recôncavo Basin wells (Geotrack Report #990)

Well	Present-day thermal gradient[*1] (°C/km)	Episode	Paleo-geothermal gradient[*2] (°C/km)
1-AO-1-BA	20	Late Cretaceous	12.0 (0.0-27.0)
		Eocene	-[*3]
		Miocene	13.0 (0.0-32.5)
1-BRN-1-BA	15	Late Cretaceous	13.0 (9.5-17.5)
		Late Cret. (AFTA only)	15.0 (12.5-18.5)
		Eocene	23.0 (12.5-27.5)
		Miocene	18.0 (14.0-20.5)
1-FPO-1-BA	15	Late Cretaceous	15.5 (13.0-18.0)
		Eocene	21.0 (13.5-30.5)
		Miocene	15.5 (9.5-19.5)
1-FVM-1-BA	15	Late Cretaceous	15.0 (13.0-17.0)
		Eocene	14.5 (9.5-21.5)
		Miocene	10.5 (0.0-17.5)
6-MGP-34-BA	20	Late Cretaceous	22.5 (18.0-27.0)
		Eocene	22.0 (18.0-26.0)
		Miocene	25.5 (17.5-31.0)

[*1] Present-day thermal gradient derived from corrected BHT values or derived from AFTA data – see Appendix A and discussion of results from individual wells in Sections 3 to 10.

[*2] Maximum likelihood paleogeothermal gradients with 95% confidence limits estimated from paleotemperatures in each episode derived from AFTA and VR data in each well, using methods described in Section 2.

[*3] Eocene constraints in this well do not provide sufficient control to allow formal estimation.

Table 13.2: Removed section estimates: Tucano and Recôncavo Basin wells (Geotrack Report #990)

	1-AO-1-BA	1-BRN-1-BA (AFTA only)	1-FPO-1-BA	1-FVM-1-BA	6-MGP-34-BA
Late Cretaceous[*1]	6200 (2050->10000)	3000 (2100-4000)	3450 (2600-4550)	3300 (2500-4350)	2650 (1900-3750)
5°C/km	>10000	*not allowed*	*not allowed*	*not allowed*	*not allowed*
10°C/km	6900-8000	*not allowed*	*not allowed*	*not allowed*	*not allowed*
15°C/km	4200-5200	**2800-3400**	**3350-3750**	**3100-3600**	*not allowed*
20°C/km	2900-3500	*not allowed*	*not allowed*	*not allowed*	3000-3500
25°C/km	**2100-2400**	*not allowed*	*not allowed*	*not allowed*	**2000-2300**
30°C/km	*not allowed*	*not allowed*	*not allowed*	*not allowed*	*not allowed*
35°C/km	*not allowed*	*not allowed*	*not allowed*	*not allowed*	*not allowed*
Eocene[*1]	-	2400 (0-3800)	700 (0-3050)	1800 (100-3500)	2050 (1450-2850)
5°C/km	*not allowed*	*not allowed*	*not allowed*	*not allowed*	*not allowed*
10°C/km	>1100	*not allowed*	*not allowed*	3650-4550	*not allowed*
15°C/km	250->10000	**2350-3050**	**2350-2750**	**1100-2400**	*not allowed*
20°C/km	0-4800	650-1450	850-1350	50-550	2250-2650
25°C/km	**0-3600**	0-450	50-450	*not allowed*	**1400-1700**
30°C/km	0-2800	*not allowed*	*not allowed*	*not allowed*	*not allowed*
35°C/km	0-2500	*not allowed*	*not allowed*	*not allowed*	*not allowed*
Miocene[*1]	3500 (600->10000)	500 (0-1800)	1450 (450-4800)	3500 (700->10000)	1250 (650-2400)
5°C/km	>10000	*not allowed*	*not allowed*	8450-11000	*not allowed*
10°C/km	4280-5450	*not allowed*	3950-4550	2700-4300	*not allowed*
15°C/km	2400-3200	**1250-1750**	**1350-1950**	**900-1700**	*not allowed*
20°C/km	1500-2200	0-350	350-450	*not allowed*	1900-2400
25°C/km	**950-1450**	*not allowed*	*not allowed*	*not allowed*	**1050-1550**
30°C/km	650-850	*not allowed*	*not allowed*	*not allowed*	550-850
35°C/km	*not allowed*	*not allowed*	*not allowed*	*not allowed*	*not allowed*

[*1] Maximum likelihood estimates of removed section with 95% confidence limits, estimated with respect to the top-Early Cretaceous unconformity at ground level, assuming a constant paleo-surface temperature of 20°C.

Note: Entries in **red bold text** represent the favoured solutions used for reconstructions in Section 14. Determination of the amount of removed section depends on the assumption that paleogeothermal gradients were linear through both the removed section and the preserved section, in each well. This assumption will not be valid if heating involved non-linear paleogeothermal gradients, which may result either because of vertical contrasts in thermal conductivity through the section, or if heating was not directly related to depth of burial but was due e.g. to hot fluid circulation. In such cases, the estimates quoted here are likely to over-estimate true amounts of removed section.

The quoted values are based on an assumed paleo-surface temperature of 20°C. These can easily be converted to apply to other values, by subtracting or adding the difference in depth equivalent to the change in paleo-surface temperature, for the appropriate paleo-gradient. For example, for a paleogeothermal gradient of 25°C/km, a decrease of 10°C in the paleo-surface temperature is equivalent to an increase of 400 metres in the amount of removed section.

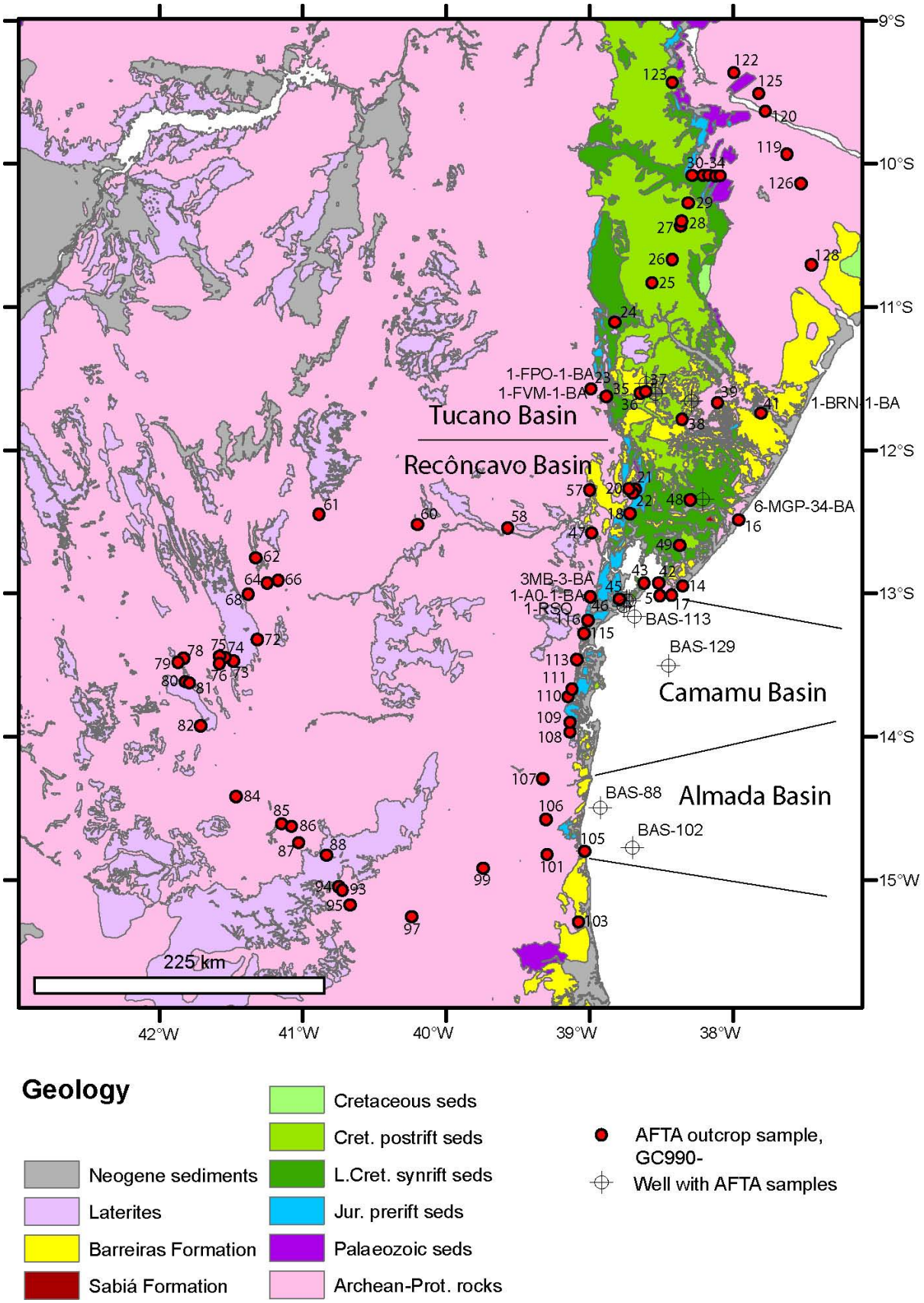

Figure 13.1: Location map showing the offshore Camamu and Almada Basins and the adjacent Onshore region..

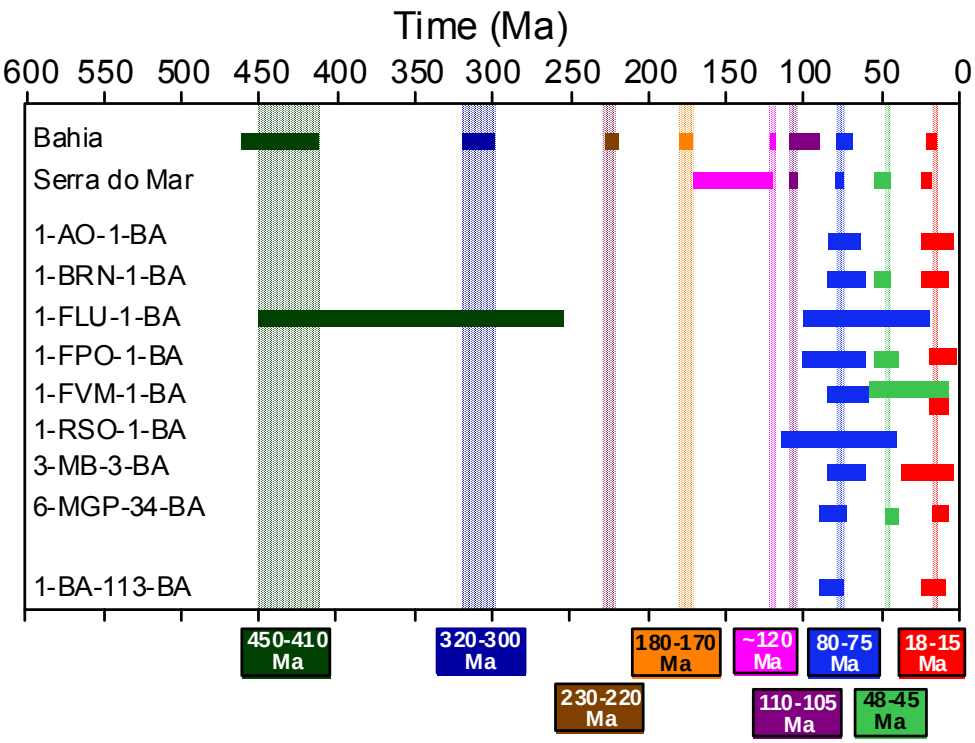

Figure 13.2: Comparison of timing constraints on dominant cooling episodes revealed by AFTA data in outcrop regions (Sections 11 and 12) and in eight wells from this study (Sections 3 though 10), together with those in offshore well 1-BAS-113-BA from Geotrack Report GC1013. Results from all wells are dominated by Late Cretaceous (blue) and Miocene (red) cooling, with many also showing Eocene (green) cooling). Late Cretaceous and Miocene cooling is also recognised in both outcrop regions, with Eocene effects also recognised in the Serra do Mar. Overall, these results suggest a very similar style of thermal history for the region over the last 80 Myr. A number of other cooling episodes are recognised from outcrops across Bahia, while Early Cretaceous cooling recognised in the Serra do Mar also appears to be synchronous with cooling in NE Brazil. Overall, a broadly similar history probably applies across the whole region, with individual regions experiencing different amounts of cooling in different events.

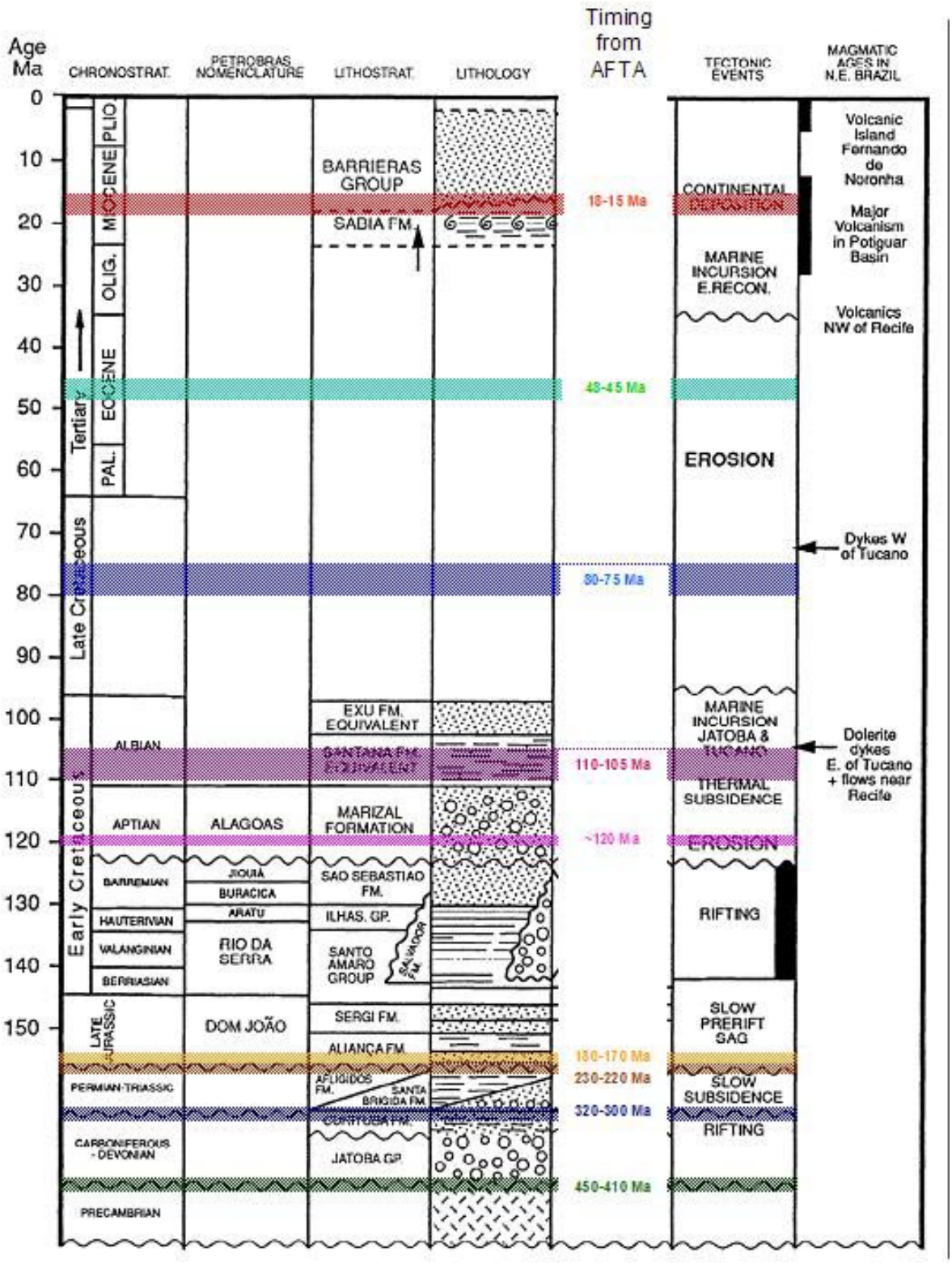

Figure 13.3: Comparison of the timing of cooling episodes identified in this study with regional geology of the Recôncavo-Tucano-Jatobá rift, from Magnavita et al. (1994).

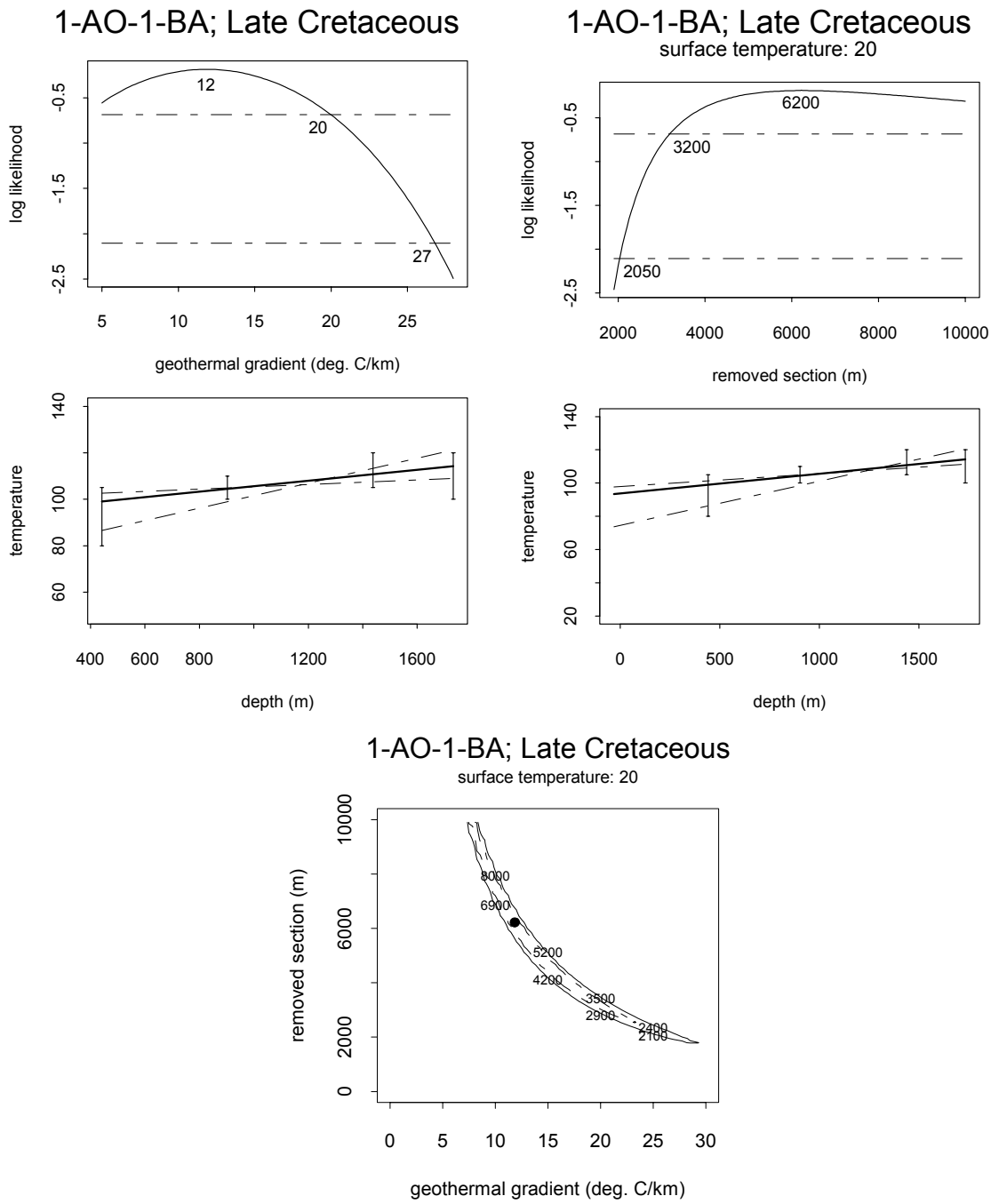

Figure 13.4: Late Cretaceous paleogeothermal gradients & removed section: well **1-AO-1-BA**

Upper: Maximum likelihood profiles of linear paleogeothermal gradient (left) and removed section (right) fitted to **Late Cretaceous** paleotemperature constraints from **AFTA and VR data** in the **1-AO-1-BA-1** well (Section 3). The methodology used to construct these profiles is outlined in Appendix C. In each plot, paleotemperature constraints are plotted against depth below the top-Early Cretaceous unconformity at ground level at the location of this well, also showing the best-fit profile (solid line) and lines (dashed) representing upper and lower 95% confidence limits. In the right-hand plot, the fitted gradients are extrapolated to a paleo-surface temperature of 20°C to determine removed section. Alternative paleo-surface temperatures can be accomodated (see text).

Lower: Crossplots of total section removed against paleogeothermal gradient, showing the ranges of paired values (within the contoured region) required to explain the **Late Cretaceous** paleotemperature constraints at the 95% confidence level, for a paleo-surface temperature of 20°C. Values printed within each plot are amounts of removed section corresponding to ±2σ limits at various values of paleogeothermal gradient. For a paleogeothermal gradient of 20°C/km, between 2900 and 3500 metres of additional section is required.

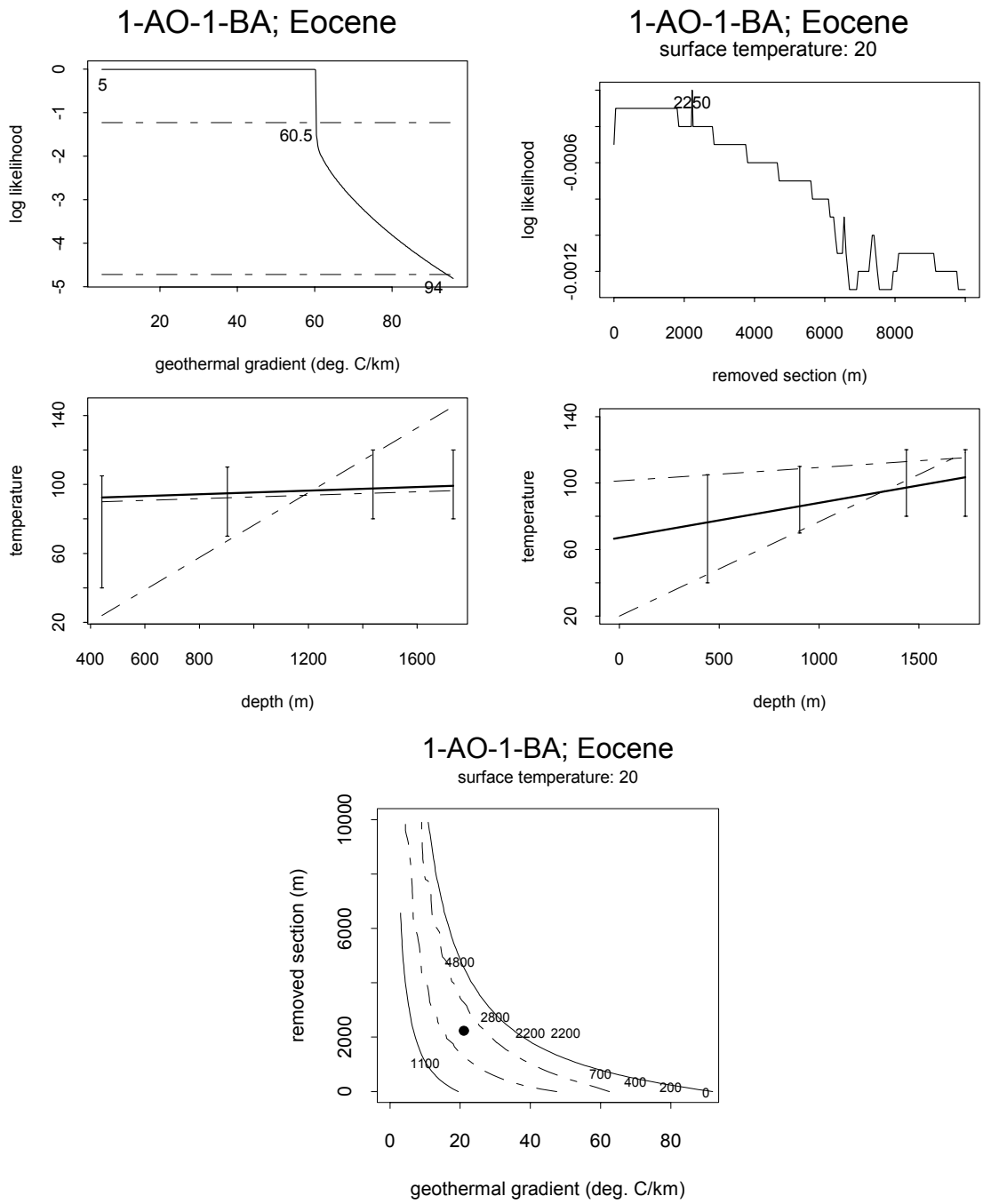

Figure 13.5: Eocene paleogeothermal gradients & removed section: well **1-AO-1-BA**

Upper: Maximum likelihood profiles of linear paleogeothermal gradient (left) and removed section (right) fitted to **Eocene** paleotemperature constraints from **AFTA and VR data** in the **1-AO-1-BA-1** well (Section 3). The methodology used to construct these profiles is outlined in Appendix C. In each plot, paleotemperature constraints are plotted against depth below the top-Early Cretaceous unconformity at ground level at the location of this well, also showing the best-fit profile (solid line) and lines (dashed) representing upper and lower 95% confidence limits. In the right-hand plot, the fitted gradients are extrapolated to a paleo-surface temperature of 20°C to determine removed section. Alternative paleo-surface temperatures can be accomodated (see text).

Lower: Crossplots of total section removed against paleogeothermal gradient, showing the ranges of paired values (within the contoured region) required to explain the **Eocene** paleotemperature constraints at the 95% confidence level, for a paleo-surface temperature of 20°C. Values printed within each plot are amounts of removed section corresponding to ±2σ limits at various values of paleogeothermal gradient. For a paleogeothermal gradient of 20°C/km, between 0 and 4800 metres of additional section is required.

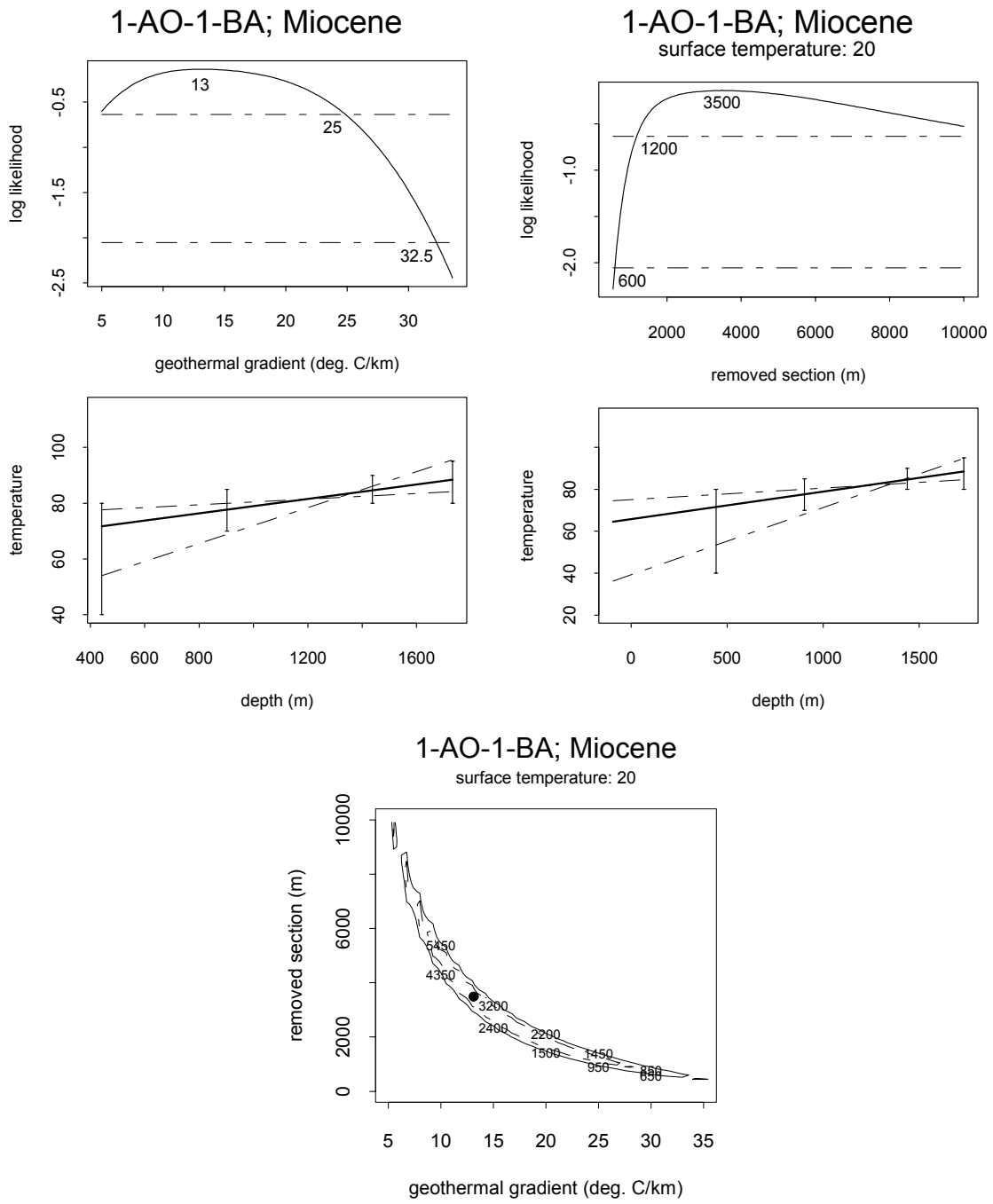

Figure 13.6: Miocene paleogeothermal gradients & removed section: well **1-AO-1-BA**

Upper: Maximum likelihood profiles of linear paleogeothermal gradient (left) and removed section (right) fitted to **Miocene** paleotemperature constraints from **AFTA and VR data** in the **1-AO-1-BA-1** well (Section 3). The methodology used to construct these profiles is outlined in Appendix C. In each plot, paleotemperature constraints are plotted against depth below the top-Early Cretaceous unconformity at ground level at the location of this well, also showing the best-fit profile (solid line) and lines (dashed) representing upper and lower 95% confidence limits. In the right-hand plot, the fitted gradients are extrapolated to a paleo-surface temperature of 20°C to determine removed section. Alternative paleo-surface temperatures can be accomodated (see text).

Lower: Crossplots of total section removed against paleogeothermal gradient, showing the ranges of paired values (within the contoured region) required to explain the **Miocene** paleotemperature constraints at the 95% confidence level, for a paleo-surface temperature of 20°C. Values printed within each plot are amounts of removed section corresponding to ±2σ limits at various values of paleogeothermal gradient. For a paleogeothermal gradient of 20°C/km, between 1500 and 2200 metres of additional section is required.

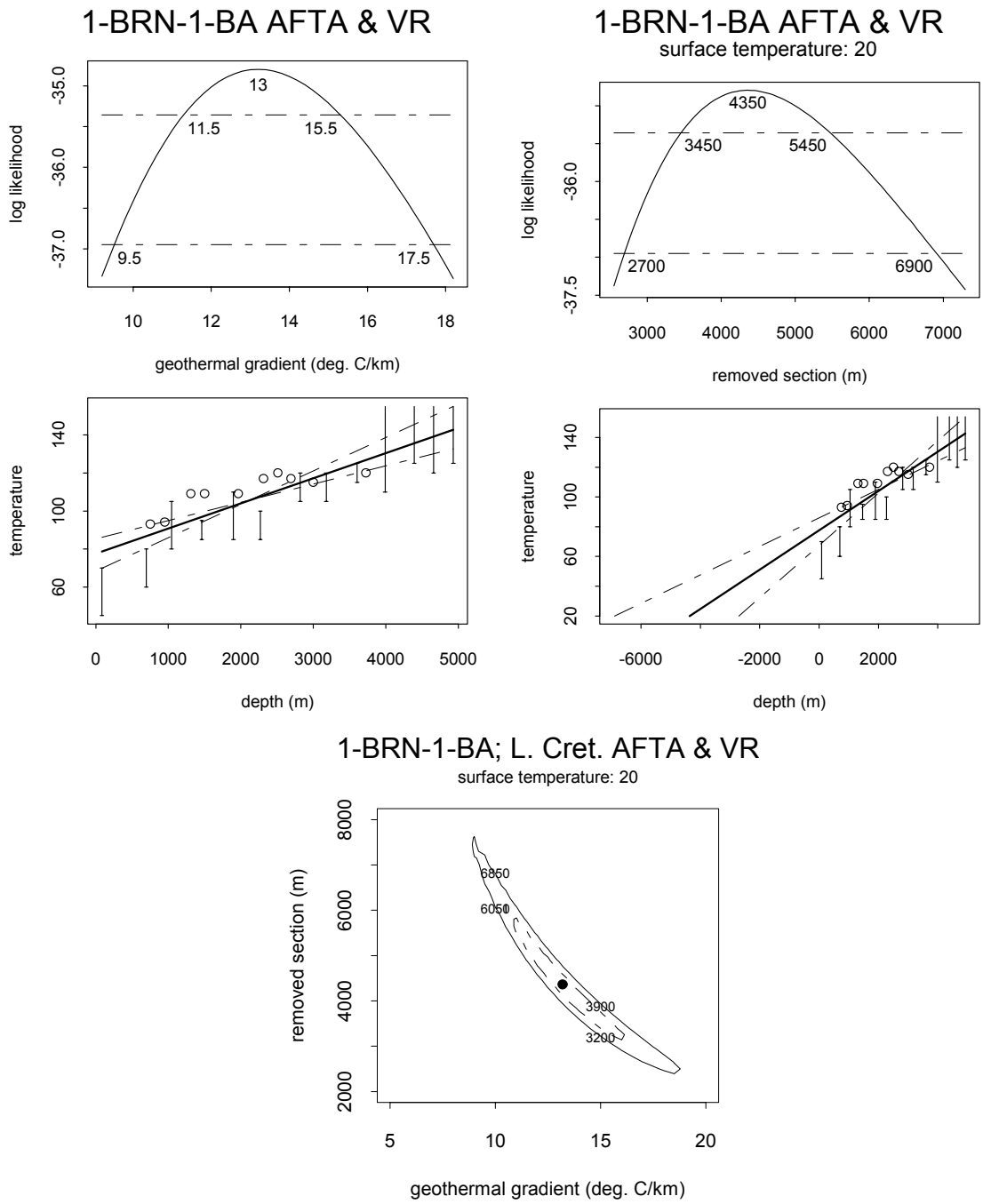

Figure 13.7: Late Cretaceous paleogeothermal gradients & removed section: well **1-BRN-1-BA**

Upper: Maximum likelihood profiles of linear paleogeothermal gradient (left) and removed section (right) fitted to **Late Cretaceous** paleotemperature constraints from **AFTA and VR data** in the **1-BRN-1-BA-1** well (Section 3). The methodology used to construct these profiles is outlined in Appendix C. In each plot, paleotemperature constraints are plotted against depth below the top-Early Cretaceous unconformity at ground level at the location of this well, also showing the best-fit profile (solid line) and lines (dashed) representing upper and lower 95% confidence limits. In the right-hand plot, the fitted gradients are extrapolated to a paleo-surface temperature of 20°C to determine removed section. Alternative paleo-surface temperatures can be accomodated (see text).

Lower: Crossplots of total section removed against paleogeothermal gradient, showing the ranges of paired values (within the contoured region) required to explain the **Late Cretaceous** paleotemperature constraints at the 95% confidence level, for a paleo-surface temperature of 20°C. Values printed within each plot are amounts of removed section corresponding to ±2σ limits at various values of paleogeothermal gradient. For a paleogeothermal gradient of 15°C/km, between 3200 and 3900 metres of additional section is required.

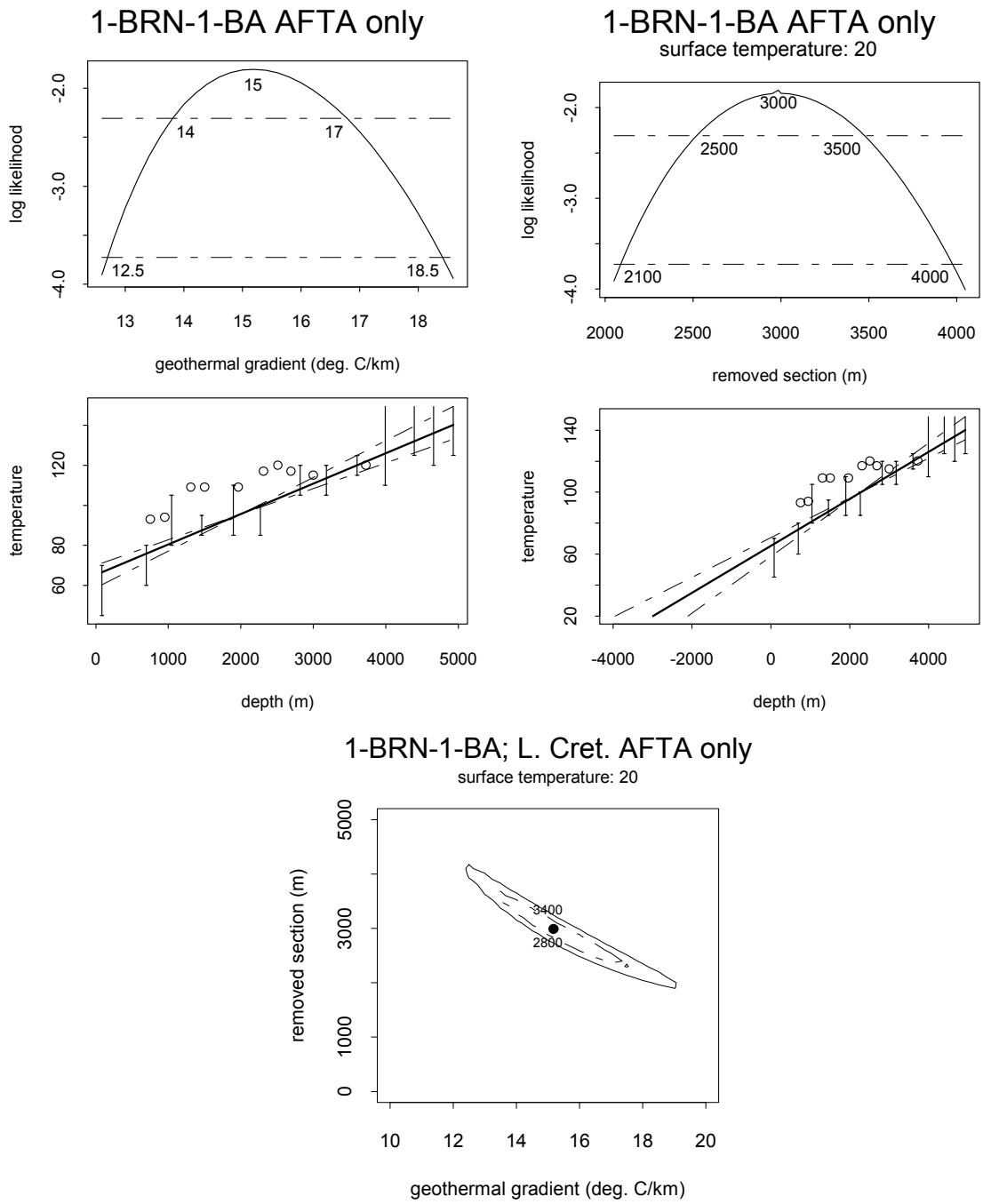

Figure 13.8: Late Cretaceous paleogeothermal gradients & removed section: well **1-BRN-1-BA; from AFTA only**

Upper: Maximum likelihood profiles of linear paleogeothermal gradient (left) and removed section (right) fitted to **Late Cretaceous** paleotemperature constraints from **AFTA only** in the **1-BRN-1-BA-1** well (Section 3). The methodology used to construct these profiles is outlined in Appendix C. In each plot, paleotemperature constraints are plotted against depth below the top-Early Cretaceous unconformity at ground level at the location of this well, also showing the best-fit profile (solid line) and lines (dashed) representing upper and lower 95% confidence limits. In the right-hand plot, the fitted gradients are extrapolated to a paleo-surface temperature of 20°C to determine removed section. Alternative paleo-surface temperatures can be accomodated (see text).

Lower: Crossplots of total section removed against paleogeothermal gradient, showing the ranges of paired values (within the contoured region) required to explain the **Late Cretaceous** paleotemperature constraints at the 95% confidence level, for a paleo-surface temperature of 20°C. Values printed within each plot are amounts of removed section corresponding to ±2σ limits at various values of paleogeothermal gradient. For a paleogeothermal gradient of 15°C/km, between 2800 and 3400 metres of additional section is required.

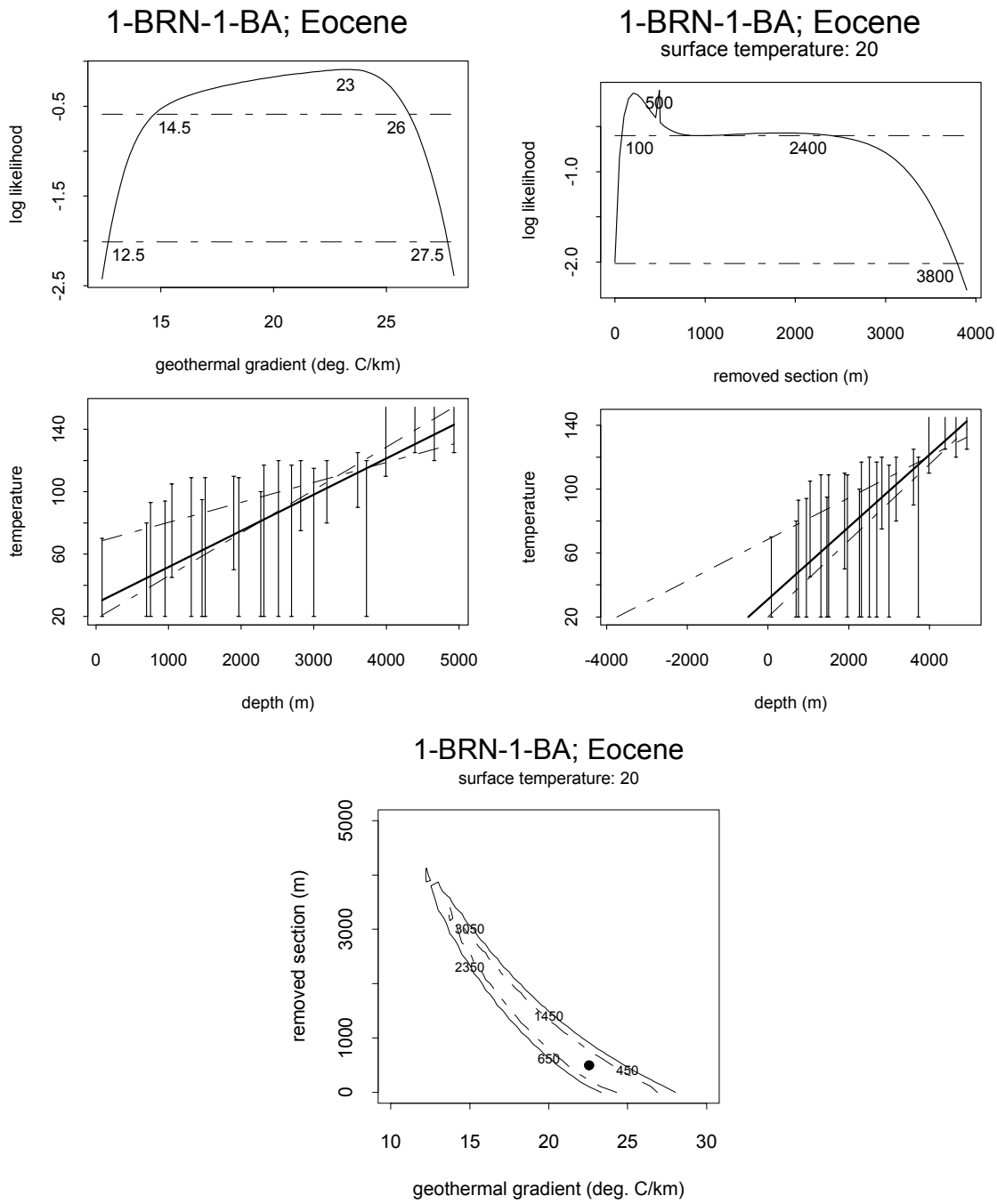

Figure 13.9: Eocene paleogeothermal gradients & removed section: well **1-BRN-1-BA**

Upper: Maximum likelihood profiles of linear paleogeothermal gradient (left) and removed section (right) fitted to **Eocene** paleotemperature constraints from **AFTA and VR data** in the **1-BRN-1-BA-1** well (Section 3). The methodology used to construct these profiles is outlined in Appendix C. In each plot, paleotemperature constraints are plotted against depth below the top-Early Cretaceous unconformity at ground level at the location of this well, also showing the best-fit profile (solid line) and lines (dashed) representing upper and lower 95% confidence limits. In the right-hand plot, the fitted gradients are extrapolated to a paleo-surface temperature of 20°C to determine removed section. Alternative paleo-surface temperatures can be accomodated (see text).

Lower: Crossplots of total section removed against paleogeothermal gradient, showing the ranges of paired values (within the contoured region) required to explain the **Eocene** paleotemperature constraints at the 95% confidence level, for a paleo-surface temperature of 20°C. Values printed within each plot are amounts of removed section corresponding to ±2σ limits at various values of paleogeothermal gradient. For a paleogeothermal gradient of 15°C/km, between 2350 and 3050 metres of additional section is required.

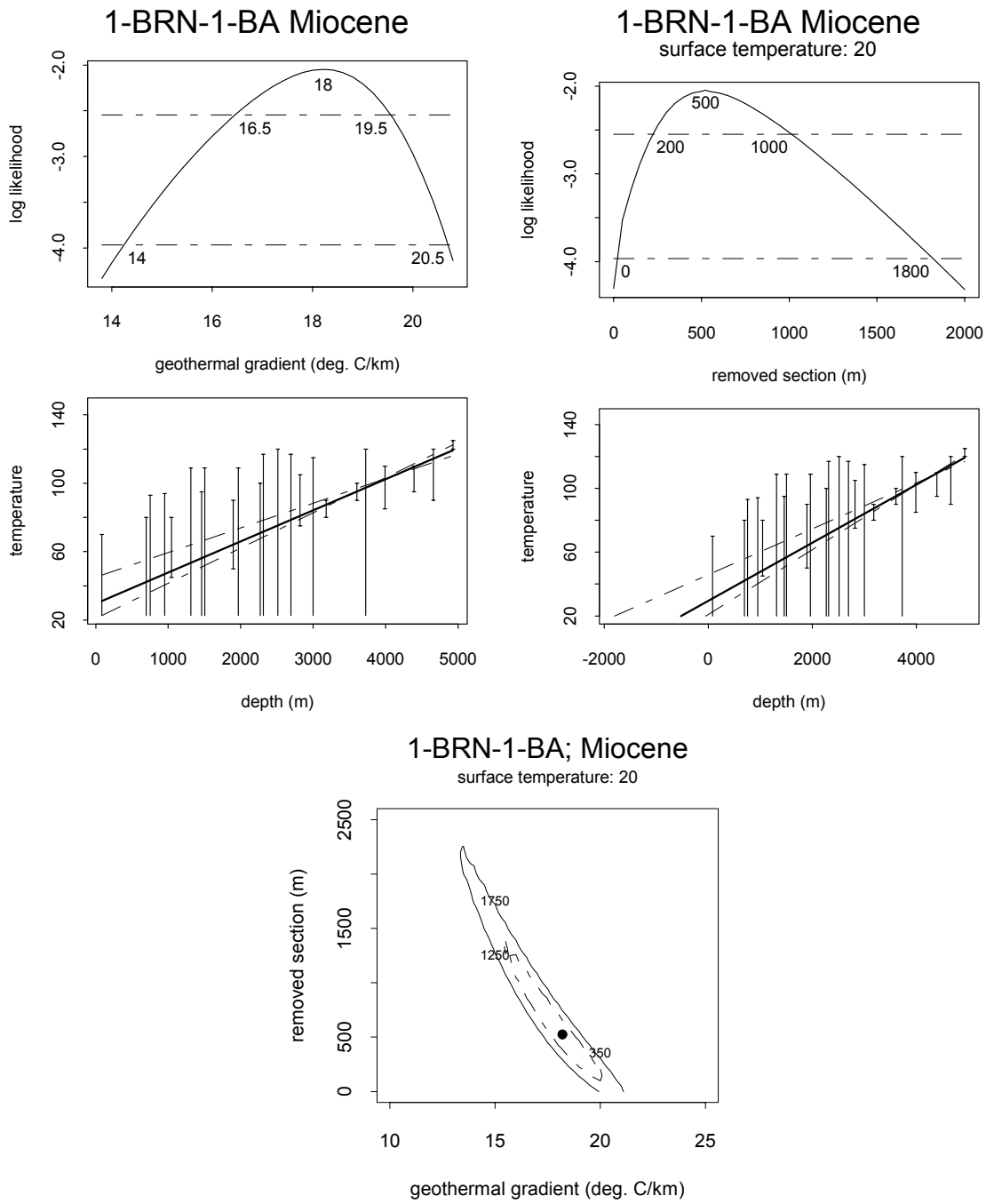

Figure 13.10: Miocene paleogeothermal gradients & removed section: well **1-BRN-1-BA**

Upper: Maximum likelihood profiles of linear paleogeothermal gradient (left) and removed section (right) fitted to **Miocene** paleotemperature constraints from **AFTA and VR data** in the **1-BRN-1-BA-1** well (Section 3). The methodology used to construct these profiles is outlined in Appendix C. In each plot, paleotemperature constraints are plotted against depth below the top-Early Cretaceous unconformity at ground level at the location of this well, also showing the best-fit profile (solid line) and lines (dashed) representing upper and lower 95% confidence limits. In the right-hand plot, the fitted gradients are extrapolated to a paleo-surface temperature of 20°C to determine removed section. Alternative paleo-surface temperatures can be accomodated (see text).

Lower: Crossplots of total section removed against paleogeothermal gradient, showing the ranges of paired values (within the contoured region) required to explain the **Miocene** paleotemperature constraints at the 95% confidence level, for a paleo-surface temperature of 20°C. Values printed within each plot are amounts of removed section corresponding to ±2σ limits at various values of paleogeothermal gradient. For a paleogeothermal gradient of 15°C/km, between 1250 and 1750 metres of additional section is required.

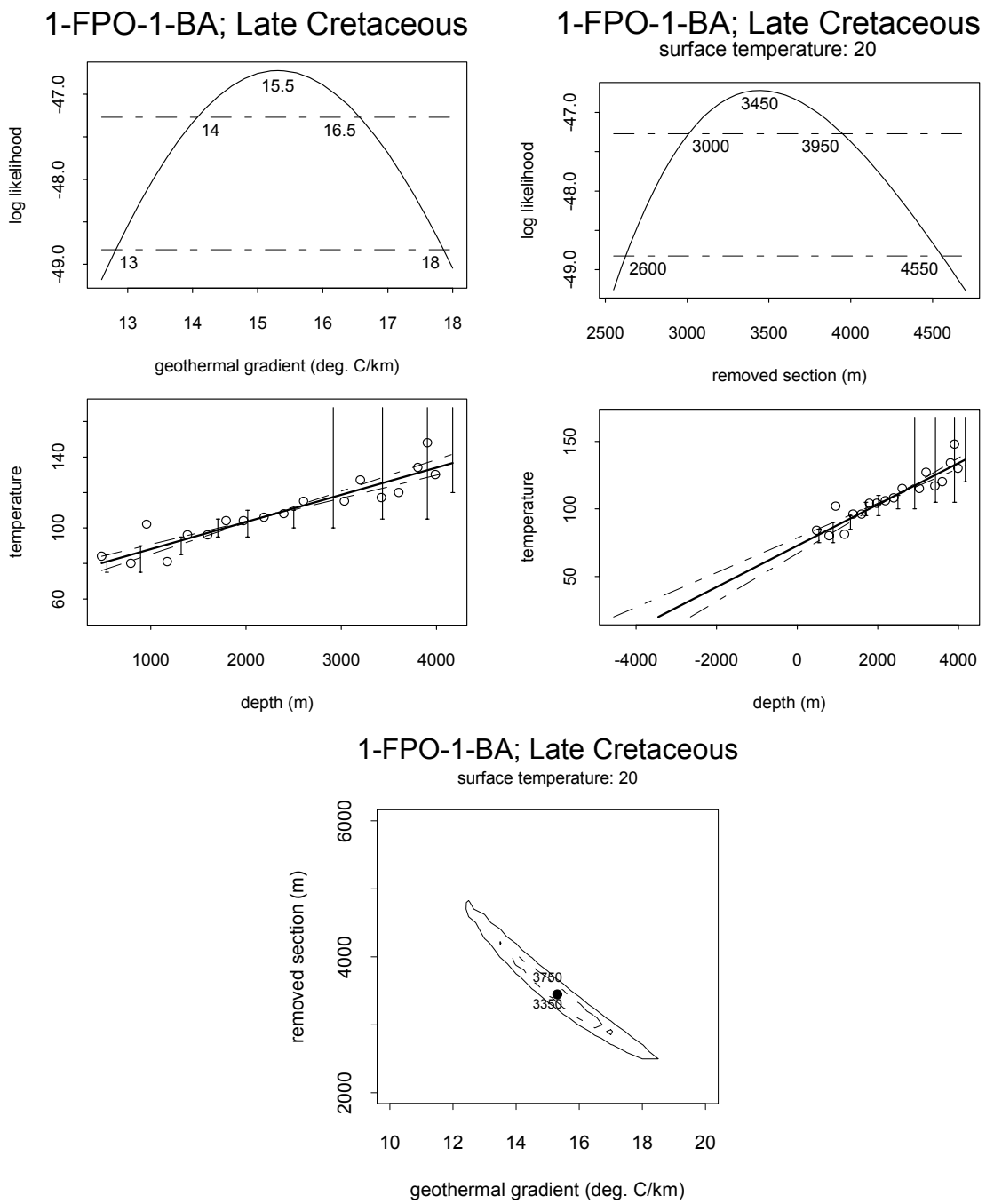

Figure 13.11: Late Cretaceous paleogeothermal gradients & removed section: well **1-FPO-1-BA**

Upper: Maximum likelihood profiles of linear paleogeothermal gradient (left) and removed section (right) fitted to **Late Cretaceous** paleotemperature constraints from **AFTA and VR data** in the **1-FPO-1-BA-1** well (Section 3). The methodology used to construct these profiles is outlined in Appendix C. In each plot, paleotemperature constraints are plotted against depth below the top-Early Cretaceous unconformity at ground level at the location of this well, also showing the best-fit profile (solid line) and lines (dashed) representing upper and lower 95% confidence limits. In the right-hand plot, the fitted gradients are extrapolated to a paleo-surface temperature of 20°C to determine removed section. Alternative paleo-surface temperatures can be accomodated (see text).

Lower: Crossplots of total section removed against paleogeothermal gradient, showing the ranges of paired values (within the contoured region) required to explain the **Late Cretaceous** paleotemperature constraints at the 95% confidence level, for a paleo-surface temperature of 20°C. Values printed within each plot are amounts of removed section corresponding to ±2σ limits at various values of paleogeothermal gradient. For a paleogeothermal gradient of 15°C/km, between 3350 and 3750 metres of additional section is required.

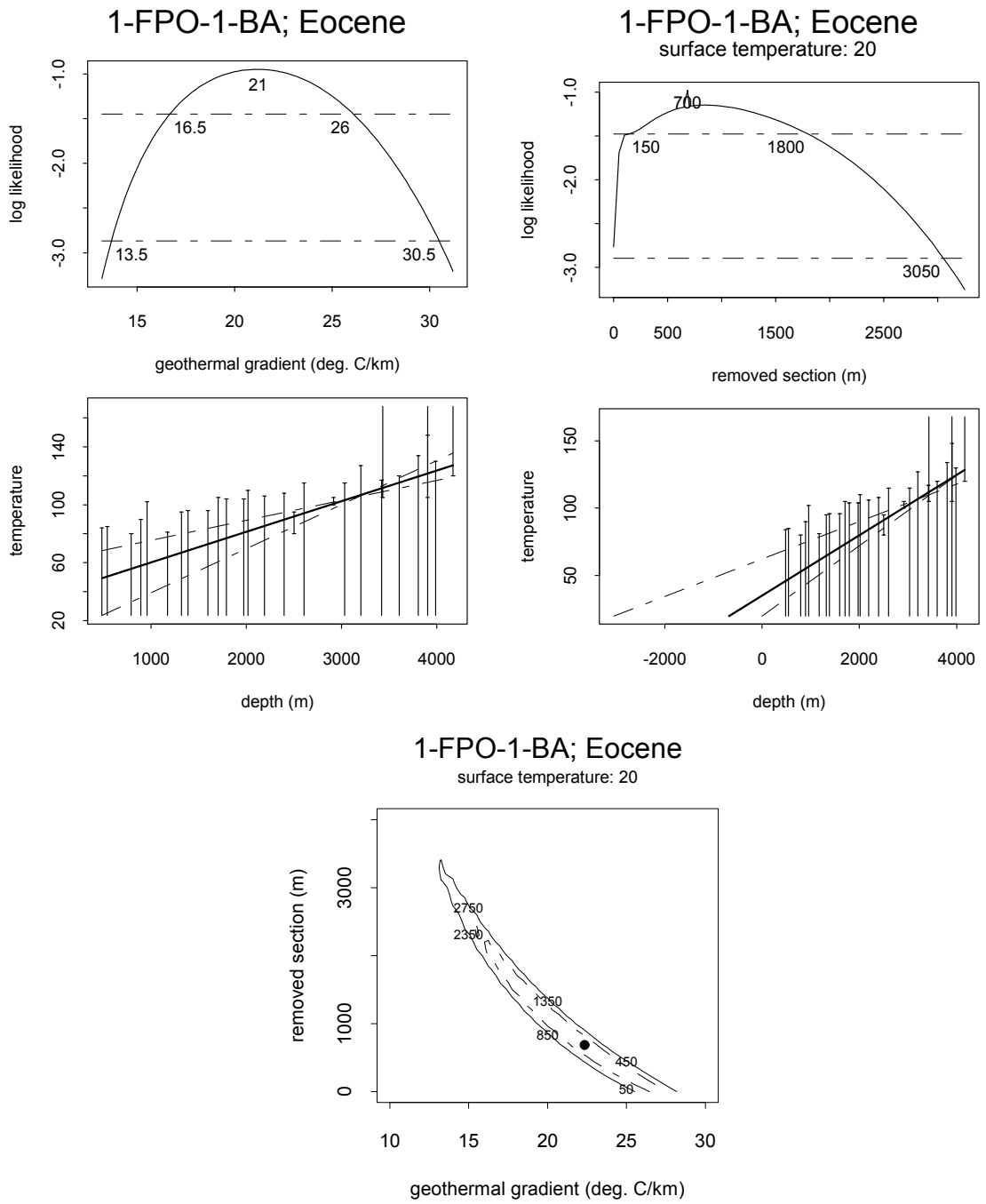

Figure 13.12: Eocene paleogeothermal gradients & removed section: well **1-FPO-1-BA**

Upper: Maximum likelihood profiles of linear paleogeothermal gradient (left) and removed section (right) fitted to **Eocene** paleotemperature constraints from **AFTA and VR data** in the **1-FPO-1-BA-1** well (Section 3). The methodology used to construct these profiles is outlined in Appendix C. In each plot, paleotemperature constraints are plotted against depth below the top-Early Cretaceous unconformity at ground level at the location of this well, also showing the best-fit profile (solid line) and lines (dashed) representing upper and lower 95% confidence limits. In the right-hand plot, the fitted gradients are extrapolated to a paleo-surface temperature of 20°C to determine removed section. Alternative paleo-surface temperatures can be accomodated (see text).

Lower: Crossplots of total section removed against paleogeothermal gradient, showing the ranges of paired values (within the contoured region) required to explain the **Eocene** paleotemperature constraints at the 95% confidence level, for a paleo-surface temperature of 20°C. Values printed within each plot are amounts of removed section corresponding to ±2σ limits at various values of paleogeothermal gradient. For a paleogeothermal gradient of 15°C/km, between 2350 and 2750 metres of additional section is required.

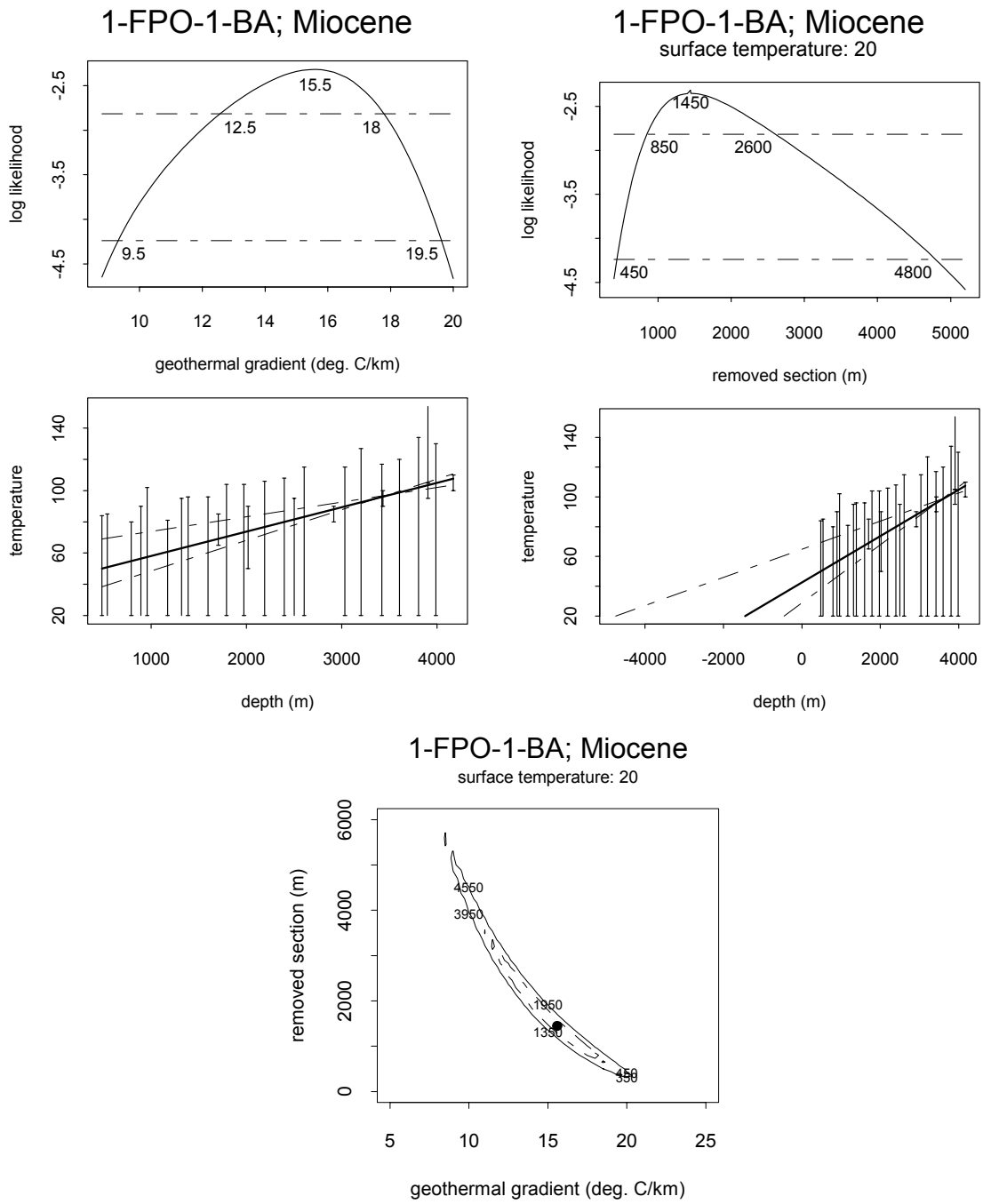

Figure 13.13: Miocene paleogeothermal gradients & removed section: well **1-FPO-1-BA**

Upper: Maximum likelihood profiles of linear paleogeothermal gradient (left) and removed section (right) fitted to **Miocene** paleotemperature constraints from **AFTA and VR data** in the **1-FPO-1-BA-1** well (Section 3). The methodology used to construct these profiles is outlined in Appendix C. In each plot, paleotemperature constraints are plotted against depth below the top-Early Cretaceous unconformity at ground level at the location of this well, also showing the best-fit profile (solid line) and lines (dashed) representing upper and lower 95% confidence limits. In the right-hand plot, the fitted gradients are extrapolated to a paleo-surface temperature of 20°C to determine removed section. Alternative paleo-surface temperatures can be accomodated (see text).

Lower: Crossplots of total section removed against paleogeothermal gradient, showing the ranges of paired values (within the contoured region) required to explain the **Miocene** paleotemperature constraints at the 95% confidence level, for a paleo-surface temperature of 20°C. Values printed within each plot are amounts of removed section corresponding to ±2σ limits at various values of paleogeothermal gradient. For a paleogeothermal gradient of 15°C/km, between 1350 and 1950 metres of additional section is required.

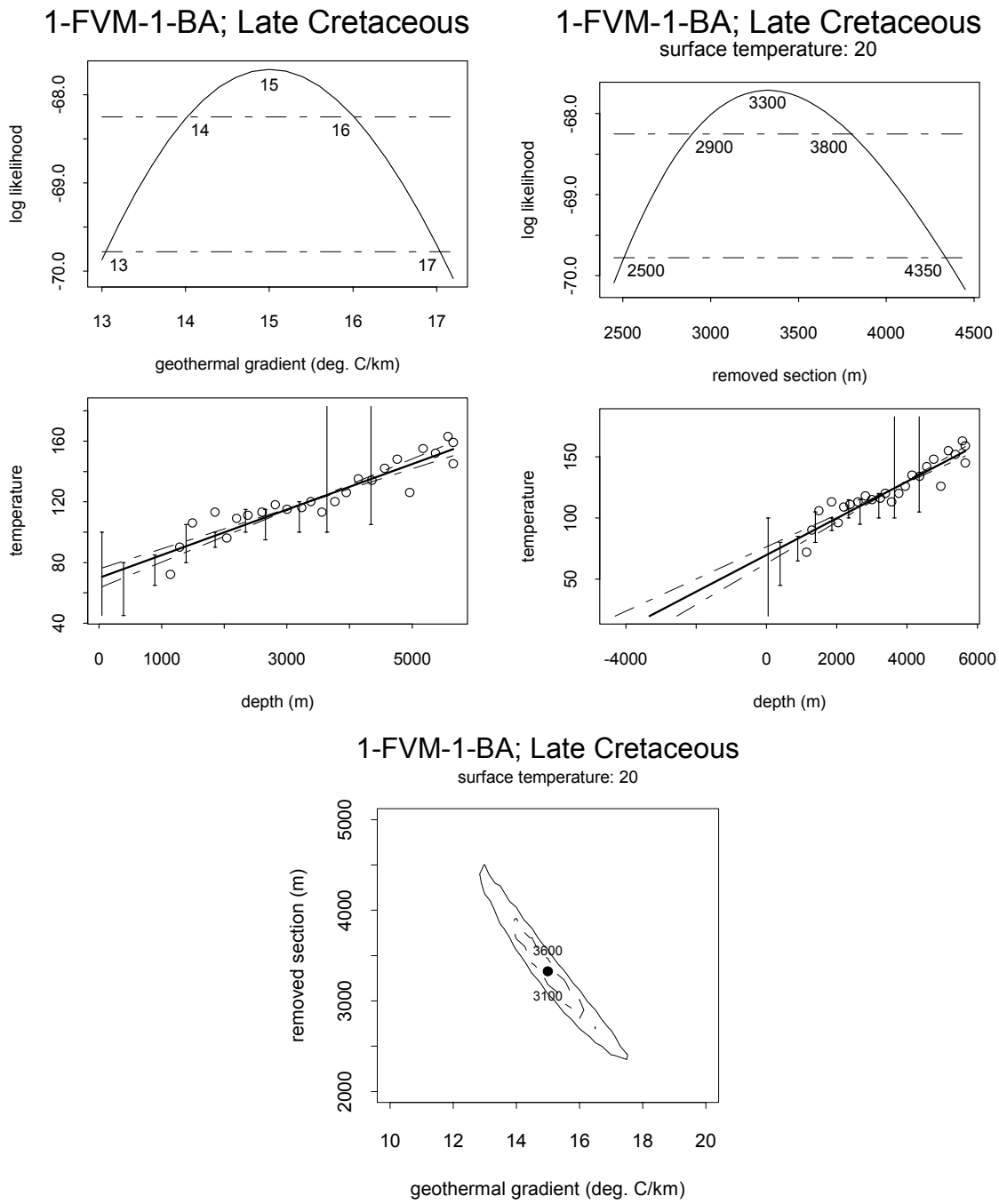

Figure 13.14: Late Cretaceous paleogeothermal gradients & removed section: well **1-FVM-1-BA**

Upper: Maximum likelihood profiles of linear paleogeothermal gradient (left) and removed section (right) fitted to **Late Cretaceous** paleotemperature constraints from **AFTA and VR data** in the **1-FVM-1-BA-1** well (Section 3). The methodology used to construct these profiles is outlined in Appendix C. In each plot, paleotemperature constraints are plotted against depth below the top-Early Cretaceous unconformity at ground level at the location of this well, also showing the best-fit profile (solid line) and lines (dashed) representing upper and lower 95% confidence limits. In the right-hand plot, the fitted gradients are extrapolated to a paleo-surface temperature of 20°C to determine removed section. Alternative paleo-surface temperatures can be accomodated (see text).

Lower: Crossplots of total section removed against paleogeothermal gradient, showing the ranges of paired values (within the contoured region) required to explain the **Late Cretaceous** paleotemperature constraints at the 95% confidence level, for a paleo-surface temperature of 20°C. Values printed within each plot are amounts of removed section corresponding to ±2σ limits at various values of paleogeothermal gradient. For a paleogeothermal gradient of 15°C/km, between 3100 and 3600 metres of additional section is required.

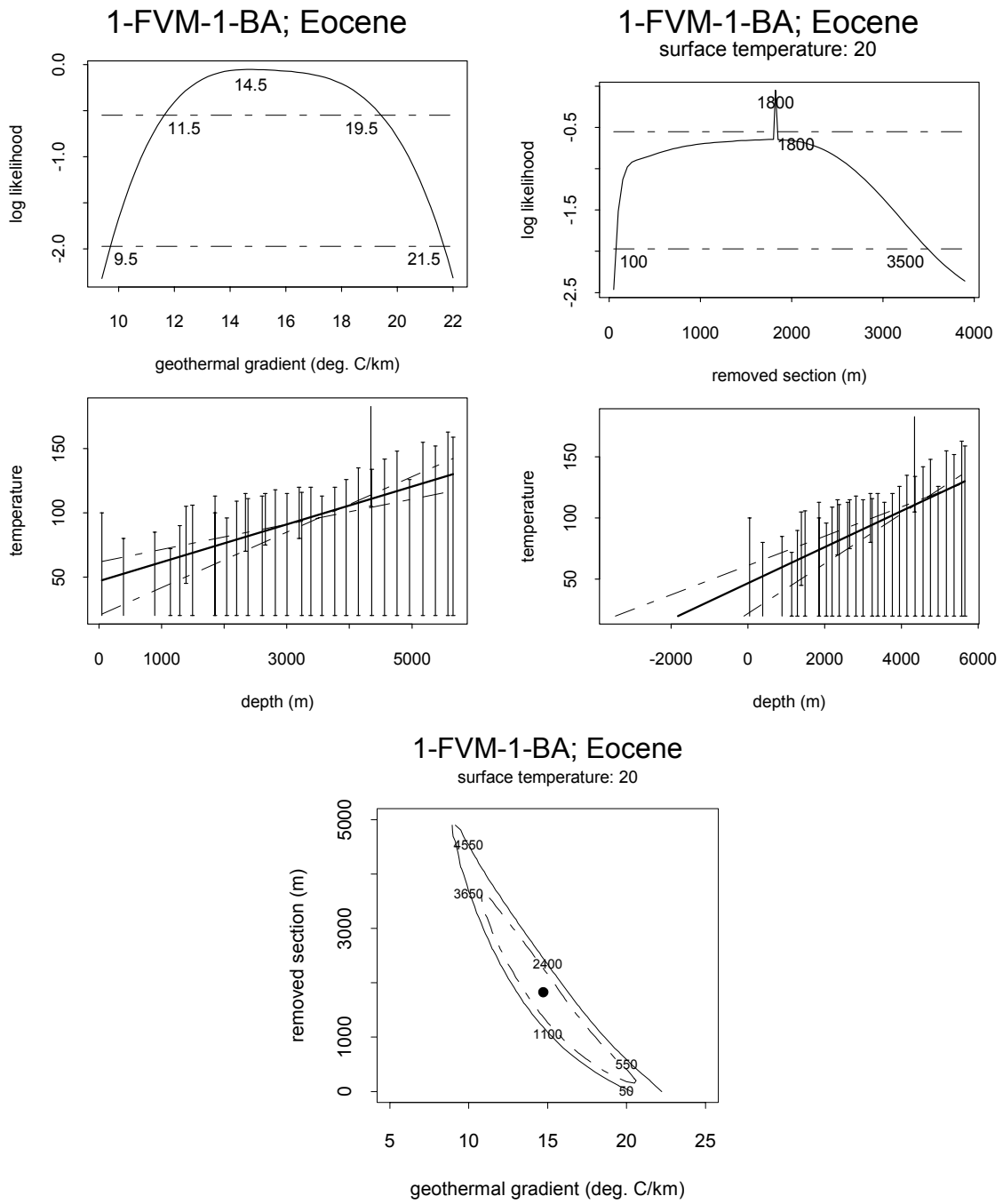

Figure 13.15: Eocene paleogeothermal gradients & removed section: well **1-FVM-1-BA**

Upper: Maximum likelihood profiles of linear paleogeothermal gradient (left) and removed section (right) fitted to **Eocene** paleotemperature constraints from **AFTA and VR data** in the **1-FVM-1-BA-1** well (Section 3). The methodology used to construct these profiles is outlined in Appendix C. In each plot, paleotemperature constraints are plotted against depth below the top-Early Cretaceous unconformity at ground level at the location of this well, also showing the best-fit profile (solid line) and lines (dashed) representing upper and lower 95% confidence limits. In the right-hand plot, the fitted gradients are extrapolated to a paleo-surface temperature of 20°C to determine removed section. Alternative paleo-surface temperatures can be accomodated (see text).

Lower: Crossplots of total section removed against paleogeothermal gradient, showing the ranges of paired values (within the contoured region) required to explain the **Eocene** paleotemperature constraints at the 95% confidence level, for a paleo-surface temperature of 20°C. Values printed within each plot are amounts of removed section corresponding to ±2σ limits at various values of paleogeothermal gradient. For a paleogeothermal gradient of 15°C/km, between 1100 and 2400 metres of additional section is required.

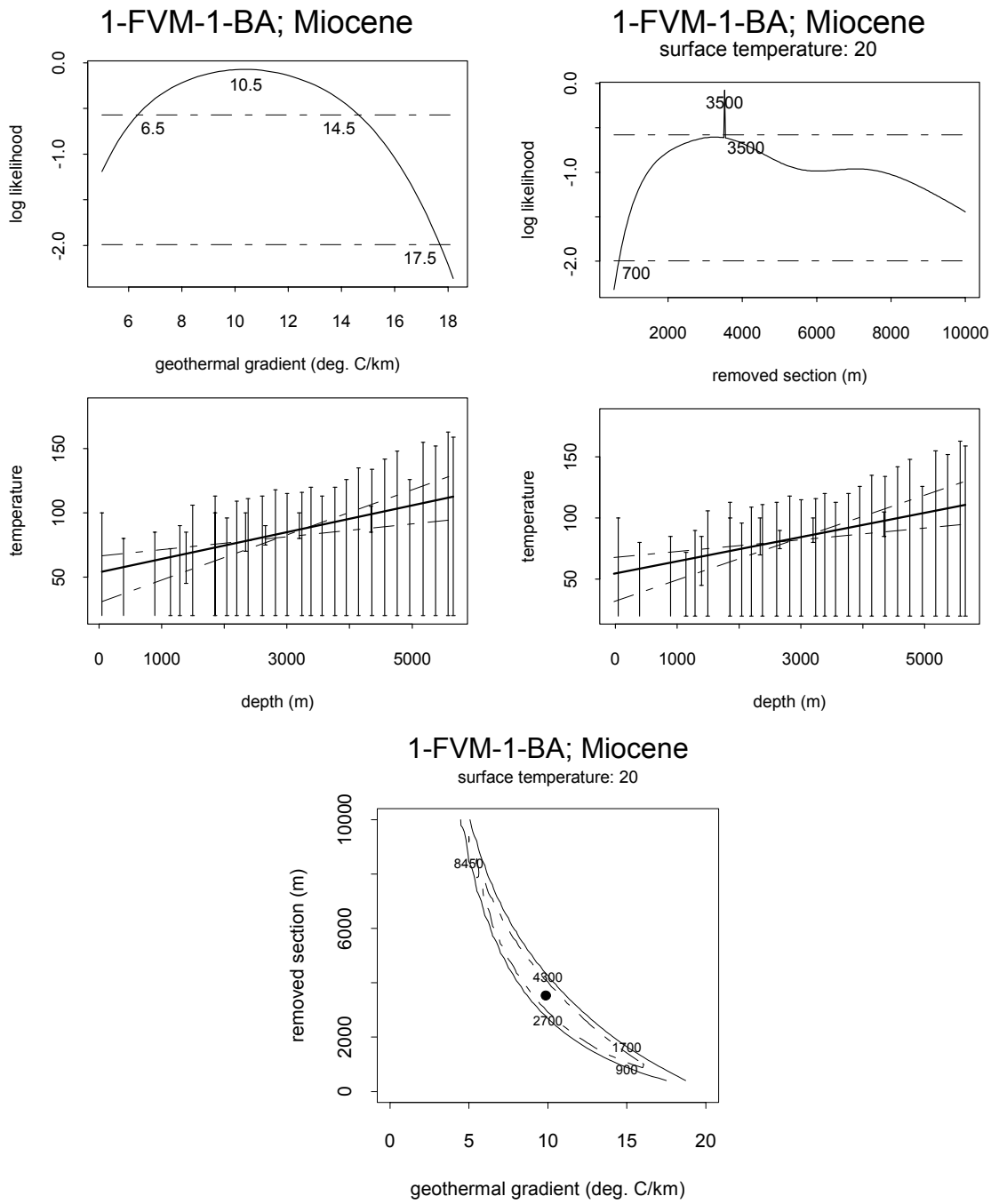

Figure 13.16: Miocene paleogeothermal gradients & removed section: well **1-FVM-1-BA**

Upper: Maximum likelihood profiles of linear paleogeothermal gradient (left) and removed section (right) fitted to **Miocene** paleotemperature constraints from **AFTA and VR data** in the **1-FVM-1-BA-1** well (Section 3). The methodology used to construct these profiles is outlined in Appendix C. In each plot, paleotemperature constraints are plotted against depth below the top-Early Cretaceous unconformity at ground level at the location of this well, also showing the best-fit profile (solid line) and lines (dashed) representing upper and lower 95% confidence limits. In the right-hand plot, the fitted gradients are extrapolated to a paleo-surface temperature of 20°C to determine removed section. Alternative paleo-surface temperatures can be accomodated (see text).

Lower: Crossplots of total section removed against paleogeothermal gradient, showing the ranges of paired values (within the contoured region) required to explain the **Miocene** paleotemperature constraints at the 95% confidence level, for a paleo-surface temperature of 20°C. Values printed within each plot are amounts of removed section corresponding to ±2σ limits at various values of paleogeothermal gradient. For a paleogeothermal gradient of 15°C/km, between 900 and 1700 metres of additional section is required.

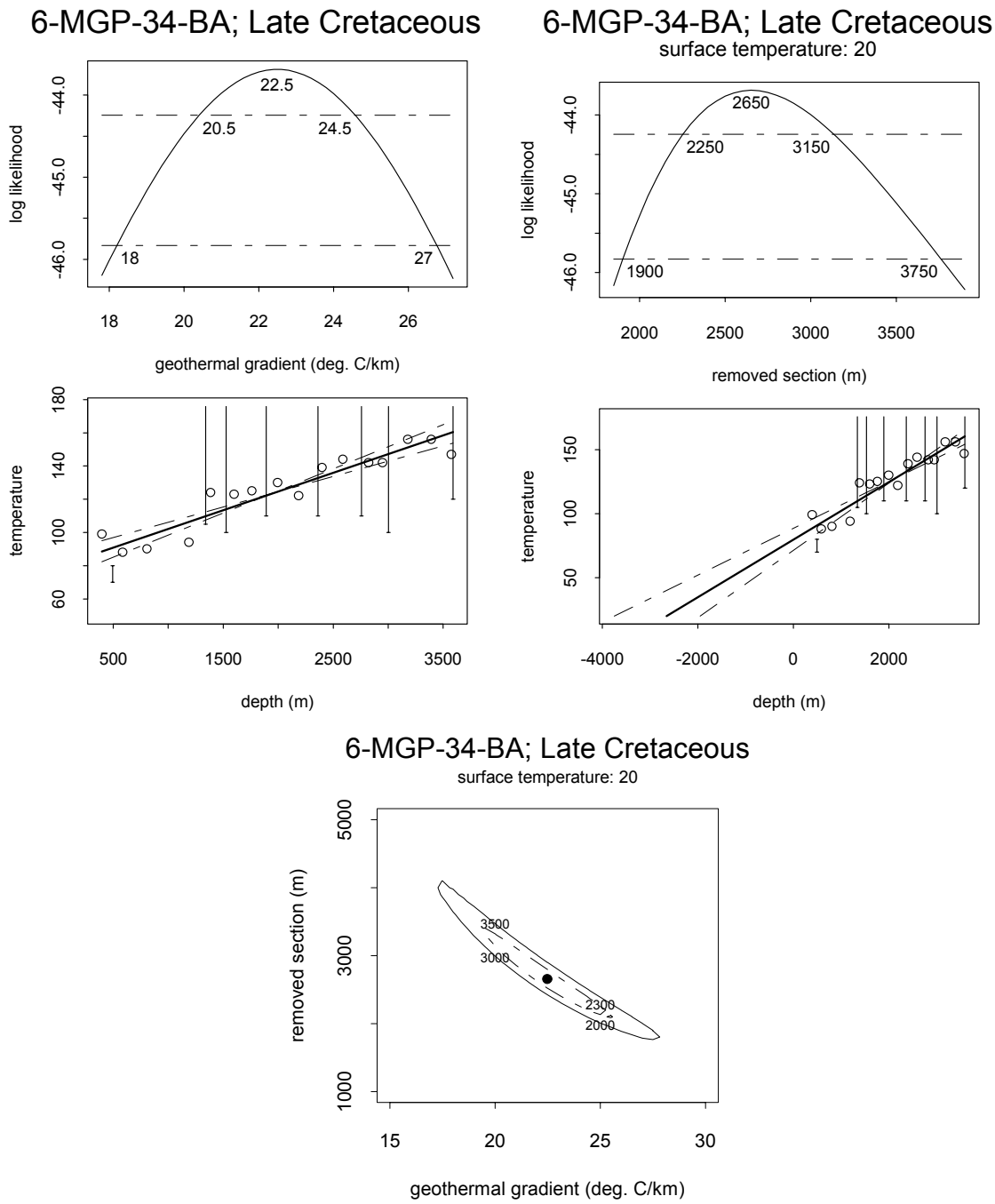

Figure 13.17: Late Cretaceous paleogeothermal gradients & removed section: well **6-MGP-34-BA**

Upper: Maximum likelihood profiles of linear paleogeothermal gradient (left) and removed section (right) fitted to **Late Cretaceous** paleotemperature constraints from **AFTA and VR data** in the **6-MGP-34-BA** well (Section 3). The methodology used to construct these profiles is outlined in Appendix C. In each plot, paleotemperature constraints are plotted against depth below the top-Early Cretaceous unconformity at ground level at the location of this well, also showing the best-fit profile (solid line) and lines (dashed) representing upper and lower 95% confidence limits. In the right-hand plot, the fitted gradients are extrapolated to a paleo-surface temperature of 20°C to determine removed section. Alternative paleo-surface temperatures can be accomodated (see text).

Lower: Crossplots of total section removed against paleogeothermal gradient, showing the ranges of paired values (within the contoured region) required to explain the **Late Cretaceous** paleotemperature constraints at the 95% confidence level, for a paleo-surface temperature of 20°C. Values printed within each plot are amounts of removed section corresponding to ±2σ limits at various values of paleogeothermal gradient. For a paleogeothermal gradient of 20°C/km, between 3000 and 3500 metres of additional section is required.

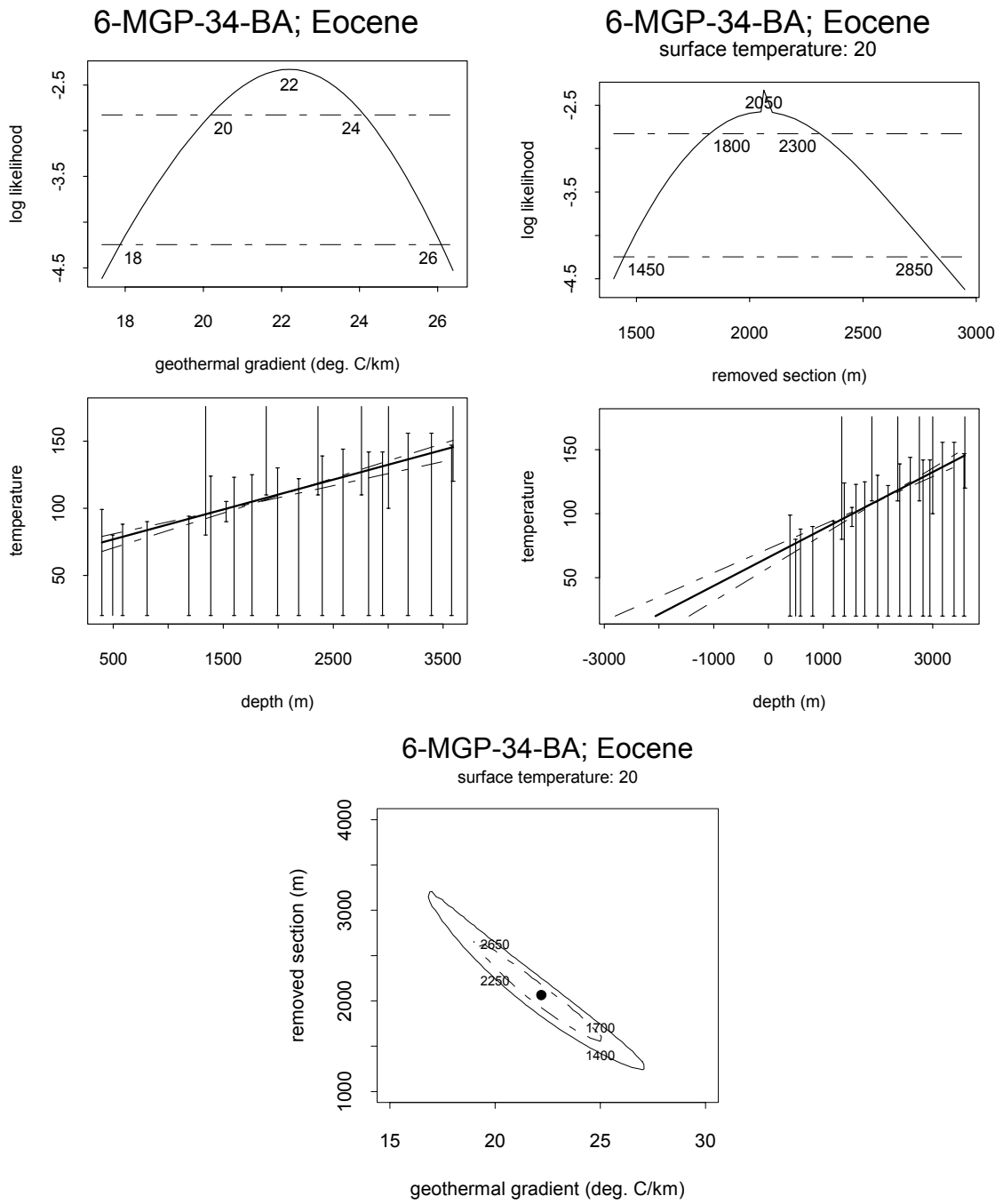

Figure 13.18: Eocene paleogeothermal gradients & removed section: well **6-MGP-34-BA**

Upper: Maximum likelihood profiles of linear paleogeothermal gradient (left) and removed section (right) fitted to **Eocene** paleotemperature constraints from **AFTA and VR data** in the **6-MGP-34-BA** well (Section 3). The methodology used to construct these profiles is outlined in Appendix C. In each plot, paleotemperature constraints are plotted against depth below the top-Early Cretaceous unconformity at ground level at the location of this well, also showing the best-fit profile (solid line) and lines (dashed) representing upper and lower 95% confidence limits. In the right-hand plot, the fitted gradients are extrapolated to a paleo-surface temperature of 20°C to determine removed section. Alternative paleo-surface temperatures can be accomodated (see text).

Lower: Crossplots of total section removed against paleogeothermal gradient, showing the ranges of paired values (within the contoured region) required to explain the **Eocene** paleotemperature constraints at the 95% confidence level, for a paleo-surface temperature of 20°C. Values printed within each plot are amounts of removed section corresponding to ±2σ limits at various values of paleogeothermal gradient. For a paleogeothermal gradient of 20°C/km, between 2250 and 2850 metres of additional section is required.

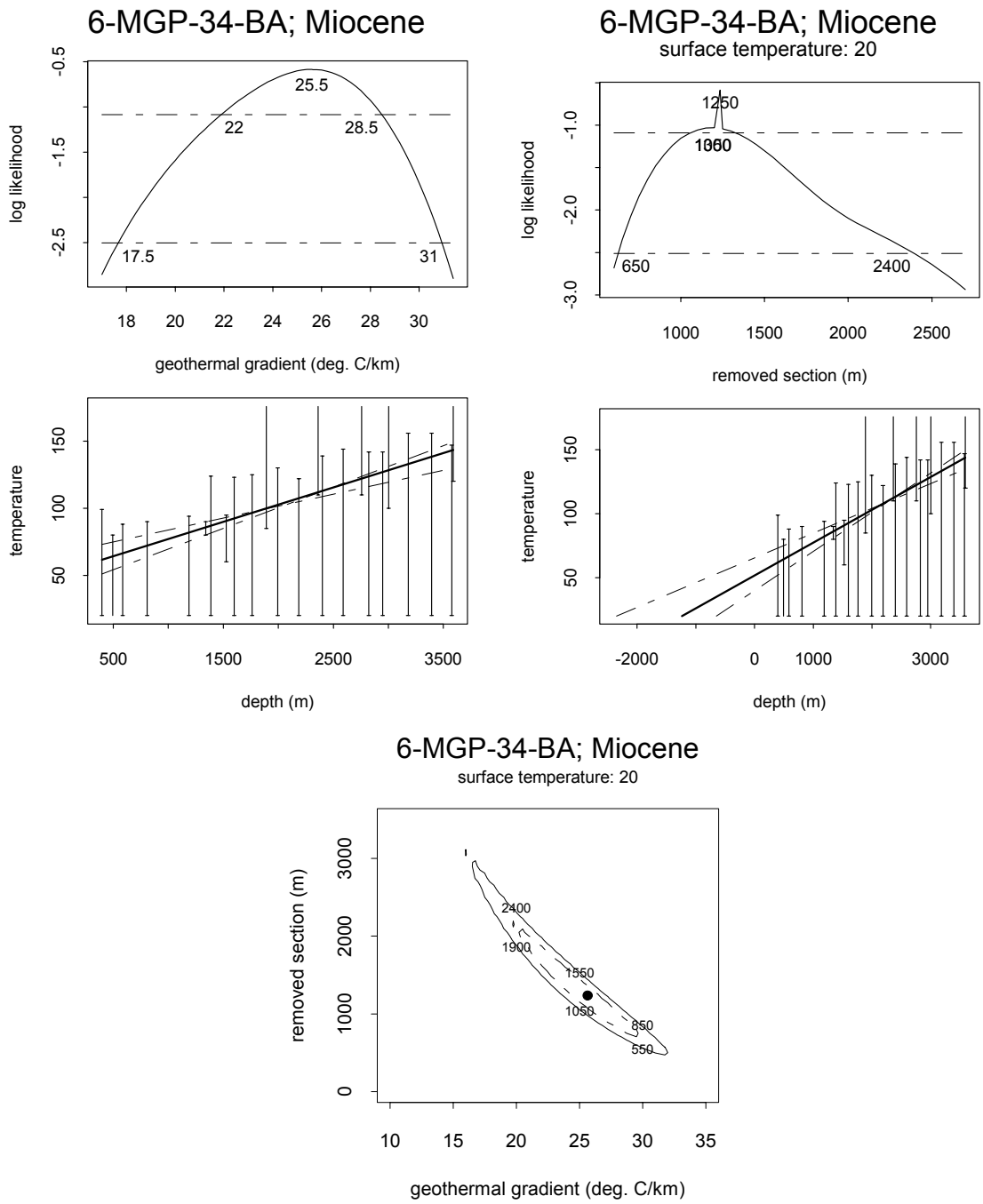

Figure 13.19: Miocene paleogeothermal gradients & removed section: well **6-MGP-34-BA**

Upper: Maximum likelihood profiles of linear paleogeothermal gradient (left) and removed section (right) fitted to **Miocene** paleotemperature constraints from **AFTA and VR data** in the **6-MGP-34-BA-1** well (Section 3). The methodology used to construct these profiles is outlined in Appendix C. In each plot, paleotemperature constraints are plotted against depth below the top-Early Cretaceous unconformity at ground level at the location of this well, also showing the best-fit profile (solid line) and lines (dashed) representing upper and lower 95% confidence limits. In the right-hand plot, the fitted gradients are extrapolated to a paleo-surface temperature of 20°C to determine removed section. Alternative paleo-surface temperatures can be accomodated (see text).

Lower: Crossplots of total section removed against paleogeothermal gradient, showing the ranges of paired values (within the contoured region) required to explain the **Miocene** paleotemperature constraints at the 95% confidence level, for a paleo-surface temperature of 20°C. Values printed within each plot are amounts of removed section corresponding to ±2σ limits at various values of paleogeothermal gradient. For a paleogeothermal gradient of 20°C/km, between 1900 and 2400 metres of additional section is required.

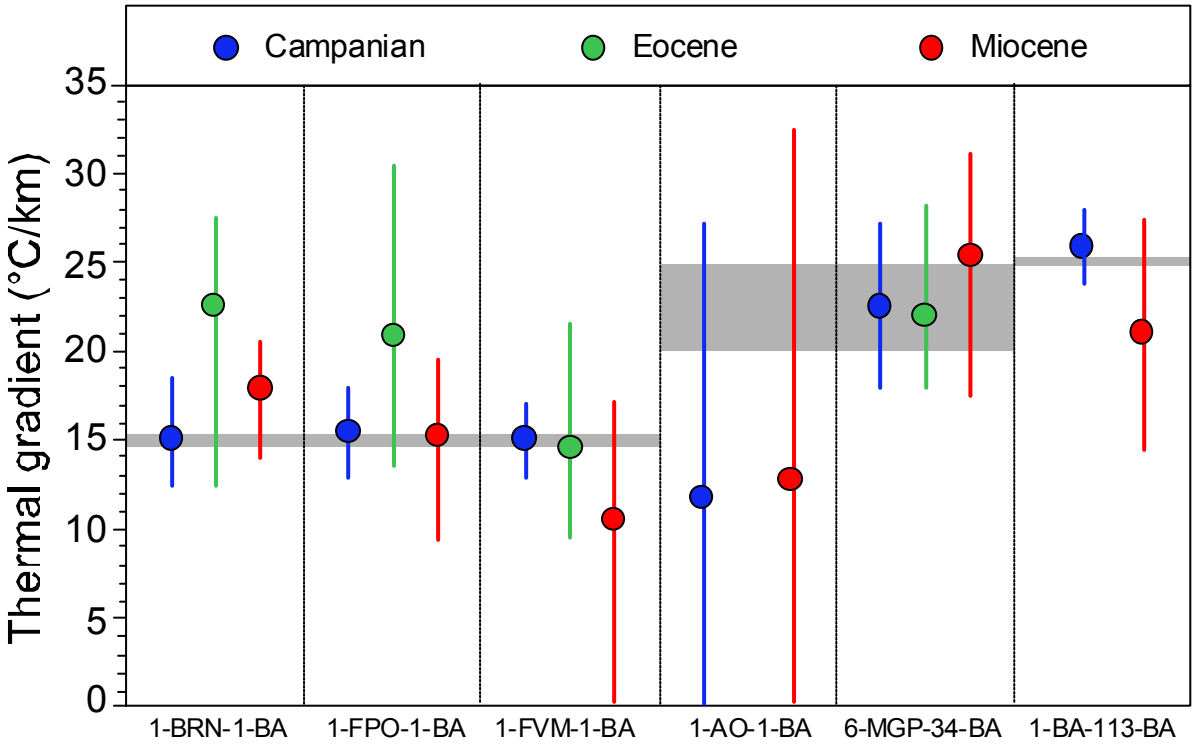

Figure 13.20: Comparison of present-day thermal gradients (grey shaded boxes) with paleogeothermal gradients obtained in this study in three episodes from five wells (from Table 13.1), plus constraints on Campanian and Miocene values from the 1-BAS-113-BA well from Geotrack Report #1013 (using the preferred Campanian value of 26°C/km based on AFTA and selected VR data). These results suggest little or no change in basal heat flow over at least the last 80 Myr.

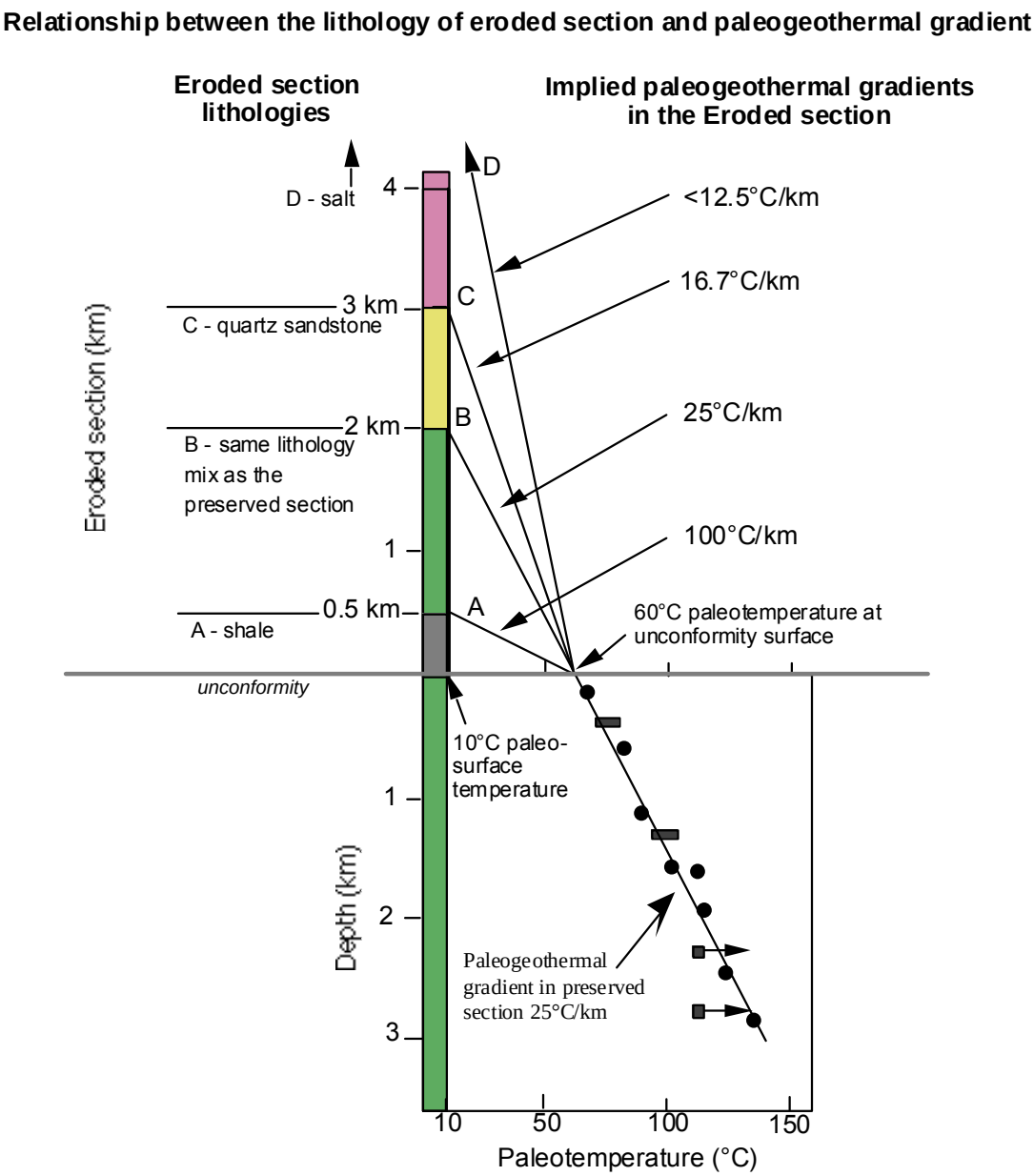

Figure 13.21: General relationship between lithology and removed section.

In the example illustrated, the paleogeothermal gradient defined by the AFTA and VR paleotemperature results in the drilled preserved section is clearly linear, indicating that large lithology-controlled thermal conductivity contrasts are not present in the section. Linear extrapolation of the paleogeothermal gradient in the preserved section to a paleo-surface temperature of 10°C suggests 2 km of section has been eroded, based on the explicit assumption that the lithologies eroded were similar to those still preserved in the drilled section. If the eroded lithologies were grossly different to those still preserved then linear extrapolation is not valid, because grossly different lithologies would produce a non-linear, "dog-leg" paleotemperature profile at the time of maximum burial. Examples are illustrated for typical lithologies. Lower eroded section estimates result from assuming finer-grained lithologies (i.e. lower thermal conductivities) removed, but this requires high paleogeothermal gradients in this section prior uplift and erosion.

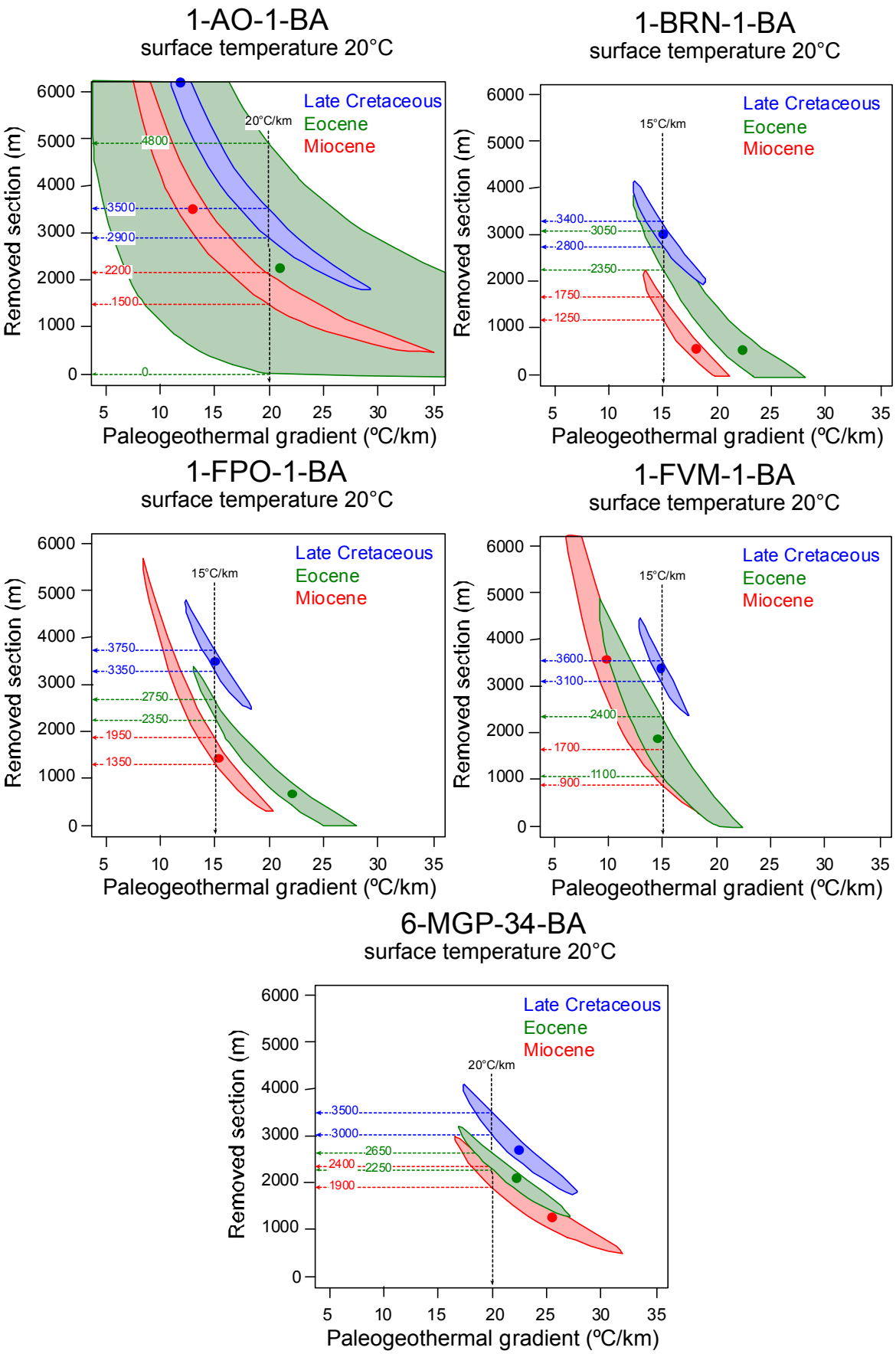

Figure 13.22: Comparison of constraints on 3 episodes in 5 wells. See text for discussion.

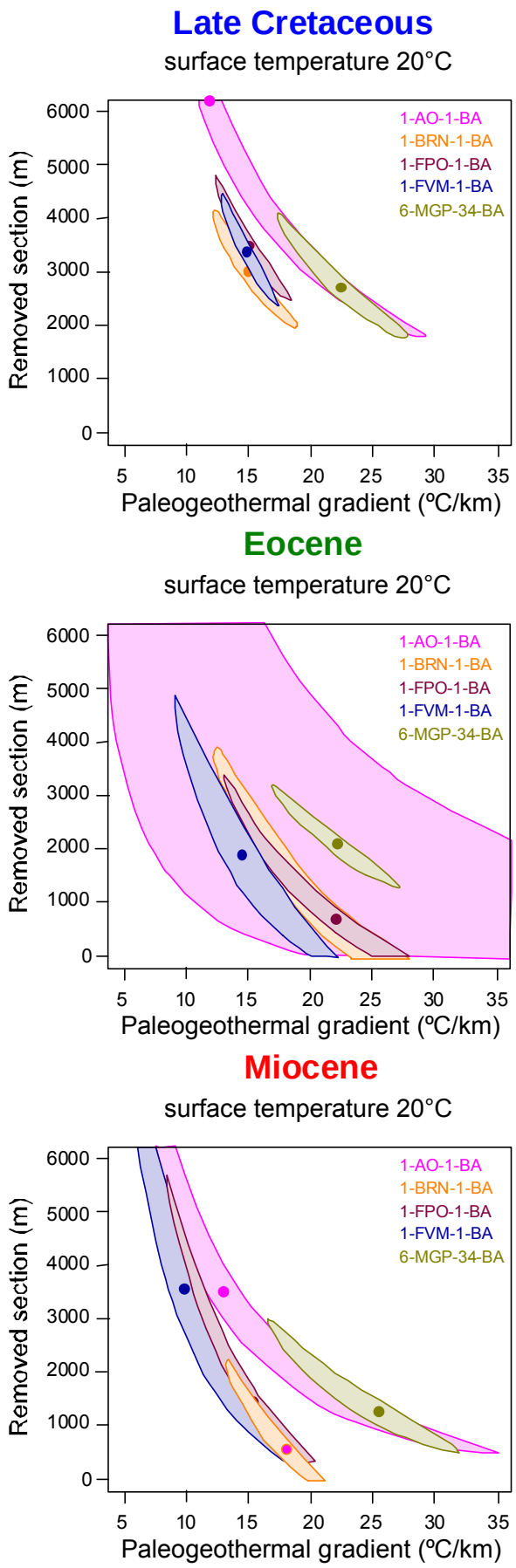

Figure 13.23: Comparison of constraints on 3 episodes in 5 wells. See text for discussion.

References

Bray, R.J., Green, P.F. and Duddy, I.R., (1992). Thermal History Reconstruction using apatite fission track analysis and vitrinite reflectance: a case study from the UK East Midlands and the Southern North Sea. In: Hardman, R.F.P. (ed.), Exploration Britain: Into the next decade. *Geological Society Special Publication*, **67**, 3-25.

Burnham, A.K. and Sweeney, J.J., (1989). A chemical kinetic model of vitrinite reflectance maturation. *Geochimica et Cosmochimica Acta.*, **53**, 2649-2657.

Gradstein, F.M., Ogg, J.G. and Smith, A.G. (2004). *A geologic time scale 2004*, Cambridge University Press.

Green P.F. (1986). On the thermo-tectonic evolution of Northern England: evidence from fission track analysis. *Geological Magazine*, **123**, 493 - 506.

Harman, R., Gallagher, K., Brown, R., Raza, A. & Bizzi, L., (1998). Accelerated denudation and tectonic/geomorphic reactivation of the cratons of northeastern Brazil during the Late Cretaceous. *Journal of Geophysical Research*, **103** No. B11, 27,091-27,105.

Japsen, P.J., Bonow, J., Green, P.F. and Cobbold, P.R. (2009). Burial and exhumation history of NE Brazil focussing on the Camamu Basin: a multidisciplinary study based on thermal, sonic and stratigraphic data and landform analysis. Final report, GEUS Report 2009/10.

Magnavita, L.P., Davison, I. and Kusznir, N.J. (1994). Rifting, erosion and uplift history of the Recôncavo-Tucano-Jatobá rift, northeast Brazil. tectonics, 13, 367-388.

Meister, E.M. 1973. Gradientes geotérmicos nas bacias sedimentares brasileiras. *Boletim Técnico da Petrobras* **16**, 221-232

Sant' Anna, L.G., Riccomini, C., Rodrigues-Francisco, B.H., Sial, A.N., Carvalho, M.D. and Moura, C.A.V. (2004), The Paleocene travertine system of the Itaborai basin Southeastern Brazil. *Journal of South American Earth Sciences*, **18**, 11-25.

Sweeney, J.J. and Burnham, A.K. (1990). Evaluation of a simple model of vitrinite reflectance based on chemical kinetics. *AAPG Bulletin*, **74**, 1559-1570.

Turner, J.P., Green, P.F., Holford, S.P. and Lawrence, S.R., (2008), Thermal history of the Rio-Muni (West Africa) – NE Brazil margins during continental breakup: *Earth and Planetary Science Letters*, **270**, 354–367.

Zalan, P.V. and De Oliviera, J.A.B. (2005). Origem e evolução estrutural do Sistema de Riftes Cenozóicos du Sudeste do Brasil. *Boletim de Geociências da Petrobras, Rio de Janeiro*, **v.13**, no 2, p. 269-300, maio/nov. 2005

AFTA data for 2 basement samples near the outcrop of the Fonseca Formation

RD93-3 Apatite BRFT09-4
Counted by: COB

Slide ref	Current grain no	N_s	N_i	N_a	ρ_s	ρ_i	RATIO	U (ppm)	Cl (wt%)	F.T. AGE (Ma)
G1167-1	4	27	40	18	2.384E+06	3.531E+06	0.675	27.6	0.11	184.9 ± 46.3
G1167-1	7	33	38	12	4.370E+06	5.032E+06	0.868	39.3	0.03	236.9 ± 56.7
G1167-1	8	19	44	50	6.038E+05	1.398E+06	0.432	10.9	0.03	118.9 ± 32.8
G1167-1	9	8	21	100	1.271E+05	3.337E+05	0.381	2.6	0.07	105.0 ± 43.7
G1167-1	10	9	47	24	5.959E+05	3.112E+06	0.191	24.3	0.03	53.0 ± 19.3
G1167-1	11	10	21	36	4.414E+05	9.270E+05	0.476	7.2	0.02	131.0 ± 50.4
G1167-1	12	18	29	24	1.192E+06	1.920E+06	0.621	15.0	0.04	170.2 ± 51.3
		124	240		7.464E+05	1.445E+06		11.3		

Area of basic unit = 6.293E-07 cm-²
χ^2 = 15.492 with 6 degrees of freedom
P χ^2) = 1.7%
Age Dispersion = 32.880%

Ns / Ni = 0.517 ± 0.057
Mean Ratio = 0.521 ± 0.083

Ages calculated using a zeta of 380.4 ± 5.7 for CN5 glass
ρ = 1.461E+06cm-² ND = 2181
ρ_D interpolated between top of can; ρ = 1.461E+06cm-² ND = 1149
bottom of can; ρ = 1.312E+06cm-² ND = 1032

POOLED AGE = 142.0 ± 16.1 Ma
CENTRAL AGE = 138.3 ± 23.5 Ma

A:

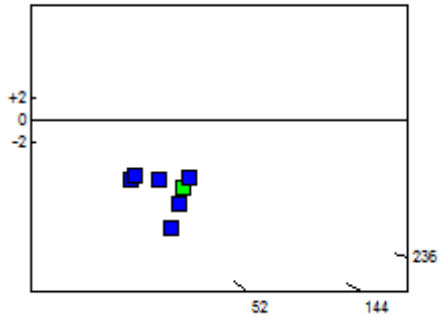

B:

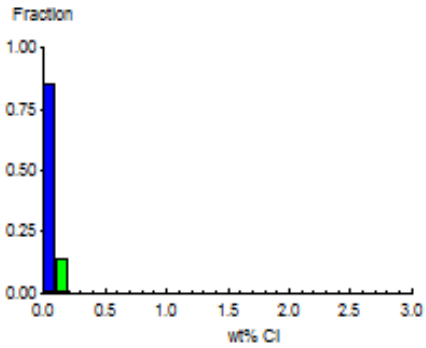

C:

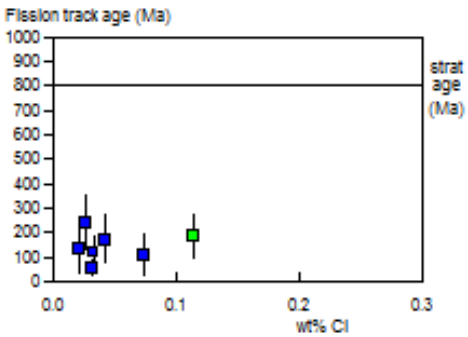

D:

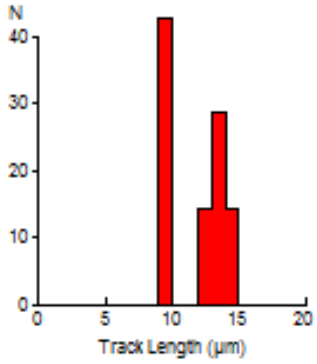

Mean track length 11.89 ± 0.90 µm Std. Dev. 2.38 µm 7 tracks

RD93-5 Apatite BRFT09-7
Counted by: MEM

Slide ref	Current grain no	N_s	N_i	N_a	ρ_s	ρ_i	RATIO	U (ppm)	Cl (wt%)	F.T. AGE (Ma)
G1171-1	3	10	23	25	6.356E+05	1.462E+06	0.435	12.0	0.01	117.3 ± 44.5
G1171-1	5	7	50	30	3.708E+05	2.648E+06	0.140	21.8	0.00	38.0 ± 15.4
G1171-1	6	8	10	35	3.632E+05	4.540E+05	0.800	3.7	0.01	214.2 ± 101.8
G1171-1	7	18	27	35	8.172E+05	1.226E+06	0.667	10.1	0.02	179.0 ± 54.7
G1171-1	8	13	29	60	3.443E+05	7.680E+05	0.448	6.3	0.02	120.9 ± 40.5
G1171-1	10	3	9	40	1.192E+05	3.575E+05	0.333	2.9	0.02	90.1 ± 60.1
G1171-1	11	1	2	18	8.828E+04	1.766E+05	0.500	1.5	0.00	134.7 ± 165.0
G1171-1	13	5	5	40	1.986E+05	1.986E+05	1.000	1.6	0.01	266.6 ± 168.8
G1171-1	14	13	20	48	4.304E+05	6.621E+05	0.650	5.4	0.02	174.6 ± 62.4
G1171-1	15	6	9	100	9.534E+04	1.430E+05	0.667	1.2	0.01	179.0 ± 94.5
G1171-1	16	23	75	45	8.122E+05	2.648E+06	0.307	21.8	0.00	82.9 ± 19.9
G1171-1	17	3	3	36	1.324E+05	1.324E+05	1.000	1.1	0.01	266.6 ± 217.8
G1171-1	18	0	5	45	0.000E+00	1.766E+05	0.000	1.5	0.00	0.0 ± 109.8
G1171-1	19	4	14	20	3.178E+05	1.112E+06	0.286	9.2	0.01	77.3 ± 43.9
G1171-1	20	14	23	28	7.945E+05	1.305E+06	0.609	10.7	0.02	163.6 ± 55.7
G1171-1	24	6	18	48	1.986E+05	5.959E+05	0.333	4.9	0.01	90.1 ± 42.6
G1171-1	26	8	14	24	5.297E+05	9.270E+05	0.571	7.6	0.02	153.7 ± 68.3
G1171-1	28	2	6	70	4.540E+04	1.362E+05	0.333	1.1	0.03	90.1 ± 73.6
G1171-1	29	18	29	60	4.767E+05	7.680E+05	0.621	6.3	0.01	166.8 ± 50.3
G1171-1	35	18	26	70	4.086E+05	5.902E+05	0.692	4.9	0.01	185.8 ± 57.2
		180	397		3.261E+05	7.193E+05		5.9		

Area of basic unit = 6.293E-07 cm-²
χ^2 = 27.357 with 19 degrees of freedom
P χ^2) = 9.7%
Age Dispersion = 27.386%

Ns / Ni = 0.453 ± 0.041
Mean Ratio = 0.520 ± 0.058

Ages calculated using a zeta of 392.9 ± 7.4 for CN5 glass
ρ = 1.386E+06cm-² ND = 2183
ρ_D interpolated between top of can; ρ = 1.386E+06cm-² ND = 1090
bottom of can; ρ = 1.389E+06cm-² ND = 1093

POOLED AGE = 122.3 ± 11.5 Ma
CENTRAL AGE = 126.9 ± 14.9 Ma

A:

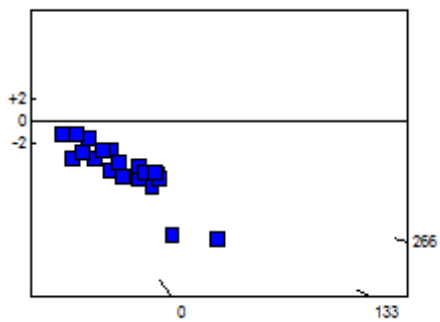

B:

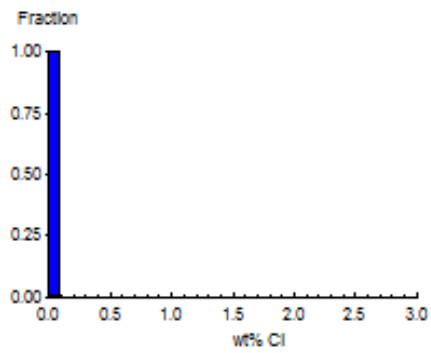

C:

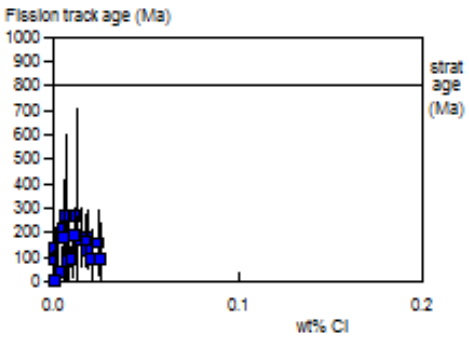

D:

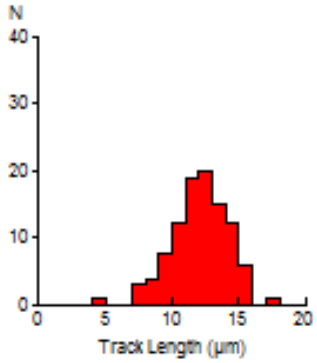

Mean track length 12.08 ± 0.21 µm Std. Dev. 2.15 µm 106 tracks

Default History predictions, RD93-5

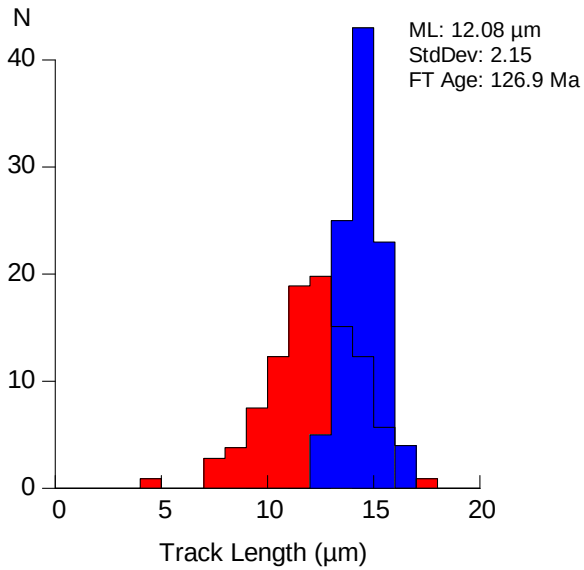

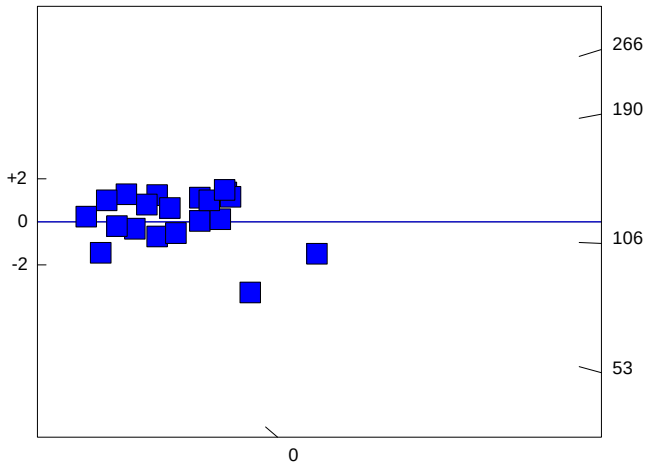

RD93-5: pooled age 126.9±14.5 Ma
$P(\chi^2) = 9.7\%$

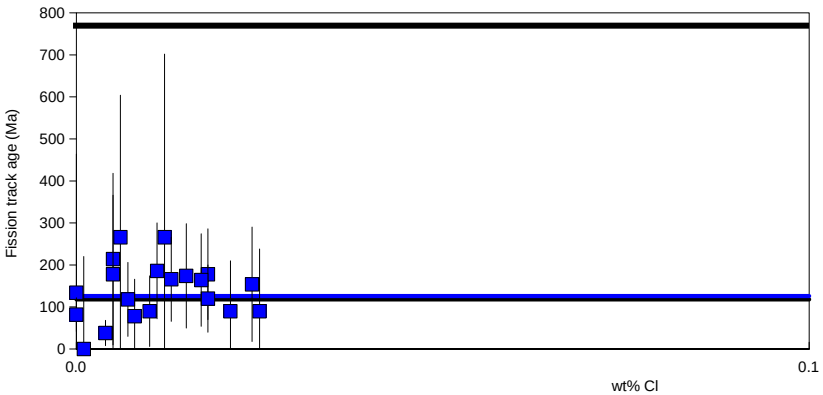

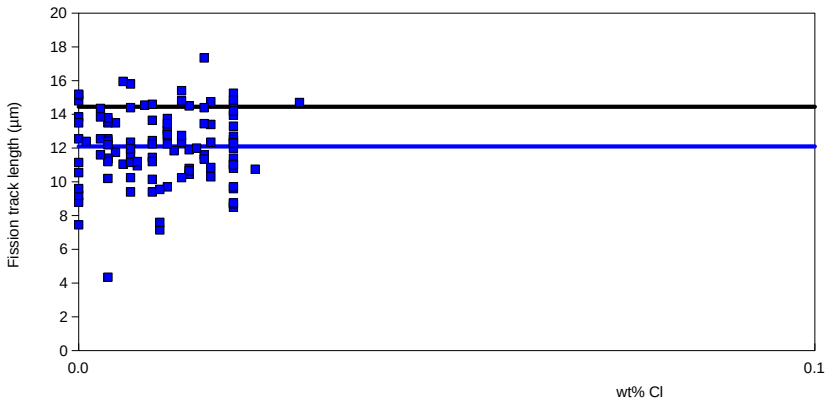

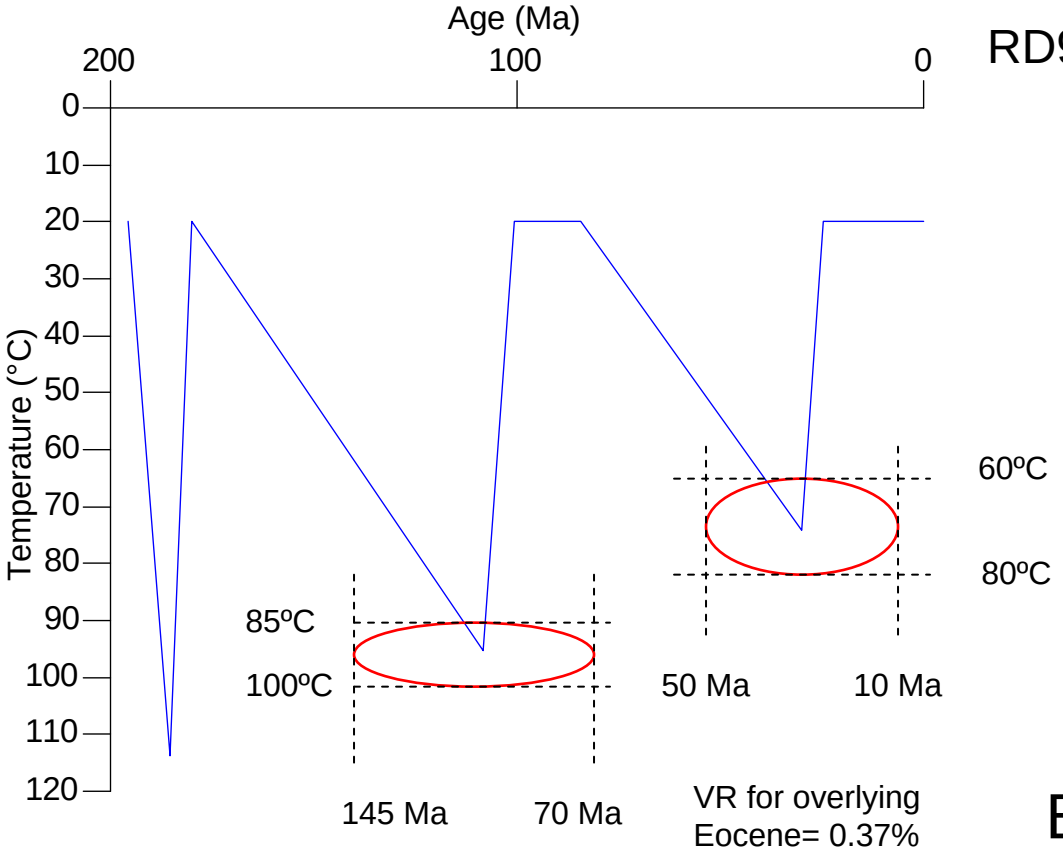

RD93-5

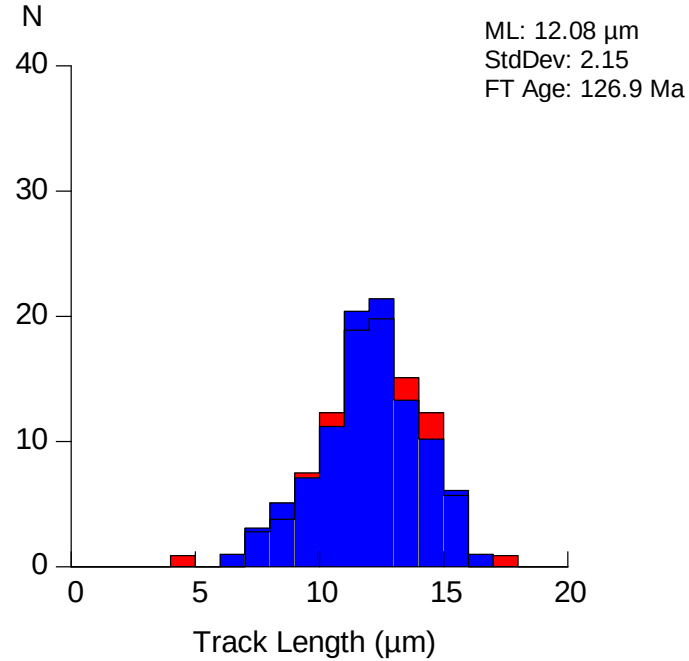

Best-fit history predictions

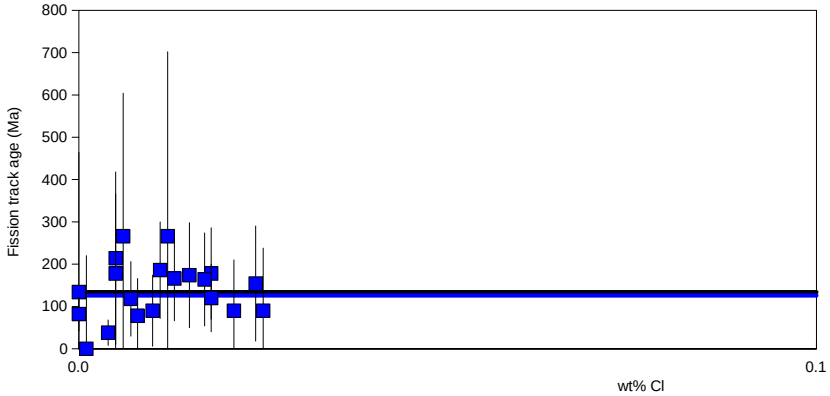

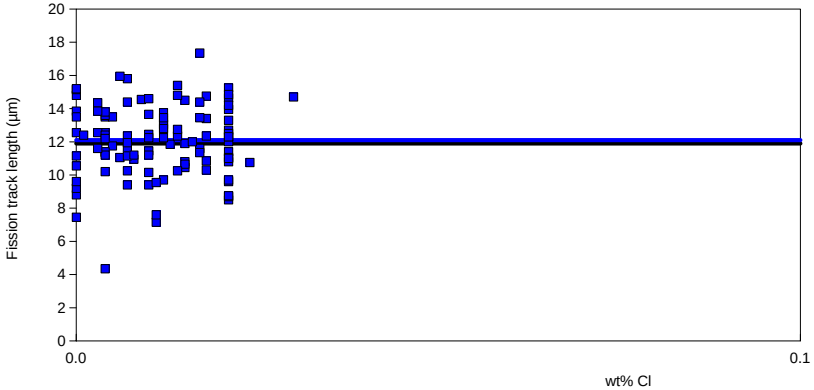

DANMARKS OG GRØNLANDS GEOLOGISKE UNDERSØGELSE RAPPORT 2009/8

Burial anomalies and magnitude of exhumation estimated from sonic data for 19 wells, onshore and offshore NE Brazil; Almada, Camamu, Recôncavo, Sanfranciscana and Tucano Basins

Peter Japsen

GEOLOGICAL SURVEY OF DENMARK AND GREENLAND
MINISTRY OF CLIMATE AND ENERGY

2. Introduction

This report is a contribution to the research project ‘Burial and exhumation history of NE Brazil focussing on the Camamu Basin: A multidisciplinary study based on thermal, sonic and stratigraphic data and landform analysis’. The project is carried out by GEUS in close cooperation with Geotrack International for StatoilHydro do Brasil Ltda and Petrobras as a multi-disciplinary research project aimed at understanding the regional burial and exhumation history of NE Brazil and the Camamu Basin. The project started in 2007 and will be finished in 2009.

The burial and exhumation history of the study area are also analyzed in reports (that are part of thus study) of apatite fission-track analysis (AFTA) data in samples from offshore wells (Geotrack report 1013) and in samples from onshore wells and outcrops (Geotrack report 990). These reports form part of the present project. These AFTA studies have identified three episodes of post-rift cooling:

- Late Cretaceous (Campanian) cooling starting in the interval between c. 80 and 75 Ma,
- Eocene cooling starting in the interval between c. 48 and 45 Ma
- Miocene cooling starting in the interval between c. 18 and 15 Ma

Whereas the Campanian and the Miocene event affected the entire onshore study area in eastern Bahia and inshore Camamu well BAS-113, the Eocene event has only been detected in deep wells in the Recôncavo-Tucano Basins.

3. Data

The study is based on log data for 19 boreholes, 5 onshore and 14 offshore (Table A-1 in Appendix A). Three wells are from the southern part of the Tucano Basin (BRN-1, FPO-1, FVM-1), 1 from Recôncavo (6-MGP-34) and one from the margin of the Sanfranciscana Basin in the western part of the state of Bahia (FLU-1). Eight offshore wells are from the Camamu Basin (BAS-21, -64, -74, -84, 97, -107, 113, -129) and 6 from the Almada Basin (BAS-71, -77, -79, -88, -102, -118). All wells drill into the Lower Cretaceous rift sequence, apart from the FLU-1 well that was drilled into Proterozoic sediments. The thickness of the drilled sequences onshore range between 1.0 km (FLU-1) and 5.6 km (FVM-1), and offshore this range is between 2.3 km (BAS-107) and 3.9 km (BAS-84).

Stratigraphic charts for the Almada, Camamu and Recôncavo Basins are shown in figures A-1 to A-3 (*Gontijo et al. 2007; Caixeta et al. 2007; Silva et al. 2007*). Composites logs and interpretations of the lithology (digital LithoLogs) were supplied for most of the wells as listed in Table A-1. A lithostratigraphic subdivision of the wells was supplied by the costumer and is listed in Table A-2. Well log data were supplied in LAS format, in most cases containing tracks with caliper, sonic transit time, density, gamma and in some cases neutron porosity (log plots in Appendix B).

3.1 Deletion of bad-hole data

Figure 3-1 shows an example of how caving may cause recording of atypical low sonic velocities; in the left panel, data points for which the caliper exceeds 13'' are marked by red dots and in the right panel, it seen that the corresponding Vp-values plot below the general trend. Consequently, log data from borehole intervals with caving have been deleted in the most extreme cases (see plots in Appendix B).

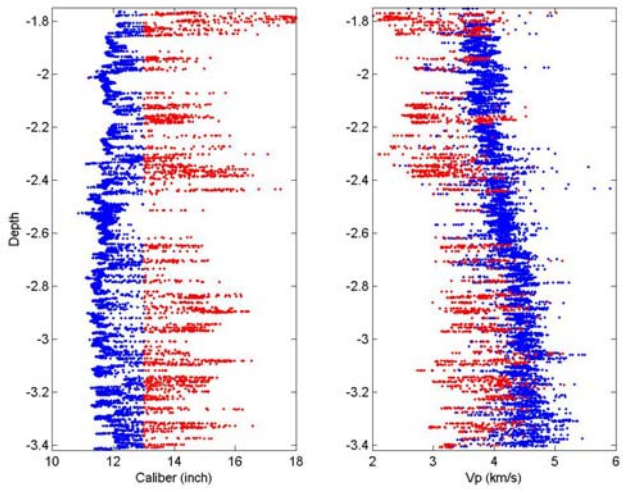

Figure 3-1. *Plots of caliper (left) and Vp (right) versus depth for well FPO-1. The size of the regular hole in this depth interval is about 12 inches, but locally the hole is more than 16'' wide. Data points for which the caliper exceeds 13'' are marked by red dots and it is seen that these bad-holed data have Vp-values below the general trend.*

3.2 Displays of sonic data

The log data for each well are displayed on double pages in Appendix B:

- Composite plots of the caliper, raw sonic, density, neutron porosity (where available) and gamma logs (upper left plots).
- Plots of caliper and sonic logs for detection of bad-hole data and a plot of the edited sonic data (lower left plots).
- Plots of the bad-hole corrected sonic log colour-coded according to the lithology as interpreted from the LithoLog (upper right plot).
- Plots with interpretation of burial anomaly based on a comparison of the edited sonic (averaged over 10-m intervals) log and the baselines for pure sandstone (BR00, BR05), pure shale (Vsh) and organic-rich shale (Vsh-o). In these plots the sonic log is colour-coded according to the main lithostratigraphic units. The full range of the sonic velocities is thus not shown in these plots and thus both data scatter and sonic variations related to lithology are suppressed (lower right plot).

The interpreted datapoints for high-velocity sandstone and low-velocity shale units in each well are displayed on both the upper and lower right plots

Details of the sonic logs as plotted in the composite logs (not included in this report) show that the quality of the sonic logs may not always allow for reliable estimates of the mean velocity of a unit; e.g. in well FVM-1 where the likely velocity around 5 km/s of a sand (?) unit at c. 4.4 km is only reached in a few data points due to considerable scatter (cf. the sonic log for the near-by FPO-1 well).

4. Velocity anomalies and burial anomalies

4.1 Estimation of maximum palaeoburial using sonic data

The technique for estimating maximum palaeoburial of a sedimentary unit – and thus the amount of erosion of its overburden – from sonic data has been known for decades (e.g. Marie 1975; Magara 1976; Scherbaum 1982; Chapman 1983; Bulat & Stoker 1986; Japsen 1993, 1998, 2000; Hillis 1995; Heasler & Kharitonova 1996; Al-Chalabi & Rosenkranz 2002). There is, however, no generally accepted methodology of how such estimates are best derived; see Corcoran & Doré (2005) for a review. The technique is based on the general observation that the sonic velocity of most sedimentary rocks increases as the porosity of the sediment is reduced through deeper burial. Porosity is reduced due to increased effective stress that causes mechanical compaction and pressure solution. Sonic velocity is increased due to porosity-reduction and stiffer grain contacts, and as these processes are considered largely irreversible, measured velocity will depend on the maximum effective stress experienced by the sedimentary rock – and hence on its maximum burial if the burial depth has been reduced by erosion. The timing of the erosion of the overburden is represented by any of the unconformities in the overburden.

A normal velocity-depth trend is thus a function that describes how sonic velocity increases with depth in a relatively homogenous, brine-saturated sedimentary formation when porosity is reduced during normal compaction (mechanical or chemical). Compaction is 'normal' when the fluid pressure of the formation is hydrostatic, and the formation is at maximum burial depth. Simple boundary conditions for such trends are that the velocity at the surface equals the velocity of the sediment when it was first deposited (Nur *et al.* 1998), and that velocity approaches the matrix velocity of the rock while the velocity-depth gradient approaches zero with increasing depth (see Japsen *et al.* 2007).

The derivation of a normal velocity-depth trend involves three steps of generalisation: 1) Identification of a relatively, laterally homogenous lithological unit, 2) selection of data points that represent normal compaction and 3) assignment of a function that expresses the velocity-depth trend (see Japsen *et al.* 2007). Few attempts have been made to constrain normal velocity-depth trends for different lithologies rather than just considering velocity-depth trends as fits of arbitrary functions to local data sets. The increase of velocity with depth for a uniform sedimentary formation (and thus the shape of the baseline) has been shown to depend on the mineralogical composition of the formation (Japsen *et al*. 2007).

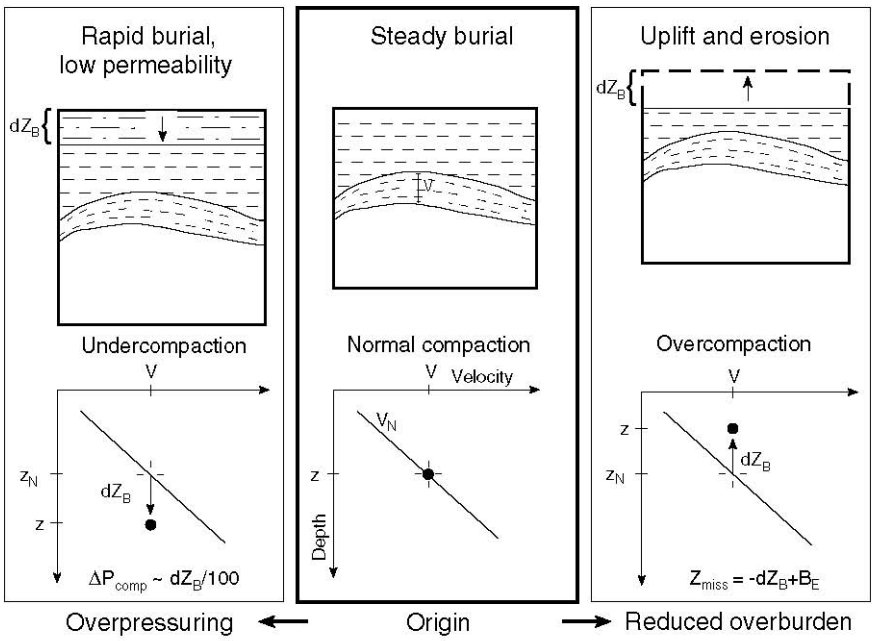

Figure 4-1. *Burial anomaly, dZ_B [m], relative to a normal velocity-depth trend, V_N, for a sedimentary formation (Eq. 4-1). In the North Sea Basin, burial anomalies of ±1 km for pre-Miocene formations result from late Cenozoic exhumation along basin margins and overpressuring due to rapid, late Cenozoic burial in the basin centre. Rapid burial and low permeability cause undercompaction and overpressure, ΔP_{comp} [MPa], and velocities low relative to depth (positive dZ_B) (cf. Eq. 4-3). Exhumation due to uplift reduce the overburden thickness, and causes overcompaction expressed as velocities high relative to depth (negative dZ_B); however, post-exhumational burial, B_E, will mask the magnitude of the missing section, Δz_{miss} (Eq. 4-2). The normalized depth, z_N, is the depth corresponding to normal compaction for the measured velocity (cf. Terzaghi's principle). Modified after Japsen (1998).*

Normal velocity-depth trends for chalk (V_N^{ch}), marine shale dominated by smectite/illite (V_N^{sh}) and quartz-dominated Triassic deposits (V_N^{B}) were defined by Japsen (1998, 1999, 2000) in such a way that the velocity at the surface agreed with those of recently deposited sediments, and that velocity did not approach infinity at depth. Velocity-depth anomalies relative to these trends were found to be in agreement with estimates of erosion along the margins of the North Sea Basin as well as with measurements of overpressure in the centre of this basin. Furthermore, these baselines are in agreement with those of previous workers even though such analytical expressions have often not fulfilled simple boundary conditions (e.g. Marie 1975; Scherbaum 1982; Bulat & Stoker 1987; Hillis 1995; Hansen 1996). Baselines for sandstone was established by Japsen *et al*. (2007) by eliminating porosity from an exponential porosity-depth relation by assuming a modified Voigt relation between sonic velocity and porosity for sandstone with different clay content.

The burial anomaly, dZ_B, is the difference between the present-day burial depth of a rock, z, and the depth, $z_N(V)$, corresponding to normal compaction for the measured velocity, V (Japsen 1998):

$$dZ_B = z - z_N(V) \tag{4-1}$$

The burial anomaly is zero for normally compacted sediments, whereas high velocities relative to depth give negative burial anomalies which may be caused by a reduction in overburden thickness when lithology is relatively homogenous over the study area, and if lateral variations of horizontal stress are minor. A positive burial anomaly may indicate undercompaction due to overpressure. To assess whether the burial anomaly for a stratigraphic unit is a measure of exhumation requires an integrated evaluation: The burial anomalies should thus agree with other estimates of erosion and should correspond geographically to where there is a missing section in the stratigraphic record. Any post-exhumational burial, B_E, will mask the magnitude of the missing (removed) overburden section, Δz_{miss}:

$$\Delta z_{miss} = -dZ_B + B_E \tag{4-2}$$

where the minus indicates that erosion reduces depth (Hillis 1995; Japsen 1998). The timing of the exhumation events is thus important for understanding the succession of events, their true magnitude and for identifying the age of the eroded succession.

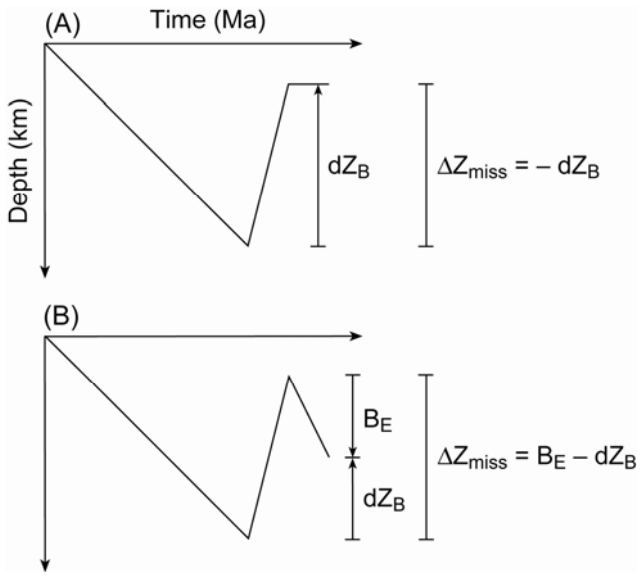

Figure 4-2. *Burial diagrams illustrating that the magnitude of the missing (or removed) section (Δz_{miss}) will be less than the magnitude of the measured burial anomaly (dZ_B) in the case of post-exhumational burial (B_E) (Eq. 4-2). (A) Exhumation followed by no deposition; (B) exhumation followed by burial.*

4.2 Overpressure-prediction from sonic data

Overpressure in the central North Sea was successfully predicted from velocity-depth anomalies for the Cenozoic succession relative to a normal velocity-depth trend for shale close to that given by Eq. (5-1) (Japsen 1999; Fig. 4-1). The overpressure results from a

balance between the load of the upper Cenozoic deposits, and the draining determined by the thickness and sealing quality of the lower Cenozoic sediments. The overpressure of an undercompacted rock, ΔP_{comp}, is proportional to the burial anomaly, dZ_B, if the effective stress is increasing with time (cf. Magara 1978; Japsen 1998). We get $\Delta P_{comp} = \Delta\rho_{up} \cdot g \cdot dZ_B$ where $\Delta\rho_{up}$ is the density contrast (wet bulk density minus pore fluid density) of the upper Cenozoic and g is the gravitational acceleration (9.807 m/s2). The equation is based on Terzaghi's principle and states that if a rock is buried at a greater depth by dZ_B without change in the effective stress (indicated by unchanged velocity), the effective stress of the added load is carried by an increase in pore pressure. If we substitute $\Delta\rho_{up} \approx 1.02 * 10^3$ kg/m^3, and dZ_B is in meters, we find that the overpressure of an undercompacted rock, ΔP_{comp} [MPa], is proportional to the burial anomaly, dZ_B [m] (Fig. 4-1):

$$\Delta P_{comp} \approx dZ_B/100 \text{ [MPa]}, \tag{4-3}$$

'which means that a burial anomaly of 1000 m may reflect overpressure due to undercompaction of 10 MPa (Japsen 1998). From the above expression we can define the effective depth, Z_{eff}, for a unit at measured depth, Z, as the depth where the same effective stress would occur during normal compaction. In the case of overpressure (ΔP) we get

$$Z_{eff} = Z - \Delta P \cdot 100 \tag{4-4}$$

where ΔP is measured in MPa and depths are in metres (cf. Japsen 1998).

In Figure 4-3 we compare the degree of undercompaction of the lower Cenozoic succession in the North Sea expressed by its burial anomaly, dZ_B^{low}, with pressure data from the underlying Chalk, ΔP_{Ch}, because pressure measurements from the lower Cenozoic shales are rare in the central North Sea. We observe that ΔP_{Ch} is proportional to dZ_B^{low}, and in the order of the overpressure predicted by Eq. (4-3). This indicates that the burial anomaly for the lower Cenozoic succession relative to the shale trend given by Eq. (5-1) is a measure of overpressure due to undercompaction. Investigation of interval velocities from almost a thousand wells revealed basin-wide differences in the physical properties of the Cenozoic deposits related to disequilibrium compaction below the mid-Miocene unconformity in the central North Sea (cf. Osborne and Swarbrick 1997).

Japsen (1998) demonstrated that positive burial anomalies for the chalk in the central North Sea were proportional to measured values of overpressure in the chalk and that the overpressure was in the order of magnitude given by Eq. (4-3).

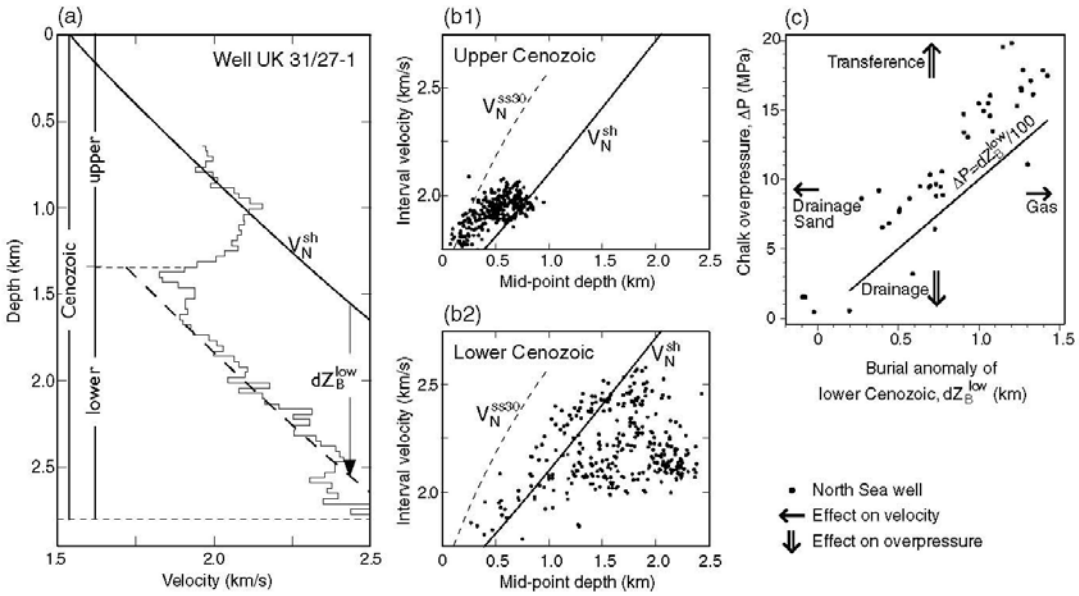

Figure 4-3. *Prediction of overpressure in the North Sea from interval velocities of the Cenozoic deposits (excluding the Danian) (cf. Figure 4-1).*
(a) Sonic log where low velocities reveal undercompaction of the lower Cenozoic sediments corresponding to measured overpressure in the underlying chalk.
(b1) and (b2) Interval velocity versus depth to the midpoint of the upper and lower Cenozoic deposits, respectively, for 322 North Sea wells.
(c) Burial anomalies for the lower Cenozoic sediments (dZ_B^{low}) versus Chalk formation overpressure (ΔP) in North Sea wells.
The upper Cenozoic deposits are close to normal compaction whereas velocity-depth anomalies for the lower Cenozoic sediments outline a zone of undercompaction in the central North Sea. The deviations from the trend line in figure (c) is due to the non-compactional sources that add to the Chalk overpressure from below (transference; cf. Osborne and Swarbrick 1997), the easier drainage from the more shallow Cenozoic section and sandy lithology; $\Delta P=dZ_B/100$ (see equation 4-3). The burial anomalies are calculated relative to the shale trend given by equation (5-1). Depths below top of sediments. V_N^{ss30}: modified Voigt model for sandstone, 30% clay content. V_N^{sh}: marine shale (Eq. 5-1). Modified after Japsen et al. (2007).

5. Normal velocity-depth trends for different lithologies

5.1 A baseline for smectite/illite-dominated shale

Japsen (2000) formulated a constrained baseline, V_N^{LJur}, for marine shale dominated by smectite/illite based on velocity-depth data for the Lower Jurassic F-1 Member of the Fjerritslev Formation from 31 Danish wells of which 28 have sonic data for the Chalk:

$$tt = 460 \cdot e^{-z/2175} + 185 \tag{5-1}$$

where transit time, *tt*, is the inverse of velocity. The baseline was reconstructed by correcting present formation depths for the effect of late Cenozoic erosion as estimated from the velocity of the overlying Chalk in these wells relative to the Chalk baseline of Japsen (2000). The corrected depths correspond to the burial of the formation prior to erosion when the sediments were at maximum burial at more locations than today. The baseline can thus be traced more easily in a plot of velocity versus the corrected depths, and is well defined at great depth where velocity-depth data for normally compacted shale at maximum burial can be difficult to identify (2.1<z<3.8 km). This formulation is a constrained, exponential transit time-depth model that fulfils reasonable boundary conditions at the surface (1550 m/s) and at infinite depth (5405 m/s); maximum velocity-depth gradient 0.6 1/s for z=2.0 km. The shale trend corresponds closely to baselines for marine shale found by other workers (Scherbaum 1982, Hansen 1996; see discussion in Japsen 1999 and in Japsen *et al*. 2007.

5.2 A baseline for the Lower Triassic Bunter 'Shale'

Japsen (2000) formulated a segmented, linear baseline, V_N^{BSh}, for the Lower Triassic Bunter Shale based on velocity-depth data from 142 British and Danish wells of which 91 have velocity-depth data for the Chalk:

$$\begin{aligned} V_N^{BSh} &= 1550 + z \cdot 0.6, & 0 < z < 1393\,\mathrm{m} \\ V_N^{BSh} &= -400 + z \cdot 2, & 1393 < z < 2000\,\mathrm{m} \\ V_N^{BSh} &= 2600 + z \cdot 0.5, & 2000 < z < 3500\,\mathrm{m} \\ V_N^{BSh} &= 3475 + z \cdot 0.25, & 3500 < z < 5300\,\mathrm{m} \end{aligned} \tag{5-2}$$

The trend indicates a pronounced variation of the velocity gradient with depth. The gradient is only 0.5 1/sin the upper part, and increases to 1.5 1/s for depths around 2 km, from where it decreases gradually with depth to 0.5 and then 0.25 1/s. The decline of the gradient with depth reflects that velocity approaches an upper limit.

The Bunter Shale baseline was reconstructed by applying the same procedure as for the Lower Jurassic shale by correcting present formation depths for the effect of late Cenozoic erosion as estimated from Chalk velocities. The trend was constructed to predict likely values near the surface (1550 m/s), and is based on reference data with corrected depths from 1600 to 5600 m (Japsen 2000). Rather than proposing a specific baseline for the Lower Triassic Bunter Sandstone, Japsen (2000) found that the trend derived for the Bunter Shale was a reasonable approximation for a data set from 133 British and Danish wells of which 87 have velocity-depth data for the Chalk. Burial anomalies for the Bunter Sandstone can thus be used to place an upper limit on estimates of erosion based on Bunter Shale data.

The dominance of smectite/illite in the distal parts of the Fjerritslev Formation, and of kaolin in the continental Bunter Shale was suggested by Japsen (2000) to be a possible explanation why baselines for these formations diverge, and why those for Bunter Shale and Bunter Sandstone converge at depth. Alternatively, the similarity of the baselines for the Bunter Shale and the Bunter Sandstone may be due to the dominance of quartz in both formations.

5.3 A revised baseline for sandstone

Japsen *et al*. (2007) found *V-z* trends for sandstone by eliminating porosity from an exponential porosity-depth relation by assuming a so-called modified Voigt relation between sonic velocity and porosity for sandstone with different clay content. The model was based on the properties of sandstone at an assumed maximum depth for practical purposes of 4 km. The resulting modified Voigt velocity-depth model for sandstone has a *V-z* gradient that decreases monotonously from values greater than 1 s^{-1} for z<0.4 km and 30% clay content; the resulting SS00 and SS05 trends thus corresponds to sandstone with a clay content of 0% and 5%. Reduction of the clay content leads to higher velocity and velocity gradient.

If we compare the modified Voigt model with the normal trend for the Bunter Shale and Sandstone, we find that the Bunter trend plot between the sandstone models for 0% and 5% clay content for depths below *c*. 2 km. The match between the modified Voigt model and the Bunter Sandstone trend supports the application of the modified Voigt model for sandstone as well as the estimation of the amount of exhumation by means of chalk velocities (because burial anomalies based on chalk velocities were used to derive the Bunter baseline). The match between the modified Voigt model and the data points for the Bunter Shale suggests that the lithology of the Bunter Shale is dominated by quartz in the wide area covered by the data set (southern and eastern North Sea Basin). Consequently, the term ‘Shale’ seems to be an indication of grain size rather than of mineralogy.

The modified Voigt model can be approximated by a modified velocity-average equation:

$$V = V_m - (V_m - V_c)e^{-z/b} \qquad (5\text{-}3)$$

where V_m is the matrix velocity of the sediment, V_c is the sonic velocity of the sediment at critical porosity (the porosity limit above which a particular sediment exists only as a suspension) and b is a decay parameter (Nur *et al*. 1998). Japsen *et al*. (2007) estimated the parameters in equation (5-3) for sandstone with varying clay content as an approximation to the modified Voigt trend for z<4 km taking V_c=1600 m/s. For 0% and 5% clay content the parameters to the modified velocity-average equation (Eq. 5-3) were found to be:

$$\begin{aligned} &\text{SS00, 0\% clay: } V_m = 5065 \text{ m/s, } b_3 = 1923 \text{ m.} \\ &\text{SS05, 5\% clay: } V_m = 4796 \text{ m/s, } b_3 = 1963 \text{ m.} \end{aligned} \tag{5-4}$$

The baselines for pure sandstone of Japsen *et al*. (2007) predict velocities around 4.5 km/s at the assumed maximum depth of 4 km (0%-%5 clay). However, the sonic data for many wells in this study show sandstone velocities that reach 5 km/s; e.g. BAS-21, -113 and FPO-1 (see Fig. 5-1 and Appendix B). Sonic velocities well above 5 km/s are characteristic of conglomerates; e.g. in well BRN-1 below 3 km.

Consequently, the pure sandstone baselines have been calibrated to match the data presented in this report, in particular well BAS-21 and -88 (Fig. 5-1).

- The sonic log for well BAS-88 displays data for a c. 1 km thick sandstone unit with a velocity-depth trend increasing from c. 3.5 to 4.25 km/s (Rio de Contas Fm). The higher velocities over this unit plot within the range given by the SS00 and SS05 trends, and the drilled sequence is thus interpreted to be at maximum burial at present.
- The sonic log for well BAS-21 displays data for a c. 2 km thick sandstone unit with a velocity-depth trend increasing from c. 4 to almost 5 km/s (Morro do Barro Fm). These velocities are much higher than predicted for the SS00 and SS05 trends for this depth interval, and the section is thus interpreted to have been deeper buried in the past. Furthermore, the data show a gradual increase of velocity with depth over the entire interval, whereas the SS00 and SS05 trends predict almost no increase in velocity. The velocity-depth gradient over this sandstone unit is about 0.5 1/s and this corresponds closely to the gradient predicted by the Bunter Shale trend for velocities around 4.5 km/s whereas the gradients of the SS00 and SS05 trends are much smaller.

To account for these observations, slightly modified baselines for pure sandstone, BR00 and BR05, are formulated by with the following parameters to the modified velocity-average equation (Eq. 5-3):

$$\begin{aligned} &\text{BR00, 0\% clay: } V_m = 5400 \text{ m/s, } b_3 = 2500 \text{ m.} \\ &\text{BR05, 5\% clay: } V_m = 5400 \text{ m/s, } b_3 = 2800 \text{ m.} \end{aligned} \tag{5-5}$$

These parameters represent only a slight modification of the parameters for SS00 and SS05 (Fig. 5-2). The modified trends plot at slightly greater depths for velocities less than c. 4.5 and 4 km/s, for BR00 and BR05, respectively, and at slightly more shallow depths for higher velocities (and thus predict smaller amounts of exhumation for high velocities). This change in curvature was made to account for the trends observed in the data and in particular to reach a velocity of 5 km/s at a more shallow depth than predicted by SS00 and

SS05 (e.g. at 8 km for SS00). The revised baselines predict velocities near 5 km/s at 6 km depth, and these values match the input data used for the original modified Voigt model. The use of 4 km as maximum depth (anchor point) in the calculations of Japsen *et al*. (2007) caused the velocity predictions for greater depths to be too small.

If we compare this model with the normal trend for the Bunter Shale and Sandstone, we find that the BR05 trend corresponds closely to the Bunter trend. Pure sandstone units are thus likely to plot in the interval defined by the BR00 and BR05 trends.

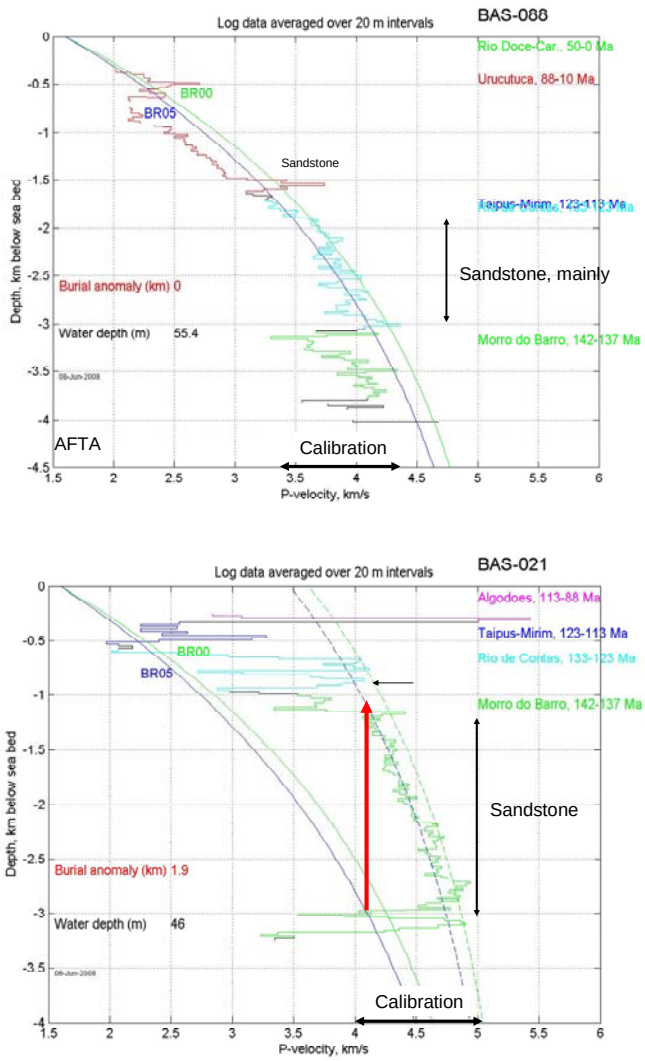

Figure 5-1. *Plots of sonic logs used for calibration of the sandstone baselines used in this study, BR00 and BR05 for 0% and 5% clay, respectively. Sandstone sonic data between c. 3.5 and 4.25 km/s in BAS-88 and between c. 4 and 5 km/s in BAS-21 are used for calibration. Whereas the drilled sequence in BAS-88 is found to be at maximum burial, the sequence drilled in BAS-21 is found to have been more 1.9 km deeply buried as indicated by the red arrow and the dashed baselines that are shifted upwards by that amount. Full plots and legend: See Appendix B.*

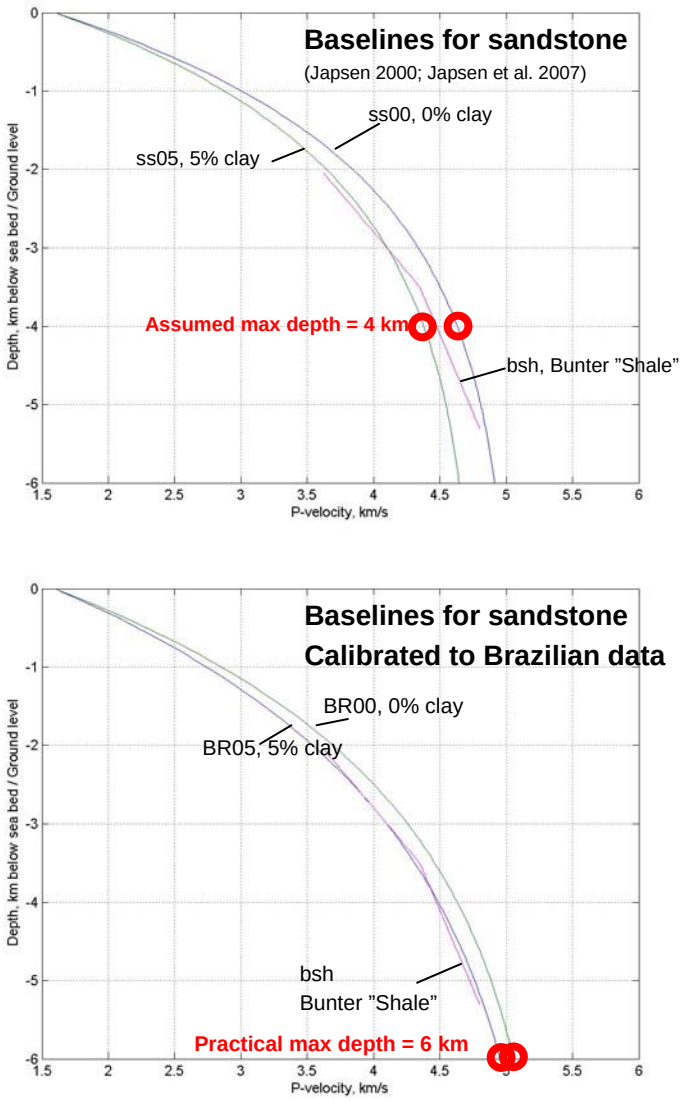

Figure 5-2. *Baselines for sandstone. Upper panel: Baseline models for 0% and 5% clay content based on a prediction of porosity and sonic velocity of consolidated sandstone with data at 4 km depth as anchor point (Eq. 5-4; Japsen et al. 2007). Lower panel: Baselines calibrated to data from wells BAS-21 and -88 (BR00 and BR05: Eq. 5-5). 'bsh': Baseline for the quartz-dominated Lower Triassic Bunter Shale, North Sea (Eq. 5-2).*

8. References

Al-Chalabi, M. & Rosenkranz, P.L. 2002. Velocity-depth and time-depth relationships for a decompacted uplifted unit. *Geophysical Prospecting* **50**, 661–664.

Bulat, J. & Stoker, S.J. 1987. Uplift determination from interval velocity studies, UK, southern North Sea. In: *Petroleum geology of north west Europe* (Ed. by J. Brooks and K.W. Glennie), pp. 293–305, Graham & Trotman.

Caixeta, J.M., Bueno, G.V., Magnavita, L.P. & Feijó, F.J. 1994. Bacias do Recôncavo, Tucano e Jatobá. Boletim Geociencias Petrobras 8, 163-172.

Caixeta, J.M., Milhomem, P.S., Witzke, R.E., Dupuy, I.S.S. & Gontijo, G.A. 2007. Bacia de Camamu. *Boletim Geociencias Petrobras* **15**, 455–461.

Chapman, R.E. 1983. *Petroleum geology*. Elsevier, Amsterdam.

Corcoran, D.V. & Doré, A.G. 2005. A review of techniques for the estimation of magnitude and timing of exhumation in offshore basins. *Earth-Science Reviews* **72**, 129–168.

Geotrack Report 990. Thermal History Reconstruction in the 1-AO-1-BA, 1-BRN-1-BA, 1-FLU-1-BA, 1-FPO-1-BA, 1-FVM-1-BA, 1-RSO-1-BA, 3-MB-3-BA and 6-MGP-34-BA wells, Tucano and Reconcavo Basins, Onshore Brazil, together with AFTA and associated thermal history interpretations in 89 outcrop samples from Bahia, NE Brazil, and 20 samples from the Serra do Mar. Green, P.F. 2009. Geotrack International, Victoria, Australia, in prep.

Geotrack Report 1013. Camamu Basin, offshore Brazil. Thermal history reconstruction in the 1-BAS-88-BA, 1-BAS-102-BA, 1-BAS-113-BA & 1-BAS-129-BA wells, based on AFTA and VR data. Green, P.F. 2008. Geotrack International, Victoria, Australia, 153 pp and appendices.

Gontijo, G.A., Milmomem, P.S., Caixeta, J.M., Dupuy, I.S.S. & Menezes, P.E.L. 2007. Bacia de Almada. *Boletim Geociencias Petrobras* **15**, 463–473.

Hansen, S. 1996. Quantification of net uplift and erosion on the Norwegian Shelf south of 66ºN from sonic transit times of shale. *Norsk Geologisk Tidsskrift* **76**, 245–252.

Heasler, H.P. & Kharitonova, N.A. 1996. Analysis of sonic well logs applied to erosion estimates in the Bighorn Basin, Wyoming. *AAPG Bulletin* **80**, 630–646.

Hillis, R.R. 1995. Quantification of Tertiary exhumation in the United Kingdom southern North Sea using sonic velocity data. AAPG Bulletin **79**, 130–152.

Japsen, P. 1993. Influence of lithology and Neogene uplift on seismic velocities in Denmark; implications for depth conversion of maps. AAPG Bulletin **77**, 194–211.

Japsen, P. 1998. Regional velocity-depth anomalies, North Sea Chalk: a record of overpressure and Neogene uplift and erosion. AAPG Bulletin **82**, 2031–2074.

Japsen 1999. Overpressured Cenozoic shale mapped from velocity anomalies relative to a baseline for marine shale, North Sea. *Petroleum Geoscience* **5**, 321–336.

Japsen 2000. Investigation of multi-phase erosion using reconstructed shale trends based on sonic data. Sole Pit axis, North Sea. *Global and Planetary Change* **24**, 189–210.

Japsen, P., Mukerji, T. & Mavko, G. 2007. Constraints on velocity-depth trends from rock physics models. *Geophysical Prospecting* **55**, 135–154.

Magara, K. 1976. Thickness of removed sedimentary rocks, paleopore pressure, and paleotemperature, southwestern part of Western Canada Basin. *AAPG Bulletin* **60**, 554–565.

Marie, J.P.P. 1975. Rotliegendes stratigraphy and diagenesis. In: *Petroleum and the continental shelf of north-west Europe* (Ed. by A.W. Woodland), pp. 205–211. Applied Science, London.

Nur, A., Mavko, G., Dvorkin, J. & Galmundi, D. 1998. Critical porosity; a key to relating physical properties to porosity in rocks. *Leading Edge* **17**, 357–362.

Osborne, M.J. & Swarbrick, R.E. 1997. Mechanisms for generating overpressure in sedimentary basins. A reevaluation. *American Association of Petroleum Geologists Bulletin* **81**, 1023–1041.

Petri, S. 1972. Foraminíferos e o ambiente de deposição dos sedimentos do Mioceno do Recôncavo Baiana. *Revista Brasileira de Geociências* **2**, 51–67.

Scherbaum, F. 1982. Seismic velocities in sedimentary rocks; indicators of subsidence and uplift. *Geologische Rundschau* **71**, 519–536.

Silva, O.B., Caixeta, J.M., Milhomem, P.S. & Kosin, M. 2007. Bacia de Recôncavo. *Boletim Geociencias Petrobras* **15**, 423–431.

Viana, C.F., da Gama Junior, E., da Araújo Simöes, I., Moura, J.A., dos Reis Fonseca, J. & Alves, R.J. 1971. Revisão estratigráfica da bacia Recôncavo/Tucano. *Buletim técnico Petrobras* **14**, 157-192.

Appendix B. Interpretation and plots of sonic data

Legend

Depths are given in km below sea bed or ground level, also in comments where depths in round numbers are indicated for reference in the diagrams. Depth is displayed as negative numbers in order to produce plots where depth increases downwards.

Log plots (left hand page)

Vp, P-velocity: Sonic p-wave velocities
rhob: Bulk density (blue curve)
Nphi: Neutron porosity converted to limestone densities, -1.6667*nphi + 2.71 (red curve)
Plots of caliper and sonic logs for detection of bad-hole data is displayed on the lower side of the left-hand page. Sonic data that correlate with bad-hole conditions are colour-coded in red on the first two plots and deleted in the final data set shown in the third plot.

Plots for interpretation of the burial anomaly (right hand page)

Upper right plot displays all sonic datapoints after removal of bad-hole data. Colour coded according to lithology according to the LithoLog, if available.

Lower right plots displays the edited sonic data averaged over intervals of 10 m.

Selected lithostratigraphic units are indicated in the diagram with a colour corresponding to the colouring of that part of the sonic log.

Biostratigraphic control on the post-Campanian succession is indicated with arrows along the depth axis.

Main unconformities are marked with green lines. Possible unconformities are indicated by dashed lines and intervals where Cenozoic unconformities may be present are marked with a green, dotted box. Abbreviations used in the names of the unconformities:

RdC	Rio de Contas Fm
RD-C	Rio Doce-Caravelas Fms
MdB	Morro do Barro Fm
TM	Taipus-Mirim Fm

Identified datapoints for low-velocity shale and high-velocity sandstone are plotted on the displays. The datapoints are readings of depth and velocity from the respective lithological units as identified on the composite log and the LithoLog if available.

Full lines indicate baselines for the respective lithologies:

sh_o (or Vsh-o) – baseline for organic-rich shale; full cyan line (Eq. 5-6).

sh (or Vsh) – baseline for shale; full red line (Eq. 5-1; Japsen 2000)

BR00, BR05 – baseline for sandstone with 0% and 5% clay; full blue and green lines (Eq. 5-5). Slightly modified in this report after Japsen et al. 2007.

Dashed lines indicate the same baselines only shifted upwards by the burial anomaly to fit the data trend.

Burial anomaly = 0: normal compaction

Burial anomaly (= magnitude of burial anomaly, rather than the formally defined negative values in case of removed overburden thickness) >0: indicative of exhumation

Exhumation = Burial anomaly + post-exhumational reburial

.

Paleocene strata).

Unconformities
Post-Algodões unconformity (110–0 Ma): Above Algodões Fm (365 m thick; Albian strata reported) and below thin cover of RD-C Fms (31 m).

Caliper
No caliper available, but the sonic data are well-defined over most of the drilled interval.

Sonic log and composite log (without sonic displayed)
Mixed lithologies above MdB, including 100 m thick RdC sandstone at c. 0.8 km.

Massive MdB sandstone between 1.3 and 3.0 km with velocities ranging between c. 4 and 5 km/s. The sonic data for this interval was used for calibration on the sandstone trends, BR00 and BR05.

Burial anomaly
1.9 ± 0.2 km (relative to the baselines) gives a good match between the sandstone data between 0.8 and 3.1 km and the absolute values and the curvature of the baselines for pure sandstone. BR00 and BR05 were calibrated after this dataset by shifting the trends towards more shallow depths than those of SS00 and SS05 and thus reducing the estimated burial anomaly.

Post-exhumational burial
0.0 km.

Removed section

1.9 ± 0.5 km (allowing for the uncertainty of the baselines); probably corresponding to the upper part of the Algodões Fm (0.4 km preserved) and the lower part of the Urucutuca Fm (missing).

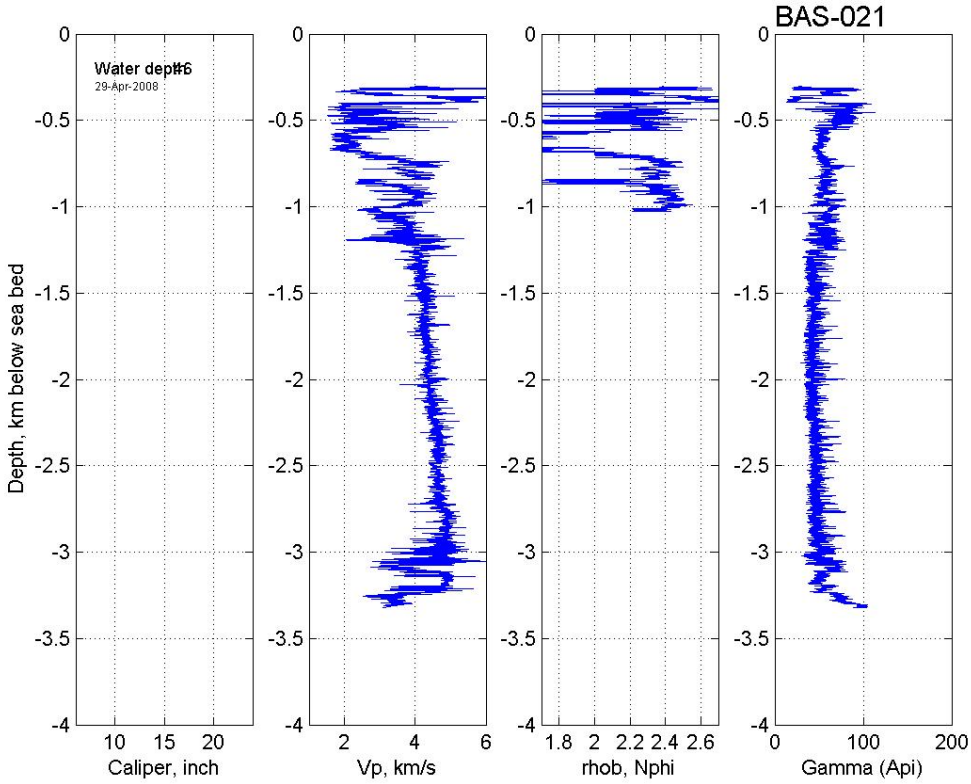
BAS-021
Water depth 46
29-Apr-2008
Depth, km below sea bed
Caliper, inch
Vp, km/s
rhob, Nphi
Gamma (Api)

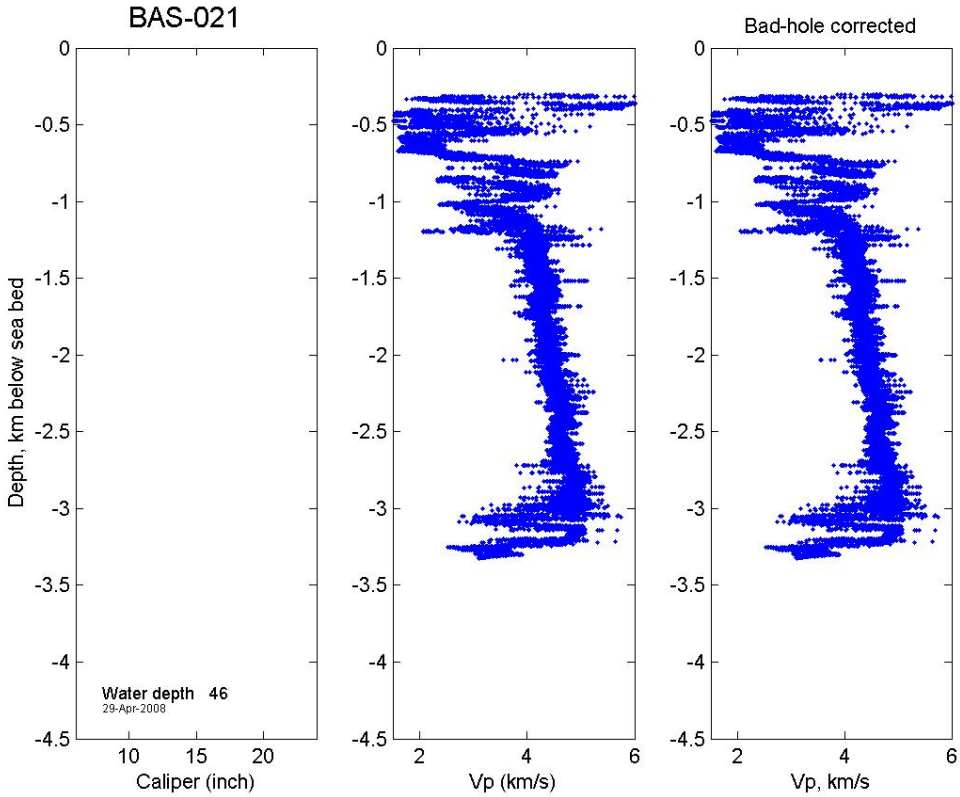
BAS-021
Bad-hole corrected
Water depth 46
29-Apr-2008
Depth, km below sea bed
Caliper (inch)
Vp (km/s)
Vp, km/s

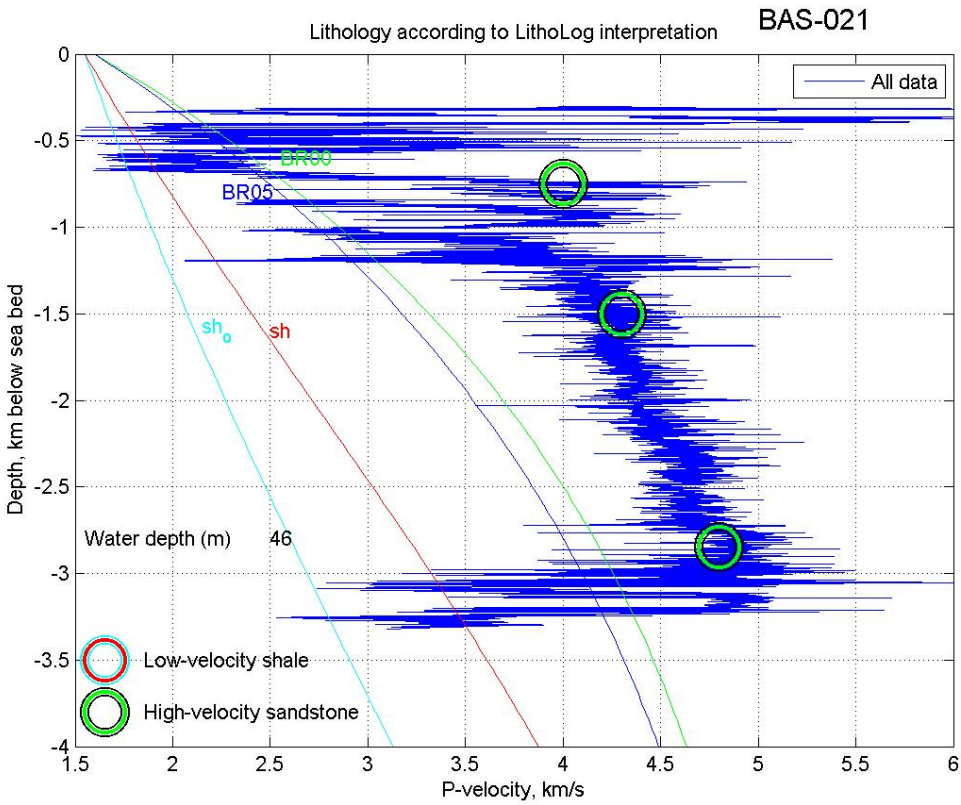

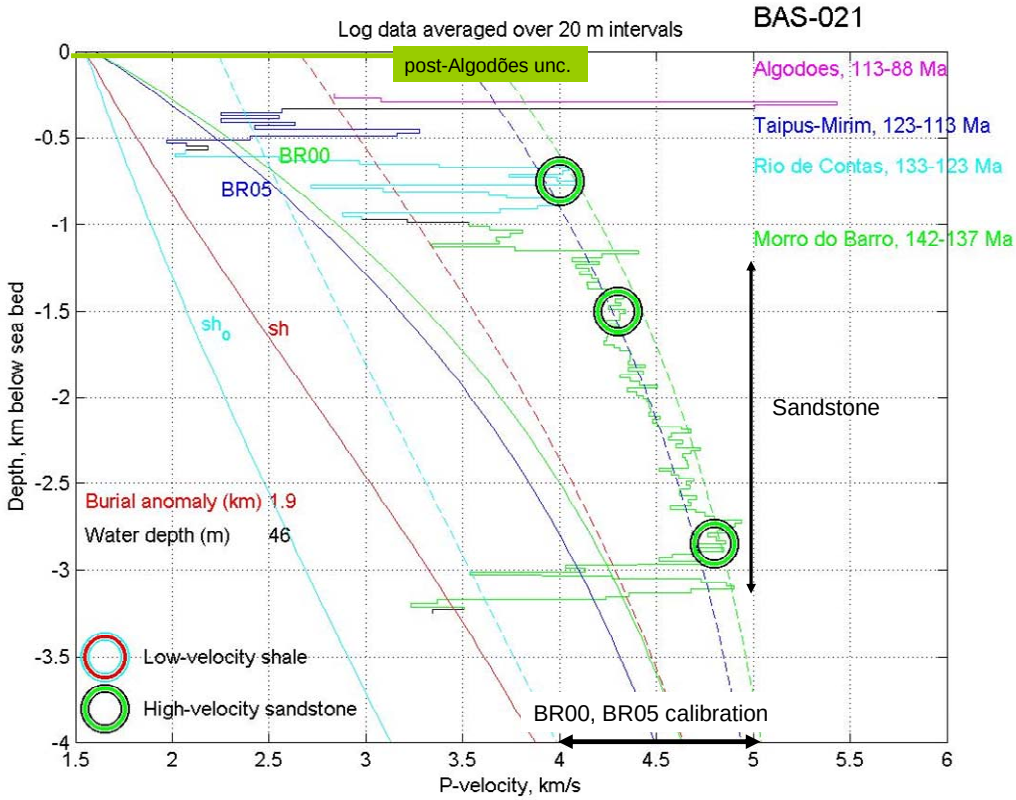

cf. BAS-74 (near-by), -97, -113 (thick MdB sandstone)

Unconformities
Post-Taipus Mirim unconformity (123–70 Ma): Above thin TM Fm (31 m) and below thick Rio Doce-Caravelas and Urucutuca Fms (1649 m) with Maastrichtian strata reported 926 m below seabed; Algodões Fm missing.

Post-Eocene unconformity (34-0 Ma): Above Late Eocene strata and within thin overlying section (242 m, RD-C Fms).

Caliper
Wide calliper range over much of the drilled interval, but only clear correlation with low velocities around 4 km.

Sonic data and composite log
Steady increase of Vp with depth over the interval from 0.9 to 1.5 km generally plotting below the sandstone baselines; dominated by shale with calcilutite intercalations (Urucutuca Fm). Low-velocity shale in the upper part of MdB. Datapoint plot near Vsh.

The RdC Fm is predominantly sandstone 1.9 to 3.1 km with velocities ranging between c. 3.5 and 4.4 km/s. The sonic data for this interval was used for calibration on the sandstone trends, BR00 and BR05.

Burial anomaly
0 ± 0.2 km (Mesozoic section relative to the baselines): The Mesozoic sequence – and thus the Cenozoic sequence as well – is at maximum burial. Based on the observation that the RdC thick sandstones plot near the baselines for pure sandstone – not only BR00 and BR05 that were partly calibrated after data from this interval, but also near the SS00 and SS05 baselines.

Post-exhumational burial
1.6 km; burial of the post-TM unconformity.

Removed section
- ; since the rift sediments are at maximum burial today any exhumation at the post-TM unconformity must be less than 1.6 km; potentially corresponding to the upper part of the TM Fm (31 m preserved), the Algodões Fm and the lower part of the Urucutuca Fm.

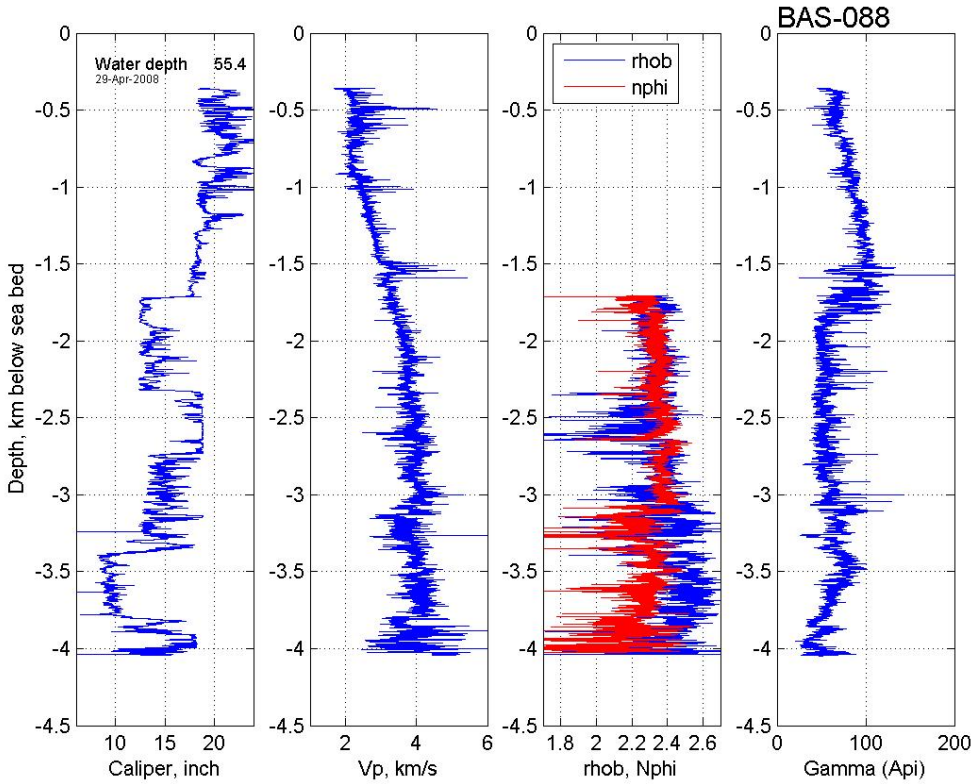
BAS-088
Water depth 55.4
29-Apr-2008
rhob
nphi
Depth, km below sea bed
Caliper, inch
Vp, km/s
rhob, Nphi
Gamma (Api)

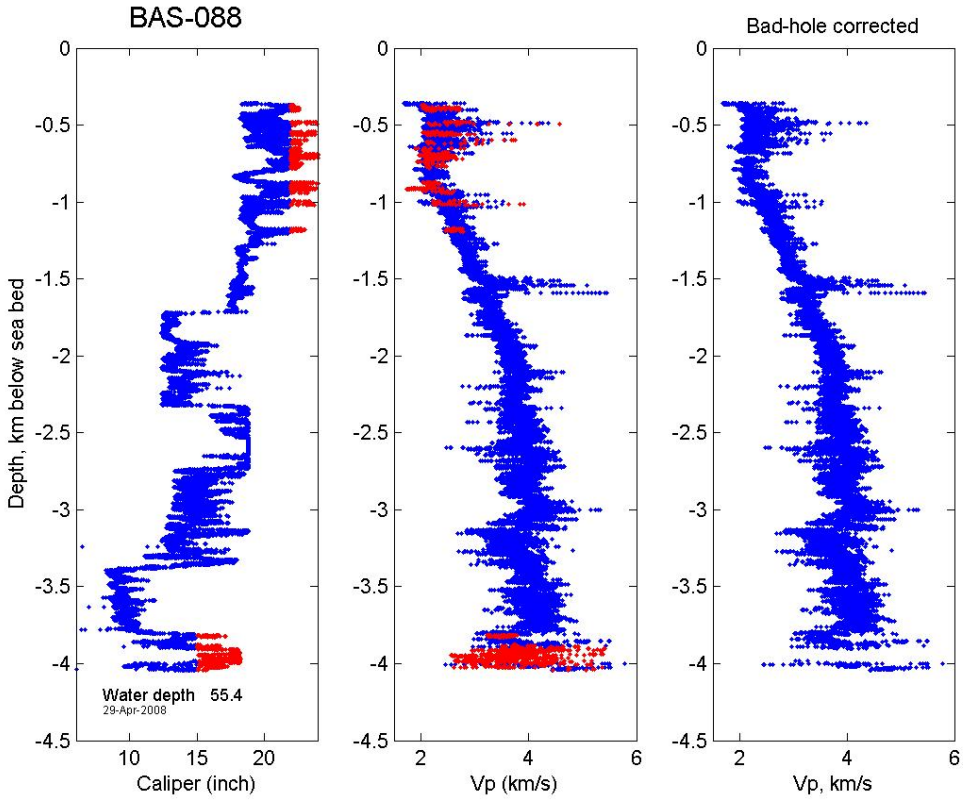
BAS-088
Bad-hole corrected
Water depth 55.4
29-Apr-2008
Depth, km below sea bed
Caliper (inch)
Vp (km/s)
Vp, km/s

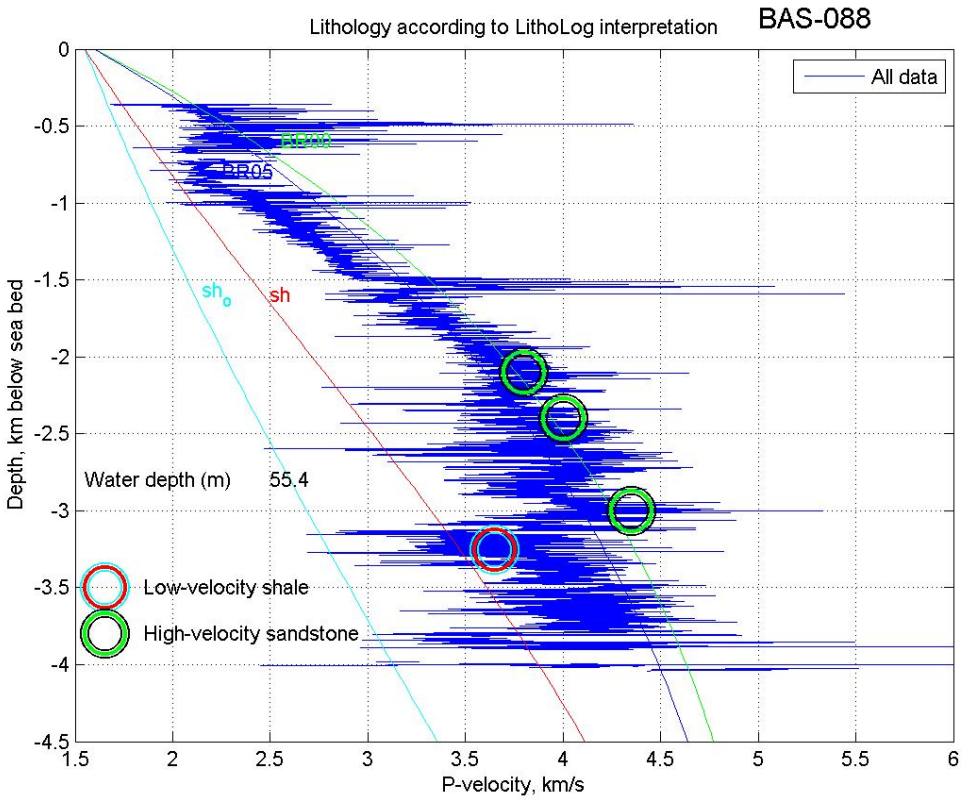

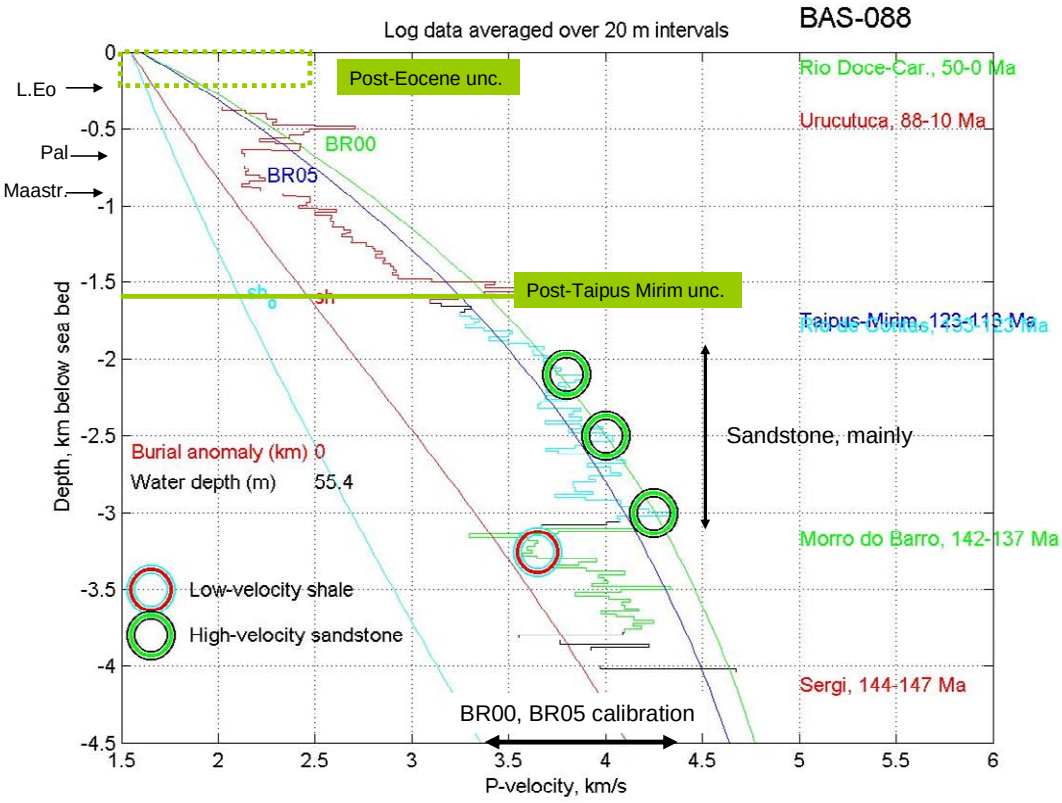

cf. BAS-118, -79 (both near-by)

AFTA

Unconformities
Post-RdC unconformity (133–0 Ma): Above thin RdC Fm (96 m) and below thin RD-C Fms (75 m); Algodões and TM Fms missing.

Caliper
Constant calliper down to 1.3 km, then moderate fluctuation down to 3.4 km and finally considerable fluctuations in the deepest part of the well (below 3.4 km) coinciding with low velocities (<4 km/s), and these datapoints are consequently deleted.

Sonic data, LithoLog and composite log
The sonic log varies significantly (e.g. between 2.5 and 4 km/s) over small depth intervals between 0.5 and 2.8 km. According to the composite log, this is due to a rapidly changing lithology (sand, shale, limestone, dolomite). Low-velocity shale units define a lower bound for the sonic data above 2.4 km and two points on this trend is highlighted.

A thick and uniform sandstone unit with small velocity variations is present in the basal part of the MdB Fm (2.8-3.4 km).

Burial anomaly
2.2 ± 0.2 km (relative to the baselines) is chosen as a good match between the baselines and the datapoints for 1) the high-velocity sand units between 2.8 and 3.4 km and 2) the low-velocity shale trend above 2.4 km.

Post-exhumational burial
0.1 km; burial of the post-RdC unconformity.

Removed section
2.3 ± 0.5 km (allowing for the uncertainty of the baselines); probably corresponding to the upper part of the RdC Fm (96 m preserved), the TM and Algodões Fms (missing) and the lower part of the Urucutuca Fm (missing).

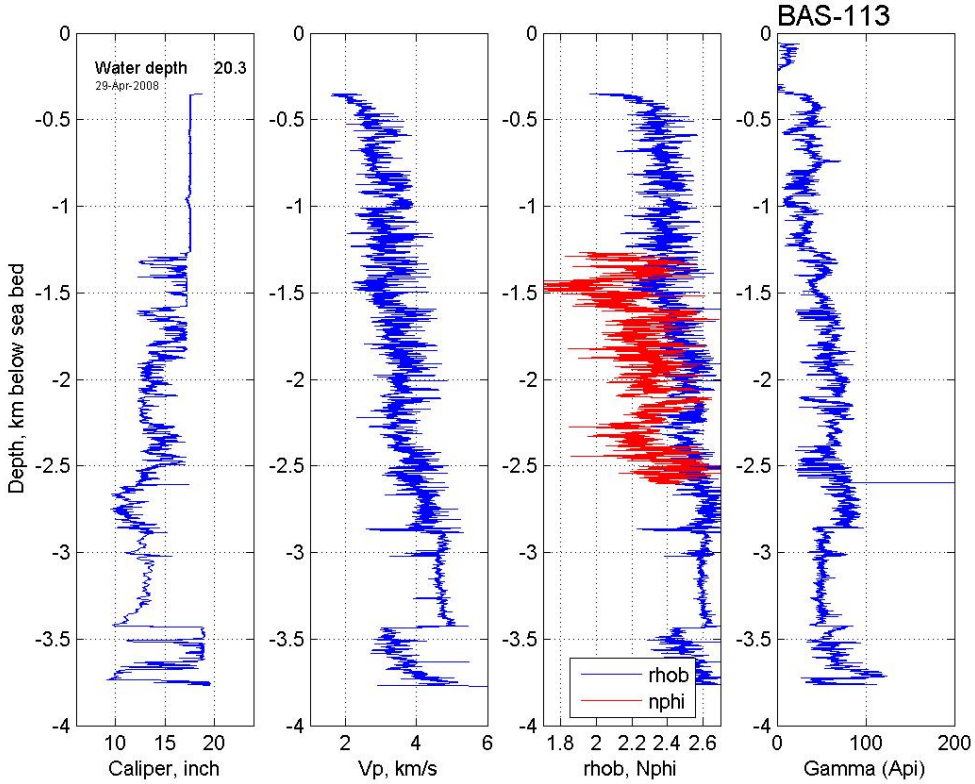
BAS-113
Water depth 20.3
29-Apr-2008
Depth, km below sea bed
Caliper, inch
Vp, km/s
rhob, Nphi
Gamma (Api)
rhob
nphi

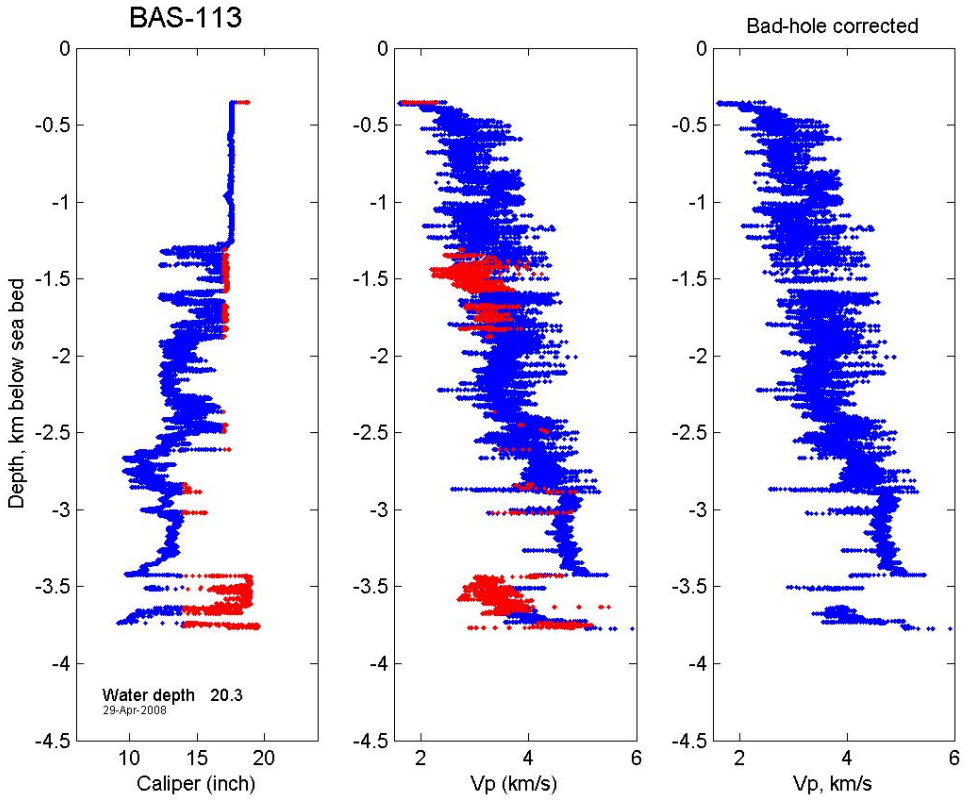
BAS-113
Bad-hole corrected
Water depth 20.3
29-Apr-2008
Depth, km below sea bed
Caliper (inch)
Vp (km/s)
Vp, km/s

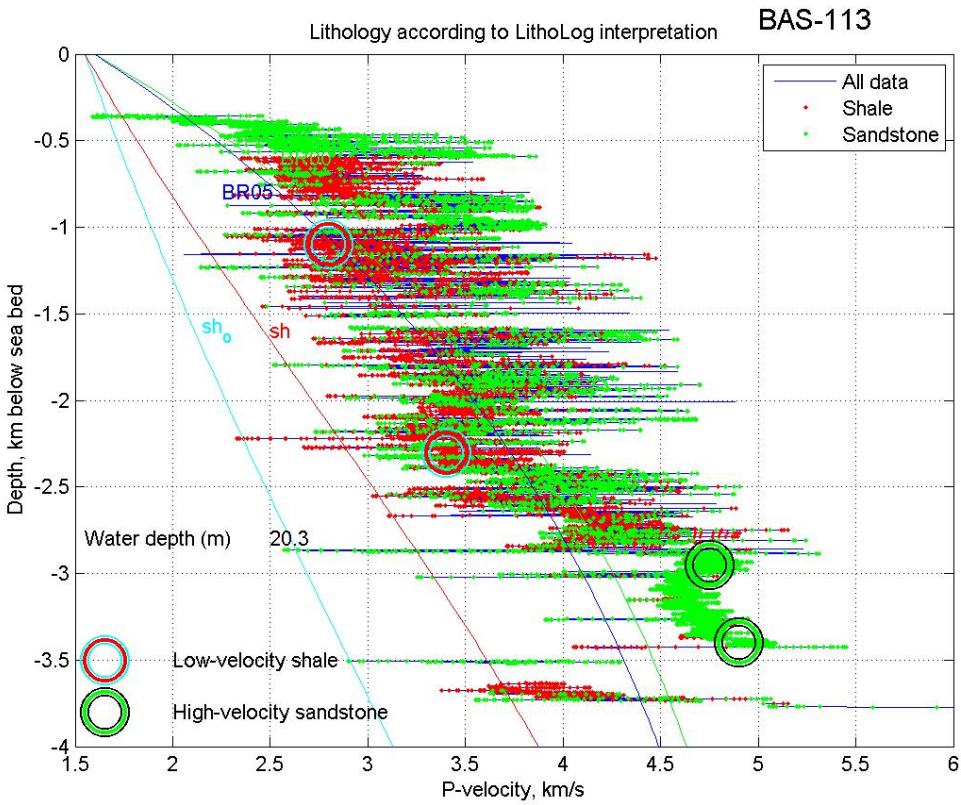

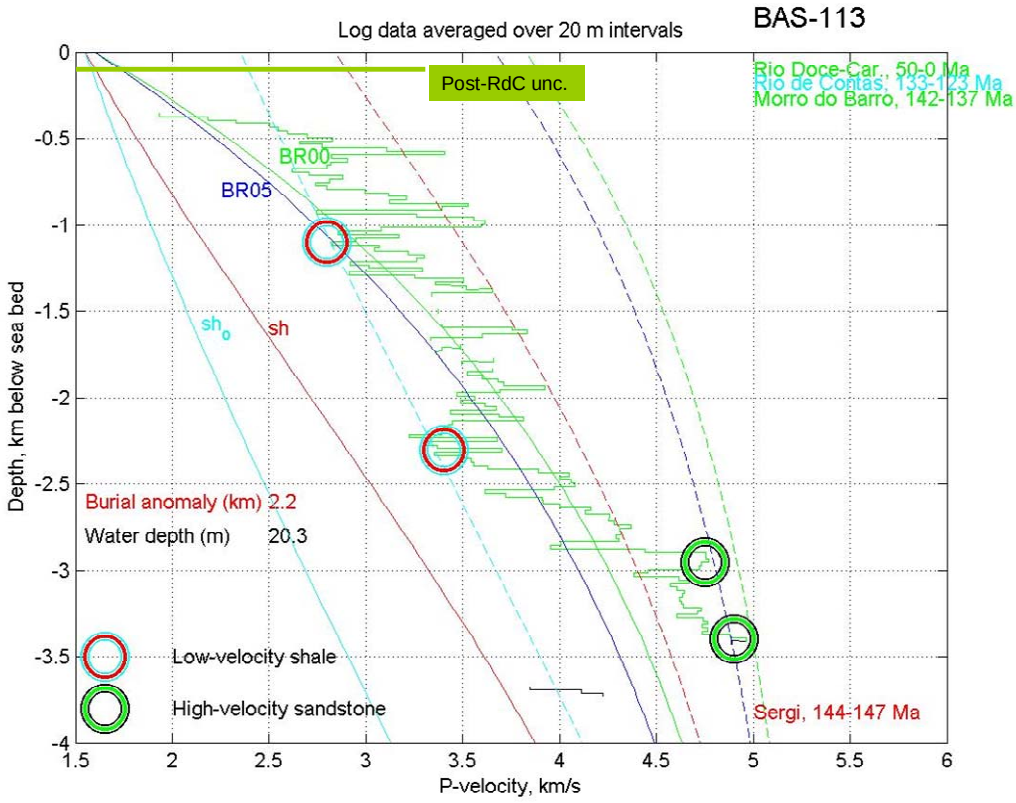

cf. BAS-84 (near-by), -21 (thick MdB)

AFTA

Unconformities
Post-Marizal unconformity (115–0 Ma): Ground level.

Caliper
Considerable variations throughout the borehole. Clear correlation between bad-hole conditions and low sonic velocities; overall trend of the data not affected by the data editing.

Sonic data and composite log
Well-defined trend of sonic velocities increasing with depth between 1 and 3.5 km; constant velocity level above 1 km and relatively low velocities in the Candeias Fm below 3.5 km. Shale dominated interval between 3.6 and 4.1 km (Candeias Fm); some scatter in the sonic data, but reliable reading at c. 4 km. Estimation of shale velocities difficult in the upper part of the well because of severe bad-hole conditions. Very low velocities in shale interval at 4.1 km with may reflect very organic-rich shales.

Thick sandstone units over a 150 m thick interval at c. 3.5 km with well-defined sonic level (Ilhas Group).

Burial anomaly
2.5 ± 0.3 km (relative to the baselines); based on sandstone data at 3.5 km consistent with estimated shale velocity of the Candeias Fm matching Vsh-o at 4.0 km. Coincidence between sonic data around 1 km and Vsh-o suggests that these sediments are organic-rich and that this condition explains the low velocities in the upper part of the borehole.

Post-exhumational burial
0 km.

Removed section
2.5 ± 0.6 km (allowing for the uncertainty of the baselines); Marizal Fm and younger units.

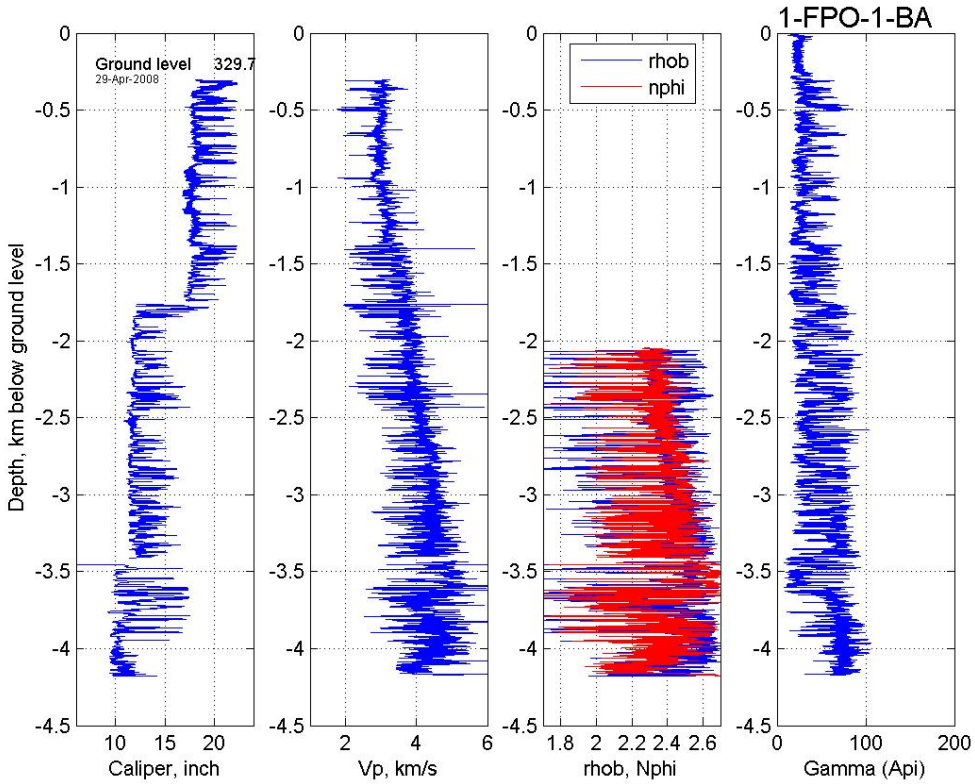
1-FPO-1-BA
Ground level 329.7
29-Apr-2008
Depth, km below ground level
Caliper, inch
Vp, km/s
rhob
nphi
rhob, Nphi
Gamma (Api)

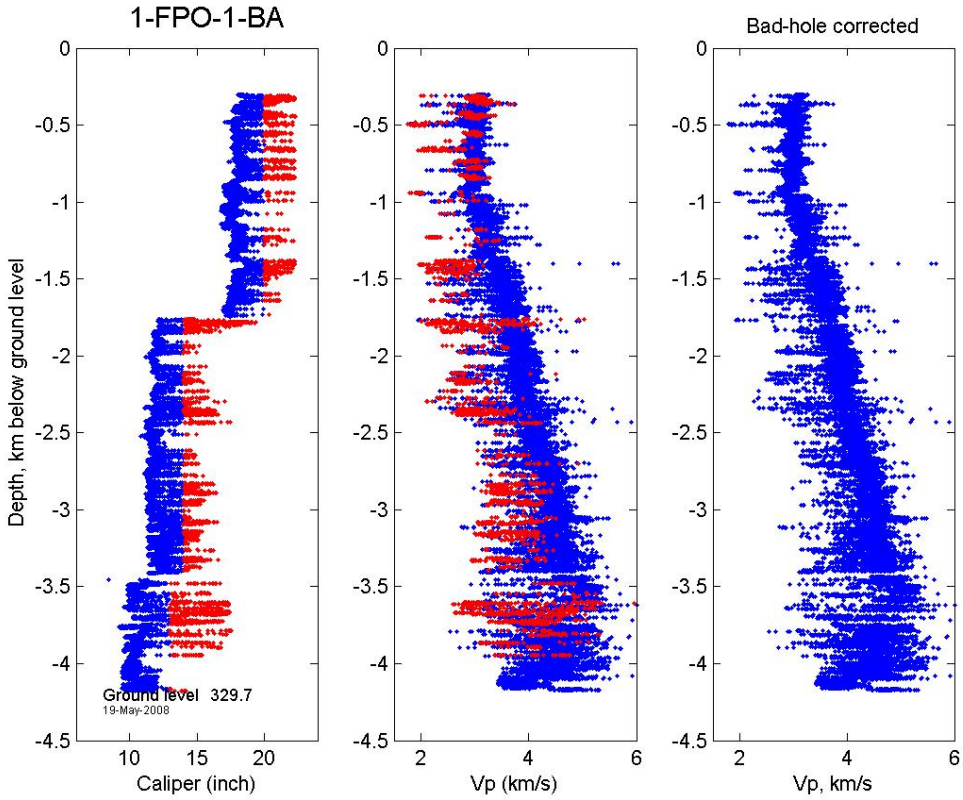
1-FPO-1-BA
Bad-hole corrected
Depth, km below ground level
Ground level 329.7
19-May-2008
Caliper (inch)
Vp (km/s)
Vp, km/s

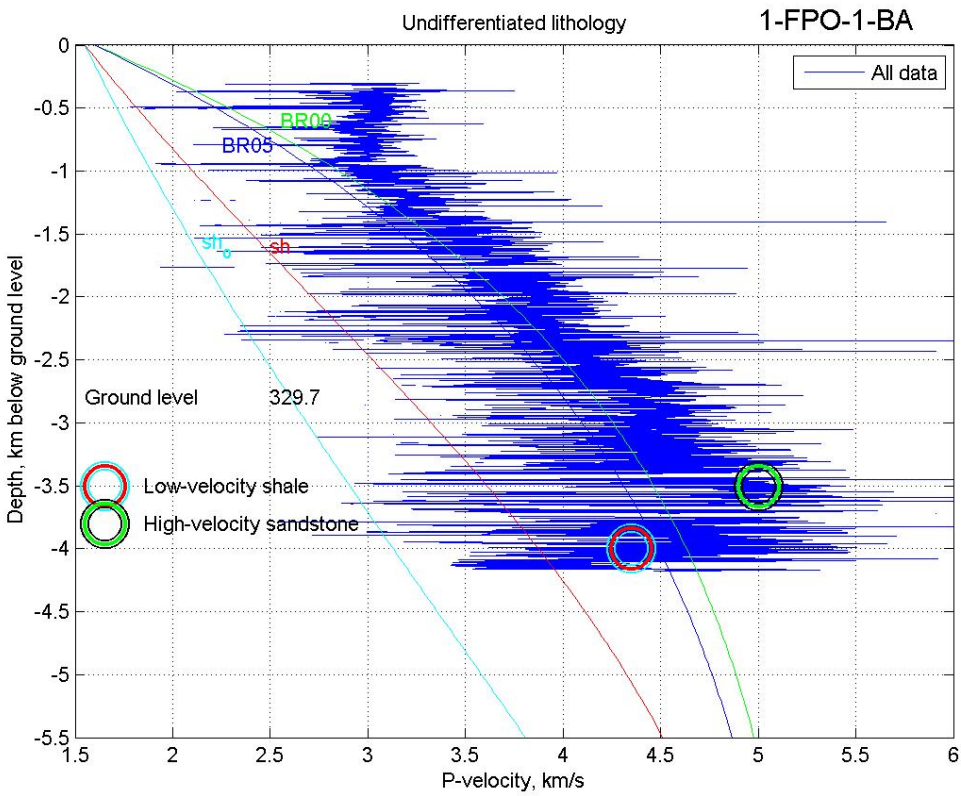

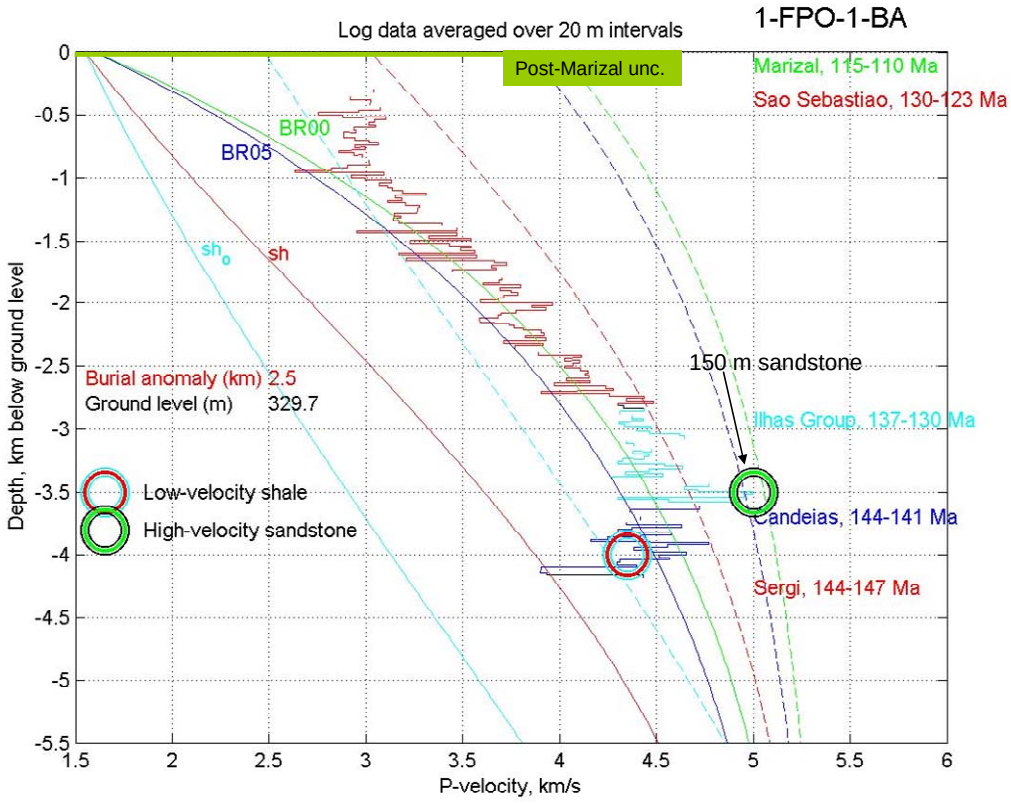

Near FVO-1

AFTA

Unconformities
Post-São Sebastião unconformity (125–0 Ma): Ground level.

Caliper
Very small variations in the caliper; few datapoints deleted due to bad-hole conditions.

Sonic data and composite log
Good-quality sonic log with a wide data range that is clearly related to the lithological changes in the drilled sequence (mainly low-velocity shale vs high-velocity sandstone units).

Low-velocity shale data: Well-defined sonic level at 1.4 km (Marfim Fm), at 2.15 and 2.85 km (Marancangalha Fm), 3.4 km (Candeias Fm).

High-velocity sandstone: Well-defined sonic level at 2.4 and 3.1 km (Marancangalha Fm) and 3.6 km (Sergi Fm; based on the raw sonic log).

Burial anomaly
2.5 ± 0.5 km (relative to the baselines); primarily based on high-velocity sandstones in the deepest part of the borehole, but also on a general fit between low-velocity datapoints and Vsh-o. Sandstone units in the shallow part of the well plot c. 0.5 km below the shifted baselines; this is interpreted as being due clay content. The two deepest shale datapoints have identical sonic values but are separated by 500 m; the low velocity for the deepest datapoint is interpreted as being due to very high organic content in the Candeias Fm which is the main source rock in the basin.

Post-exhumational burial
0 km.

Removed section
2.5 ± 0.8 (allowing for the uncertainty of the baselines); São Sebastião Fm and younger units.

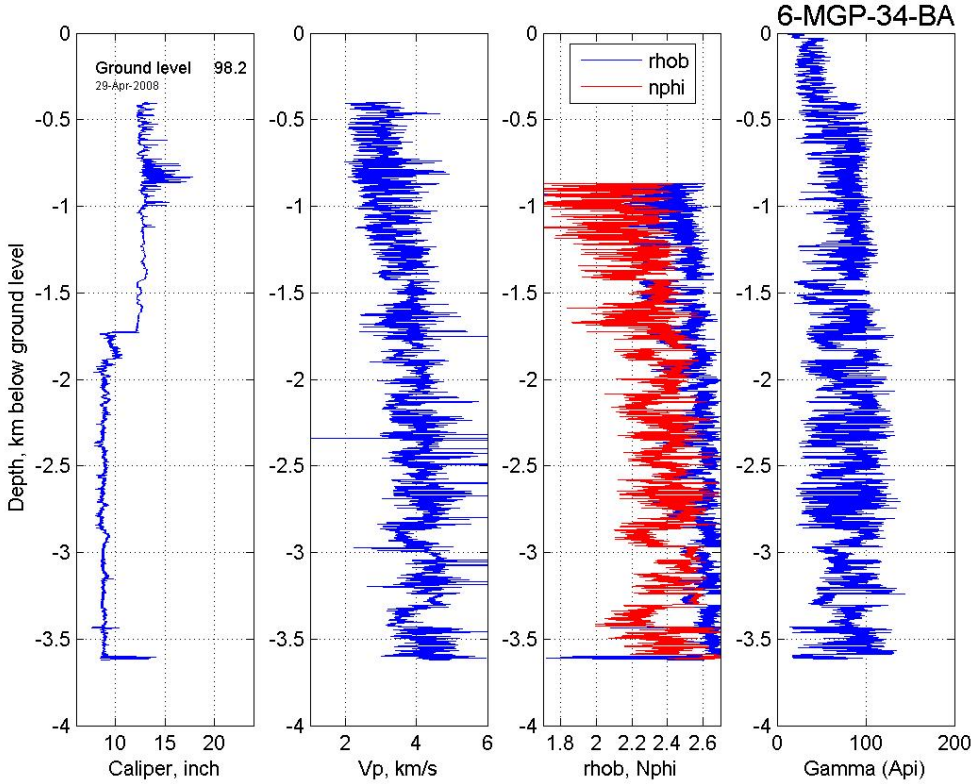
6-MGP-34-BA
Ground level 98.2
29-Apr-2008
rhob
nphi
Depth, km below ground level
Caliper, inch
Vp, km/s
rhob, Nphi
Gamma (Api)

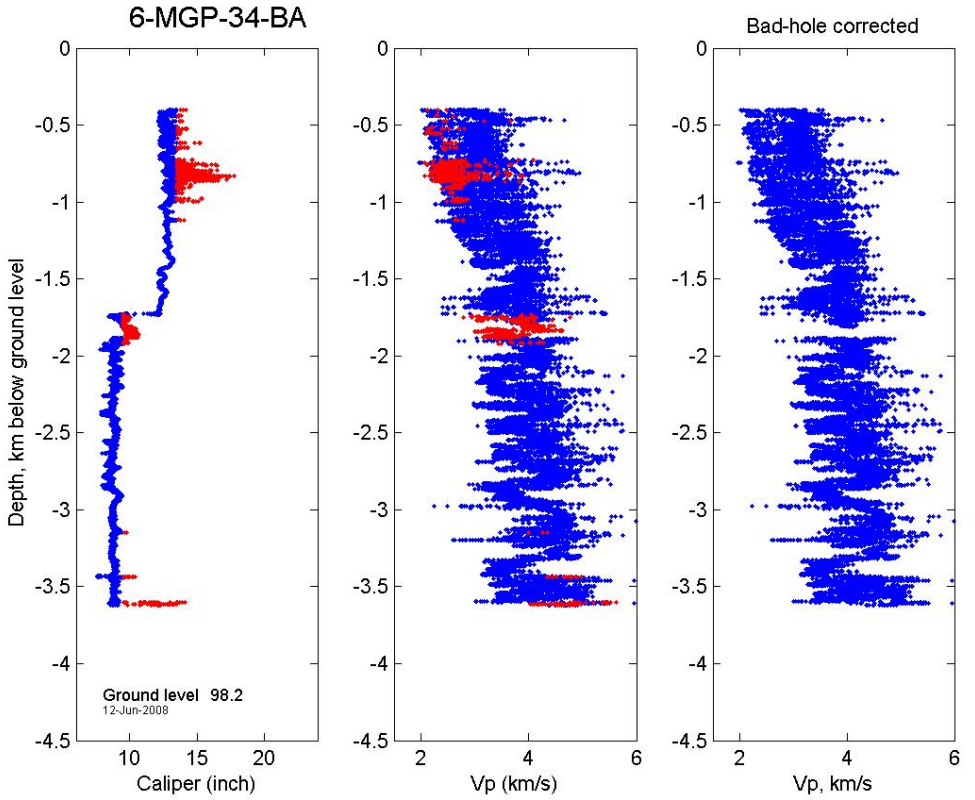
6-MGP-34-BA
Bad-hole corrected
Ground level 98.2
12-Jun-2008
Depth, km below ground level
Caliper (inch)
Vp (km/s)
Vp, km/s

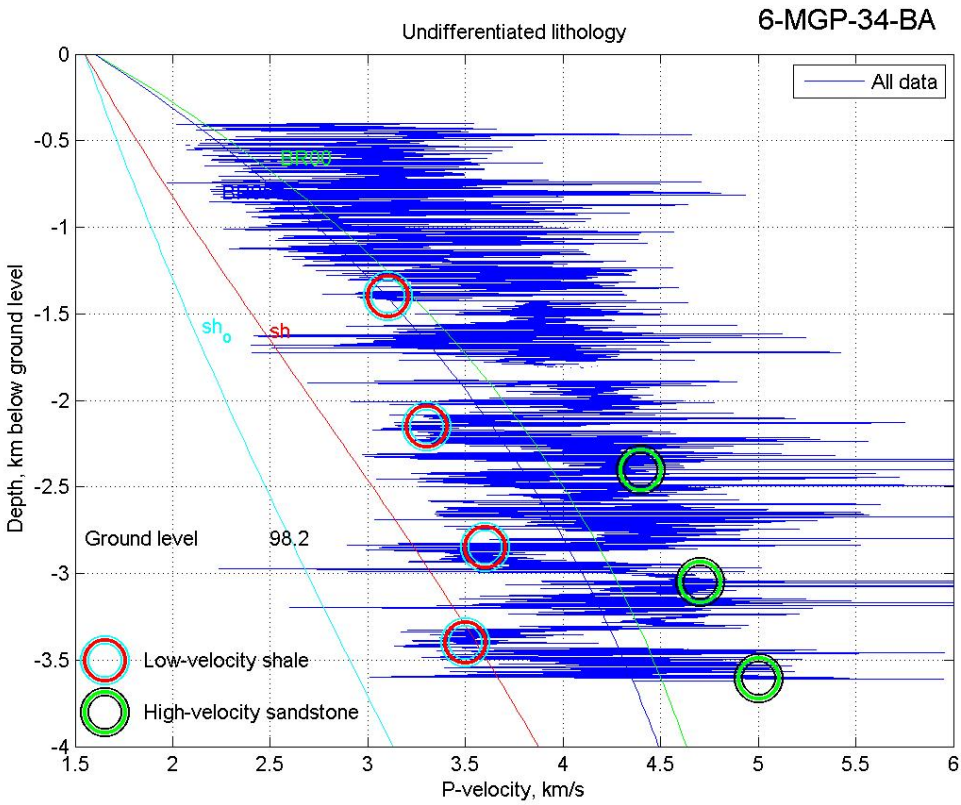

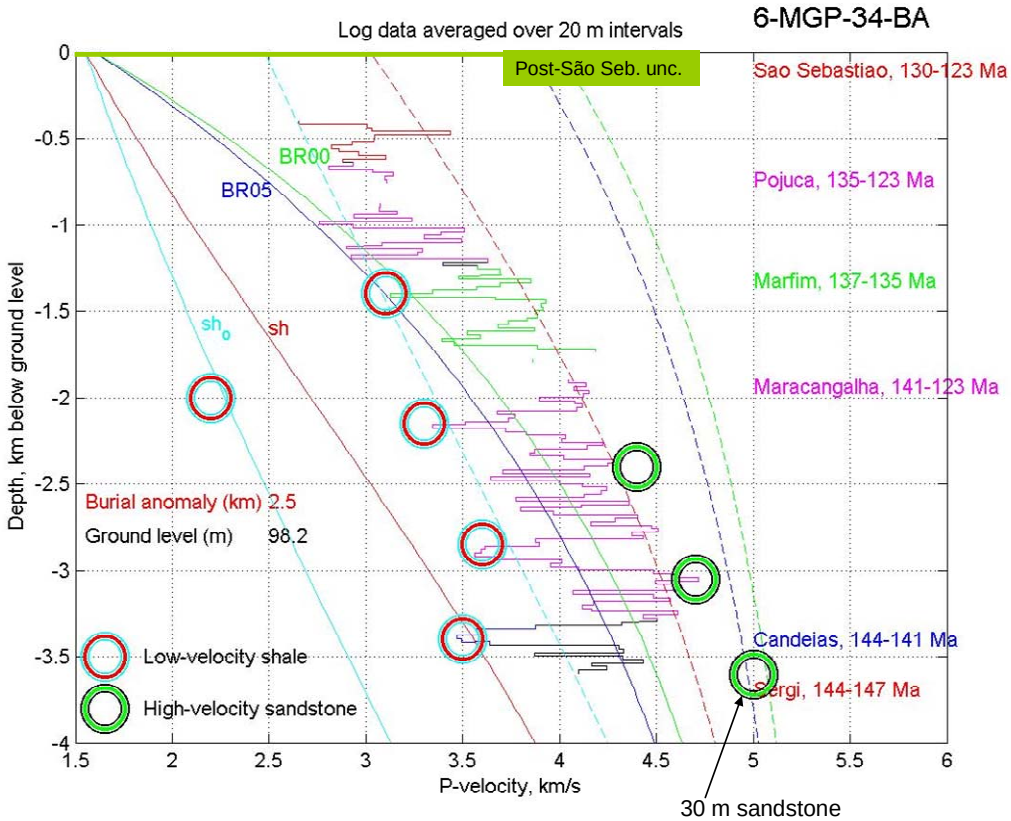

Between BRN-1 and BAS-113

AFTA

DANMARKS OG GRØNLANDS GEOLOGISKE UNDERSØGELSE RAPPORT 2009/9

Relative denudation chronology in NE Brazil based on mapping of large-scale landforms

Contribution to the project "Burial and exhumation history of NE Brazil focussing on the Camamu Basin: a multidisciplinary study based on thermal, sonic and stratigraphic data and landform analysis"

Funded by StatoilHydro do Brasil and Petrobras

Johan M. Bonow

Confidential report

Copy No.

To be released 01.03.2014

GEOLOGICAL SURVEY OF DENMARK AND GREENLAND
MINISTRY OF CLIMATE END ENERGY

GEUS

1. Summary **3**

2. Background **5**

2.1 Geomorphology 6
2.2 The approach of landscape analysis 6
2.3 The study area 6

3. Method of landscape analysis **9**

3.1 Method of surface mapping 9

4. Geomorphological results **13**

4.1 Topographical overview 13
4.2 The denudation surfaces 20
4.2.1 The higher surface 21
4.2.2 The lower surface 22
4.2.3 The coastal plain 22
4.2.4 Illustrations of the surface mapping 22
4.3 The surfaces in relationship to geology 24

5. Geomorphological implications and discussion **27**

5.1 Surface chronology and timing of events 28

6. Conclusions **29**

7. References **30**

1. Summary

This report documents the geomorphological investigations in NE Brazil for StatoilHydro do Brazil, in the research project “Burial and exhumation history of NE Brazil focussing on the Camamu Basin: A multidisciplinary study based on thermal, sonic and stratigraphic data and landform analysis”. The outcome of the entire project is reported by Japsen et al. (2009).

The aim of this report is 1) to document the landscape observations, 2) to map peneplains (denudation surfaces) of different age and 3) to make a relative chronology for the tectonic landscape development in the study area. The documentation is based on extensive field work, and observations of landforms and their relationship to the geology. The surfaces have been mapped by aid of a contour map and profiles constructed from digital elevation data (SRTM). The mapping has been complemented with information from the fieldwork and the geological maps.

The geomorphological analysis of the large-scale landforms has lead to identification of two major denudation surfaces of regional extent, the higher and the lower surface, and the coastal plain, all in stepped sequence following the valleys (Fig. 23). These surfaces all cut across rocks of different age and of different resistance. It is therefore concluded that their formation was governed by erosion relative to a general base level. The wide extent of the higher and lower surface suggests that they developed over a significant time interval with stable base-level conditions because a long time span will reduce the lithological and structural influence on the shape of these surfaces. Further any significant change of base level cannot have occurred as that would have resulted in rejuvenation of the relief.

The higher surface is well-developed across Chapada Diamantina and Planalto de Conquista. The elevation of the surface is c. 1200 m a.s.l. over Chapada Diamantina and c. 900 m a.s.l. over Planalto de Conquista, but despite that the higher surface is tilted towards the southeast they can be correlated. Therefore it is concluded that they were formed as one coherent surface. The higher surface cuts across Precambrian basement, but over wide areas Cenozoic laterites and weathered basement are preserved below the surface, thus constraining its final formation age to the Cenozoic. A winding escarpment usually separates the higher surface from the lower.

The lower surface can be identified from the coast at c. 200 m a.s.l. and it follows the major valleys up to c. 500 m a.s.l., as far as 250 km from the coast. At its upper reaches the escarpment up to the higher surface is usually pronounced. The lower surface cuts across the Aptian sedimentary sequence in the Recôncavo-Tucano Basins and Precambrian basement along the flanks. A thin cover of the Miocene-Pliocene(?) Barreiras Formation is present in areas where the lower surface is present and it is thus difficult to map the relationship between the lower surface and this cover.

The coastal plain is rather narrow, mainly defined along the major rivers. It is incised into the Barreiras Formation.

Based on the relationship between the surfaces and the geology the following relative sequence of events is suggested: The higher surface was developed during the Cenozoic and is probably Paleogene in age, based on that both the higher surface and the laterites are currently being destroyed by erosion along the escarpments that outline the plateaux. Consequently, the laterites must have formed at the end of the denudational event that formed the higher surface.

The lower surface post-dates the higher surface and is suggested to be Neogene in age. The coastal plain is post-Barreiras, and this combined with the immature dissection of the landscape observed over much of the coastal zone indicates that it is a young feature.

At least some of the base level changes recorded by the denudation surfaces must be tectonic in origin, in particular the pronounced step of 500 to 700 metres between the higher and the lower surface. This step reflects the amount of uplift prior to the formation of the lower surface.

Differences in lithology and structure have influenced the development and preservation of the surfaces across the study area. Resistant rocks assist in preservation of old surfaces and halt new surfaces to develop. The rivers in areas of resistant rocks tend to form deep canyons whereas the formation of new surfaces is much faster in areas with less resistant rocks and such areas will also be the first to be rejuvenated after a base level change. Long-term denudation significantly reduces the lithological influence on the surface development.

2. Background

The aim with this report is 1) to document the landscape observations 2) to map peneplains of different age, and 3) to make a relative chronology for the tectonic landscape development in NE Brazil (Fig. 1). This report is the results of the detailed analysis based on landscape mapping (this report) and fieldwork (Japsen et al, 2007).

The geomorphological data and the interpretations presented here is part of the overall effort to integrate the results from the AFTA data for conclusions about the thermochronology history of the subsurface rocks (Apatite fission track analysis), the geological record and the large-scale landscape analysis (geomorphology) for conclusions about the relative chronology for denudational events. The purpose of this integration is to construct a regional model for the morphotectonic evolution in NE Brazil. This part will primarily deal with the geomorphology. The details of AFTA will be reported separately (Green 2008, in press). The details of the geological development as well as the integration of all data will be reported in Japsen et al. (2009).

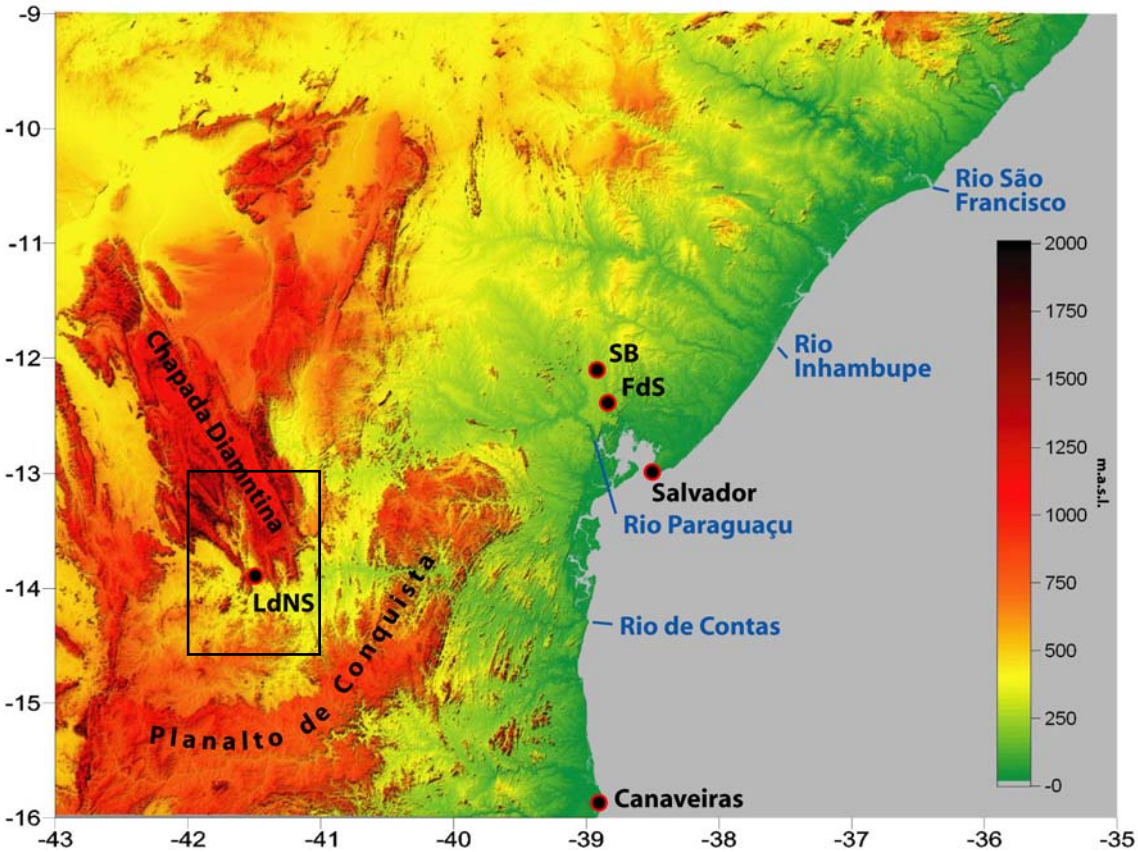

Fig. 1. The study area with place names used in this report. The black rectangle marks the location of fig 22. SB-Santa Bárbara, FdS-Feira de Santana, LdNS- Liveramento de Nossa Senhora.

2.1 Geomorphology

2.2 The approach of landscape analysis

The framework of the landscape development is based on relationships between different denudation-surfaces in stepped sequence and geology separated into basement and cover rocks (e.g. Lidmar-Bergström, 1982, 1988, 1989, 1995, 1996, Lidmar-Bergström et al., 2000, 2007; Bonow et al., 2003, 2006a, 2006b, 2007; Bonow, 2005). The denudation surfaces are thought to reflect a base-level to which it will grade. The longer time available for a surface to form, the more extensive it will be and also less controlled by different lithological conditions. Thus a surface will continue to develop, at different rate due to climatic conditions, until the base level to which it grades will change. Thus will a lowered base level (e.g. due to uplift) cause valley incision and rejuvenation of the relief, subsequently leading to the development and formation of a new. lower erosion surface. The step (escarpment or knick-point) in the landscape between the valley floor and a higher surface will thus show the amount of base level change. On the other hand will an elevated base level (e.g. due to subsidence) cause burial of the previously formed surface, thus preserving the surface and landscapes from a certain time.

2.3 The study area

Geomorphological studies regarding general landscape development are few in Brazil, and no detailed investigation has been made of the landscapes in study area. Generally the Brazilian landscapes have been looked upon as a result of regional uplift at the time of break-up of the Gondwana (e.g. Zonneveld, 1993; Ab'Sáber 2000 and references therein), ephasising the pre-Cenozoic development, a conclusion also derived from landscape studies in central Argentina (Demoulin et al. 2005). Recent geomorphological studies of northern Brazil have suggested a generally continuous rise of the landmass since rifting (Peulvast and Claudino Sales 2004, Peulvast et al. 2008). However, Valadão (1998) regarded the stepped landscapes in NE Brazil to reflect mainly a Cenozoic development. Based on river patterns and sedimentary record in the scale of South America, Potter (1997) regarded the continent to mainly have been stable since break up.

The most complete geomorphological analysis so far of NE Brazil has been made by Lester King (King 1956, 1967). His work has had a significant impact of the geomorphological thinking in more recent geomorphological literature, but also on literature describing different aspects of tectonics and stratigraphy often relate to his different erosion surfaces. Therefore will his surface mapping and thoughts briefly be reviewed in this report. King's mapping was mainly field based (e.g. King 1967 p 233), and occasionally based on less accurate topographical maps. Today mapping of denudation surfaces (i.e. peneplains) can be made based on high resolution digital elevation models. A new method of such systematic surface mapping has therefore been possible to develop (e.g. Lidmar-Bergström 1988; Bonow et al., 2006 and references therein, see section above). This method of mapping has been applied in this study and is described in the method chapter below.

In NE Brazil, including the present study area, King identified four different denudation surfaces that he interpreted to represent cyclic, low-relief base-level governed erosional surfaces (Fig. 2). King regarded the highest surface to be the oldest and that the youngest surfaces subsequently formed after break-up of the Gondwana supercontinent in the Cretaceous. King called the surface formed a *pediplain* and the formation process for *pediplanation,* in which the surface formed from the valleys by widening by parallel scarp retreat (King 1953). King's terminology shall be seen in the light of his desire to differentiate his landscape model from the one by Davis (1899), "The geographical cycle" which described the landscapes to develop by slope decline, thus not resulting in stepped surfaces. The end result of the denudation cycle, Davis (1899) named the *peneplain*, which is indistinguishable in appearance from the *pediplain*.

In NE Brazil King (1967) interpreted that the two oldest surfaces (and highest) were Mesozoic in age and he named them *Gondwana* and *post-Gondwana*. The Gondwana surface was thought as a pre-break-up surface that had developed across both present South America and Africa. In Brazil, Gondwana and post-Gondwana surfaces are only well preserved in the highest areas in the interior. According to King (1967), only small areas exist of these surfaces in the study area, specifically in Chapada Diamantina and in the north respectively south part of Planalto de Conquista. More frequent, according to King (1967), is the early Cenozoic *Sul-Americana* surface, that is well preserved and dominating in the highlands of Chapada Diamantina, and with remnants on the Planalto de Conquista. Its age is determined as it is regarded to cut across silicreted sands of presumed early Cenozoic age, in locations west of the São Francisco river, thus far west of the study area. The erosional cycle *Velhas* is not present in the Chapada Diamantina, but exists on the flanks of the Planalto de Conquista. The Velhas is regarded to have been formed during the late Cenozoic and is characterised by a smooth surface occasionally with inselbergs. King (1956, 1967) assign the main part of the study area to belong to the youngest cycle, the *Paraguaçu*, which he mapped also into the coastal area and he thought that this cycle was due to recent tilting along the present coast line.

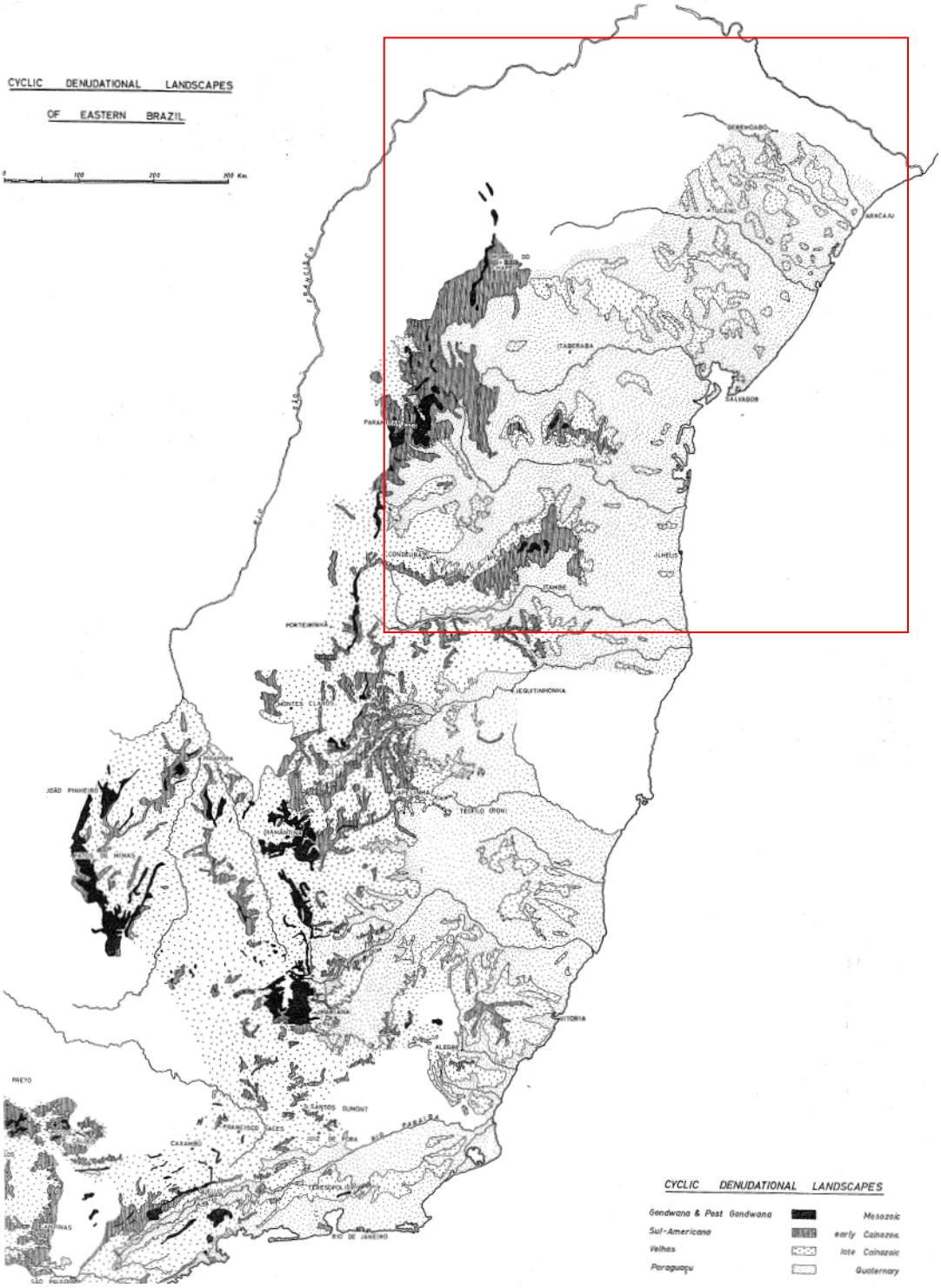

Fig. 2. Lester King's map of “cyclic denudational landscapes” in NE Brazil (Fig. 121 in King 1967, here slightly cropped). The red box marks the study area in this report.

3. Method of landscape analysis

The large-scale landforms were analysed in two steps: 1) Mapping of different erosion surface, and 2) Comparing the mapped surfaces with the geology. The Shuttle Radar Topography Mission (SRTM) was used as the basic elevation data set. The spacing between data points is approximately 90 m (Jarvis et al., 2008). The information about the general geology was extracted from the geology map of Brazil (CPRM, 2001) and the details from the geology map of Bahia (Dalton de Souza et al. 2003). This resulted in an erosion surface map.

3.1 Method of surface mapping

The SRTM was used as the basic elevation data set and was used to construct a contour map with 100 m contours (Fig. 3) using Surfer Software (Golden Software 2002). The DEM was also used to extract topographical profiles in north to south and west to east respectively, spaced at every 0.1 degrees (Fig. 4). Centred along the topographical profile a 0.2 degree wide corridor was extracted and analysed for maximum and minimum height values. The resulting three profiles (i.e. topographical, maximum and minimum) were plotted together in a single profile (Fig. 5). The profiles were made with a length-scale equal to the constructed contour map, so that they easily can be compared, but the vertical scale was exaggerated five times, so that break-of-slope becomes easier to identify. In areas where the topographical line and the maximum line coincide, it shows where the altitude level is for the surface, which can be mapped on the contour map.

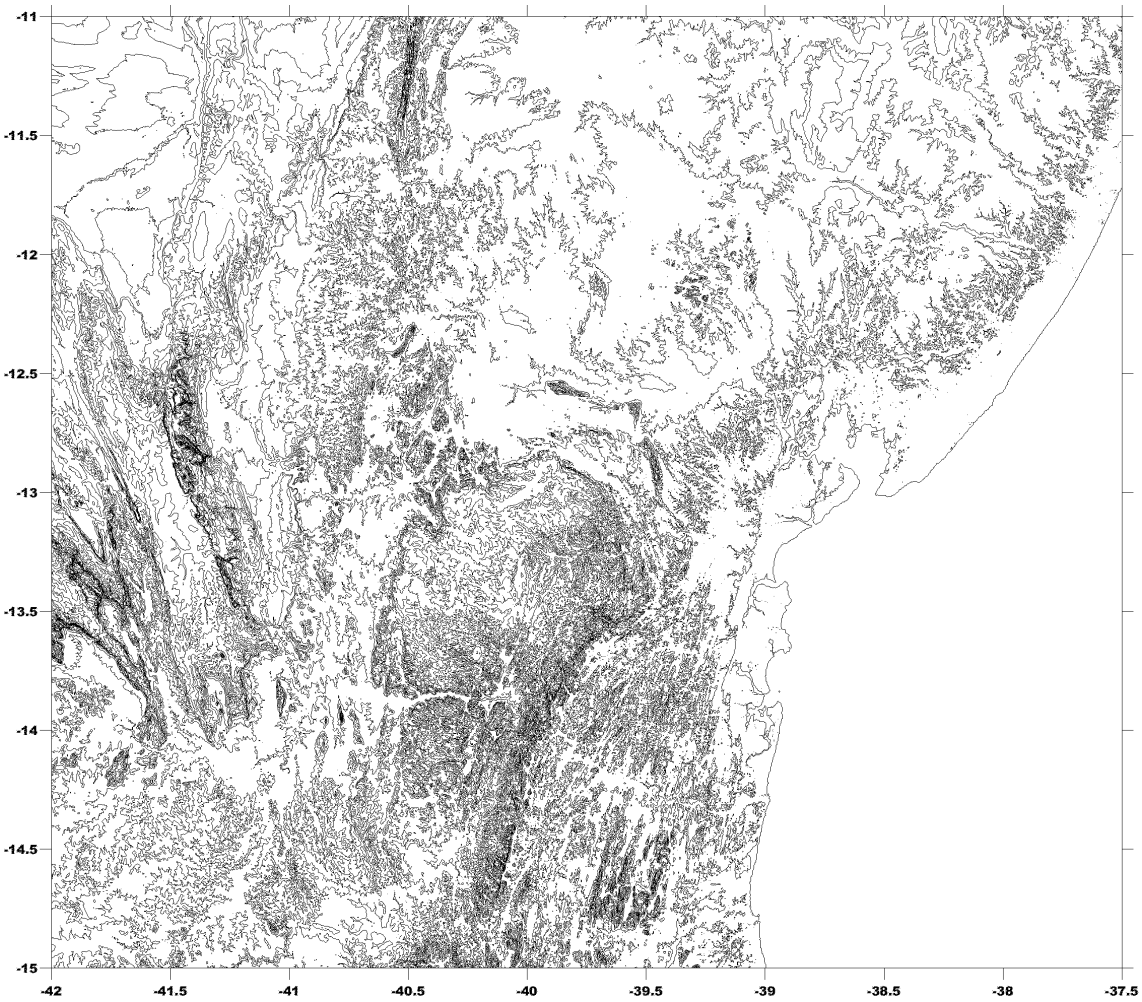

Fig. 3. The contour map with 100 m contours used as the base for the surface mapping. The map was constructed from elevation data obtained by the SRTM- mission (Jarvis et al., 2008).

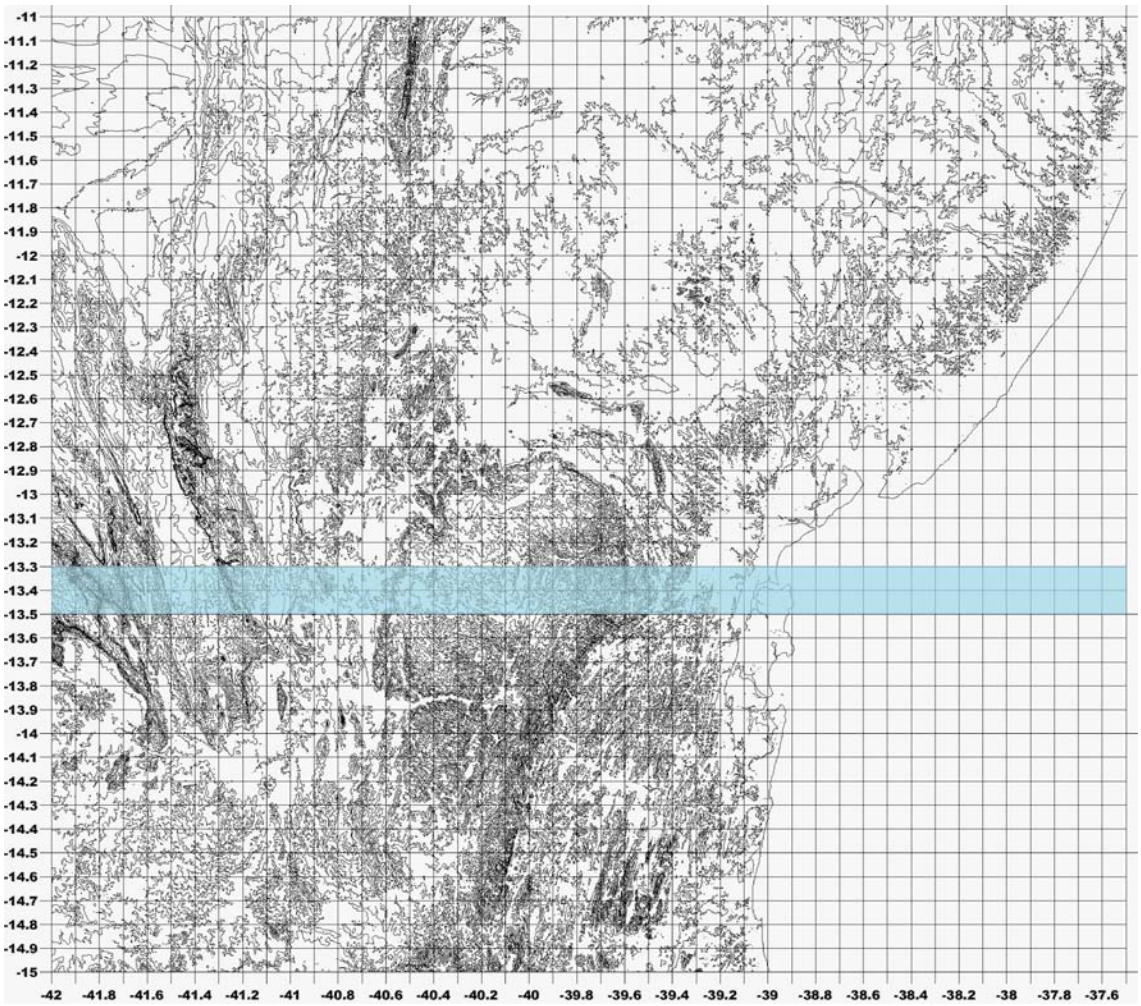

Fig. 4. The map shows an example for one of all the 80 constructed profiles (West-East and North- South) used to identify different peneplains. The blue area mark the corridor for the maximum and minimum values plotted together with the profile along latitude -13.4. The systematic construction of overlapping corridors allow inclined surfaces to be mapped on the contour map.

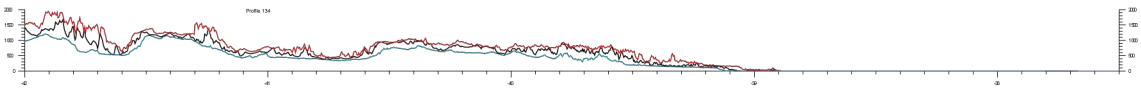

Fig 5. Example of a profile used for the analysis of surfaces. The red and blue line in the profile is the maximum respectively minimum values for the blue corridor in the figure above. The black line is the topographical line along the -13.4 latitude. The coincidence between the red and black line illustrates where the surface level can be seen in the contour map. Based on the contour map, surface levels were plotted onto the profiles and the profiles was used to extend the surface mapping from well preserved areas to less preserved areas.

From the contour map several areas with extensive coherent levels could be identified, e.g. Chapada Diamantina, Planalto de Conquista and the areas west of the Recôncavo-Tucano-Jatobo basin. As a consequence these areas could be used as a first starting point in order to begin the surface mapping. The identification of surfaces was made by combining

coherent areas on the contour map in combination with cross interpretation of these areas in different single profiles (topographical, maximum, minimum). In this way different surfaces can be followed from profile to profile, showing surface outliers, steps between different surfaces, offsets within a surface and the tilt of each surface or tectonic block. Rapid change of inclination in the contours was used to determine the extent for mapping of each surface. Thus, this kind of mapping allows the identification of both sub-horizontal and inclined surfaces (Lidmar-Bergström 1988, 1996; Bonow et al. 2006). I must be emphasised that it is very important to use the combination of profiles and contour map, and trying to interpret surfaces along single profile lines can never give any confidence in landscape levels and identification of tectonic blocks, a method unfortunately common among many authors. Thus, the profiles shown in this report are only illustrations to the mapping. To further support the identification of surfaces ordinary topographical maps were consulted. The lithological influence on the surfaces was checked against geological maps. By doing this it is possible to distinguish between flat areas due to resistant rocks and surfaces formed by denudation by fluvial systems (cf Japsen et al in press). Field work, including documentation of landforms, in the study area took place in 2007 (Japsen et al. 2007).

4. Geomorphological results

This section presents a topographical overview of the study area, an overview description and illustration of the different surfaces, and some more detailed maps and photographs.

4.1 Topographical overview

Three areas with different characteristics were identified (Fig. 6): 1) A coastal plain, developed as incised valleys up to 200 m a.sl. (Figs 7, 8, 9), A low inland plain, developed along the major valleys up to 500 m a.s.l and 250 km from the present coastline (Figs 10, 11, 12, 13, 14, 15, 16, 17, 18) and 3) A highland plain in the interior above 1000 m a.s.l. (Figs 19, 20, 21).

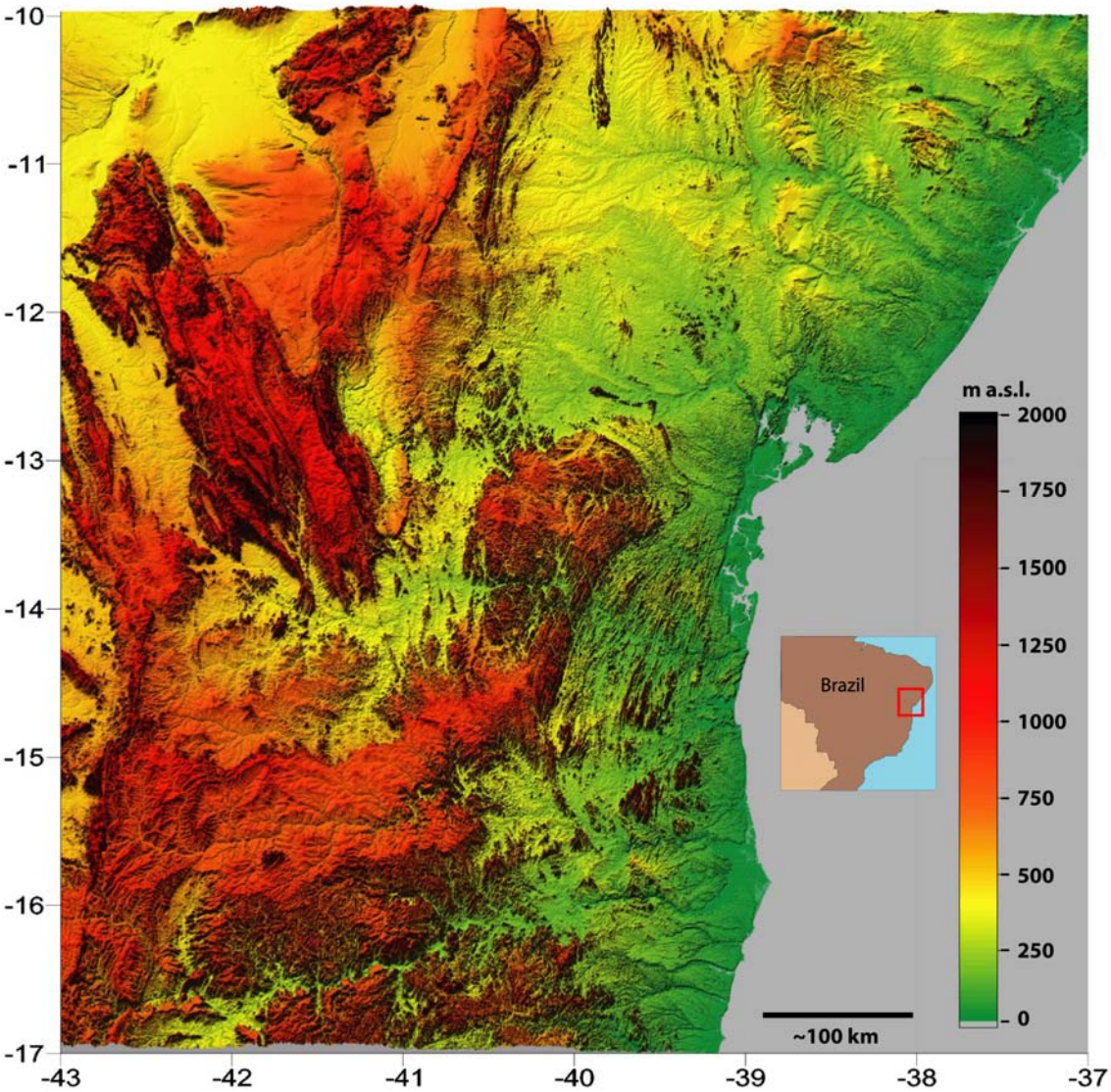

Fig. 6. The topography of the study area. The high areas of Chapada Diamantina and Planalto de Conquista are dominant in the central and western part, while lowland plains dominate in the eastern and coastal areas. Many of the details in topography are structurally controlled. See fig 1 for place names.

The coastal areas are generally characterised by a narrow low-land plain, gently sloping inland towards the west (Fig. 6). The coastal plain is cut into the Miocene-Pliocene(?) Barreiras Formation. The incision has also occurred along valleys that usually are rather narrow and the surface thus of limited wideness, but for Rio Imhambupe and Rio Paraguaçu (Fig. 1), where the backward erosion is extensive along the rivers and here the surface is also of some wideness. In this area the incision is far beyond the Barreiras Formation and have cut into either the Tucano Basin (Rio Imhambupe) or into the basement areas (Rio Paraguaçu) (Figs 1, 6).

Fig. 7. At Canaveiras, the present coastal areas are low-lying and very flat. Occasionally there is a small escarpment (c 30 m high) within the coastal plain, showing the most recent development of denudation. This scarp is probably erosional. Photo location: S 15' 33"; W 39' 00", see also Fig.1.

Fig. 8. The well preserved and wide coastal plain at Canaveiras, cut across the Barreiras. The summits of the inselbergs in the background are at about 500 m a.s.l. Photograph towards the west. Photo location: S 15' 30"; W 39' 12".

Fig. 9. This incised valley is thought to represent the latest incision in the study area, thus belonging to the coastal plain. The landscape is of valley in valley type and the top of the valley shoulders here are gently sloping and eventually merges with the lower surface at higher elevation. Photograph from southern Sergipe. Photo location: S 10' 50"; W 37' 34".

At about 200 m a.s.l., the coastal plain is replaced by a less tilted plain (Figs 10, 11) extending up to about 500 m a.s.l. and the valleys in the plain are shallow and wide (Fig. 12). This lower inland plain is of widest extent in the northern part of the study area. It has developed to a distance of more than 200 km from the coast, but occurs also to less extent along the larger rivers in the southern part as well as far into the interior (Fig 6). It is generally slightly tilted towards the sea in the east. This plain is of low relative relief, often less than a few tenth of metres, but occasionally mountain complexes (Fig. 14) or isolated inselbergs, consisting of resistant bedrock (often granitic intrusions) (Fig. 15), rises considerably above the plain. This is especially prominent in the northern part of the study area. Commonly, at the upper reaches of the plain, there is a more or less well developed escarpment (Figs 16, 17, 18).

Fig. 10. The low-relief inland plain, here cut across basement rocks in northwest Sergipe. The horizon is only broken by some low inselbergs. Photograph towards northwest Photo location: S 09' 53"; W 37' 38".

Fig. 11. The low-relief plain west of Feira de Santana, here at c 200 m a.s.l.. Photograph towards the north. Photo location: *c.* S 12' 20"; W 39' 00".

Fig. 12. The low-relief plain has wide and shallow valleys. Photograph towards the west c. 100 km west of Feira de Santana. Photo location: S 12' 29"; W 39' 50".

Fig. 13. Small ridges of resistant rocks rise slightly above the low-relief plain. Photo location: S 12' 32"; W 39' 34".

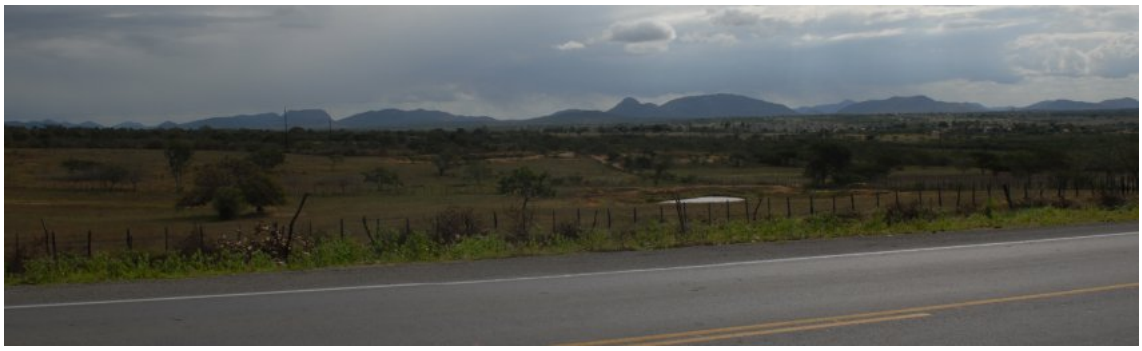

Fig. 14. A hill complex of crystalline rock at the western side of the Tucano Basin. In the foreground is the Jurassic sequence, but the border to the basement is far east of the complex, thus not seen in the topography. Photograph towards northwest, 5 km south of Santa Bárbara. Photo location: S 11' 58"; W 38' 58".

Fig. 15. Inselberg on the low relief plain 125 km west of Feira de Santana. The plain is here at c. 250 m a.s.l.. Inselbergs are sometimes regarded as the last remnant of an older landscape, but here the summit is well below the higher surface in the landscape. Photo location: S 12' 31"; W 40' 03".

Fig. 16. The low plain, here at c 350 m a.s.l. is limited by a sharp break-of-slope at its uppermost part. The summits of the escarpment are at c. 1300 m a.s.l. (dotted line). Photo location: S 12' 38"; W 41' 10".

Fig. 17. The low plain in the westernmost part of the study area, here at c. 500 m a.s.l. is clearly bordered by escarpments. The escarpment to the left is part of Chapada Diamantina and in the centre-left is part of the Planalto de Conquista. Photograph towards the south-east just outside Liveramento de Nossa Senhora (c.f. Fig 22). Photo location: S 13' 40"; W 41' 50".

Fig. 18. Detail of the contact between the escarpment and the low plain. The bottom of the valley is at c 500 m .a.s.l. and the summit of the escarpment is at c. 1100 m a.s.l.. Photograph towards the west outside Liveramento de Nossa Senhora (c.f. Fig. 22). Photo location: S 13' 37"; W 41' 48".

Above the escarpment another plain of low relief has been identified at between c 900-1200 m a.s.l., dominating the landscape in the western and central part of the study area (Fig. 6). The lower altitude occurs in Planalto de Conquista area, while the higher altitudes are common in Chapada Diamantina area (Figs 19, 20, 21, 22). Both these areas have wide and shallow valleys incised in the surfaces, but usually the surface is more dissected than the lower surface. In the Chapada Diamantina area there is some higher relief, up to slightly above 2000 m a.s.l., represented by rather narrow ridges of resistant rocks. Thus

relatively flat areas of large areal extent occur both in high and in low positions of the landscape, and it seemed possible to map their extent in more detail.

Fig. 19. The high plain in Chapada Diamantina is limited in the east by a resistant bedrock ridge. The plain reaches out of sight to the north and is here at about 1200 m a.s.l. (c.f. Fig. 22). Photo location: S 13' 28"; W 41 28".

Fig. 20. In the west and in the east the plain is bordered by ridges of resistant rocks, rising a few hundred metres above the plain. Note the shallow valley slightly incised into the plain (red arrow). (c.f. Fig. 22). Photo location: S 13' 28"; W 41' 28".

Fig. 21. The high plain on the Planalto de Conquista plateau is at c. 900 m a.s.l, and the inselbergs in the background rises to slightly above 1000 m a.s.l.. Photo location: S 14' 49'; W 40' 50'.

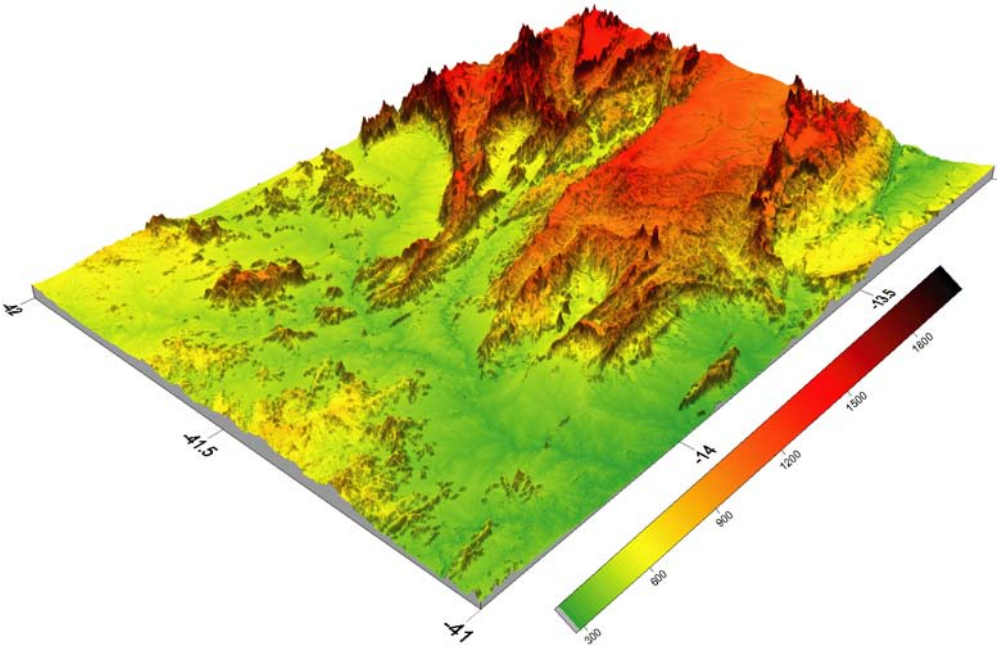

Fig. 22. 3D model of Chapada Diamantina. The higher surface is between 1200-1300 m a.s.l. and it is incised by shallow valleys. The escarpment to the lower surface is pronounced and around 700 m high. Location in Fig. 1.

4.2 The denudation surfaces

Based on the method described above, two major and regionally developed surfaces were identified and mapped; here labelled the higher surface (HS) and the lower surface (LS). Both these surfaces cut across different types of bedrock. Therefore they are interpreted as denudation surfaces controlled by a general base level (Fig. 23). A younger denudation generation (or surface), here labelled the coastal plain, has also been identified. It is developed as a rather narrow incised valley below the lower surface, and it is almost only along the river Rio São Francisco, that it has developed as a surface beyond the immediate river valley. The relief above the higher surface is highly irregular and it has not been possible to identify any coherent surface here.

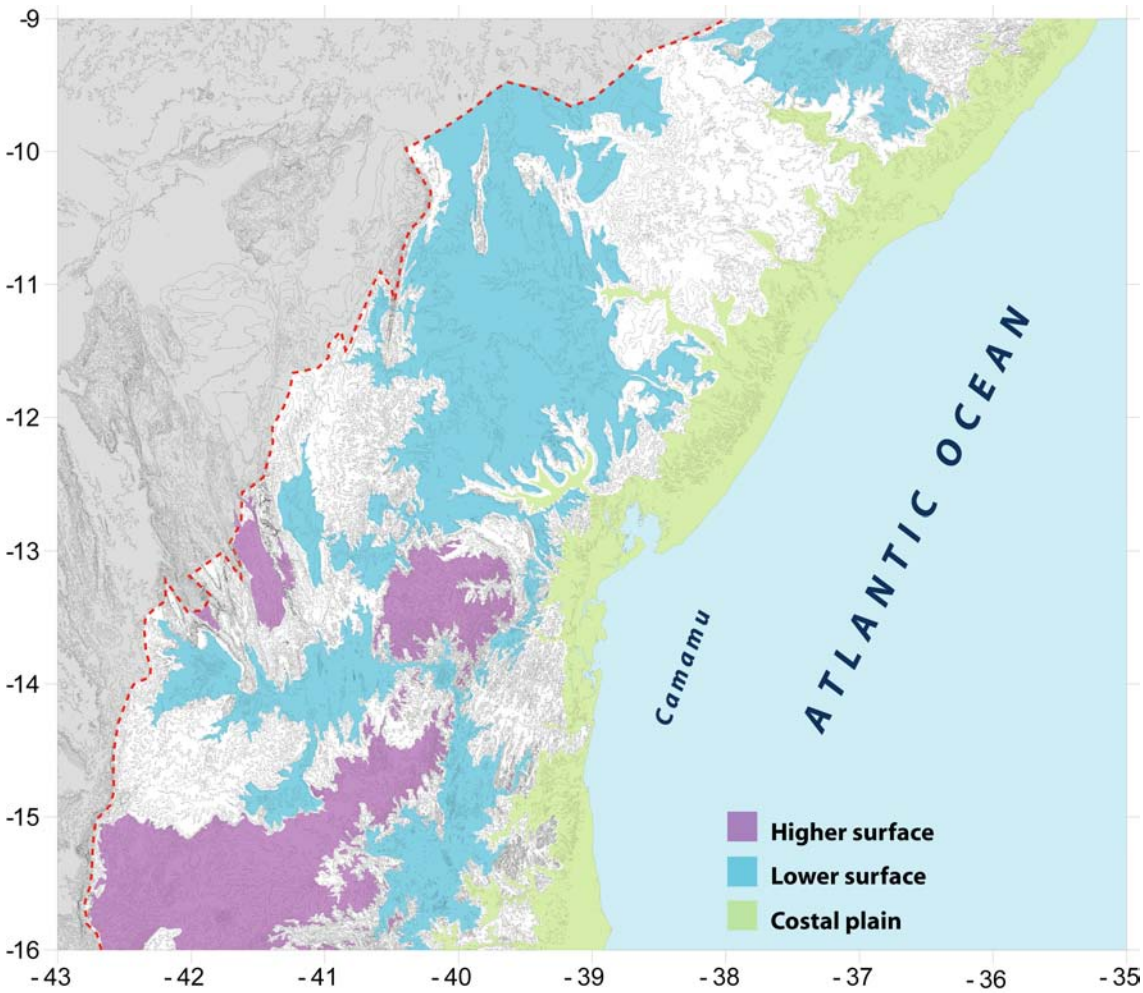

Fig. 23. The three denudation surfaces in the study area all cut across bedrock of different age and resistance. The white in the map are areas with slopes or areas that not have any identifiable coherent surfaces (e.g. ridges). The map is limited by the present coast and the water divide (red line).

4.2.1 The higher surface

The higher surface is a regional surface, and it is preserved in the southern and central part of the study area, i.e. Planalto de Conquista and Chapada Diamantina (Fig. 23). Mainly it is coherent with very few break-of-slopes within the surface, that could indicate offsets of the surface after its formation. The area, on which the surface exists, is thus regarded to be on a coherent tectonic block that has been internally stable since the formation of the higher surface. The mapping on the contours and correlation through the profiles (Figs 3 ,4) shows that the surface is tilted towards the south-east. The surface is at the highest elevation in Chapada Diamantina area, between c. 1300-1100 m.a.s.l., and at lower elevations in the Planalto de Conquista area, around 900 m a.s.l.(Figs. 19, 20, 21, 22)

4.2.2 The lower surface

The lower surface is also a regional surface, but it is more widespread than the higher surface (Fig. 23). It is developed along the major rivers in the area, i.e. Rio São Francisco, Rio Paraguaçu and Rio de Contas. It is especially well developed in the central part of the study area, north of Planalto de Conquista along the Rio Paraguaçu. Here it forms a coherent area covering more than 45.000 km^2. The lower surface is clearly a denudation surface as it cuts across rocks of different age and resistance. The mapping shows that the surface is tilted towards the coast, thus at highest elevation in the west. It can be followed from about 500 m a.s.l. at its upper reaches and down to about 200 m a.s.l where the lower surface is cut off by the more steeply tilted coastal plain. However the lower surface exact relationship to the Barreiras Fomration is unclear, whether it cuts off or if the Barrieras Formation is on top of the lower surface. At the lower surface's upper reaches the transition to the higher surface is often sharp, characterised by a winding escarpment (Figs 16, 18, 22).

4.2.3 The coastal plain

The coastal plain is tilted and can be followed from the present coast up to about 200 m a.s.l. (Fig. 23). The incision dissects the lower surface and the Barreiras at the coast. But how wide the plain has grown varies considerably across the study area. The surface is especially wide along the rivers Rio São Francisco and Rio Paraguaçu . At c 150 m a.s.l. the surface associated with the Rio Paraguaçu is wide, but narrows noticeably, and here the river forms a canyon before it enters the sea. Thus it is possible that the river here is antecedent. (Figs 7, 8, 9).

4.2.4 Illustrations of the surface mapping

Four profiles have been selected to illustrate the mapping (Figs 23, 24, 25, 26). In the profiles the location for the higher and lower surface has been indicated, and these lines for the surface line are based on the mapping made on the contour map (Fig. 23).

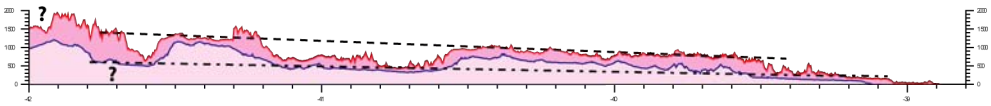

Fig. 24. West-east profile along -13.4 degrees.

Fig. 24 is drawn to illustrate how the landscape appears in a profile where the higher surface is well preserved. In the west, lies Chapada Diamantina where the surface is at c 1200 m a.s.l., and in the east the surface cross Planalto de Conquista, at c 900 m a.s.l., before it ends at the coast. The correlation in the western areas is not clear, but maybe the surfaces also exist on the west side of the present water divide. The mapping shows that the surface is clearly tilted generally towards the southeast, which appears as an east tilting in the profile. The surface is preserved in areas with metamorphic rocks that are resistant to weathering. No clear breaks can be seen in the profile line that could indicate movements on indi-

vidual tectonic blocks. The lower surface can clearly be seen in the east along the coast. Some inselbergs rises from the surface that almost can be correlated with the level for the higher surface. In the central part of the profile the lower surface forms a bottom level along the incised river Rio de Contas that cuts across the high area south of this profile (c.f. Figs 6, 23).

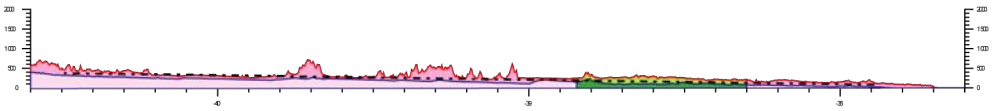

Fig. 25. West-east profile along -11.3 degrees. Note that no change of inclination occurs despite the crossing of the Tucano Basin.

Fig. 25 shows the situation in the northern part of the study area where the lower surface is well developed, but also where the higher surface (if it ever existed here) has been totally obliterated. In the west the profile starts east of the northern part of Chapada Diamantina. The lower surface is here at its uppermost reaches at c 500 m a.s.l. and the interpretation is that it is slightly tilted towards the east. In the eastern parts the lower surface cut across the Recôncavo-Tucano-Jatobo Basin, but the difference in geology cannot clearly be seen in the regional pattern. In the central part resistant rocks form hill complexes and inselbergs, however the cross correlation with other profiles from the mapping indicates that the summits do not reach the level for the higher surface (cf. Fig. 26).

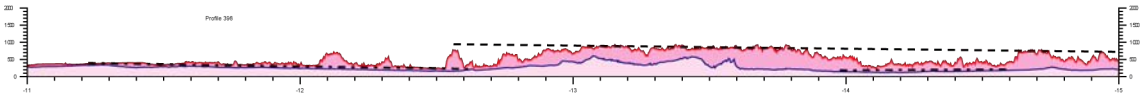

Fig. 26. North-south profile along -39.8 degrees.

Fig 26 is a north-south profile relatively close to the sea. It crosses the easternmost part of Planalto de Conquista, where the higher surface is well preserved. The line for the higher surface shows the slight tilt of the surface towards the southeast. To the north the surface seems to have been eroded and cannot be seen in the landscape. The summits of the inselbergs in the northern part do not correspond to a projected surface level, thus suggesting that it has been significantly eroded. The lower surface is well represented in the profile. In the southern part the line represents a valley network of incised valleys, in a landscape otherwise dominated by ridges (c.f. Fig.6). Although not clear at all in the profile, but in the surface map (Fig. 23) the lower surface has a very different appearance in the landscape in the northern part. Here the lower surface is well developed and wide with only shallow valleys, but for some inselbergs and mountain complexes. The lower surface here is tilted towards the Rio Paraguaçu, situated immediately north of the highland area.

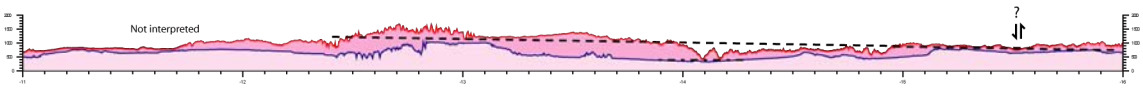

Fig. 27. North-south profile along -41.5 degrees.

Fig. 27 is selected to illustrate the correlation of surface level between Chapada Diamantina (in the centre) and Planalto de Conquista in the south in the westernmost part of the study area, and also to show the appearance of the lower surface at its uppermost reaches. Above the upper surface level some narrow ridges which clearly stand above the

higher surface. The correlation from Chapada Diamantina to the eastern areas shows that the surface might be offset in the eastern part. This is marked in Fig 27 and coincide with a rather large valley in west-east direction (cf. Fig. 6). If true this offset is small, around 100 m, and must have occurred post surface formation. The lower surface is typically concave with a low-point in the valley centre as can be seen in the blue bottom line. The valleys have dissected the higher surface, and the sharp break-of-slope in the maximum line shows the position of escarpments, that separates the lower surface from the higher.

4.3 The surfaces in relationship to geology

The landscape analysis has resulted in a geomorphological map of different surfaces (Fig. 23). This map has been analysed in relationship to the basement geology and to the sedimentary sequences within the study area, in order to distinguish between flat areas due to resistant rocks and surfaces formed by denudation by fluvial systems. The result of this analysis is imbedded in the surface map (Fig. 23). To demonstrate how the geology influences on the development and preservation of surface, an example will be shown here from Chapada Diamantina and the area east of it (Fig. 28). The area is typical for the study area, with north-south trending ridges (folds), containing rocks of different age and resistance.

The lower surface (blue in Fig. 28) is at its uppermost reaches, and the latest development is clearly connected to the geology. The Rio Paraguaçu has cut across an area with granitic and gneissic rocks (e.g. PP2myml, A2mo) and into an area with limestone and calcite (NP2sa and NP2snl, bluish in geology map). While the surface is of limited extent in the granitic/gneissic areas the surface has widen considerable in the limestone area. Thus the conclusion is that the erosion has been much faster in the latter area, and the local lithology have enhanced the development of the lower surface. But at the same time will a surface formed across resistant rocks last much longer than if it is formed across easily eroded rocks. Therefore this is the most likely case in areas with quartzitethat is the case in both Chapada Diamantina and Planalto de Conquista. However the geology will only temporary halt the denudation and eventually only minor, low, ridges of the more resistant strata will be left in the landscape (c.f. Figs 13, 14). The final result after long time of denudation will be a rather flat landscape also in areas with very different geology (see Fig. 25 as an example).

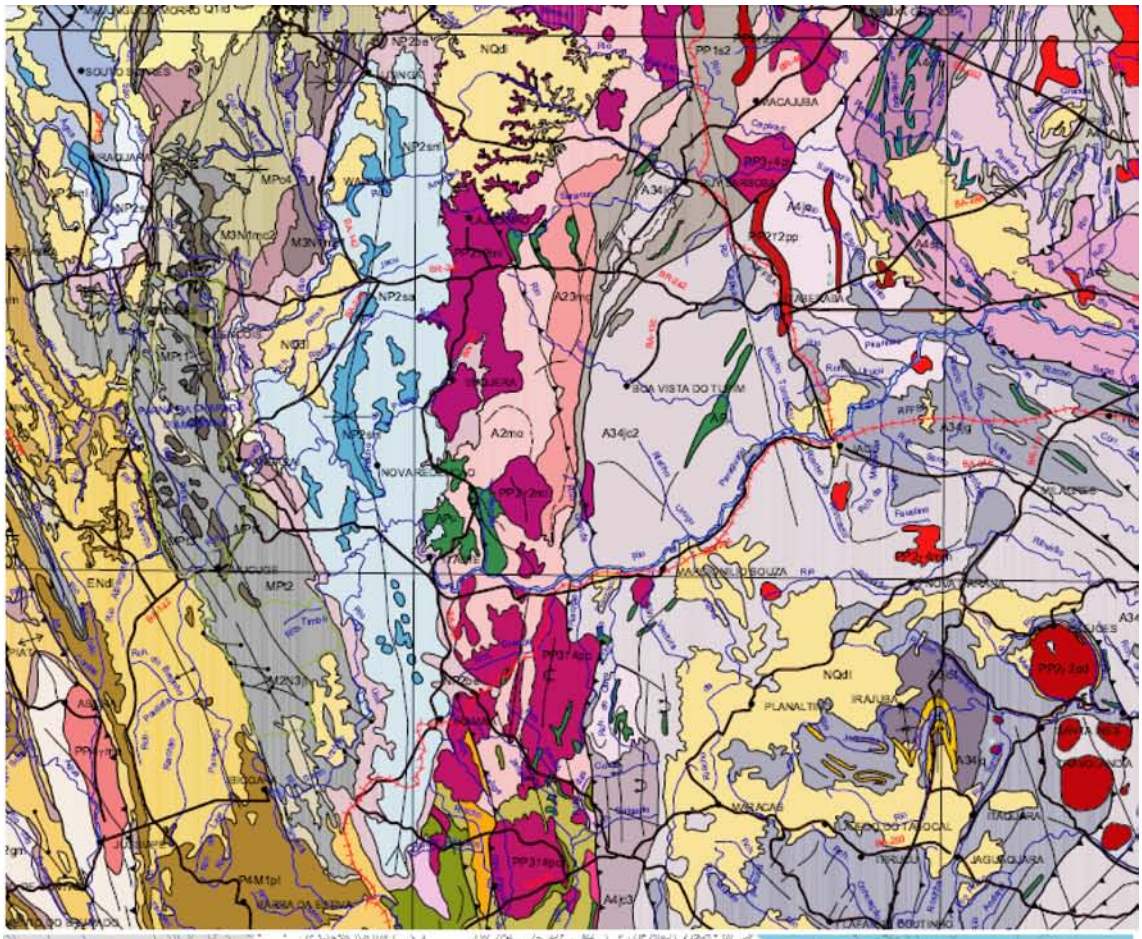
NQdl
PP1s2
MACAJUBA
NP2sa
A2mo
A34jc2
BOA VISTA DO TUPIM
MPt2
ENdl
NQdl
PLANALTIN
IRAJUBA
MARACAS
ITAQUARA
JAGUAQUARA
A4jc3

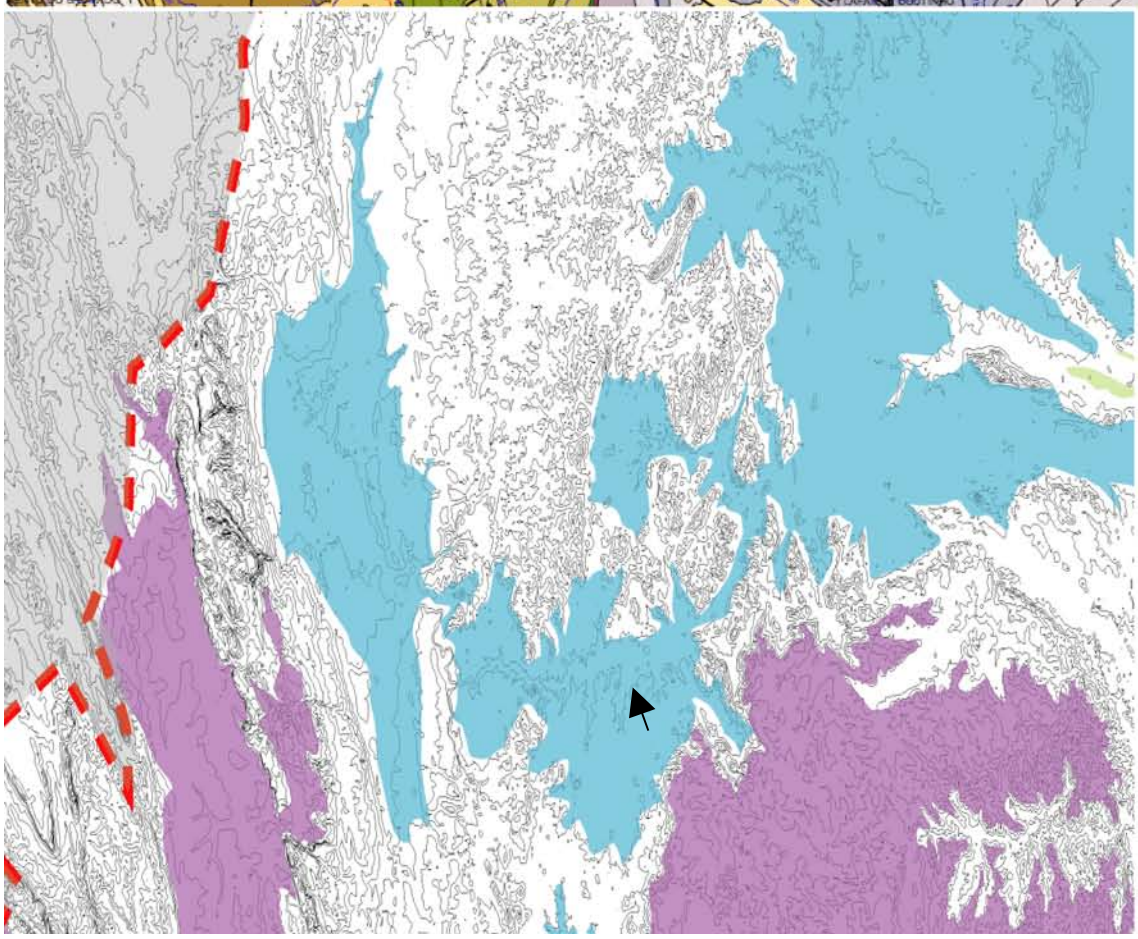

Previous page: Fig. 28. A selection of the Bahia geology map (Dalton de Souza et al. 2003) and from the surface map (Fig. 23.), covering the same area. To the left is Chapada Diamantina and to the right Planato de Conquista. The bedrock is all basement. Lower map: Blue-lower surface, Pink-higher surface. Contours 100 m, the black arrow points at the 300 m contour line. Red-water divide.

5. Geomorphological implications and discussion

The surface mapping in the area (Fig. 23) shows that two major surfaces (peneplains), can be followed along the major valleys as an inclined plain, and the mapping further shows that the surfaces cut across rocks of different age and resistance (Fig. 28). These conditions leave no other options than that the surfaces must have been governed by a general base level. The condition that the surfaces are regional shows that they must have been formed at a time with tectonically stable conditions. The denudation of resistant rocks to form a surface also suggests a long time for the development of surfaces. Therefore, the regional, low-relief surfaces in the study area are witnesses of two different periods when the landscapes were at low elevation and close to the general base level. Thus a relative denudation chronology can be constructed, however that history may not include all the burial and exhumation events that may have occurred in the landscape, but likewise is significant and detectable by other methods (e.g. AFTA, Green 2008, in press).

The higher surface is only preserved in areas with resistant rocks, but it seems highly likely that it originally was completed across a much wider area, indicated by remnants in the east (e.g. inselbergs) that once may have reached the level for the higher surface. The higher surface may also have been present in the west, but in that case it has been deeply cut by the headwaters of the São Francisco river. A candidate for the preserved surface in the west could thus be the Cretaceous rocks in the São Francisco Basin, presently under destruction in its eastern part by the São Francisco river.

The relief above the higher surface may or may not be part of an older surface. If ever existed, it has been significantly eroded. Any attempt to constrain that surface, e.g. as an envelope surface has limited value in landscape analysis.

The lower surface was developed at the expanse of the upper surface due to base-level change. The backward erosion has resulted in winding escarpments, and the winding is especially pronounced in areas with large differences in bedrock resistance. As the amount of base level change, estimated from the valley floor of the lower surface to the elevation of the higher surface, is about 700 m, the change must have had a tectonic component. The lower surface is represented in the whole study area and it is occasionally wide also far away from the present base level. In the eastern part of the study area the lithology play an insignificant role for the surface appearance, while in the west it has mainly developed in areas with less resistant rocks (c.f. 28).

King's geomorphological map (Fig. 2) (King 1967) is in overview analogous to the new map presented here, but for the details, especially the borders for the different surfaces. King identified a high area, which he divided into two surfaces (named Sul-Americana and Velhas) and a low-land plain, (Paraguaçu), in which the former two surfaces are almost analogous to the higher surface and the latter to the lower surface of this study. A difference is that King does not acknowledge a coastal plain cutting off the lower surface, which has implications for the event chronology and timing for surface development in the area (see further discussion in Japsen et al. 2009).

5.1 Surface chronology and timing of events

This latest base-level change has resulted in incision of rivers along the coast and in the the Recôncavo and the Tucano Basin, dissecting Barreiras and Marizal Formations. The apparent rapid dissection of the lower surface here suggests that this is due to relatively recent base level change and must post-date the Barreiras. The age constraints on the Barreiras group are rather broad, between Miocene-Pliocene(?) (Arai and Shimabukuro, 2003). Anyhow the rapid incision together with the preservation of the easily eroded sediments, still forming coherent patches of a once larger surface, indicates that this latest event most probably is young. Such surface would have been rapidly dissected, unless covered or situated in a low position close to the base level.

The lower surface cut across both basement and the rift section. Therefore must the surface post-date the Aptian Marizal formation. However from the geomorphological mapping it is not totally clear whether the lower surface cuts across the Barreiras or if the Barreiras is deposited on the lower surface. The relationship is not clear because the intersection angle is to low to provide a definitive answer. This leaves two possibilities: If the Barreiras are deposited onto the lower surface, the basement beneath the Barreiras is an exhumed surface, with the consequence that another erosional event is required. If so that event is pre-Barreiras, but post higher surface. If the lower surface cuts the Barreiras and basement, the lower surface must be post Barreiras. If however the Barreiras can be of two different ages as suggested by Arai and Shimabukuro (2003), this relationship might be different in other parts of the study area.

The higher surface is primarily found in areas with Proterozoic rocks, thus badly constraining its formation age. However the surface is corresponding to large areas covered with Cenozoic laterites, thus this shows that the higher surface formed in post-Cretaceous times. Further, because some extensive time is needed to form the lower surface after completion of the higher surface, it seems likely that the higher surface formed during the Paleogene, while the lower surface formed mainly in the Neogene and the coastal plain from the Late Pleistocene to present. The landscape as seen today is thus reflecting tectonics and base-level changes in the Cenozoic.

6. Conclusions

The geomorphological analysis of the large scale landscapes at the passive Atlantic margin of NE Brazil shows two major denudation surfaces formed along the major rivers, the higher and the lower surface, and a minor surface in the present coastal areas, the coastal plain (Fig. 23). The higher surface is situated at 1200 to 900 m a.s.l in Chapada Diamantina and Planalto de Conquista. The higher surface is cut across Precambrian basement, and occasionally covered by Cenozoic laterites. The higher surface must therefore be Cenozoic and most likely Paleogene in age, thus formed long after the rift-flank uplift. The lower surface cuts across basement and the rift sequence in the Recôncavo-Tucano Basin and must therefore be post-Aptian in age. The lower surface is extensive and has developed by eroding the higher surface, and this condition suggests that the surface is probably Neogene in age. The coastal plain cut into the Barreiras Formation, constraining its age to post-Miocene, but the rapid development of incision suggest that this reflects a much more recent base-level change.

The height difference of c 500-700 metres between the higher and the lower surface suggests that the base level change must have had a tectonic component.

Resistant rocks facilitate preservation of old surfaces while less resistant rocks facilitate the formation of new surfaces. However long-term denudation decreases the lithological influence significantly of surface the appearance.

7. References

Ab'Sáber, A.N., 2000: Summit surfaces in Brazil. Revisita Brasileira de Geociências **30** (3), 515– 516.

Arai, M. and Shimabukuro, S. 2003: the Tortonian unconformity and its relation with the stratigraphic framework of the Barreiras group and correlative units (Neogene, Brazil). 3rd Latinamerican Congress of Sedimentology (Belém, June 8 – 11, 2003), Abstracts - Symposium Theme 2, p. 263-264.

Bonow J.M., 2005: Re-exposed basement landforms in the Disko region, West Greenland - disregarded data for estimation of glacial erosion and uplift modelling. Geomorphology **72**: 106–127.

Bonow J.M., Lidmar-Bergström K. and Näslund JO. 2003: Palaeosurfaces and major valleys in the area of the Kjølen Mountains, southern Norway – consequences of uplift and climatic change. Norsk Geografisk Tidsskrift **57**: 83–101.

Bonow J.M, Japsen P., Lidmar-Bergström K., Chalmers J.A. and Pedersen A,K.: 2006a. Cenozoic uplift of Nuussuaq and Disko, West Greenland - elevated erosion surfaces as uplift markers of a passive margin. Geomorphology **80**: 325–337.

Bonow J.M., Lidmar-Bergström K. and Japsen P. 2006b: Palaeosurfaces in central West Greenland as reference for identification of tectonic movements and estimation of erosion. Global and Planetary Change **50**: 161–183.

Bonow, J.M., Lidmar-Bergström, K., Japsen, P., Chalmers, J.A. and Green, P.F. 2007: Elevated erosion surfaces in central West Greenland and southern Norway: their significance in integrated studies of passive margin development. Norwegian Journal of Geology **87** (1-2), 197–206

CPRM 2001: Geological map of Brazil, 1 : 5,000,000. 1 CD.

Dalton de Souza, J., Kosin, M., Melo R.C., Santos, R.A., Teixeira, L.R., Sampaio. A.R., Guimarães, J.T., Viera Bento, R., Borges, V.P.,

Martins, A.A.M., Arcanjo, J.B., Loureiro, H.S.C. and Angelim, L.A.A. 2003: Mapa Geológico do Estado ba Bahia – Escala 1:1,000,000. Salvador: CPRM, 2003, Versão 1,1, Programas Carta Geolo´gica do Brasil ao Milinésimo e Levantamentos Geológicos do Brasil (PLGB), Convēnio de Cooperação e Apoio Técnico-Científico CBPM-CPRM.

Davis, W.M. 1899: The geographical cycle. Geographical Journal **14**: 481-504

Demoulin, A., Zarate, M. and Rabassa, J. 2005: Long-term landscape development: a perspective from southern Buenos Aires ranges of east central Argentina. Journal of South American Earth Sciences **19**: 193-204.

Green, P.F. 2008: Geotrack Report 1013: Camamu Basin, offshore Brazil. Thermal history reconstruction in the 1-BAS-88-BA, 1-BAS-102-BA, 1-BAS-113-BA & 1-BAS-129-BA wells, based on AFTA and VR data. Geotrack International, Victoria, Australia, 153 pp and appendices.

Green, P.F. in prep: Geotrack Report 990: Thermal History Reconstruction in the 1-AO-1-BA, 1-BRN-1-BA, 1-FLU-1-BA, 1-FPO-1-BA, 1-FVM-1-BA, 1-RSO-1-BA, 3-MB-3-BA and 6-MGP-34-BA wells, Tucano and Recôncavo Basins, Onshore Brazil, together with AFTA and associated thermal history interpretations in 89 outcrop samples from Bahia, NE Brazil, and 20 samples from the Serra do Mar. Geotrack International, Victoria, Australia. in prep.

Golden Software, 2002: Surfer 8-Contouring and 3D Surface Mapping for Scientists and Engineers, ver 8.02. Golden Software Inc., Colorado.

Japsen, P., Bonow, J.M., Cobbold, P.R. and Pedreira, A.J. 2007. Burial and exhumation history of North-East Brazil. Field work 2007. Danmarks og Grønlands Geologiske Undersøkelse, Rapport **2007/66**, 75pp.

Japsen, P., Bonow, J.M., Green, P.F., Chalmers, J.A. and Lidmar-Bergström, K., in press: Formation, uplift and dissection of planation surfaces at passive continental margins. Earth Surface Processes and Landforms.

Japsen, P., Bonow, J.M., Green, P.F. and Cobbold, P.R. 2009: Burial and exhumation history of NE Brazil focussing on the Camamu Basin: a multidisciplinary study based on thermal, sonic and stratigraphic data and landform analysis. Final report. GEUS Report **2009/10**.

Jarvis, A., Reuter, H. I., Nelson, A. and Guevara, E., 2008: Hole-filled seamless SRTM data V4, International Centre for Tropical Agriculture (CIAT), available from http://srtm.csi.cgiar.org.

King, L.C., 1953: Canons of landscape evolution. Bulletin of the Geological Society of America **64**, 712-752.

King, L.C., 1956: A geomorfologia do Brasil oriental. Revisita Brasileira deGeografica **18** (2), 3 –121.

King, L.C., 1967: The morphology of the earth (2nd edn). Oliver & Boyd, Edinburgh.

Lidmar-Bergström K. 1982: Pre-Quaternary geomorphological evolution in southern Fennoscandia. Sveriges Geologiska Undersökning C 785.

Lidmar-Bergström K. 1988: Denudation surfaces of a shield area in south Sweden. Geografiska Annaler **70A**: 337–350.

Lidmar-Bergström K. 1989: Exhumed Cretaceous landforms in south Sweden. Zeitschrift für Geomorphologie, Neue Folge Suppl. bd **72**: 21–40.

Lidmar-Bergström K. 1995: Relief and saprolites through time on the Baltic Shield. Geomorphology **12**: 45–61.

Lidmar-Bergström K. 1996: Long term morphotectonic evolution in Sweden. Geomorphology **16**: 33–59.

Lidmar-Bergström K, Ollier, C.D. and Sulebak, J.R. 2000: Landforms and uplift history of southern Norway, Global and Planetary Change **24**: 211–231.

Lidmar-Bergström K., Näslund, J.-O., Ebert, K., Neubeck, T. and Bonow, J.M. 2007: Cenozoic landscape development on the passive margin of northern Scandinavia. Norwegian Journal of Geology **87** (1-2), 181–196.

Peulvast, J.P. and Claudino Sales V. 2004: Stepped surfaces and palaeolandforms in the northern Brazilian «Nordeste»: constraints on models of morphotectonic evolution. Geomorphology **62**: 89–122.

Peulvast, J.P., Claudino Sales, V., Bétard, F. and Gunell, Y 2008: Low post-Cenomanian denudation depths across the Brazilian Northeast: Implications for long-term landscape evolution at a transform continental margin, Global and Planetary Change **62:** 39–60

Potter, P.E. 1997: The Mesozoic and Cenozoic palaeodrainage of South America: a natural history. Journal of South American Earth Sciences **10**: 331-344.

Valadão, R.C. 1998: Evolição de Longo-Termo do Relevo do Brasil Oriental (Desnudação, Superfícies de Aplanamento e Soerguimentos Crustais). PhD-thesis, Universidade Fedral da Bahia, Instituto de Geociências.

Zonneveld, J.I.S. 1993: Planations and summit levels in Suriname (S. America). Zeitschrift für Geomorphologie, Suppl. Bd. **93**, 29–46.